

**UNIVERSITY OF MODENA AND REGGIO EMILIA**

**Ph.D school in: Food and agricultural science, technology and biotechnology**

---

Dean of Ph.D school: Prof. Alessandro Ulrici

XXXIII Cycle

**Phenotypic and genomic analysis of *Komagataeibacter* strains to elucidate the cellulose biosynthesis mechanism**

Candidate: Salvatore La China

Tutor: Dr. Maria Gullo

# Table of contents

<b>Abstract</b>	<b>3</b>
<b>Riassunto</b>	<b>4</b>
<b>Thesis outline</b>	<b>6</b>
<b>Chapter 1</b>	<b>9</b>
<i>Oxidative fermentations and exopolysaccharides production by acetic acid bacteria: a mini review</i>	
<b>Chapter 2</b>	<b>22</b>
<i>Biotechnological production of cellulose by acetic acid bacteria: current state and perspectives</i>	
<b>Chapter 3</b>	<b>39</b>
<i>Kombucha tea as a reservoir of cellulose producing bacteria: assessing diversity among Komagataeibacter isolates</i>	
<b>Chapter 4</b>	<b>51</b>
<i>Exploring K2G30 genome: A high bacterial cellulose producing strain in glucose and mannitol based media</i>	
<b>Chapter 5</b>	<b>65</b>
<i>Genome sequencing and phylogenetic analysis of K1G4: a new Komagataeibacter strain producing bacterial cellulose from different carbon sources</i>	
<b>Chapter 6</b>	<b>77</b>
<i>Characterization of bio-nanocomposite films based on gelatin/polyvinyl alcohol blend reinforced with bacterial cellulose nanowhiskers for food packaging applications</i>	
<b>Chapter 7</b>	<b>93</b>
<i>Mechanical and structural properties of environmental green composites based on functionalized bacterial cellulose</i>	

<b>Chapter 8</b>	<b>106</b>
<i>General discussion and future perspectives</i>	
<b>Supplementary materials</b>	<b>111</b>
<b>References</b>	<b>124</b>
<b>Organizations</b>	<b>155</b>
<b>Acknowledgments</b>	<b>156</b>
<b>Curriculum vitae and list of publications</b>	<b>158</b>

# Abstract

Acetic acid bacteria are versatile organisms converting a number of carbon sources into biomolecules of industrial interest. Such properties, together with the need to limit chemical syntheses in favor of more sustainable biological processes, make acetic acid bacteria suitable organisms for food, chemical, medical, pharmaceutical and engineering applications. At current, well-established bioprocesses by acetic acid bacteria are those derived from the oxidative pathways that lead to organic acids synthesis, such as acetic acid and gluconic acid, vitamin C and ketones. Others applications of acetic acid bacteria derive from their ability to produce exopolysaccharides. Among exopolysaccharides, bacterial cellulose is one of the most important biopolymer that actually is receiving more attention for sustainable industrial applications. The reasons why bacterial cellulose is an attractive biopolymer lies in its physical-chemical properties, and mechanical properties, as well as in the biodegradability and not toxic features. Among its physical-chemical properties stand out purity, considering that it consists of glucose monomers, high water-holding capacity, high crystallinity index and biocompatibility. All of these features make bacterial cellulose suitable for the use as native polymer or in composite materials.

Within the *Acetobacteriaceae* family, the genus *Komagataeibacter* includes species of interest for the production of bacterial cellulose, especially the species *Komagataeibacter xylinus*, which is considered the model organism for the study of the biological e biochemical mechanisms of bacterial cellulose synthesis.

Kombucha tea, a beverage originated from Asia continent, produced from black and green tea supplemented with sucrose, is a selective food matrix for recovering cellulose producing acetic acid bacteria. The occurrence of at least two microbial groups, yeasts and acetic acid bacteria, which establish a symbiotic relationship, allows the production of a sparkling, low alcoholic, acidic beverage, containing a layer of bacterial cellulose on the surface.

The aim of this PhD thesis was to study the biological mechanisms of cellulose production in acetic acid bacteria. Bacterial strains from UMCC (Unimore Microbial Culture Collection) culture collection, isolated from Kombucha tea, were typed and selected for their ability to produce bacterial cellulose. A polyphasic study was performed on two strains, including the whole genome sequencing focusing the analysis of genes involved in cellulose synthesis, and a phenotypic characterization mainly aimed at the detection of the best carbon for cellulose production.

This approach allowed also the taxonomic identification of the two strains, highlighting issues of taxonomic allocation within the *Komagataeibacter* genus.

The bacterial cellulose obtained by the conditions set up in this study, was used to develop two bio-based materials. The first material is a combination of bacterial cellulose with gelatin and polyvinyl-alcohol that is a promising innovative biomaterial for food packaging uses; the second one is a bio-based composite material composed of bacterial cellulose and inorganic compounds (titanium dioxide and clay), which properties outline the application as high performance membrane for biomedical use.

# Riassunto

I batteri acetici sono microrganismi versatili in grado di convertire fonti di carbonio in biomolecole di interesse industriale. Nell'era in cui c'è una forte necessità di ridurre la sintesi chimica di materiali, a favore di produzioni mediate da processi biologici sostenibili, i batteri acetici rivestono un ruolo chiave per diverse applicazioni in campo chimico, biomedico, farmaceutico, alimentare e ingegneristico. Attualmente, i bioprocessi consolidati che vedono coinvolti i batteri acetici sono principalmente legati allo sfruttamento del loro potenziale ossidativo con produzione di acidi organici, come l'acido acetico e l'acido gluconico, la vitamina C e i chetoni. Altre applicazioni dei batteri acetici riguardano le loro abilità nella produzione di esopolisaccaridi. In particolar modo, la cellulosa batterica è, senza dubbio, uno dei biopolimeri che attualmente sta ricevendo molta attenzione per applicazioni industriali sostenibili. Quello che rende la cellulosa di origine microbica un polimero così attraente risiede sicuramente nelle proprietà chimico-fisiche e meccaniche, così come nella non tossicità e biodegradabilità. Tra le caratteristiche chimico-fisiche peculiari della cellulosa batterica spiccano la purezza, considerando che è composta esclusivamente da monomeri di glucosio, alto grado di cristallinità, elevata capacità di ritenzione idrica e biocompatibilità. Queste proprietà consentono l'utilizzo della cellulosa batterica sia nella forma nativa che in combinazione con altri materiali.

All'interno della famiglia *Acetobacteriaceae*, il genere *Komagataeibacter*, include specie di grande interesse per la produzione di cellulosa, in modo particolare la specie *Komagataeibacter xylinus*, considerata il modello per lo studio dei meccanismi biologici e biochimici che regolano la produzione di cellulosa.

Una delle matrici di origine alimentare da cui è possibile isolare ceppi del genere *Komagataeibacter* è una bevanda fermentata chiamata *Kombucha tea*, originaria del continente asiatico, e tradizionalmente prodotta fermentando tè nero o tè verde addizionato di saccarosio. La coesistenza di almeno due gruppi microbici, quali lieviti e batteri acetici in associazione simbiotica, è responsabile della trasformazione in una bevanda frizzante a basso contenuto alcolico, acidula e caratterizzata da una presenza di cellulosa sulla superficie.

Lo scopo del presente lavoro di tesi è stato quello di approfondire i meccanismi biologici di produzione di cellulosa batterica. Ceppi batterici isolati da *Kombucha tea* e posseduti dalla collezione microbica UMCC (*Unimore Microbial Culture Collection*) sono stati genotipizzati e selezionati sulla base della capacità di produzione di cellulosa batterica. Due ceppi sono stati oggetto di uno studio polifasico che ha previsto sia il sequenziamento dell'intero genoma, finalizzato alla conoscenza dei geni coinvolti nel meccanismo di regolazione e produzione di cellulosa, che uno studio fenotipico di caratterizzazione delle migliori fonti di carbonio per la produzione di cellulosa batterica. Tale approccio ha permesso anche l'identificazione dei due ceppi, evidenziando alcune problematiche di collocazione tassonomica all'interno del genere *Komagataeibacter*. La cellulosa ottenuta da uno dei due ceppi, in condizioni ottimizzate nel presente studio, è stata utilizzata per lo sviluppo di due materiali, di cui uno ha dato risultati promettenti per applicazioni nel campo del confezionamento alimentare, in combinazione con gelatina-polivinil alcool; l'altra ha riguardato lo sviluppo di un materiale composito con composti

inorganici (biossido di titanio e argilla) le cui caratteristiche ne delineano l'impiego come membrane ad alta prestazione in applicazioni biomedicali.

# Thesis outline

This PhD thesis was carried out at the Department of Life Sciences of the University of Modena and Reggio Emilia, between years 2017 and 2020. The manuscript deals with the research project performed during the three years focused on the development of new strategies for the production of bacterial cellulose. The main goal of the research project was to integrate different experimental approaches in order to understand the biological meaning and the molecular machinery that lead cellulose production in prokaryotes. This research project is an example of a multidisciplinary approach which considered different aspects related to environmental microbiology, food microbiology and material sciences, used to develop new materials with high impact in a wide range of applications, especially in biomedical field and food packaging. Furthermore, the use of bacterial cellulose for the development of new advanced bio-based materials represent an eco-friendly approach with the main focus on the substitution of plastic-based materials. The main characters of this thesis are acetic acid bacteria, especially strains belong to the *Komagataeibacter* genus. We will deal with the isolation of the strains used in this project, followed by the cellulose production using reference and alternative media and finally will introduce two applications. A detailed outline of the thesis book is reported below.

**Chapter 1** introduces acetic acid bacteria, especially those involved in industrial applications. This chapter is will give to the readers an overview about the versatility of acetic acid bacteria from industrial point of view, starting from the old one application for vinegar production. The chapter is divided based on the production of compounds derived from oxidative processes, as vinegar, gluconic acid, vitamin C (keto-gulonic acid), dihydroxyacetone, and bioprocess that lead to the production of exopolysaccharides as bacterial cellulose and levan.

**Chapter 2** is focused on the biotechnological and industrial aspects of bacterial cellulose production by acetic acid bacteria. This chapter will describe the main structural features of bacterial cellulose, linking those features to the suitability of this biopolymer for a wide range of uses, especially for biomedical applications and for food packages. In order to explain the structural properties, the biological and biochemical processes were described based on the state of art. A detailed description of the cellulose synthase complex, the enzymes responsible of cellulose production, was reported in this chapter, offering an overview of the biochemical pathways involved in the biopolymer production and a comparison of the already described strains, in order to highlight the differences that occur in strains able to synthesize exopolysaccharide, especially at genetic level. In this chapter a biological meaning was highlighted, focusing the cellulose role in the bacterial life and acetic acid bacteria as a model for the mechanism of biofilm formation. At the end, the main biotechnological applications of bacterial cellulose were analyzed, given in this way a complete overview the cellulose production starting from the biology to the industrial applications.

Chapter 1 and chapter 2 provide scientific notions on which the experimental approach adopted in this thesis book was adopted. In **Chapter 3** the isolation procedures of bacteria able to produce cellulose was reported. The food matrix, represented by a fermented beverage called *Kombucha tea*, was described from technological point of view, highlighting the benefits and health features of *Kombucha tea* consumption. Since the production of *Kombucha tea* is characterized by a double fermentation by a peculiar microbial community represented by yeasts and bacteria, the interaction of microorganisms and the cooperation relationships were described. The experimental for the

selection of strains able in cellulose production and, especially, of acetic acid bacteria related to the genus *Komagataeibacter* was described. A total of 46 strains were analyzed based on fingerprint techniques. The cellulose production abilities of the target strains were evaluated and based on the results collected, two strains were chosen in order to study the biological mechanisms of cellulose production and the versatility in term of utilize of different carbon sources.

In **Chapter 4**, the first target strain isolated was described. The strain K2G30 (UMCC 2756) was chosen because its high ability in cellulose production. Indeed, among the full set of isolates screened in chapter 3, K2G30 achieved the higher yield of cellulose production. The genome of K2G30 was sequenced and the genes related to the cellulose synthase complex were identified and analyzed. In comparison with the available genomes of other *Komagataeibacter* strains sequenced, K2G30 was characterized by four copies of the catalytic subunits of cellulose synthase complex. The presence of the four subunits of the catalytic core of cellulose synthase could justify the higher yield obtained of cellulose. The phylogeny of K2G30 was inferred using a concatenation of 16S and 23S rDNA sequences, retrieved from the full genome sequence. The taxonomical assignment of K2G30 resulted from the alignment of the full 16S-23S rRNA sequence shows a clusterization with the type strain of *K. xylinus* (LMG1515<sup>T</sup>). Furthermore, K2G30 was tested using three different carbon sources (glucose, mannitol and xylitol), of which, mannitol and xylitol, could be easily recovered from agricultural wastes. The highest yield was achieved using mannitol, meaning that K2G30 is a suitable strain for producing bacterial cellulose at industrial level. Moreover, considering that mannitol is a carbon source available in many agricultural wastes, K2G30, can be considered an added value for sustainable bacterial cellulose production.

From the set of isolates screened in chapter 3, another isolate stood out for its abilities in cellulose production and was described in **chapter 5**. The strain K1G4 (UMCC 2947), clustered in a different group from the fingerprint analysis, was recognized to be a different strain of *K. xylinus* than K2G30. As in the case of K2G30, the gDNA of K1G4 was sequenced and the operon of cellulose synthase complex was reconstructed. Differently from K2G30, the strain K1G4 exhibited 3 copies of the catalytic subunits of cellulose synthase complex, justifying the lower obtained yield. In contrast of the approach used in chapter 4 for the taxonomic assignment, in this experiment the power of the phylogenetic analysis was improved using the full operon sequence of K1G4, retrieved from the genome project. As for K2G30, also K1G4 was assigned to *K. xylinus* species, based on the phylogenetic tree obtained. K1G4 was also tested to assay its abilities in cellulose production and correlate the results obtained from both phenotypic and genomic sequence analysis. In order to compare the two strains, also K1G4 was tested using three different carbon sources. Differently from K2G30, the carbon sources tested here did not include xylitol, given the low results obtained from K2G30 project. Xylitol was substituted by glycerol, another carbon source that could be recovered from wastes derived from diesel refining processes. The best result obtained in term of yield of cellulose was achieved using mannitol medium. About glycerol and glucose, K1G4 used the two carbon sources with the same efficiency. Compared to K2G30, the bacterial cellulose yield obtained using K1G4 was lower for these two carbon sources.

Based on the results obtained in the two previous chapters, K2G30 was chosen for the next step, represented by the development of one application. In the **chapter 6**, the cellulose obtained from K2G30 was used to develop a new composite biopolymer that could be used in food packaging, in order to replace plastic-based materials. Cellulose produced by *K. xylinus* K2G30 was blended with gelatin and polyvinyl alcohol (PVA), two valuable polymers for replacing plastic materials. The obtained polymer was studied and evaluated in term of the structure, mechanical properties and color properties. The results obtained from this study highlighted that the biopolymer obtained



possessed all properties that makes it suitable to partially replace or reduce the use of the existing petroleum-based packaging materials available in the market.

In **Chapter 7**, the cellulose produced by K2G30 was used for the formulation of new functionalized biomaterial suitable to build up hydrophilic porous membranes or plastic-like film, as candidate for the replacement of existing petroleum-based materials. Although the aim of this study was similar to the project of the previous chapter, the approach was completely different. In this case, two inorganic material were used to create two different blended materials with different features in terms of structures, mechanical properties and morphology properties. The two materials used in this study were Titanium dioxide (TiO<sub>2</sub>) and inorganic ceramic Clay. The two polymers obtained using the two different cellulose fillers displayed a completely different properties, making them suitable for different applications.

# Chapter 1

## Oxidative fermentations and exopolysaccharides production by acetic acid bacteria: a mini review

Salvatore La China, Gabriele Zanichelli, Luciana De Vero, Maria Gullo

Department of Life Sciences, University of Modena and Reggio Emilia, Via G. Amendola, 2, Pad. Besta, 42122, Reggio Emilia, Italy

**This chapter is published as:**

**La China S**, Zanichelli G, De Vero L, Gullo M. Oxidative fermentations and exopolysaccharides production by acetic acid bacteria: a mini review. *Biotechnol Lett* (2018) 40, 1289–1302. <https://doi.org/10.1007/s10529-018-2591-7>

## Abstract

Acetic acid bacteria are versatile organisms converting a number of carbon sources into biomolecules of industrial interest. Such properties, together with the need to limit chemical syntheses in favor of more sustainable biological processes, make acetic acid bacteria appropriate organisms for food, chemical, medical, pharmaceutical and engineering applications. At current, well-established bioprocesses by acetic acid bacteria are those derived from the oxidative pathways that lead to organic acids, ketones and sugar derivatives. Whereas emerging applications include biopolymers, such as bacterial cellulose and fructans, which are getting an increasing interest for the biotechnological industry. However, considering the industrial demand of high performing bioprocesses, the production yield of metabolites obtained by acetic acid bacteria, is still not satisfying. In this paper we review the major acetic acid bacteria industrial applications, considering the current status of bioprocesses. We will also describe new biotechnological advances in order to optimize the industrial production, offering also an overview on future directions.

## Introduction

The acetic acid bacteria (AAB) group includes highly versatile organisms, able to produce a great variety of compounds used in food and beverages, chemical, medical, pharmaceutical and engineering fields (Mamlouk and Gullo, 2013; De Roos and De Vuyst, 2018). The genus *Acetobacter* includes species (i.e. *Acetobacter pasteurianus* and *A. aceti*) of interest for the food industry because of the ethanol-oxidizing activity that is beneficial in vinegar production and detrimental in other fermented beverages like wine, beer and cider (Bartowsky and Henschke, 2008; Wu et al., 2010; Sengun and Karabiyikli, 2011).

*Gluconacetobacter* and *Komagataeibacter* genera, on the other hand, comprise highly versatile species, having a great variety of metabolic abilities including acetic acid and gluconic acid production, nitrogen fixation and bacterial cellulose production. For instance *K. europaeus*, which is the main species involved in industrial vinegar production, *K. xylinus*, which is designated as a model organism of bacterial cellulose (BC) synthesis and *Ga. diazotrophicus* that includes strains of interest for their endophytic activity (Mamlouk and Gullo, 2013).

Within *Gluconobacter* genus, *G. oxydans* plays a leading biotechnological role because of its importance for the industrial production of gluconic acid, dihydroxyacetone, Vitamin C (L-ascorbic acid) precursors and miglitol (Adachi et al., 2003; De Vero et al., 2010; Sainz et al., 2016b; Dikshit and Moholkar, 2019). Recently, species of *Gluconobacter*, *Gluconacetobacter*, *Komagataeibacter*, *Kozakia* and *Neosassa* genera have been investigated for their ability to produce fructans such as levan-type exopolysaccharides (LT-EPS). Such compounds are getting increasing attention due to their possible use in medical, pharmaceutical and foods fields (Jakob et al., 2012a; Brandt et al., 2016).

This review focuses on the metabolic potential of AAB taking into account their versatility in the bioconversion of carbon substrates into valuable bioproducts, such as organic acid, ketones and exopolysaccharides (Table 1-1). Is it known that other metabolites, not discussed in this paper, are of industrial interest, however here, we will focus on acetic acid, gluconic acid, dihydroxyacetone, 2-keto-L-gulononic acid, BC and fructans, as representative of both consolidated and emerging applications of AAB (Table 1-2).

## Main bioconversions having industrial impact

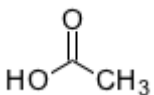
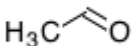
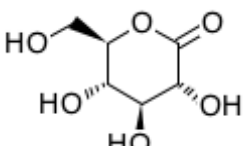
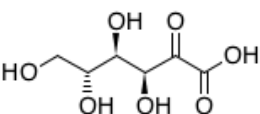
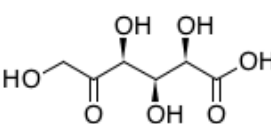
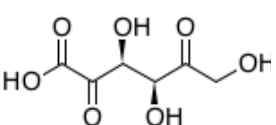
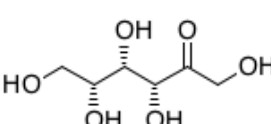
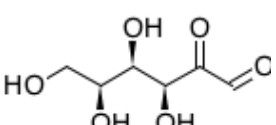
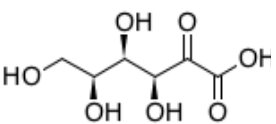
The oxidation of carbon sources by AAB is responsible for the production of a number of industrially relevant compounds. In such processes, sugars, alcohols and sugar alcohols are incompletely oxidized to the corresponding products, which are accumulated in large amounts in the medium. These pathways, the so called oxidative fermentations, involve a set of membrane-bound dehydrogenases, located in the periplasmic region of the cell membrane. Considering their primary structure, membrane-bound dehydrogenases of AAB (also called primary dehydrogenases) can be divided into five groups: quinoprotein-cytochrome complex, molybdoprotein-cytochrome complex, flavoprotein-cytochrome complex, membrane-bound quinoprotein, and other proteins (Adachi and Yakushi, 2016). They first extract the electrons from the substrates; then transfer them to the terminal oxidase via ubiquinone, which generates proton-motive force for ATP generation (Matsushita et al., 1994). The respiratory chain is involved only in the partial oxidation, but not in the complete oxidation of these substrates to CO<sub>2</sub> and H<sub>2</sub>O. The assimilation pathways of partially oxidized products (for instance those related to acetic acid, ketogluconates or dihydroxyacetone), operating in the cytoplasm, generally, are active only in the late growth or in the stationary phase (Toyama et al., 2005). Historically, AAB have been known for their ability to produce acetic acid by oxidation of ethanol. This reaction can occur either on the periplasmic side of the cell membrane or in cytosol. On the periplasmic side, ethanol is first oxidized to acetaldehyde by a membrane bound pyrroloquinoline quinone-dependent alcohol dehydrogenase (PQQ-ADH) and then acetaldehyde is further oxidized to acetic acid by aldehyde dehydrogenase (ALDH), which belong to the molybdoprotein-cytochrome complex. In the cytosol, the pathway is identical, but the bioconversion is operated by both a NAD-dependent ADH [EC 1.1.1.1] and ALDH [EC 1.2.1.3]. After ethanol depletion, the accumulated acetic acid is used by cells via acetyl CoA synthase and phosphoenolpyruvate carboxylase.

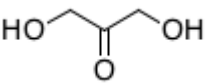
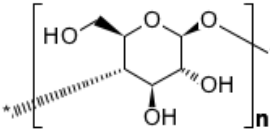
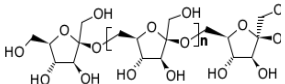
The high versatility of AAB emerges when we consider sugars metabolism, which can generate a number of oxidation products and exopolysaccharides like BC and fructans. Glucose oxidation, as mainly studied in *G. oxydans*, leads to the synthesis of glucono- $\delta$ -lactone acid in a reaction catalyzed by the membrane-bound pyrrolo-quinolinequinone-dependent gluconate dehydrogenase (PQQ-GDH). Glucono- $\delta$ -lactone is stable in acid conditions, but it can spontaneously hydrolyses to gluconic acid under neutral and alkaline conditions or can be converted to gluconic acid by a membrane-bound gluconolactonase (Ameyama et al., 1981; Matsushita et al., 1994).

Gluconic acid can be further oxidized to 2-keto-D-gluconate by the flavoprotein gluconate dehydrogenase (FAD-GADH) or to 5-keto-D-gluconate by the PQQ-glycerol dehydrogenase (PQQ-GLDH), a polyol-dehydrogenase (also known as D-sorbitol dehydrogenase (SLDH)) which have a broad substrate specificity (Saichana et al., 2015). 2-keto-D-gluconate is oxidized to 2,5-diketo-D-gluconate acid by the flavoprotein 2-keto-D-gluconate dehydrogenase (FAD-2KGADH) [EC 1.1.99.4]. Both, 5-keto-D-gluconate and 2,5-diketo-D-gluconate, are intermediate products of the synthesis of 2-keto-L-gulonic acid, a precursor in the vitamin C process. The substrates for the production of 2-keto-L-gulonic acid can be glucose, D-sorbitol or L-sorbose, respectively. When D-glucose is used as substrate, 2-keto-L-gulonic acid is formed via 2,5-diketo-D-gluconate, as mentioned before (Sonoyama et al., 1982). In the case of D-sorbitol as substrate, it is first oxidized to L-sorbose (PQQ-GLDH) and then to L-sorbosone by the flavoprotein L-sorbose dehydrogenase (FAD-SDH) (Sugisawa et al., 1991). If L-sorbose is utilized as substrate, 2-keto-

L-gulonic acid is produced via L-sorbose (Hoshino et al., 1990). Finally, L-sorbose is oxidized to 2-keto-L-gulonic by L-sorbose dehydrogenase (SNDH), which cofactor remain unknown (Adachi and Yakushi, 2016).

**Table 1-1.** Properties and application field of the main compounds produced by acetic acid bacteria

Chemical compound	Key enzyme involved in the biosynthesis- Precursor compound	Main biotechnological application
 Acetic acid (C <sub>2</sub> H <sub>4</sub> O <sub>2</sub> )	-ALDH [ EC 1.2.1.-] -Acetaldeide	Food, chemical
 Acetaldeide ( C <sub>2</sub> H <sub>4</sub> O)	-PQQ-ADH [EC 1.1.2.8] -Ethanol	Food, chemical
 Glucono-δ-lactone (C <sub>6</sub> H <sub>10</sub> O <sub>6</sub> )	-PQQ-GDH [EC 1.1.5.2] -Glucose	Food, pharmaceutical, chemical
 2-keto-D-gluconate (C <sub>6</sub> H <sub>10</sub> O <sub>7</sub> )	-FAD-GADH [EC 1.1.99.3] -Gluconic acid	Food, pharmaceutical, chemical
 5-keto-D-gluconate (C <sub>6</sub> H <sub>10</sub> O <sub>7</sub> )	-PQQ-GLDH [EC 1.1.99.22] -Gluconic acid	Food, pharmaceutical, chemical
 2,5-Diketo-D-gluconate (C <sub>6</sub> H <sub>8</sub> O <sub>7</sub> )	-2KGADH [EC 1.1.99.4] -2-keto-gluconate	Food, pharmaceutical, chemical
 L-sorbose ( C <sub>6</sub> H <sub>12</sub> O <sub>6</sub> )	-PQQ-GLDH [EC 1.1.99.22] -D-sorbitol	Pharmaceutical, cosmetic, food
 L-Sorbose (C <sub>6</sub> H <sub>10</sub> O <sub>6</sub> )	-FAD-SDH [EC 1.1.99.12] -L-Sorbose	Pharmaceutical, cosmetic, food
 2-keto-L-gulonate (C <sub>6</sub> H <sub>10</sub> O <sub>7</sub> )	-SNDH [ EC:1.1.1.-] -L-sorbose	Pharmaceutical, cosmetic, food

Chemical compound	Key enzyme involved in the biosynthesis- Precursor compound	Main biotechnological application
 <p>Dihydroxyacetone (C<sub>3</sub>H<sub>6</sub>O<sub>3</sub>)</p>	-PQQ-GLDH [EC 1.1.99.22] -Glycerol and other polyols	Pharmaceutical, chemical, cosmetic
 <p>Cellulose ((C<sub>6</sub>H<sub>10</sub>O<sub>5</sub>)<sub>n</sub>)</p>	-CS [EC 2.4.1.12] -UDP-glucose	Food, biomedical, cosmetic, engineering
 <p>Levan (C<sub>18</sub>H<sub>32</sub>O<sub>16</sub>)</p>	-LS [EC 2.4.1.10] -Fructose	Food, medical, pharmaceutical

In AAB, sugars can be also used as monomeric units for the synthesis of exopolysaccharides chains, such as BC and fructans. BC is produced from activated glucose (UDP-glucose) as starting material, thanks to cellulose synthase complex (CS) activity that forms 1,4- $\beta$ -glucan chains. The CS is constituted by different subunits that work in a concerted way. The polymerization mechanism of 1,4- $\beta$ -glucan chains to form crystalline structure is characterized by events series that occur in that so called terminal complex (TC), outside the cell. 16 CSs are localized in each TC that form 16 glucan chains. The first polymerization event occurs between glucan chains in order to form a protofibrils, thanks to the establishment of hydrogen bonds and Van der Waals forces. Protofibrils from adjacent TC polymerize to form microfibrils and finally the wound ribbon (Ross et al., 1991). Among fructans, LT-EPS are synthesized by the extracellular enzyme levansucrase (or sucrose 6-fructosyltransferase, which catalyses the transfer of D-fructosyl residues from sucrose to a growing fructan chain by trans-fructosylation (Han and Clarke, 1990; Donot et al., 2012). Once sucrose is completely depleted, levansucrase cleaves the  $\beta$ (2–6) linkages of the newly-formed levan chain, causing the consecutive release of the terminal fructose units until a branching point is reached (Chambert et al., 1974; Méndez-Lorenzo et al., 2015).

## Acetic acid

Acetic acid has two major areas of production: the first one is food-grade vinegar and the second one chemically synthesized acetic acid (mainly produced from petrochemical sources, such as carbonylation of methanol and oxidation of n-butane), a commodity that has become an important feedstock for the chemical industry (Vidra and Németh, 2018). The market for acetic acid is growing at ca. 5% per year and estimated to 16,155 metric tons by 2020. Over 65% of global production of pure acetic acid is obtained by chemical synthesis and not biologically. The chemical process via methanol carbonylation, ensures high starting acetic acid concentrations (35–45%), high yield (about 99% from methanol) and low production costs. While the main disadvantage of the biological production, is the cost to recover low concentrations of acetic acid (4–12%) from fermentation broths (Rogers et al., 2014; Murali et al., 2017). The acetic acid obtained by microbial oxidative conversion of ethanol-containing substrates, is world-wide referred to vinegar. Although in vinegar industry the bioconversion of ethanol in acetic acid is defined highly efficient (about

90–95% of the stoichiometric yield) (Jiménez-Hornero et al., 2009), many evidences underline the need of further optimization. Considering the applied aspects of the fermentation process, it is remarkable to emphasize that a main difference between vinegar production and most other fermented foods and beverages (e.g. sourdough for bread production, dairy products, sausages wine and beer) is the kind of microbial culture used.

In particular, to obtain vinegar, fermentations are developed by mixed microbial cultures, without using selected starter cultures (SSCs), at both small and large scale (Hidalgo et al., 2010; Gullo et al., 2014; Mas et al., 2014). Practically, heterogeneous AAB cultures are propagated by back-slopping procedure and reused to start up subsequent fermentation cycles. The selective pressure due to acetic acid, allows keeping relatively stable the AAB population. This procedure ensures low production costs, high performance and does not require specialized expertise to perform the fermentation. However, to minimize risks of fermentation breakdown and/or undesired metabolites, the introduction of SSCs is considered an appropriate technological tool for vinegar industry (Ndoye et al., 2006; Gullo and Giudici, 2008).

Regarding the design and application of SSCs for submerged fermentation, first Sokollek and Hammes (1997) proved the importance of specific media to reach high cell yields and to revitalize the culture after storing, preserving the viability of industrial cultures (Sokollek and Hammes, 1997). SSCc were also applied in static system characterized by a long fermentation time (acetic acid produced about 6% v/v). In this case a main characteristic is the attitude of the strain to persist along scaling up in not or less controlled processes (Giudici et al., 2009; Gullo et al., 2009). More recently 90 g/L of acetic acid were achieved by a SSC produced from *A. pasteurianus* UMCC 1754 in commercial red wine, whereas 60 g/L were produced using the same strain to ferment cooked grape must at 20% of sugars (Gullo et al., 2016). These studies confirmed the feasibility to manage vinegar fermentations by SSCs, as well as the versatility of AAB strains to adapt to different substrates in controlled fermentations.

In vinegar fermentation process, AAB are exposed to different chemical-physical stressors such as the initial ethanol amount, the increasing concentration of acetic acid and the heat generated during acetic acid production. These factors strongly affect cell growth and consequently the final acetic acid yield. Thanks to advances in the genetic engineering, different studies have been conducted to understand tolerance mechanisms and how to improve the resistance of AAB to the above mentioned parameters. These studies are mainly focused on acetic acid resistance, which is considered the main stressor under industrial conditions. This is due to the undissociated acetic acid that once penetrates the cell membrane, disintegrates membrane transport processes and causes an increase of acidity into the cell. Qi and co-workers (2013) obtained a high-acetic acid producing *A. pasteurianus* mutant (CICIM B7003-02) by UV mutagenesis under acidic stress that showed enhanced fermentation ability and higher tolerance to acetic acid compared to the wild type (Qi et al., 2014). Concerning the mechanisms involved in tolerance to acetic acid and temperature, a study highlighted the relevance of chaperons system. In particular, GroEL and GroES subsystem seems to be involved in those mechanisms. Indeed, an increase of both production and tolerance to acetic acid was highlighted in a mutant strain of *A. pasteurianus* that exhibits *rpoH*, a gene that regulates the expression of GroES GroEL system and other chaperons, overexpressed. Whereas a disruption of *rpoH* induces to a higher sensitivity to ethanol, acetic acid and temperatures compared to the wild-type (Okamoto-Kainuma Akiko et al., 2011).

**Table 1-2.** Consolidated and emerging applications of acetic acid bacteria treated in this study

Product	Phase of application/Industrial exploitation			Organism	References
	Developed process	Early applications	Research phase		
<b>Acetic acid</b>	Vinegars by no SSCs	Vinegars by SSCs	Improvement of tolerance mechanisms to physiological stressors; production of pure acetic acid for chemical field	<i>Acetobacter spp.</i> , <i>Gluconacetobacter spp.</i> , <i>Komagataeibacter spp.</i>	Sokollek and Hammes (1997), Rogers et al. (2006), Gullo et al. (2016), Qui et al. (2013), Matsutani et al. (2013)
<b>Gluconic acid</b>	Fermentative process	-	Genetic engineered strains to improve product yield; optimization of chemical-physical parameters to enhance the production	<i>G. oxydans</i>	Li et al. (2016) and Merfort et al. (2006)
<b>Dihydroxyacetone</b>	Fermentative process	-	Minimization of substrate/product inhibition using engineered <i>G. oxydans</i> strains; Research of low cost substrates	<i>G. oxydans</i>	Gätgens et al. (2007), Li et al. (2010) Lu et al (2012), and Moholkar (2018)
<b>2-keto-L-gulonic acid</b>	Two steps fermentation process	One step fermentation (microbial direct production)	Evaluation of genetic engineered strains; yield improvement  Investigations on target pathway to obtain a direct production	<i>G. oxydans</i>	Saito et al (1997) and Gao et al. (2014)
<b>Cellulose</b>	Static cultivation for food, pharmaceutical, cosmetic and engineering applications	Tissue repair (burns, ulcers), materials, non-caloric bulking agent	Optimization of culture systems and research of high yield strains  Research of low cost carbon sources	<i>Komagataeibacter spp.</i> , <i>Gluconacetobacter spp.</i>	Muongman et al. (2011), Gullo et al. (2017), Son et al. (2001), Thompson and Hamilton (2001) and Kuo et al. (2010)
<b>Fructans</b>	-	Non-alcoholic beverages as sweetener or dietary fibre	Selection of strains for biomedical and food applications	<i>Gluconobacter spp.</i> , <i>Neoasaia spp.</i> , <i>Kozakia spp.</i> , <i>Gluconacetobacter spp.</i>	Jacob et al. (2012b), Bello et al (2001), and Abdel-Fattah et al., 2012Abdel-Fattah et al. (2012)

<sup>a</sup>SSCs (selected starter cultures)



Matsutani and co-workers (2013), instead, improved the thermotolerance of the strain *A. pasteurianus* SKU1108 by repeated cultivation cycles under high-temperature conditions. The mutant strain (SKU1108-TH-3), produced 30 g/L of acetic acid at 37 °C and acquired the ability to ferment at a temperature of 3 °C higher than the wild-type strain (Matsutani et al., 2013).

Among mechanisms involved in the tolerance to acetic acid, also the systems to discharge the intracellular acetic acid play a key role. Proteomics studies on *A. aceti* confirmed that different proteins are induced by high acetic acid concentrations. The protein AatA, a putative ABC transporter, seems to have a relevant role in acetic acid tolerance. The disruption of this protein caused a reduction of acetic acid tolerance but not of lactic acid and propionic acid, suggesting that AatA protein functions as specific exporter of intracellular acetic acid (Méndez and Salas, 2001). The described alteration of acetic acid tolerance mechanisms can also affect the genome integrity, as demonstrated in *A. pasteurianus* (strain AC2005). In this strain it was proved that the activation of DNA repairs mechanism induced by acetic acid, protects the DNA and resolves genomic damages. The UvrA protein, a nucleotide repair excinuclease, was found to be upregulated in the presence of high acetic acid concentration, resulting in an improvement of acetic acid fermentation (Zheng et al., 2018).

Although the controversial issues in using engineered organisms, all these findings support the evidence that mechanisms of tolerance, discussed above, are key traits in AAB selection for the SSCs design.

## Gluconic acid

Gluconic acid and its salts are multifunctional bulks extensively used in industries. The global market of gluconic acid achieves USD 51.6 million in 2016, and is expected to reach USD 66.92 million by 2022 (QYResearch Reports 2017). Gluconic acid is used by pharmaceutical industry as chelating agent of divalent metals, in hygiene because of its sequestering action in alkaline media and in building industries to prevent color variations (Singh and Kumar, 2007; García-García et al., 2017). Beyond its use in pharmaceutic, gluconic acid is also exploited to improve the sensorial complexity of foods and in vinegar production, in which it contributes significantly to lower the pH (lower pKa than that acetic acid) (Giudici et al., 2016). Also, glucono-d-lactone is widely used in the food industry as a preservative for cured meat-based sausage (Cañete-Rodríguez et al., 2016). Gluconic acid derivatives, such as 2-keto-D-gluconic acid and 5-keto-L-gluconic acid are also valuable industrial compounds. 2-keto-D-gluconic acid is used as a building blocks in chemical synthesis of heterocycles compounds (Stottmeister et al., 2005). 5-keto-D-gluconic acid is used as an antioxidant in the food industry, a reducing agent in the textile industry and a chiral compound for chemical synthesis (Hermann et al., 2004).

Given its wide use in different industrial sectors, the enhancement of gluconic acid production aimed to maximize the yield, has been widely studied. There are two major aspects to consider in the gluconic acid production: the metabolism of the organism used and the chemical-physical parameters of the processes. Among AAB the most used strains for gluconic acid production belong to *G. oxydans* species. As mentioned above when *G. oxydans* grows on glucose, most of the glucose is oxidized in gluco- $\delta$ -lactone and, then into gluconic acid. Further oxidation of gluconic acid leads to the formation of ketogluconates such as 2-keto-D-gluconate and 5-keto-D-gluconate, which are undesirable products in the gluconic acid production process. The production

ratio of gluconic acid, 2-keto-D-gluconate and 5-keto-D-gluconate is strictly strain-dependent and linked to growth conditions that influence the activity of FAD-GADH and PQQ-GLDH enzymes (SHINAGAWA et al., 1983; Ano et al., 2011; Sainz et al., 2016b). In order to improve the yields of these compounds, different studies have been conducted by using genetic engineering approaches. The overexpression of the genes encoding for the membrane-bound enzymes such as the PQQ-GDH, FAD-GADH and PQQ-GLDH can direct the glucose oxidation pathways to one of above mentioned compounds (gluconic acid, 2-keto-D-gluconate and 5-keto-D-gluconate). Shi et al. (2014), for example, achieved an increase of two fold in the 2-keto-D-gluconate productivity by overexpressing the *ga2dh* gene, codifying for FAD-GADH (Shi et al., 2014a). Merfort et al. (2006), on the other hand, obtained an increase of both gluconic acid and 5-keto-D-gluconate by equipping the strain *G. oxydans* MF1 with a plasmid that allows the overexpression of both PQQ-GDH and PQQ-GLDH (Merfort et al., 2006). Some studies highlighted the role of some chemical-physical parameters, such as pH, glucose concentration, presence of calcium carbonate (CaCO<sub>3</sub>) and aeration rate, in the gluconic acid production. A high gluconic acid production was achieved keeping the pH below 3.5-4 in glucose media since ketogluconates formation is suppressed at low pH (Roehr et al., 2001). At pH higher than 5 the formation of ketoacids was favored. Another parameter in the gluconic acid and its ketoacids production is CaCO<sub>3</sub>. The presence of CaCO<sub>3</sub> in the culture medium considerably promotes the ketoacids production by shifting the chemical equilibrium towards the acids formation, due to the low solubility of ketogluconates calcium salts. The aeration rate also affects the production yield since O<sub>2</sub> is a substrate for different enzymes involved in gluconic acid pathways. A recent study showed that the O<sub>2</sub> concentration should be kept at a saturation level, included in a range of 20-30%, to achieve the highest gluconic acid production yield (García-García et al., 2017).

## Dihydroxyacetone

Dihydroxyacetone is a non-chiral compound used in the pharmaceutical industry as a cosmetic tanning agent and as an intermediate for the synthesis of various organic chemicals and surfactants. The global market of dihydroxyacetone is estimated in 2000 tons per year (Pagliaro et al., 2007)(Lux and Siebenhofer, 2013). Chemical synthesis of dihydroxyacetone through catalytic reaction of formaldehyde has low selectivity, thus industrial production is mainly operated by oxidation of glycerol via PQQ-GLDH, using *G. oxydans* strains (Hekmat et al., 2003; Chozhavendhan et al., 2018). Despite of many efforts in improvement of strains, it has been reported that, the microbial process of dihydroxyacetone by *G. oxydans* requires further optimization to maximize the yield and then the economic convenience. Main drawbacks in the microbial process are substrate (glycerol) and product (dihydroxyacetone) inhibition on bacterial growth (Macauley et al., 2001). Enhanced yield of microbial dihydroxyacetone production was obtained by immobilizing *G. oxydans* cells to a polyvinyl alcohol support. However, a dramatic reduction of the activity of immobilized cells, due to the loss of the electron transfer ability of the organism, was observed after only five operation batches (Wei et al., 2007). Gätgens et al. (2007) obtained an increased dihydroxyacetone production by overexpressing sldAB protein, coding for PQQ-GLDH in *G. oxydans* MF1 (Gätgens et al., 2007). In a study aimed to reduce product inhibition and simultaneously increase dihydroxyacetone production, the overexpression of GLDH and the interruption of *adhA* gene in *G. oxydans* allowed to obtain 134 g/L of dihydroxyacetone from 140 g/L of glycerol (Li et al., 2010). Moreover, mutants from *G. oxydans*

with significant increased production of dihydroxyacetone, during a selection time of 25-50 transfers, have been obtained by adaptive laboratory evolution experiments using glucose as the sole carbon source (Lu et al., 2012).

Recently, dihydroxyacetone was produced from crude glycerol, a by-product of biodiesel industry. By repeated-batch experiments with four times crude glycerol feeding (10 g/L each time), a dihydroxyacetone concentration of 36 g/L (89.88% conversion rate within 96 h of fermentation) was obtained. The conversion of crude glycerol into value-added chemicals such as dihydroxyacetone, could contribute to a more economic feasible biodiesel production (Dikshit and Moholkar, 2019).

## 2-Keto-gulonic acid as intermediate of vitamin C synthesis

Vitamin C is used in a wide range of industrial fields, such as pharmaceutical, food and beverage and cosmetic. The global revenue is expected to reach USD 1083.8 million by 2021 (QYResearch Reports 2017). Until 1990s, vitamin C was produced by Reichstein process, a combined chemical and microbial method involving five chemical steps and one microbial fermentation by which D-sorbitol is converted in L-sorbose. More recently, different processes have been studied in order to offer eco-friendly fermentations as an alternative to the chemical synthesis. These alternative processes enhanced the role of AAB as biocatalysts for the production of vitamin C, because of their ability to synthesize 2-keto-gulonic acid by different pathways, as full described by Shinjoh and Toyama (2016) (Shinjoh and Toyama, 2016). Actually, the most used species in Vitamin C production is *G. oxydans* (Pappenberger and Hohmann, 2014). Saito and co-workers (1997) obtained 2-keto-gulonic acid from D-sorbitol at high yield (200 g per L of D-sorbitol converted to 200 g per L of L-sorbose) by a recombinant *G. oxydans* strain (T-100) (Saito et al., 1997). Both the strains and enzymes were protected by a patent of Fujisawa Pharmaceutical Co., Ltd. The strain *G. oxydans* WSH-003 was proved to be efficient in the production of high amount of L-sorbose and it is industrially exploited to produce vitamin C via two-step fermentation process.

Enhanced production of L-sorbose (+25% respect to the wild strain) was obtained by engineering WSH-003 on which artificial poly (A/T) tails were added to the gene that encodes for PQQ-GLDH (Xu et al., 2014). Another study on WSH-003 showed the possibility to produce 2-keto-gulonic acid at high yield (40 g/L) via one step fermentation (direct conversion of D-sorbitol to 2-keto-gulonic acid) by heterologous recombination of FAD-SDH and PQQ-GLDH genes derived from *Ketogulonicigenium vulgare*. In this study, the 2-keto-gulonic acid production yield was eight fold higher than that obtained using independent expression of the FAD-SDH and PQQ-GLDH dehydrogenases (Gao et al., 2014).

## Bacterial cellulose

BC is a versatile biopolymer that can be used in a large variety of applications, including food (e.g. non-caloric bulker), pharmaceutical and biomedical products (e.g. cosmetics, skin substitute for burn wounds) and engineering (e.g. diaphragms for electro-acoustic transducers, paint additives, coatings and as reinforcement material) (Jonas and Farah, 1998; Ku et al., 2011; Gullo et al., 2018). The global BC market is estimated at 207.36 million USD in 2016 and is expected to reach 497.76 million USD by the end of 2022 (QYResearch Reports 2017). By the way, BC production at industrial scale is limited by the low yield and high production cost. The availability of suitable

AAB strains and the optimization of both culture media and the production process seem to be key elements to overcome these limitations (Ruka et al., 2012; Kuo et al., 2015; Gullo et al., 2017). BC synthesis is highly variable within AAB, for example among *K. xylinus* strains isolated from Kombucha tea, the yield ranged from 0 to 12 g/L for the majority of strains. One strain (UMCC 2756) achieved a BC yield of over 23 g/L on a glucose-based medium (50 g/L) in 10 days of static cultivation (Gullo et al., 2017). On the other hand, Son and co-workers (2001) isolated a high BC-producing strain from apples (*Acetobacter* sp. A9), which achieved a BC yield of 15, 2 g/L using a medium at 40 g/L of glucose in agitated system (Son et al., 2001).

Although the influence of carbon sources on BC production has been largely investigated, results seem discordant. Some authors reported the highest BC yield in glucose-only medium, whereas other obtained best results in media containing either mannitol or arabitol (Oikawa et al., 1995c, 1995a; Son et al., 2001). Moreover, the addition of a small amount of ethanol to a glucose medium seems to stimulate BC production. This occurs since ethanol acts as an additional energy source, allowing the cells to use glucose mainly for BC synthesis (Krystynowicz et al., 2002; Gullo et al., 2017).

As described previously, AAB can use glucose to produce different compounds, such as gluconates and BC or to produce energy via glycolysis. To improve glucose utilization efficiency for BC production, Kuo et al. (2016), generated the mutant strain *K. xylinus* GDH-KO in which the gene encoding for PQQ-GDH was knocked out through homologous recombination of a defective *gdh* gene (Kuo et al., 2016). The mutant strain showed an increase in the BC production of about 40 and 230% compared to the wild-type strain in static and shaken culture, respectively. Furthermore, the gluconic acid formation in the mutant strain was negligible.

In order to reduce the costs of feedstock while contributing to environmental impact reduction, various low-cost alternative carbon sources have been evaluated. In particular, researches focused on relatively cheap agricultural products or waste containing glucose (Thompson and Hamilton, 2001; Kuo et al., 2010). Although results are encouraging, many issues related to the yield and quality of the BC produced from these sources are still to be solved.

## Fructans

The interest for fructans produced by bacteria arises from general properties of these compounds, like bio-compatibility, bio-degradability and biomedical properties such as antioxidant and anti-inflammatory. Fructans can be also used in cosmetic industry in the skin cream preparation and moisturizers. In the last years different studies focused fructans production by AAB, especially for food industry applications. The relevance of microbial fructans rather than plants fructans is due to their chemical-physical properties; in particular, the degree of polymerization is higher for microbial fructans compared to plant fructans (Srikanth et al., 2015).

Among fructans produced by AAB, LT-EPS are linear polymers that are useful in different fields. Molecular size of LT-EPS is the most relevant property that influences their functional characteristics such as rheological, technological and health properties (Esawy et al., 2011; Benigar et al., 2014). In food industries, LT-EPS have great potential as stabilizer, emulsifier, eco-friendly adhesive and bio-thickener, as well as anti-tumor and cholesterol-lowering agents (De Vuyst et al., 1998; Yoo et al., 2004). Moreover, they are considered prebiotic since their hydrolysis products, which are short-chain fructooligosaccharides (FOS), show the ability to preferentially stimulate the growth of intestinal bifidobacteria (Roberfroid et al., 1998).

So far, LT-EPS are seldom applied in the food industry due to the lack of commercially available preparations with defined structure. However, they are used in some commercial non-alcoholic beverages (e.g. in some ultra-high-fructose syrups) as sweetener or dietary fiber (Dal Bello et al., 2001). Moreover, a promising application seems to be the use of LT-EPS to improve the dough rheology and taste of gluten-free (Jakob et al., 2012b; Ua-Arak et al., 2017). In particular, an increase of loaf volume and a reduction of bread staling rate were observed after the addition of LT-EPS produced by different AAB (Jakob et al., 2013). Comparative studies demonstrated that LT-EPS with higher molecular weight and branching at position 3 of the glucose monomer have a superior water-binding capacity and thus, affect more positively the bread characteristics (Rühmkorf et al., 2012; Ua-Arak et al., 2016).

Concerning nutritional and health-promoting aspects, it has been demonstrated, by *in vivo* studies that, LT-EPS exhibit antitumor even antiviral activities and anti-inflammatory properties by stimulating interferon response (Yoo et al., 2004; Rairakhwada et al., 2007; Esawy et al., 2011). Last advance in the field of drug delivery systems is the development of polysaccharide-based nanometric carriers. LT-EPS are particularly suitable for this application since they have large number of reactive hydroxyl groups, high biocompatibility and self-degrading ability in human system (Srikanth et al., 2015). At this regard, thin-nanostructured films of pure and oxidized LT-EPS by matrix-assisted pulsed laser evaporation were developed. *In vitro* tests revealed high potential for cell proliferation especially for oxidized LT-EPS (Sima et al., 2011).

## Conclusions and future directions

The use of AAB in bioprocesses spans from consolidated applications mainly linked to the oxidative fermentation pathways (acetic acid in vinegar production, gluconic acid, 2-keto-gulonic acid and dihydroxyacetone) to biopolymer production, such as BC and fructans, that although well studied at academic level, are still largely unexploited (Table 1-2).

The industry demand of cost-effective bio-based productions that comprises first high yield, no by-products formation and stability of strain performance during time in industrial conditions, are recognized as main factors limiting AAB exploitation. To fulfill the industry demand also established bioprocesses in which AAB are common applied, require further optimization, as in the case of acetic acid for vinegar production. Although there are many studies on strains improvement and processes optimization, the modern vinegar production is conducted via mixed AAB cultures. This system, on the one hand, allows to perform processes with low technological requirements and investments, on the other hand, it limits the full exploitation of the metabolic potential of selected strains. Considering both the requirements of the fermentation processes and the technological traits of selected strains, further growth of production yield is achievable by adopting rational strain selection approaches. Moreover, selection of strains could allow to differentiate marketable products, enhancing the portfolio of vinegars and related fermented beverages. Gluconic acid and derivatives, 2-keto-L-gulonic acid and dihydroxyacetone are industrially obtained by microbial fermentation using AAB, but obtaining higher production yield is still an open issue. Combining the use of selected wild and engineered strains with optimal process parameters is pivotal to overcome current limits.

Among emerging products from AAB, bacterial cellulose and fructans have received increasing attention because of their high potential in a wide array of applications, but actually the low production yield and high cost, limit the development of large-scale processes. However, the wide

applied research in this area is providing the basic platform for optimization of industrial biopolymers processes using AAB.

The improvements of the use of AAB can be achieved by advance in molecular biology and genetic engineering researches that, at this time, provide the best approach in order to optimize and improve the production process and yield of the different bioproducts. Finally, since sustainability is a main industry issue, the optimization of processes from waste and low cost raw materials could further positively affect the industrial application of AAB.

# Chapter 2

## Biotechnological production of cellulose by acetic acid bacteria: current state and perspectives

Maria Gullo<sup>1</sup>, Salvatore La China<sup>1</sup>, Pasquale Massimiliano Falcone<sup>2</sup>, Paolo Giudici<sup>1</sup>

<sup>1</sup>Department of Life Sciences, University of Modena and Reggio Emilia, Via G. Amendola, 2, Pad. Besta, 42122, Reggio Emilia, Italy

<sup>2</sup>Department of Agricultural, Food and Environmental Sciences, University Polytechnical of Marche, Breccie Bianche 2, Ancona, Italy  
Department of Life Sciences, University of Modena and Reggio Emilia, Via G. Amendola, 2, Pad. Besta, 42122, Reggio Emilia, Italy

**This chapter is published as:**

Gullo M, **La China S**, Falcone PM, Giudici P. Biotechnological production of cellulose by acetic acid bacteria: current state and perspectives. *Appl Microbiol Biotechnol* (2018) 102, 6885–6898. <https://doi.org/10.1007/s00253-018-9164-5>

## Abstract

Bacterial cellulose is an attractive biopolymer for a number of applications including food, biomedical, cosmetics, and engineering fields. In addition to renewability and biodegradability, its unique structure and properties such as chemical purity, nanoscale fibrous 3D network, high water-holding capacity, high degree of polymerization, high crystallinity index, light transparency, biocompatibility, and mechanical features offer several advantages when it is used as native polymer or in composite materials. Structure and properties play a functional role in both the biofilm life cycle and biotechnological applications. Among all the cellulose-producing bacteria, acetic acid bacteria of the *Komagataeibacter xylinus* species play the most important role because they are considered the highest producers. Bacterial cellulose from acetic acid bacteria is widely investigated as native and modified biopolymer in functionalized materials, as well as in terms of differences arising from the static or submerged production system. In this paper, the huge amount of knowledge on basic and applied aspects of bacterial cellulose is reviewed to the aim to provide a comprehensive viewpoint on the intriguing interplay between the biological machinery of synthesis, the native structure, and the factors determining its nanostructure and applications. Since in acetic acid bacteria biofilm and cellulose production are two main phenotypes with industrial impact, new insights into biofilm production are provided.

## Introduction

Bacterial cellulose (BC) production has been reported for a variety of bacteria species, including *Rhizobium leguminosarum*, *Burkholderia* spp., *Pseudomonas putida*, *Dickeya dadantii*, *Erwinia chrysanthemi*, *Agrobacterium tumefaciens*, *Escherichia coli*, and *Salmonella enterica* species (Chawla et al., 2009; Jahn et al., 2011). Within acetic acid bacteria (AAB), different genera have been reported to be cellulose producers, such as *Gluconacetobacter*, *Acetobacter*, and *Komagataeibacter* (Gullo et al., 2012; Valera et al., 2014). *Komagataeibacter xylinus* is considered a microbial model in BC production due to its ability to utilize a variety of sugars and the large amount of BC produced in liquid cultures (Table 2-1). The structure of BC produced by living cells is intimately linked to its synthesis, and the organization and arrangement of cellulose-synthesizing sites on the cell membrane are crucial for the parallel assembly of glucan chains (Brown, 1996).

BC is the main active component of the biofilm produced by AAB, which are well known as biofilm producer organisms (Gullo and Giudici, 2008). Biofilm production is linked to signaling molecules that control also the synthesis of BC and its detachment in response to environmental factors (Davies et al., 1998). In AAB, biofilm phenotype was first investigated by Louis Pasteur who conducted a systematic study on the “mother of vinegar” showing that it was a mass of living microorganisms causing acetic acid fermentation (Pasteur, 1864); the organism was described as *Mycoderma aceti* and biofilm formation was recognized as synonymous of acetic acid fermentation in wine.

In the era in which the nanomaterial research evolves rapidly, complex structural features, biocompatibility, mechanical, and physicochemical properties of BC are considered of main interest.



**Table 2-1.** Bacterial cellulose productivity (g/L/days) by AAB in different conditions

Present name <sup>a</sup>	Carbon source/feedstock		System	Time (days)	Productivity (g/L/days)	Reference
	Type	Amount (g/L)				
<i>K. xylinus</i> AX2-16	Glucose	25	Static	8	1.47	Zhong et al., 2013
<i>K. hansenii</i> PJK=KCTC10505BP	Glucose	10	Submerged	2	0.86	Jung et al., 2005
	Acetic acid	1.5 mL				
	Succinate	2				
	Ethanol	10				
<i>K. xylinus</i> BRC5=KCCM 10100	CSL:	80	Submerged	2	7.65	Hwang et al., 1999
	Glucose	20				
	Citric acid	1.15				
<i>K. rhaeticus</i> P1463	Apple juice		Static	14	0.68	Semjonovs et al., 2017
	Glucose	3				
	Fructose	12.4				
	Sucrose	4.6				
<i>K. hansenii</i> B22	Apple juice:		Static	14	0.50	Semjonovs et al., 2017
	Glucose	3				
	Fructose	12.4				
	Sucrose	4.6				
<i>K. xylinus</i> K2G30=UMCC 2756	Glucose	50	Static	15	1.31	Gullo et al., 2017
	Ethanol	14				
<i>K. xylinus</i> ATCC 23767 <sup>T</sup>	CSL:		Static	7	0.41	Cheng et al., 2017
	Glucose	3.87				
	Xylose	29.61				
	Mannose	1.84				
	Acetic acid	18.73				
<i>K. xylinus</i> BCRC 12334	Glucose	60	Static	14	0.52	Kuo et al., 2015
<i>K. xylinus</i> ATCC 23770	HFS:		Static	7	1.57	Cavka et al., 2013
	Glucose	14.1				
<i>K. hansenii</i> M2010332	Glucose	55	Static	7	2.33	Li et al., 2012
	Citric acid	1				
	Ethanol	20				
<i>Gluconacetobacter</i> sp. st- 60-12 and <i>Lactobacillus</i> sp. st-20	CSL:	40	Submerged	3	1.4	Seto et al., 2006
	Sucrose	40				
<i>K. xylinus</i> BPR2001	CSL:		Submerged	2.5	3.2	Noro et al., 2004
	Fructose	40				
	Inositol	0.002				
<i>K. xylinus</i> BPR2001	CSL:		Static	3	1.8	Bae and Shoda, 2005
	Sucrose	37				

CSL corn steep liquor, HFS hydrolysate fiber sludges

<sup>a</sup>The present names of AAB species are reported, according to LPSN [bacterio.net](http://bacterio.net) (Euzéby, 1997).

Moreover, new biotechnological studies highlight differences in terms of cellulose synthase (CS) complex structural organization, operons, and gene content among BC producers. For instance, these differences can lead to the formation of natural chemical modified cellulose, such as phosphoethanolamine cellulose, as recently discovered (Thongsomboon et al., 2018). These evidences can bring new opportunities to obtain modified cellulosic materials suitable for conventional and innovative applications.

A number of authoritative papers, covering characteristics and potential applications of both native and functionalized BC, have been published. However, as known, researches on the technological transfer are underestimated, in particular, those concerning the biological machinery of the CS complex, the efficient production of BC, and the tailored functionalities for the intended use.

In this mini-review, the BC produced by AAB is evaluated considering the structure, the molecular components of CS, and the biofilm formation. This study contributes to a more efficient exploitation of the state of the art, linking the scientific knowledge to the production of BC for specific biotechnological uses.

## **Interplay between native structure of bacterial cellulose and properties**

Irrespective of the natural source, the common primary structure of the BC consists of long-chain (1-4)-linked  $\beta$ -D-glucan chains developing from nano to macroscopic scale in a 3D network, reaching a degree of polymerization up to 20,000 (Habibi et al., 2010). Such linkages give an extended secondary structure with a specific ribbon-like conformation. The tertiary structure is the result of intermolecular hydrogen bonds and van der Waals forces: all  $\beta$ -1,4-D-glucan chains rings adopt a  ${}^4C_1$  chair conformation, stabilizing the entire structure through an intramolecular hydrogen bond network by hydroxyls and ring oxygen among glucose residues. Each repeating unit has a directional chemical asymmetry with respect to its molecular axis (a hemiacetal unit and hydroxyl group). The molecular directionality underpins the parallel-up structure of native BC (Koyama et al., 1997).

All BC properties strictly depend on the specific characteristics of the architecture from nano- to macro-scale, which is linked to both intracellular biosynthesis and extracellular self-assembling mechanisms. It is widely accepted that BC is synthesized within the bacterial cell as individual molecules, which undergo spinning in a hierarchical order at the bacterial sites of biosynthesis. BC molecules are aligned on the side of the cell surface before bunching together to form ultra-fine bundles embedding crystalline cellulose, having only a limited number of defects or amorphous domains (Brown, 1996, 2004).

According to Brown 1996, each microfibril is extruded in a specific region of the outer membrane, called terminal complex (TC), that consists of three subunits (BC-synthesizing sites) and each subunit contains at least 16 CS catalytic sub-units. Each catalytic subunit produces a single  $\beta$ -1,4-glucan chain; 16 glucan chains from a single BC-synthesizing site assemble to form a protofibril of about 2-20 nm in diameter. The protofibrils combine spontaneously to form ribbon-shaped microfibrils of approx. 80.4 nm in diameter and finally a 3D hierarchical network of bundles. All the BC chains in one microfibril can be elongated virtually limitless by the CS complex, while hierarchical ordering follows very closely polymerization and spinning kinetics of the glucan chains.

Studies focused on BC behavior under diluted hydrolyzing conditions evidenced that the nanopolymers are able to nucleate as spherical or spindle-shaped microdomains, leading the liquid medium into a transition state (tactoid) between isotropic and macroscopic liquid crystalline phases showing chiral-nematic ordering (Habibi et al., 2010). Native BC from AAB has been

shown to have fibers alternating needle-shaped microdomains with one dominant crystal structure, i.e., cellulose I sub-allomorph I $\alpha$  arranged in parallel configurations (Iguchi et al., 2000).

Very appealing properties of native BC from AAB origin from the polyol nature, the chemical directionality, the crystallinity degree, and the very fine ultrastructure. Moreover, such unique structure lends to a plethora of chemical and physical transformations modulating the hydrophilic/lipophilic balance, the aggregation's change, and the hierarchical organization. From these events, a rich suite of new materials or platforms for further transformations in which BC is treated as a host of non-native chemical functionalities can be developed. Furthermore, different types of artificially encased nanoparticles, including metals, are highly important in order to design AAB cellulose derivatives with tailored nanostructure and functional properties.

Among the most investigated properties of BC from AAB, there are high water-holding capacity (more than 90%), insolubility in most of the solvents, high polymerization degree (4000–20,000 expressed as hydroglucose units) (Gullo et al., 2017), and high crystallinity degree (80–90%).

Both AAB biofilms and BC derivatives have been investigated for their rheological properties such as the Young's modulus and yield strength measured in compressive or tensile conditions, as well as storage and loss moduli measured into the time and frequency domains. Such properties mainly depend on the microfibril geometry at nanometric scale and on the degree of crystallinity of BC. Iguchi et al. found that AAB biofilm behaves quite differently from pure hydrogels. The complex of the intra- and intermolecular hydrogen bonds of BC determines the relatively high elastic properties of the biofilm, while its viscous properties are determined by the interstitial voids and channels separating the microcolonies, which contain the liquid phase, mainly constituted by water that acts as structure plasticizer (Iguchi et al., 2000). The authors observed that under tensile stress, AAB biofilm shows "elastic" (instantaneously reversible) behavior only under very small deformations and time domain followed by a "viscoelastic" (time-dependent reversible) and "plastic" (stress-dependent irreversible) behavior. Such complex behavior was attributed to the fact that fibrils reorient their chiral ordering along tensile loading direction reorganizing their position, while fiber-on-fiber frictional slippage could lead to an irreversible process of energy loss. When compressed, the AAB hydrogel releases its water content deforming with high stiffness but without crack formation and propagation; the release of water is the main event causing plastic deformation (Frensemeier et al., 2010). The rheological behavior of BC hydrogel produced by a *K. xylinus* strain was investigated under in-water uniaxial cycling conditions by Gao et al. They postulated that the formation of entanglements and rearrangements of BC fibers fragments are the main factors causing irreversible deformation under loading, unloading, and reloading regimes (Gao et al., 2015).

Iguchi et al. (2000) investigated BC sheets derived from AAB biofilms after heating-pressure treatment. They recorded very high tensile Young's modulus of about 16–18 GPa: authors observed that microfibrils become tightly bound by inter-fibrillar hydrogen bonds and align in pile of thin layers with very high density. Both tensile strength and elongation decreased with the pressure applied during film preparation; the formation of microcracks was postulated the most probable cause of the decrease of mechanical toughness of the BC films. Through purification steps, the same authors improved the mechanical toughness of BC sheets reaching 30 GPa for the Young's modulus and superb acoustic characteristics; they suggested to use them in the manufacture of high-performance acoustic diaphragms. BC films have been also investigated for their fundamental rheological properties under dynamic oscillatory experiments as a function of

temperature or relative humidity. The dynamic modulus decreased from 15 to 9 GPa with the increase of temperature, while  $\tan\delta$ , i.e., the ratio between loss and storage moduli, showed two maxima at around 50 and 230 °C that were attributed to desorption of water and BC degradation, respectively (Iguchi et al., 2000). Thermomechanical behavior of BC films produced from *K. xylinus* (UMCC2756) strain has been investigated by Gullo et al. (2017)(Gullo et al., 2017). Authors found that this strain is able to produce a unique biofilm containing the allomorph I $\alpha$  as the only crystal form of cellulose and a large amount of freezable water (about 12.9% in weight). The plasticizing effect of the absorbed water resulted in a crossover of the storage modulus across the 0 °C.

Shaw et al. (2004) attempted to provide a rheological standpoint supporting the BC environmental functionality and its ability to maintain the bacterial biofilm in a stable homeostatic growth regime. All bacterial biofilms behave as elastic/viscoelastic/plastic polymeric material, i.e., they show elastic solid-like response to short time scale mechanical stimuli (stress or deformation), structure recovery ability under intermediate time scale stimuli conditions, as well as plastic response under long time scale stimuli. This complex structural behavior might provide a significant clue towards explaining biofilm robustness against different environmental mechanical stresses. The elastic structural elements absorb stress energy through rapid mechanical stimuli. The viscoelastic structural elements absorb stress energy through time-dependent and reversible deformation. Plastic properties relax the structural internal stress through nonreversible steady-state deformation rate requiring very long time to reach the new structural equilibrium. The relaxation time of a bacterial biofilm, i.e., the time taken for deformation to entirely account for initial reversible deformation, was approximately estimated about 18 min for a number of bacteria. A possible survival significance of this characteristic time scale is that it is the shortest period over which a bacterial biofilm can mount a phenotypic response to environmental transient mechanical stimuli (Shaw et al., 2004).

## **Tuning of biotechnological factors for different biofilm morphologies and cellulose nanostructures**

Temperature, hydrodynamic conditions, culture medium composition, and surface structure of the material used for BC deposition can be selectively modulated to produce different biofilm morphologies and a plethora of nanostructures. Under static growth regime, for example, pellicles of several centimeters height are usually produced (Figure 2-2a), while spheres could be produced under agitated growth conditions (Figure 2-2b). Continuous supply of air and suitable carbon sources is primarily required, but elevated temperatures and extremely low ionic concentrations favor the amorphous formation of BC with respect to the crystalline one.

The use of additives into the growth medium, including carbohydrates, proteins, and isoenzymes, may be considered effective for the construction of a functional fiber-network structure. The role of additives in the culture medium could be linked to their ability to compete for hydrogen bonds with the  $\beta$ -1-4 glucan chains, affecting the self-assembling process of formation of both the secondary and tertiary structure of BC network; for example, high molecular weight polysaccharides and cation starches may be used to produce cellulosic composites (Iwata et al., 1998).

Another way to control the BC structure from nano- to macro-scale is linked to the possibility to finely tune both the viscosity and shear rate of the liquid medium in which AAB grow. The morphology of the biofilm growing in submerged conditions is markedly different, as a function of the flow regime, i.e., laminar or turbulent (Stoodley et al., 1998). Furthermore, biofilms produced at high shear rates tend to be more isotropic with adhering properties: shear rates apply into the laminar flow in which BC bundles align along with a field of tangential and parallel forces, leading both bulk and surface ordering. Drag forces act opposite to the relative motion of BC bundles with respect to the surrounding fluid, being proportional to the speed for a laminar flow and the squared speed for a turbulent flow. Even though the ultimate cause of a drag is viscous friction, the turbulent drag is independent from fluid viscosity. Therefore, at relatively high shear rates, as cells divide, the drag forces tend to push daughter cells in the downstream direction, allowing cell to grow larger, many of them merging to form a biofilm with porous structure. The bacterial growth can affect the flow regime by switching from “isolated roughness” or “wake interaction flow” to “skimming flow” with the formation of a plethora of microenvironments inside the biofilm experiencing different flow regimes (Nowell and Church, 1979). The opportunity to choose the characteristics of surface at the region of BC deposition opens up a new window to control the cellulose nanostructure formation. In this regard, the use of nematically ordered liquid crystalline BC has been used as molecular-imprinting templates allowing the newly synthesized BC to deposit along precise nanotracks (Kondo, 2007).

## Cellulose synthase machinery

The BC bioassembly is a very complex and well-structured machinery, reflecting the series of events that led to its synthesis. In Figure 2-1, the CS complex, as described in *Komagataeibacter* members, is depicted. It includes a series of subunits working in a concerted way that synthesize and export the  $\beta$ -glucan chains in the extracellular space. CS uses activated glucose monomers by uridine-diphosphate (UDP-glucose) as precursor and is regulated by bis-(3',5')-cyclic-dimeric-guanosine monophosphate (c-di-GMP), a key mediator of the biofilm regulation cycle (Ross et al., 1987). The catalytic subunit of CS is a  $\beta$ -galactosyltransferase named BC synthase A (BcsA) and belongs to the glycosyltransferase family 2 (GT-2) (Saxena and Brown, 1995). It is a membrane integrated protein of eight  $\alpha$ -helix transmembranes (TM 1–8). The BcsA C-terminal contains a cytosolic domain

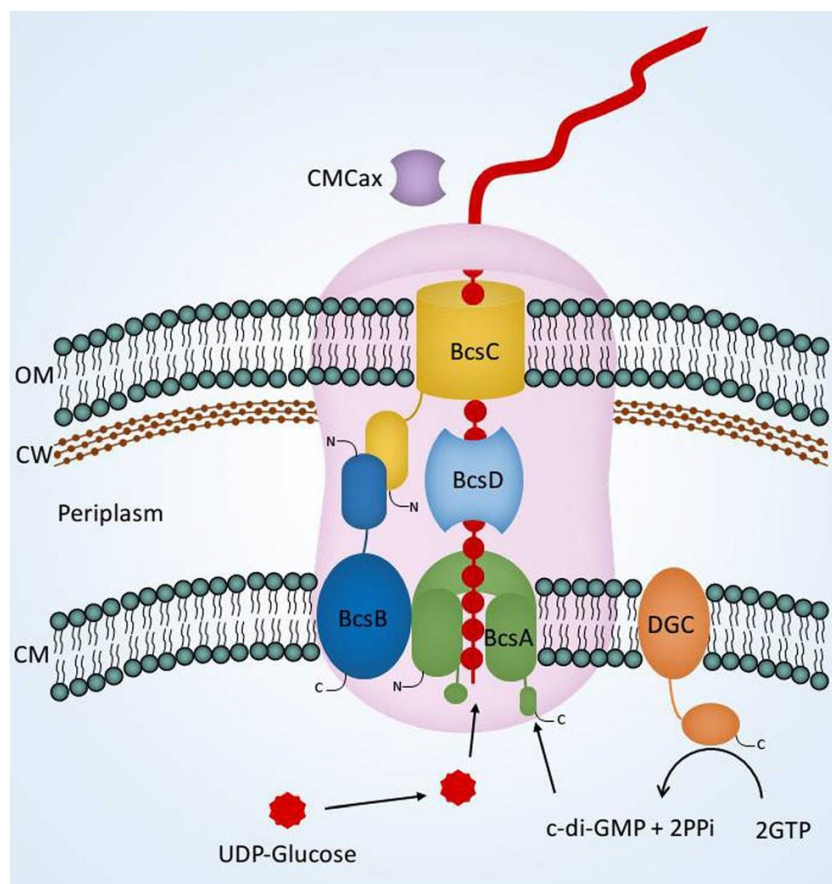


**Figure 2-1.** Cellulose synthase complex in *Komagataeibacter*. From outside: OM, outer membrane; CW, cell wall; CM, cytoplasmic membrane.

named PilZ, responsible for c-di-GMP binding (Ross et al., 1987). The TM 3-8 helices form a membrane channel across the cytoplasmic membrane, which is utilized for glucan chain translocation in the periplasm during elongation (Morgan et al., 2013). The catalytic subunit is a GT-A domain inserted between the TM-4 and the TM-5 (Lairson et al., 2008). The mechanism of reaction proposed for the addition of monomer of UDP-glucose is a classical SN<sub>2</sub>-like substitution reaction, in which the C-4 hydroxyl group of the rising glucan chain (acceptor) binds the anomeric C-1 carbon of UDP-glucose (donor). This reaction is facilitated by bivalent metal ions (Mn<sup>2+</sup> and Mg<sup>2+</sup>) (Brown et al., 2012).

BcsA is associated to another subunit of CS complex, called BcsB. BcsB is a periplasmic protein anchored to the cytoplasmic membrane by a C-terminal  $\alpha$ -helix, together with a preceding periplasmic helix, tightly interacting with the catalytic BcsA subunit. The dome-shaped protein forms two copies of a repeating unit of a carbohydrate-binding domain (CBD) that is C-terminally fused to an  $\alpha/\beta$  domain resembling a flavodoxin-like domain (Morgan et al., 2013). The CBD is structurally related to carbohydrate-binding modules (Christiansen et al., 2009), which form classical  $\beta$ -strand-rich jelly roll motifs interacting with carbohydrates either via the  $\beta$ -sheet surface or with the edges of the jelly roll (Shoseyov et al., 2006). Based on this architecture of the sub-complex BcsA-BcsB, the role of BcsB seems related only to the translocation of rising glucan chain formed by BcsA (Omadjela et al., 2013). This sub-complex is characterized by similarities

in terms of structure and functional mechanisms among BC producing bacteria. In AAB, CS complex includes other two Bcs proteins (BcsC and BcsD). BcsC is a large protein having a C-terminal anchored in the outer membrane and a large N-terminal in the periplasmic region. The C-terminal region, about 300 residues, forms an 18-stranded  $\beta$ -barrel in the outer membrane that allows the exportation of the glucan chain in the extracellular space. The periplasmic region (N-terminal) includes tetra-tricopeptide-like repeats, consisting of 34-residue tandem repeats that adapt helix-turn-helix tertiary structures and are frequently involved in mediating protein-protein interactions (Keiski et al., 2010). The N-terminal region could interact with BcsB protein, guiding the glucan chain exportation via the C-terminal  $\beta$ -barrel (Du et al., 2016). The structure and arrangement of the BcsD protein itself indicate a cylinder with the presence of a functional complex unit in the form of an octamer (Hu et al., 2010). The octamer is localized in the periplasm with an orientation parallel to the long axis of the cell. BcsD seems to play an integral role helping the alignment of the linear TCs along the longitudinal axis of the cell (Mehta et al., 2015).

CS complex of AAB contains other accessories proteins named CcpAx, CMCax, and BglAx that are codified by the same operon of Bcs proteins. These proteins are not fundamental for the BC biosynthesis itself, but they are involved in the correct glucan chains formation. CcpAx is codified only by *Komagataeibacter* members and is required for the BC synthesis in vivo. The function of CcpAx is unclear: it has been hypothesized that it can be involved in the structural organization of the TC, cooperating with BcsD. In vitro studies showed the interactions between CcpAx and BcsD proteins, demonstrating their possible cooperation (Sunagawa et al., 2013). From these studies, it can be deduced that CcpAx plays a key role in the maintenance of native structure of BC. CMCax is an endo- $\beta$ -1,4-glucanase identified for the first time in *K. xylinus* (Standal et al., 1994). It is a single domain protein of the glycosylhydrolase family, containing a signal sequence in the N-terminal region for its secretion in the periplasmic space (Römling, 2002). CMCax is formed by 11  $\alpha$ -helixes and seven  $\beta$ -strands organized in a six-barrel motif (Yasutake et al., 2006). The localization of this protein is not well identified but it was supposed to be in the neighborhood of extrusion pore of CS. Recent in vitro BC biosynthesis studies revealed that CMCax is able to degrade single glucan chains but not the crystalline polymer (Nakai et al., 2013), suggesting that it may reduce the twisting of microfibrils. BglAx is a  $\beta$ -glucosidase that seems to have also the glucosyltransferase activity (Tajima et al., 2001). Studies on *K. hansenii* ATCC 23769 highlight that BglAx is not necessary for BC synthesis but the interruption of its gene causes a yield reduction. It was proposed that the concerted action of CMCax and BglAx is necessary for maintaining the structural characteristics of cellulose Ia (Deng et al., 2013).

Many differences occur in BC-producing bacteria in terms of proteins content and complex organization. Recently, it was demonstrated that *E. coli* and *S. enterica* are able to produce naturally modified cellulose (phosphoethanolamine cellulose), which contributes to the extracellular matrix assembly and to biofilm structure (Thongsomboon et al., 2018). In these bacteria, BcsE, BcsF, and BcsG proteins were found. BcsG is an integrated membrane protein that interacts with periplasmic portion of BcsF protein and seems to be necessary for BC modification. BcsF protein represents the link between BcsG and BcsE, a soluble protein able to bind c-di-GMP, providing a regulation mechanism for BcsG activity (Thongsomboon et al., 2018).

## Genetic structure of cellulose synthase

Because of differences in gene order and gene content among BC-producing bacteria, the *bcs* operons were classified into three major types (Römling and Galperin, 2015). The first type of operon is peculiar of *K. xylinus* and the presence of *bcsD* gene is the distinguishing feature to classify this operon in subtypes (referred to *bcsI*, *bcsII*, and *bcsIII*). The second type (*E. coli*-like type) includes two additional genes, *bcsZ* and *bcsQ*, and the absence of *bcsD*. This locus contains also a divergent operon containing genes *bcsE*, *bcsF*, and *bcsG*, codifying proteins involved in natural BC modification (Thongsomboon et al., 2018). The third type of operon, well described in *A. tumefaciens*, is organized in two convergent operons, *celABCG* and *celDE*, in which the first three genes are orthologues of *bcsA*, *bcsB*, and *bcsZ*, whereas the other are specific for this operon type. This type of operon usually includes also another gene, named *bcsK*, that codifies for a BcsC-like tetratricopeptide containing protein (Römling and Galperin, 2015). Within AAB of *Komagataeibacter* genus, four genomes were whole sequenced and analyzed with respect to CS organization and functions: *K. xylinus* E25, *K. nataicola* RZS01, *K. medellinensis* NBRC 3288 and *K. hansenii* AY201 (Table 2-2). In addition, also other six *Komagataeibacter* strains were sequenced but the genome analysis is still incomplete (<https://www.ncbi.nlm.nih.gov/>).

The genes codifying CS subunits, first described in *K. xylinus*, are organized in an operon named *bcsABCD* (referred also as *acsABCD*). Some AAB contain multiple operons copies involved in BC production as those found in *Komagataeibacter*, namely *bcsI*, *bcsII*, and in some cases also a third copy referred as *bcsIII* (Table 2-2). In the *bcsABCD* operon, the first discovered four genes were those encoding for BcsA, BcsB, BcsC, and BcsD subunits (Wong et al., 1990). *bcsA* and *bcsB* codifying for the catalytic subunit were found to be fused, but any polypeptide of the same size was found, suggesting that post-translational processing generated the two subunits (Chen and Brown, 1996). Although in vitro studies showed that only *bcsA* and *bcsB* are essential for BC synthesis, all the enzymes codified by the genes of *bcsI* are required to obtain BC with the final structure in vivo, since *bcsC* and *bcsD* are involved in the exportation and/or packing of the glucan chains at the cell surface (Wong et al., 1990; Römling, 2002). The operon *bcsI* includes also accessories enzymes operating in concert with the CS, such as an endo- $\beta$ -1,4-glucanase (CMCax) and cellulose complementing factor (CcpAx), which are in the upstream region of the operon (Standal et al., 1994; Sunagawa et al., 2013). Studies in which the *ccpax* gene was interrupted demonstrated low BC crystallinity (Nakai et al., 2002). Disruption of *cmcax* gene drastically reduced BC yield and caused structure alterations resulting in cellulose II (Nakai et al., 2013). An overexpression of *cmcax* gene instead led to high enzymatic activity (Kawano et al., 2002; Morgan et al., 2013).

Flanked to *bcsA*, *bcsB*, *bcsC*, and *bcsD* genes, in down-stream region, the gene *bglAx* encoding BglAx was found (Tonouchi et al., 1995). In most strains belonging to *Komagataeibacter* genus, the second *bcs* operon (*bcsII*) does not display the full enzymatic set of the CS complex. Indeed, it contains the *bcsAB2* gene or only *bcsA2* and *bcsC2*. In some species of *Komagataeibacter*, *bcsAB2* or *bcsA2* and *bcsC* genes are interrupted by the presence of other two genes (*bcsX* and *bcsY*) (Table 2-2).



**Table 2-2.** BCS operons in *Komagataeibacter* species

Species/strain <sup>a</sup>	Accession number	Size (Mbp)	Whole/draft	BCS operon	BCS gene	Reference
<i>K. nataicola</i> RZS01 CGMCC 10961	CP019875	3.48	Whole genome	<i>bcsI</i> <i>bcsII</i>	<i>bcsA1</i> ; <i>bcsB1</i> ; <i>bcsC1</i> ; <i>bcsD</i> ; <i>cmcax</i> ; <i>ccpax</i> ; <i>bglxa</i> <i>bcsA2</i> ; <i>bcsY</i> ; <i>bcsX</i> ; <i>bcsC2</i>	Zhang et al., 2017
<i>K. hansenii</i> ATCC 53582	PRJEB10804	3.27	Draft genome	<i>bcsI</i> <i>bcsII</i> <i>bcsIII</i>	<i>bcsA1</i> ; <i>bcsB1</i> ; <i>bcsC1</i> ; <i>bcsD</i> ; <i>cmcax</i> ; <i>ccpax</i> ; <i>bglxa</i> ; <i>bcsAB2</i> ; <i>bcsY</i> ; <i>bcsX</i> ; <i>bcsC2</i> ; <i>bcsAB3</i> ; <i>bcsC3</i>	Florea et al., 2016
<i>K. hansenii</i> ATCC 23769 =AY201	CM000920	3.55	Draft genome	<i>bcsI</i> <i>bcsII</i> <i>bcsIII</i>	<i>bcsA1</i> ; <i>bcsB1</i> ; <i>bcsC1</i> ; <i>bcsD</i> ; <i>cmcax</i> ; <i>ccpax</i> ; <i>bglxa</i> ; <i>bcsAB2</i> ; <i>bcsAB3</i> ; <i>bcsC3</i>	Iyer et al., 2010
	LUCI01000000	3.35	Whole genome	<i>bcsI</i> <i>bcsII</i> <i>bcsIII</i>	<i>bcsA1</i> ; <i>bcsB1</i> ; <i>bcsC1</i> ; <i>bcsD</i> ; <i>cmcax</i> ; <i>ccpax</i> ; <i>bglxa</i> ; <i>bcsAB2</i> ; <i>bcsAB3</i> ; <i>bcsC3</i>	Pfeffer et al., 2016
<i>K. medellinensis</i> NBRC 3288	AP012159	3.14	Whole genome	<i>bcsI</i> <i>bcsII</i>	<i>bcsA1</i> ; <i>bcsB1-N</i> ; <i>bcsC1</i> ; <i>bcsD</i> ; <i>cmcax</i> ; <i>ccpax</i> ; <i>bglxa</i> ; <i>bcsAB2</i> ; <i>bcsY</i> ; <i>bcsX</i> ; <i>bcsC2-N</i>	Matsutani et al., 2015
<i>K. xylinus</i> E25	NZ_CP004360	3.45	Draft genome	<i>bcsI</i> <i>bcsII</i>	<i>bcsA1</i> ; <i>bcsB1</i> ; <i>bcsC1</i> ; <i>bcsD</i> ; <i>cmcax</i> ; <i>ccpax</i> ; <i>bglxa</i> ; not available	Kubiak et al., 2014
<i>K. xylinus</i> JCM 7664 <sup>b</sup>	AB015802	-	-	<i>bcsI</i> <i>bcsII</i>	<i>bcsA1</i> ; <i>bcsB1</i> ; <i>bcsC1</i> ; <i>bcsD</i> ; <i>cmcax</i> ; <i>ccpax</i> ; <i>bglxa</i> ; <i>bcsAB2</i> ; <i>bcsY</i> ; <i>bcsX</i> ; <i>bcsC2</i>	Umeda et al., 1999
<i>K. europaeus</i> 5P3	CADS01000001	3.99	Draft genome	<i>bcsI</i> <i>bcsII</i>	<i>bcsA1</i> ; <i>bcsB1</i> ; <i>bcsC1</i> ; <i>bcsD</i> ; <i>cmcax</i> ; <i>ccpax</i> ; <i>bglxa</i> ; not available	Andres- Barrao et al., 2011
<i>K. oboediens</i> 174Bp2	CADT01000000	4.18	Draft genome	<i>bcsI</i> <i>bcsII</i>	<i>bcsA1</i> ; <i>bcsB1</i> ; <i>bcsC1</i> ; <i>bcsD</i> ; <i>cmcax</i> ; <i>ccpax</i> ; <i>bglxa</i> ; not available	Andres- Barrao et al., 2011

<sup>a</sup> Only genomes with detected and described bcs operons were considered

<sup>b</sup> No genome sequence available

(*bcsX* and *bcsY*) (Table 2-2). About BcsY protein, sequence comparisons show that it could play a role in the BC modification, such as in the acetyl cellulose production via transacylase (Umeda et al., 1999). In *Komagataeibacter* genus, only *K. medellinensis* NBRC 3288 was reported to be

no BC producer. The recent genome sequencing of this strain highlighted two mutations localized in both operons. In the *bcsABCD*, a disrupted *bcsB1* gene (BcsB1-N; locus\_tag: GLX\_25040-GLX\_25100) was found, due to a frameshift mutation, whereas in *bcsII*, the *bcsC2* gene seems to be corrupted by an insertion sequence (BcsC-N; locus\_tag: GLX\_27490-GLX\_27560) (Matsutani et al., 2015).

## Biofilm formation in acetic acid bacteria

Biofilm can be described as a social consortium of cells embedded in an extracellular matrix that undergo developmental programs resulting in a predictable “life cycle” (McDougald et al., 2012). The need for bacteria to switch from planktonic to biofilm form is a response to their chemical physical environment. The extracellular matrix of a biofilm provides protection to bacteria cells from harsh conditions. It acts as a support avoiding cell washout across liquid flow by the attachment to a surface; it protects cells against antimicrobial compounds by limiting the diffusion of these compounds and increases cell density, enhancing factors for antibiotic resistance, as in the case of eDNA (plasmids) and DNA exchange by conjugation. The extracellular matrix of biofilm produced by bacteria is composed of proteins, exopolysaccharides (EPS), and extracellular DNA. Poly-N-acetylglucosamine (PAG) and BC are main components of the EPS fraction and in particular the BC that was first identified as a biofilm matrix component in gram negative bacteria in 2001 (Zogaj et al., 2001; Rabin et al., 2015). Formation of biofilm is a regulating mechanism and some bacteria use signaling molecules to modulate it. In gram negative bacteria, acyl-homoserine lactones (AHLs) mediate quorum sensing (QS) system. In AAB, QS system is not well studied; however, some studies revealed that they use QS to modulate a number of functions. Iida et al. described the correlation between QS and oxidative fermentation in *K. intermedius* (NCI1051). *K. intermedius* produces three different AHLs, N-decanoyl-L-homoserine lactone, N-dodecanoyl-L-homoserine lactone, and an N-dodecanoyl-L-homoserine lactone. The GinI/GinR quorum sensing system found in *K. intermedius* controls the expression of *ginA*, which in turn represses oxidative fermentation, including acetic acid and gluconic acid fermentation (Iida et al., 2008). The QS system N-AHL-dependent GinI/GinR detected in *K. intermedius* is a LuxI/LuxR type system that is homologous to LasI/LasR pathway, well described in *Pseudomonas aeruginosa* (Passos da Silva et al., 2017). Further studies on wild-type and mutants of *K. intermedius* strains revealed that GinI/ GinR QS system is not involved in BC production. This QS regulation system seems to provide some advantages to the population contrasting toxicity of acetic acid by decreasing the growth rate (Iida et al., 2008). In BC-producing AAB, there are no pieces of evidence about the role of quorum quenching (QQ) mechanisms. Valera et al. found a possible candidate involved in QQ, a protein named GqqA, which affects BC biofilm formation, but the molecular mechanism remains unknown (Valera et al., 2016). Well documented in the signaling system of AAB is the central role of c-di-GMP as second messenger contributing to the regulation of bacteria behaviors. c-di-GMP was described for the first time as an allosteric activator of the CS in *K. xylinus* (Ross et al., 1987). It regulates also other bacterial processes such as cell motility, transition between sessile and planktonic lifestyle, cell division, and pathogenesis (McNamara et al., 2015). It is synthesized from two GTP molecules by diguanylate cyclase (DGC) characterized by GGDEF domain and degraded by phosphodiesterase (PDE) to 5'-phosphoguanylyl-(3'-5')-guanosine (pGpG) or GMP. Then, the intracellular concentration of c-di-GMP is regulated by the activity of DGC and PDE. Another level of regulation is provided by specific effector binding

proteins, which vary among bacteria (Ross et al., 1991). The c-di-GMP levels can be influenced also by environmental factors such as oxygen availability. In *K. xylinus*, the synthesis or hydrolysis of c-di-GMP is dependent of PAS domain DGC protein, a well-characterized domain sensitive to oxygen levels (Chang et al., 2001; Qi et al., 2009).

## Using vinegar as a model for biofilm and cellulose formation in acetic acid bacteria

In liquid surface, as it has been experienced for long time during the alcohol-to-acetic acid conversion required for vinegar production, the growth of AAB is observed mainly as a biofilm. The biofilm is formed step-by-step and matures close-to-surface, with different shape and thickness. In regular vinegar fermentations, biofilm looks like a very thin layer that persists during fermentation (Figure 2-2c). Disturbing the liquid, biofilm is destroyed, and it is still formed after some days. However, since vinegar production is mainly conducted without selected microbial cultures, anomalous fermentations are often observed (Giudici et al., 2009a). The most frequent irregular fermentation is due to the formation of a thick EPS layer formed by BC, which is undesired in vinegar production (Gullo and Giudici, 2008).

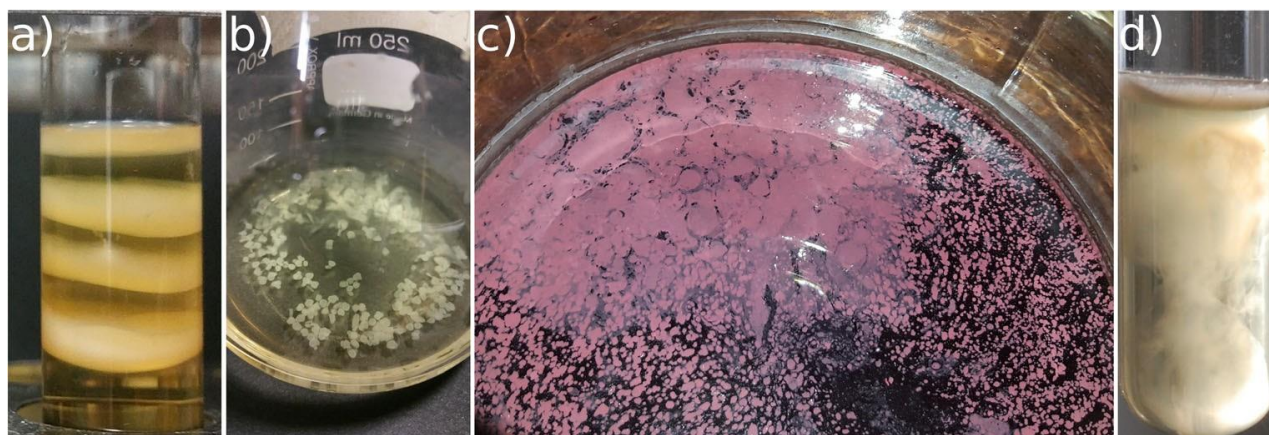


**Figure 2-2.** Different morphologies of biofilm and bacterial cellulose in AAB: BC produced by *K. xylinus* UMCC2756 as multilayer biofilm under static growth regime (a); BC produced by *K. xylinus* UMCC2756 as spheres under agitated growth regime (b); thin biofilm produced during wine vinegar fermentation (c); filamentous biofilm growth by a high BC producing isolate under static growth regime (d).

Moreover, a broad spectrum of environmental factors including the concentration of oxygen, nutrients or toxic compounds, as well as mechanical stresses can trigger both the biofilm formation and transition to planktonic cells. Macroscopic changes in shape and texture have been well documented during vinegar processes under different operative conditions (Gullo et al., 2016). The vinegars AAB biofilm must be considered as a complex hydrogel of living and death AAB cells embedded in the extracellular matrix (Figure 2-3). The predictable behavior of AAB biofilm in vinegar production is intended, at least, for the following three aims: (i) to protect the living cells towards the acetic acid accumulation, (ii) to maintain the optimum osmotic and carbon source levels required for growth and survival, and (iii) to be responsive to external mechanical stresses. From one hand, the 3D network of BC bundles is able to compartmentalize the mother liquor within microenvironments that surrounds the living cells, acting as a selective physical barrier controlling diffusion-limited solute transfer between the biofilm and liquid medium bulk.

It is generally reported that AAB-forming biofilm grows at the air surface of liquids. However, as long-time experience at laboratory scale, the site of biofilm formation is not the free surface of the liquid medium, but the submerged layer close to the free surface, since the interstitial liquid voids and channels separating microcolonies are the preferential site for BC production. The upper surface of the biofilm/BC layer, as produced under static growth conditions, undergoes high rate of evaporation reaching shortly lower values of water activity, limiting cell growth. Gullo et al. 2017 recently studied the optimal conditions to produce high BC yield by *K. xylinus* UMCC2756. Under static regime, a well-structured and thick pellicle containing only Ia cellulose was obtained. The biofilm has developed through several phases including the transition from single cells initially dispersed in the liquid bulk to mature biofilm (Gullo et al., 2017). Macroscopic observation of the layer formed by pure culture of *K. xylinus* clearly shows that the submerged layer is filamentous (Figure 2-2d), whereas microscopic examination of such biofilm shows that the number of living cells is higher with respect to the upper surface. All these findings are in accordance with the theory underpinning the dynamic of solute gradient (oxygen, water, and nutrients). The oxygen tension in gaseous phase of 10 and 15% with respect to the atmospheric conditions plays a lead to an increase of both BC production and yield (Watanabett and Yamanaka, 1995). However, irrespectively of the effective oxygen concentration within the biofilm, the major hurdle for living cells to grow onto the upper layer is the poor nutrient availability due to the limited mass transfer from the liquid bulk through the BC matrix, especially of high molecular weight solutes such as sugars. Due to both the low solute permeability and water availability, the optimal growth conditions increase from the biofilm surface towards the filamentous and submerged layers of the biofilm themselves (Figure 2-3).

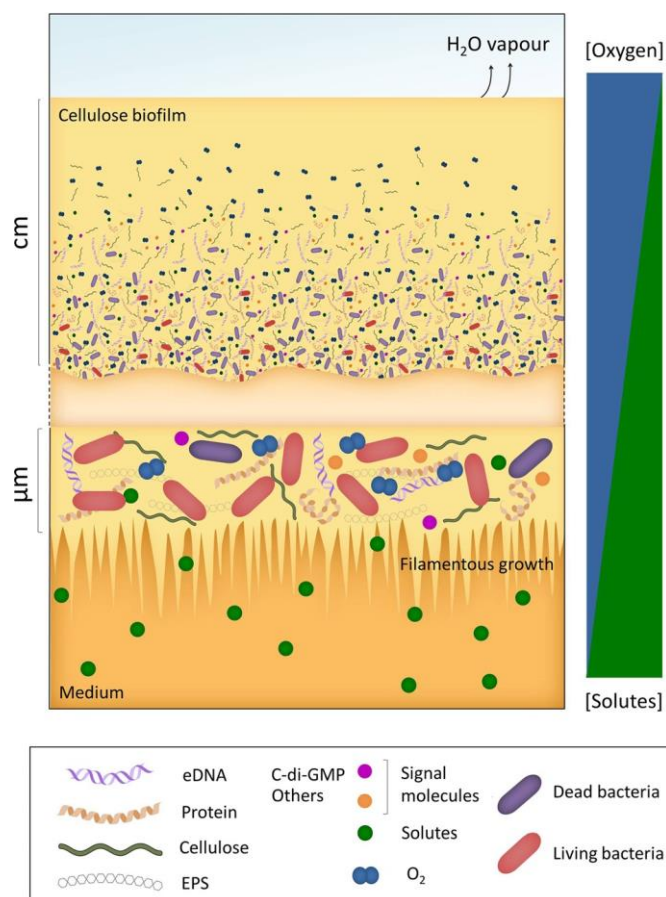


**Figure 2-3.** The structure of biofilm in AAB. Upper side centimeter (cm): BC biofilm formation occurs at the down surface due to solutes availability and oxygen diffusion across the matrix. In the upper surface, cell growth is limited due to evaporation and low solutes availability; lower side micron ( $\mu\text{m}$ ): BC biofilm formation in the early phase, with oxygen and solute availability. Biofilm filamentous AAB growth is displayed

All these evidences are also corroborated by several studies regarding the effect of surface dehydration on the isolation and maintenance of living AAB cells in culture media. Indeed, cultivation of slow-growing AAB was improved by developing and optimizing double agar media and semisolid media in which AAB cells grow preferentially within the space at higher relative humidity. Instead, it has been proven that the growth of certain biofilm forming AAB in single agar media is strongly inhibited especially when the incubation is conducted without relative humidity control (Entani et al., 1985; Kittelmann et al., 1989; Sievers et al., 1992; Mamlouk and Gullo, 2013).

## Acetic acid bacteria and main process issues

From literature, it emerges that, to efficiently switch from a laboratory to an industrial strain, several bottlenecks need to be overcome. The availability of high-producing strains, the carbon substrates utilized as starter material, and the optimization of culture methods seem to be the main requirements for an efficient BC synthesis (Gullo et al., 2017). Several studies focused on the characterization of robust AAB strains, which display suitable technological traits for BC production; however, most of them are well studied at laboratory scale but never tested at industrial scale.

However, the advance in genetic engineering and biotechnology field during the last decades provided different mutant strains able to produce high BC yield (Shigematsu et al., 2005). One of the targets of knockdown was pyrroloquinoline quinone cofactor-dependent glucose dehydrogenase (GDH-PQQ), the enzyme responsible for gluconic acid production from glucose (Cañete-Rodríguez et al., 2016). Silencing GDH-PQQ, most of glucose was available for BC production. One of the most recent work displays the knockout of GDH-PQQ in *K. xylinus* BCRC12334, which produced both a higher BC yield (about 40 and 230% compared to the wild-type strain) and a reduction of gluconic acid formation (Kuo et al., 2015). From Table 2-1, it can be deduced that many efforts in BC production, aimed to optimize culture conditions, have been done. Different studies covered the best combination of the carbon sources and the production system.

To reduce the cost of BC production, different strategies were tested using low costs and waste products as carbon sources. High BC productivity was obtained using molasses from corn steep liquor (CSL) added with citric acid in *K. xylinus* BCR5 culture (Table 2-1). Second hand fruits, which are not marketable, are also considered potential sustainable raw materials for BC production. Currently, however, although the use of low costs feedstocks as carbon sources seems appealing, it needs to be carefully evaluated not only for the produced BC yield but also for the upstream and downstream process steps necessary to remove microbial inhibitors, contaminants, and color.

The most investigated methods to produce BC comprise static and submerged regimes by which uniform smooth gels and spheres can be obtained, respectively (Islam et al., 2017). The need of

customized bioreactors for BC production, however, is still an open issue in order to increase BC yield for the intended use.

## **The industrial era of bacterial cellulose**

BC possesses higher surface area than plant cellulose and is a very malleable material. Also, distinct types of artificially encased nanoparticles, including metals, are of huge interest in order to design AAB celluloses with tailored nanostructure and functional properties.

Native BC does not require any purification steps that can cause alterations of its structural and physicochemical properties. From this prerequisite, it is clear that it can be suitable for a number of biomedical applications. Most of these are very emerging applications, thanks also to the advances in tissue engineering and in regenerative medicine. BC is used as artificial skin, artificial blood vessels, and hemostatic materials. One of the most important uses of BC in the biomedical field is as wound healing scaffolds (Picheth et al., 2017). Many BC-based scaffolds are approved by the Food and Drug Administration (FDA) because of the high purity in terms of low proteins and endotoxic units (Petersen and Gatenholm, 2011). During the last years, many brands (such as Biofill®, Gengifill®, Bionext®, and Xcell®) developed BC biodevices that can be used in a wide variety of regenerative medicine applications. These devices are characterized by different effects, such as pain relief, fast skin regeneration, and reduction of inflammatory response (Rajwade et al., 2015). Furthermore, BC is also applied in drug delivery approaches, in which modified variants of BC are used. Such modifications can enhance BC-based delivery properties. In BC hydrogels combined with carboxymethyl cellulose (CMC) and ibuprofen sodium as drug model, it was shown that CMC influences the swelling and drug release, suggesting that BC-CMC hydrogels could be exploited in controlled drug delivery (Pavaloiu et al., 2014).

Thanks to the stabilizing effect of oil-water emulsion, low toxicity, and ability to hydrate the skin without the need of surfactants, BC is extensively used in the cosmetic field for facial mask creams and as a powder in facial scrubs in association with other natural materials (as olive oil, Vitamin C, Aloe vera extract, and powdered glutinous rice).

An emerging BC application in cosmetics is the production of contact lenses, due to its transparency, light transmittance, and permeability to liquids and gases. Contact lenses produced from BC can be used also in drug delivery for treatment of the cornea (Ullah et al., 2016).

BC plays a key role also in the food industry. As dietary fiber, BC is labeled as generally recognized as safe (GRAS) by the FDA (Shi et al., 2014b). The ability to acquire flavors and colors, makes BC a suitable adjuvant for foods and beverages. Moreover, as a food additive, it is used worldwide for its gelling and thickening properties. The most common BC derivatives used in food are the CMC and hydroxypropyl methylcellulose due to their structure-stabilizing properties. Traditionally, BC occurs in the manufacturing of “nata de coco” and Kombucha tea. Nata de coco is a Philippine dessert produced from fermented coconut water. The obtained BC is chopped into minute sections and immersed in syrup of sugar (Iguchi et al., 2000), whereas Kombucha tea is a beverage obtained from sugared tea in which an association of yeasts and AAB conducts the fermentation (Mamlouk and Gullo, 2013). Monascus-BC complex, which combines limited calories and high fiber content with those of *Monascus* fungi (healthy nutrients), was proposed as meat or seafood replacement for vegetarian diet (Ng and Shyu, 2004). Also, BC is used in low cholesterol diet, thanks to serum lipids and cholesterol-lowering effect (Chau et al.,

2008). When compared with other dietary fibers, BC have several main advantages: (i) separability from biofilm without chemical treatments; (ii) biosynthesis and growth conditions can be modulated tailoring structure and functionalities directly in situ and in process; and (iii) complete indigestibility in the human intestinal tract (Pokalwar et al., 2010). Moreover, BC with its hydrogel-like texture could be a new material for salads and low-calorie desserts. The gel by itself is too hard to bite, but it becomes edible through processing either with sugar alcohol or with alginate and calcium chloride aiming to immobilize the water of gelatinous BC (Keshk, 2014). In the production of high quantity food, the need of new technology, based on the use of enzymes, is required. In the recent decades BC has been evaluated also for its ability to immobilize enzymes, such as laccases. Laccases are enzymes used to improve the organoleptic properties, such as color and flavor of beverages and oils. They can also improve the quality of sauces, concentrates, and soups by the process of deoxygenation (Osma et al., 2010). Modification of BC is also extensively used in food packaging to increase safety and shelf-life. Antimicrobial effect was shown by adding sorbic acid in mono and multilayer BC against *E. coli* (K12-MG1655) (Jipa et al., 2012). Finally, application of BC in heavy metal removal such as mercury and arsenic has been proved. Adsorption of mercury resulted fast with no effect on adsorption rate for long time, whereas, for arsenic, fast adsorption at alkaline pH range was observed (Gupta and Diwan, 2017).

## Conclusion and perspectives

Native and functionalized BC is considered a high appealing biopolymer by the industry. Several considerations derived by scientific literature indicate *K. xylinus*, among bacteria, as the most studied species for BC production. The BC produced by *K. xylinus*, like BC produced by other bacteria, has high degree of purity: this characteristic supported a great interest for industrial uses, where purity is a prerequisite. Moreover, *K. xylinus*, as a model organism for BC production, is well known concerning the molecular machinery of CS complex and it is also considerable for the obtained BC yield in different conditions.

Studies about BC structure highlighted as the supramolecular assembly can be modulated to obtain specific attribute of the BC membranes. This aspect is particularly important to enlarge the applicability in different uses: the advances in the BC synthase machinery regarding the bioassembling modality, as well as genomic and proteomic data, revealed the high potential of these approaches to obtain high performing AAB strains. Observing the biofilm grow modality of AAB, a lot of information on the ideal site and conditions for BC synthesis can be deduced; this information is significant to create conditions to synthesize a high BC yield. However, these aspects are not well known for AAB, especially the factors that determine biofilm/BC synthesis. Therefore, studies to fill the gaps in the knowledge of QS system in AAB can be really advantageous. A huge amount of literature on the evaluation of specific strains cultivated in different media and conditions has been published; it can be deduced that the stability of the production process strictly depends on the carbon source and possible BC activators.

Currently, the use of sustainable sources (low costs and waste feedstocks) is reported as a frontiers goal, but careful considerations should be made. The use of low costs and waste feedstocks need to be analyzed with respect to the process as a whole, estimating all advantages and disadvantages in order to obtain the required yield and a good quality of BC from these sources.

# Chapter 3

Kombucha tea as a reservoir of cellulose producing bacteria: assessing diversity among *Komagataeibacter* isolates

Salvatore La China<sup>1</sup>, Luciana De Vero<sup>1</sup>, Kavitha Anguluri<sup>1</sup>, Marcello Brugnoli<sup>1</sup>, Dhouha Mamlouk<sup>1</sup>, Maria Gullo<sup>1</sup>

<sup>1</sup>Department of Life Sciences, University of Modena and Reggio Emilia, Reggio Emilia, Italy

**This chapter was published as:**

**La China S**, De Vero L, Anguluri K, Brugnoli M, Mamlouk D Gullo M. Kombucha tea as a reservoir of cellulose producing bacteria: assessing diversity among *Komagataeibacter* isolates. *Appl. Sci.* (2021) 11, 1595. <https://doi.org/10.3390/app11041595>



## Abstract

Bacterial cellulose (BC) is receiving a great deal of attention due to its unique properties such as high purity, water retention capacity, high mechanical strength, and biocompatibility. However, the production of BC has been limited because of the associated high costs and low productivity. In light of this, the isolation of new BC producing bacteria and the selection of highly productive strains has become a prominent issue. Kombucha tea is a fermented beverage in which the bacteria fraction of the microbial community is composed mostly of strains belonging to the genus *Komagataeibacter*. In this study, Kombucha tea production trials were performed starting from a previous batch, and bacterial isolation was conducted along cultivation time. From the whole microbial pool, 46 isolates were tested for their ability to produce BC. The obtained BC yield ranged from 0.59 g/L, for the isolate K2G36, to 23 g/L for K2G30—which used as the reference strain. The genetic intraspecific diversity of the 46 isolates was investigated using two repetitive-sequence-based PCR typing methods: the enterobacterial repetitive intergenic consensus (ERIC) elements and the (GTG)<sub>5</sub> sequences, respectively. The results obtained using the two different approaches revealed the suitability of the fingerprint techniques, showing a discrimination power, calculated as the D index, of 0.94 for (GTG)<sub>5</sub> rep-PCR and 0.95 for ERIC rep-PCR. In order to improve the sensitivity of the applied method, a combined model for the two genotyping experiments was performed, allowing for the ability to discriminate among strains.

## Introduction

The attraction of bacterial cellulose (BC) as a natural biopolymer, produced by microorganisms, arises from its main functional properties and subsequent applications, especially in the biomedical, food, and engineering fields (Robotti et al., 2018; Haghighi et al., 2020; Barbi et al., 2021). Bacteria able to synthesize cellulose can be considered ubiquitous since they have been found to inhabit different ecosystems. They can be isolated from environmental sources (such as soil and plants), from insects, humans, and from food sources (Valera et al., 2018).

Within the family *Acetobacteraceae*, the genus *Komagataeibacter* includes species, such as *K. xylinus*, *K. europaeus* and *K. hansenii*, that have been described as cellulose producing organisms (Gullo et al., 2018). The main studied strains belong to the *K. xylinus* species, which is recognized as the model organism for studying the mechanism of BC synthesis (Son et al., 2001; La China et al., 2018).

One of the most important reservoirs in which it is possible to detect strains belonging to the *Komagataeibacter* genus is kombucha tea, a fermented beverage traditionally produced in Asia, probably originating from the northeast of China (Coton et al., 2017). Kombucha tea is characterized by a microbial community in which different microbial groups, mainly yeasts and bacteria, live in a symbiotic lifestyle (Laureys et al., 2020). Among bacteria groups, acetic acid bacteria are the main functional organisms, although lactic acid bacteria are also found; moreover, among yeasts, strains of the genera *Saccharomyces* and *Zygosaccharomyces* have been described (Sievers et al., 1995). Kombucha tea production consists of two fermentation reactions operated by yeasts and acetic acid bacteria (Arikan et al., 2020). The symbiotic relation between yeast and bacteria is established during the fermentation process, in which the yeasts are capable of hydrolysing sucrose, the main substrate for Kombucha tea production, into glucose and fructose, and then ethanol. Acetic acid bacteria use glucose, fructose and ethanol to produce gluconic acid, glucuronic acid, acetic acid, and BC (Gaggia et al., 2018; Villarreal-Soto et al., 2018).

Kombucha tea can be considered as a dynamic environment, rapidly changing its composition, acting as an ecophysiological reservoir of very specialized organisms. Considering the occurrence and function of acetic acid bacteria within kombucha, previous studies have described *K. xylinus* as the main species.

The ability of *K. xylinus* strains to produce BC is highly variable, making the selection of the best ones a crucial step in order to obtain candidate strains for large scale BC production. In fact, the availability of selected organisms in producing BC is a requirement for exploiting them as industrial machinery. The production of BC is mainly influenced by two factors. The first one is represented by the carbon sources used in the medium (Singhsa et al., 2018; Gullo et al., 2019); pure carbon sources could increase the production cost, making the process unsustainable. The second issue is related to the ability of the organism to grow and produce BC in the selected conditions (Mamlouk and Gullo, 2013). Some studies have described the abilities of strains belonging to the *Komagataeibacter* genus for producing BC at different yields (Gullo et al., 2018).

In this work, acetic acid bacteria were collected from liquid and pellicle fraction of kombucha tea samples. In total, 46 isolates were screened for their ability to produce BC and for the main phenotypic characteristics. Moreover, they were typed by applying a fingerprint analysis based on (GTG)<sub>5</sub> repetitive elements and Enterobacterial Repetitive Intragenic Consensus (ERIC) elements in order to assay the intraspecific genetic diversity.

## Materials and Methods

### Kombucha Preparation, Sampling and Physico-Chemical Determinations

Two native local kombucha precultures (P1 and P2) were provided by the National Institute of Applied Sciences and Technology (INSAT, Tunisia), previously cultivated on two different substrates: black tea (P1) and green tea (P2). Each preculture was composed of kombucha cellulose pellicle with approximately 200 mL of starter culture. Duplicates of kombucha, referred to green tea kombucha (GTK) and black tea kombucha (BTK), were prepared and inoculated according to Jayabalan et al. (Jayabalan et al., 2007). Briefly, sucrose 10% (w/v) was added to demineralized water and allowed to boil. Afterwards, 1.2% (w/v) black or green tea (Les Jardins du thé, Office Tunisien du Commerce, Tunisia) was added and allowed to infuse for about 5 min. After filtration of tea leaves through a sterile sieve, 200 mL of tea was poured into 500 mL glass jars that had been previously sterilized at +121 °C for 20 min. Once the sucrose–tea solution had cooled at room temperature, 10% (v/v) of the fermented tea (of the previous fermentation brew from kombucha with the same origin, in this case black or green tea as substrate, corresponding to the aforementioned starter culture) was added. Then, 3% (w/v) of representative pellicle fragments cut from the preculture were placed in the culture light side up. The jars were covered with a sterile gauze and fixed with an elastic band. Fermentations were carried out in the dark for 12 days. All experiments were carried out aseptically.

Cell morphology and direct observation of samples were carried out using optical microscopy at 100X of magnification, using C. Zeiss microscope apparatus (Axiolab).

Titrate acidity was determined by neutralizing samples at pH 7.2 with 0.1 N of NaOH (it was assumed that all media acidity was due to acetic acid) and expressed as % (wt/wt); pH was measured by CRISON, MicropH, 2002 pHmeter. Ethanol, expressed as % (v/v), was checked by densitometry measure using a hydrostatic balance after distillation.

### Plating and Isolation

Plating was performed immediately after sampling. Therefore, 10 mL of 0.1% (w/v) peptone water was added to 1 g of black or green kombucha pellicle in a sterile stomacher bag that was vigorously shaken for 5 min in a laboratory blender STOMACHER® 400 (Seward, England) to obtain a uniform homogenate. Samples (1 mL each) of the homogenate and liquid phase were 10-fold serially diluted in 0.1% (w/v) peptone water, from which aliquots (0.1 mL) were plated on GYC medium (10 g/L yeast extract, 50 g/L glucose, 15 g/L CaCO<sub>3</sub>, 9 g/L bacteriological agar) and ACB agar medium (30 g/L yeast extract, 1 mL of a 22 g/L bromocresol green solution, 20 g/L bacteriological agar). The media were previously autoclaved at 121 °C for 15 min and after 20 mL/L of filtered ethanol 95% (v/v) was added aseptically to the ACB medium. A total of 0.2 mL of cycloheximide hydroalcoholic solution at 25% m/v was added directly to petri dishes.

Plates were incubated at +28 °C for 72–120 h. Colonies were picked up from a suitable dilution of each sample on GYC and ACB agar media, grown for 3–5 days at +28 °C and purified through subculturing and plating. Pure kombucha isolates were named and strains were cultivated on the corresponding isolation medium for 3–5 days at +28 °C (Mamlouk, 2012). Long-term preservation methods of the strains were performed according to the standard procedures of the Microbial Resource Research Infrastructure—Italian Joint Research Unit (MIRRI-IT) (De Vero et al., 2019). Specifically, a seed lot of the strains was stored at –80 °C, adding glycerol 50% (v/v) to the liquid media. The strains with significant cellulose production were deposited in the University of Modena and Reggio Emilia (UNIMORE) Microbial Culture Collection (UMCC, [www.umcc.unimore.it](http://www.umcc.unimore.it)).

## Phenotypic Characterization

Strains were phenotypically characterized by determination of cell morphology, gram staining, catalase activity, potassium hydroxide (KOH) test, consumption of calcium carbonate and oxidation of ethanol and acetic acid on ACB agar medium, as previously reported in Gullo et al. (2012).

The BC production test was carried out by collecting the pellicles and boiling them in 4 mL of 5.0% NaOH solution for 2 h. Cellulose was confirmed when the pellicle did not dissolve after boiling (R. Navarro et al., 1999). Strains *K. xylinus* (DSM 2004) and *G. oxydans* (DSM 3503) were used as positive and negative controls, respectively. Tests were conducted in triplicate.

The amount of BC was estimated, as reported by Gullo et al. Gullo et al. (2017). Briefly, pellicles were washed with distilled water and then treated with 1% NaOH at 90 °C for 30 min. Treated BC was washed twice with distilled water, the pH of the residual water was determined; the washing step was repeated until reaching neutral pH. Drying was conducted at 80 °C. BC weight was measured by analytical balance (Gibertini E42S) (Hwang et al., 1999). The yield of BC produced was expressed in grams of dried BC per liter of broth.

## Genomic DNA Extraction, RFLP and Amplification of (GTG)<sub>5</sub>/REP-PCR and ERIC Elements

Genomic DNA extraction was performed on liquid cultures, which were previously incubated for 72 hrs at +28°C. Flasks were vigorously shaken to remove the embedded cells from BC, the liquid medium was transferred to a sterile tube and centrifuged at 12,000× g for 5 min. gDNA was extracted using the method previously proposed by Gullo et al. (2009). gDNA was checked by 3% gel agarose in 1X TBE buffer and quantified by spectrophotometric measure (NanoDrop ND-1000). Band sizes were determined using a 100 bp DNA ladder (Invitrogen, Carlsbad, CA, USA).

RFLP analysis on the full-length 16S rRNA gene was performed using *RsaI* and *AluI* endonucleases (Fermentas, Hanover, ND, USA), incubating at +37 °C for 2 h. The restriction reaction was stopped by incubation at 80 °C for 20 min. The fragments were checked on 3% gel agarose in 1X TBE buffer and sizes were determined using 100 bp DNA ladder (Invitrogen).

(GTG)<sub>5</sub> rep-PCR fingerprinting was carried out according to the method of Versalovic et al. (1994), with some minor modifications. Isolates were subjected to REP-PCR with a single oligonucleotide GTG<sub>5</sub> (5'-GTGGTGGTGGTGGTGGTGGT-3'). Samples were incubated for 5 min at 94 °C and then cycled 35 times at 94 °C for 30 s, 40 °C for 1 min, and 72 °C for 4 min. The samples were incubated for 7 min at 72 °C for final extension and kept at 4 °C. ERIC elements were initially amplified according to Versalovic et al. (1991) using the primers ERIC 1R (5'-ATGTAAGCTCCTGGGGATTAC-3') and ERIC 2 (5'-AAGTAAGTGGGGTGAGCG-3'). Samples were incubated for 5 min at 94 °C and then cycled 30 times at 94 °C for 30 s, 57 °C for 30 s, and 65 °C for 4 min. The final extension was performed at 65 °C at 8 min and kept at 4 °C until tested. The reproducibility of ERIC/PCR was also tested by amplifying gDNA from randomly chosen strains several times. For both rep-PCR, pattern band lengths were determined by comparison against a 100 bp plus DNA ladder for the smallest bands and by 1 Kbp DNA ladder for the largest bands (Takara Bio, Inc., Otsu, Shiga, Japan).

### **Statistics and Clustering Analysis of (GTG)<sub>5</sub> and ERIC Rep-PCR Patterns**

Patterns obtained from (GTG)<sub>5</sub> and ERIC rep-PCR runs were imported into BioNumerics tool, package version 8. The cluster analysis was performed calculating Dice coefficients using a tolerance of 1% and optimization of 1%. Clustering based on Dice coefficients was performed using the unpaired group method with arithmetic average (UPGMA) method. For each fingerprint assay, the cluster cut-off analysis was applied to define the most reliable clusters. The cophenetic correlation index was used as a statistical tool to evaluate the quality of branches. For each of the genotyping experiments, the discriminatory index (D), expressed as the probability that two strains consecutively taken from a sample would be placed into different clades, was calculated as described by Hunter and Gaston (Hunter and Gaston, 1988).

Correlation analysis was performed considering the most abundant clades (Clade 5, 6 and 7), in order to obtain statistically significant results. The Spearman correlation index was calculated using the Hmisc v4.4–2 R package (Harrell and Dupont 2014) implemented in R v 4.0.3 (R Development Core Team, 2014). The correlation plot was obtained using the Corrplot v 0.84 package (Taiyun and Viliam 2017).

## **Results**

### **Kombucha Characteristics and Isolated Strains**

Within 3 days of cultivation in 600 mL beakers, the two kombucha tea samples, GTK and BTK, demonstrated a thin exopolysaccharide layer that became thicker with time (from 2–3 mm to 10 mm at the end of the cultivation period). Optical microscopy observations showed a high number of free bacterial and yeast cells, as well as aggregates of cells within the matrix, making cell counting uncertain and not enlightening even from the first day of fermentation.

Titrate acidity reached a maximum of 12 g/L at the end of fermentation in the black kombucha trial (GTK) and 6 g/L in the green one (BTK). pH dropped from approximately 3.7 to 2.75 for both samples, as a result of acid formation. Although no inhibition compounds were determined in this study, the difference in the final amount of acetic acid of the GTK and BTK samples could be due to the occurrence of more antibacterial compounds in GTK (Battickh et al., 2013). Ethanol was nearly 0 at the beginning of the

cultivation time and reached 0.28% (v/v) and 0.30% (v/v) at the final time, for samples GTK and BTK, respectively. The low value of observed ethanol is in agreement with the gradual increase in acetic acid during cultivation time.

The isolation was performed from preculture (P1 and P2) and samples at 0, 6, and 12 days of cultivation. A total of 122 isolates were selected based on the colony and/or cellular morphologies. Microscopically, presumptive acetic acid bacteria cells appeared in single or grouped pairs or short chains, Gram-negative, catalase-positive, and KOH positive. A total of 46 isolates, which oxidized both ethanol and acetic acid, as confirmed by the ethanol chalk–ethanol test on GYC and the colorimetric assay on ACB, and produced a well-defined cellulose layer and/or formed both a cellulose layer and cellulose particles dispersed in the surrounding liquid, were considered in this study (Table 3-1).

**Table 3-1.** Features of 46 isolates from Kombucha tea used in this study. Site of isolation and RFLP analysis. In bold are reported the strains deposited in UNIMORE Microbial Culture Collection (UMCC) collection; within the brackets is the assigned accession number.

* Strain	Sample	Time	BC (g/L)	Colony Morphology	Liquid Growth	<i>AluI</i> (pb)	Group	<i>RsaI</i> (bp)	Group	Reference
K1A18	liquid	6	4.0448 ± 0.0008	green cellulosic	cellulose layer	-	-	1, 400, 425, 550	A	This study
K1A34	liquid	12	5.6214 ± 0.0010	green with light cellulosic edge	cellulose layer	150, 450, 800	1	1, 400, 425, 550	A	This study
K1A6	liquid	0	3.0024 ± 0.0009	cellulosic small	cellulose layer	150, 450, 800	1	1, 400, 425, 550	A	This study
K1A7	liquid	0	1.5886 ± 0.0004	cellulosic	cellulose layer/deposit	150, 450, 800	1	1, 400, 425, 550	A	This study
K1A8	liquid	0	2.5886 ± 0.0002	cellulosic	cellulose layer	150, 450, 800	1	1, 400, 425, 550	A	This study
K1A9	liquid	0	3.4014 ± 0.0004	green cellulosic	cellulose layer	-	-	-	-	This study
<b>K1G2</b> (=UMCC 2964)	liquid	P1	4.7895 ± 0.0014	white cellulosic edge	cellulose layer/deposit	150, 450, 800	1	1, 400, 425, 550	A	Gullo et al., 2012
K1G22	liquid	12	0.7057 ± 0.0003	cellulose light	cellulose layer/deposit	150, 450, 800	1	1, 400, 425, 550	A	Gullo et al., 2012
K1G23	liquid	12	4.8122 ± 0.0003	dark cellulose	cellulose layer	150, 450, 800	1	1, 400, 425, 550	A	Gullo et al., 2012
K1G24	liquid	12	4.1210 ± 0.0001	white cellulose	only cellulose deposit	-	-	1, 400, 425, 550	A	Gullo et al., 2012
K1G3	liquid	P1	2.1857 ± 0.0052	light beige	cellulose layer	150, 450, 800	1	1, 400, 425, 550	A	Gullo et al., 2012
K1G4	liquid	0	1.1738 ± 0.0032	cellulosic	cellulose layer/deposit	150, 450, 800	1	1, 400, 425, 550	A	Gullo et al., 2012
K1G5	liquid	0	4.9590 ± 0.0027	cellulosic	cellulose layer/deposit	150, 450, 800	1	1, 400, 425, 550	A	Gullo et al., 2012
K1G6	liquid	0	5.3676 ± 0.0025	white cellulosic	cellulose layer/deposit	150, 450, 800	1	1, 400, 425, 550	A	Gullo et al., 2012
<b>K2A10</b> (=UMCC 2965)	liquid	0	5.0405 ± 0.0008	cellulosic green small	cellulose layer	150, 450, 800	1	1, 400, 425, 550	A	This study
K2A28	liquid	6	5.8962 ± 0.0007	green cellulosic	cellulose layer	150, 450, 800	1	1, 400, 425, 550	A	This study
K2A32	pellicle	6	5.6143 ± 0.0001	green cellulosic	cellulose layer	-	-	-	-	This study
K2A33	liquid	6	0.6414 ± 0.0005	green cellulosic	cellulose layer	150, 450, 800	1	1, 400, 425, 550	A	This study
K2A44	liquid	12	5.1971 ± 0.0002	small green	cellulose layer/deposit	150, 450, 800	1	1, 400, 425, 550	A	This study

K2A45	pellicle	12	5.2133 ± 0.0004	light edge	cellulose layer	150, 450, 800	1	1, 400, 425, 550	A	This study
K2A46	liquid	12	5.7833 ± 0.0001	dark center light edge	cellulose layer	150, 450, 800	1	1, 400, 425, 550	A	This study
K2A47	pellicle	12	5.8019 ± 0.0001	blue medium displayed	cellulose layer	150, 450, 800	1	1, 400, 425, 550	A	This study
K2A7	liquid	0	4.6076 ± 0.0007	green cellulosic small	cellulose layer	150, 450, 800	1	.00, 450, 550	B	This study
K2A8	liquid	0	4.4781 ± 0.0004	green cellulosic small	cellulose layer	-	-	-	-	This study
K2G1	liquid	P2	6.8843 ± 0.0004	cellulosic	cellulose layer/deposit	150, 450, 800	1	1, 400, 425, 550	A	This study
K2G10	liquid	0	4.9752 ± 0.0016	cellulosic small	cellulose layer/deposit	150, 450, 800	1	.00, 450, 550	B	Gullo et al., 2012
K2G11	liquid	0	1.0638 ± 0.0003	white cellulosic	cellulose layer/deposit	150, 450, 800	1	1, 400, 425, 550	A	Gullo et al., 2012
K2G12	liquid	0	6.2805 ± 0.0001	small cellulosic	cellulose layer/deposit	150, 450, 800	1	1, 400, 425, 550	A	Gullo et al., 2012
K2G14	liquid	0	7.7414 ± 0.0005	white cellulosic	cellulose layer/deposit	150, 450, 800	1	1, 400, 425, 550	A	Gullo et al., 2012
K2G15	liquid	0	7.5448 ± 0.0001	creamy	cellulose layer/deposit	150, 450, 800	1	.00, 450, 550	A	Gullo et al., 2012
K2G2	pellicle	P2	6.2548 ± 0.0004		cellulose layer/deposit	150, 450, 800	1	1, 400, 425, 550	A	Gullo et al., 2012
<b>K2G29</b>	pellicle	6	7.5848 ± 0.0002	cellulosic	cellulose layer	150, 450, 800	1	.00, 450, 550	B	Gullo et al., 2012
=UMCC 2967)										
K2G30	pellicle	6	23.1829 ± 0.0001	cellulosic	cellulose layer/deposit	150, 450, 800	1	.00, 450, 550	B	Gullo et al., 2012
K2G31	pellicle	6	1.1267 ± 0.0007	cellulosic	cellulose layer/deposit	-	-	-	-	Gullo et al., 2012
<b>K2G32</b>	liquid	6	9.9976 ± 0.0003	cellulosic	cellulose layer/deposit	150, 450, 800	1	1, 400, 425, 550	A	Gullo et al., 2012
=UMCC 2968)										
K2G34	liquid	6	6.6614 ± 0.0001	cellulosic	cellulose layer	-	-	-	-	Gullo et al., 2012
K2G35	liquid	6	1.9314 ± 0.0005	cellulosic	cellulose layer/deposit	150, 450, 800	1	1, 400, 425, 550	A	Gullo et al., 2012
K2G36	liquid	6	0.5929 ± 0.0004	yellow cellulosic	cellulose layer	150, 450, 800	1	.00, 450, 550	B	Gullo et al., 2012
<b>K2G38</b>	liquid	6	9.6957 ± 0.0009	cellulosic	cellulose layer	150, 450, 800	1	1, 400, 425, 550	A	Gullo et al., 2012
=UMCC 2969)										
<b>K2G39</b>	liquid	6	10.3957 ± 0.0001	cellulosic	cellulose	150, 450, 800	1	.00, 450, 550	B	Gullo et al., 2012

=UMCC 2970)

<b>K2G41</b>	liquid	6	9.1443 ± 0.0003	cellulosic	cellulose layer	150, 450, 800	1	00, 450, 550	B	Gullo et al., 2012
--------------	--------	---	-----------------	------------	-----------------	---------------	---	--------------	---	--------------------

=UMCC 2971)

<b>K2G44</b>	pellicle	12	5.9500 ± 0.0005	dark brown cellulose	cellulose layer/deposit	150, 450, 800	1	0, 400, 425, 550	A	Gullo et al., 2012
--------------	----------	----	-----------------	----------------------	-------------------------	---------------	---	------------------	---	--------------------

=UMCC 2972)

<b>K2G46</b>	liquid	12	9.1195 ± 0.0007	brown cellulose	cellulose layer/deposit	-	-	-	-	Gullo et al., 2012
--------------	--------	----	-----------------	-----------------	-------------------------	---	---	---	---	--------------------

<b>K2G5</b>	liquid	P2	8.0605 ± 0.0003	white cellulosic	cellulose layer	-	-	0, 400, 425, 550	A	Gullo et al., 2012
-------------	--------	----	-----------------	------------------	-----------------	---	---	------------------	---	--------------------

=UMCC 2966)

<b>K2G6</b>	liquid	P2	7.7533 ± 0.0003	white cellulosic	cellulose layer/deposit	150, 450, 800	1	0, 400, 425, 550	A	Gullo et al., 2012
-------------	--------	----	-----------------	------------------	-------------------------	---------------	---	------------------	---	--------------------

<b>K2G8</b>	liquid	0	6.8343 ± 0.0002	white cellulosic	cellulose layer	150, 450, 800	1	0, 400, 425, 550	A	Gullo et al., 2012
-------------	--------	---	-----------------	------------------	-----------------	---------------	---	------------------	---	--------------------

(-) not detected; \* Strain labeling: K (Kombucha tea); 1 (BTK); 2 (GTK); A (ACB medium); G (GYC medium); Number: progressive number. BC: bacterial cellulose; BTK: black tea kombucha; GTK: green tea kombucha.



Qualitative cellulose tests confirmed their ability to produce BC. Significant macroscopic diversity in the cellulosic material was observed, coupled with high variability in terms of amount of BC, as reported in Figure 3-1. The strains with a BC production level of at least higher than 4 g/L were deposited in the UMCC culture collection with the code reported in Table 3-1.

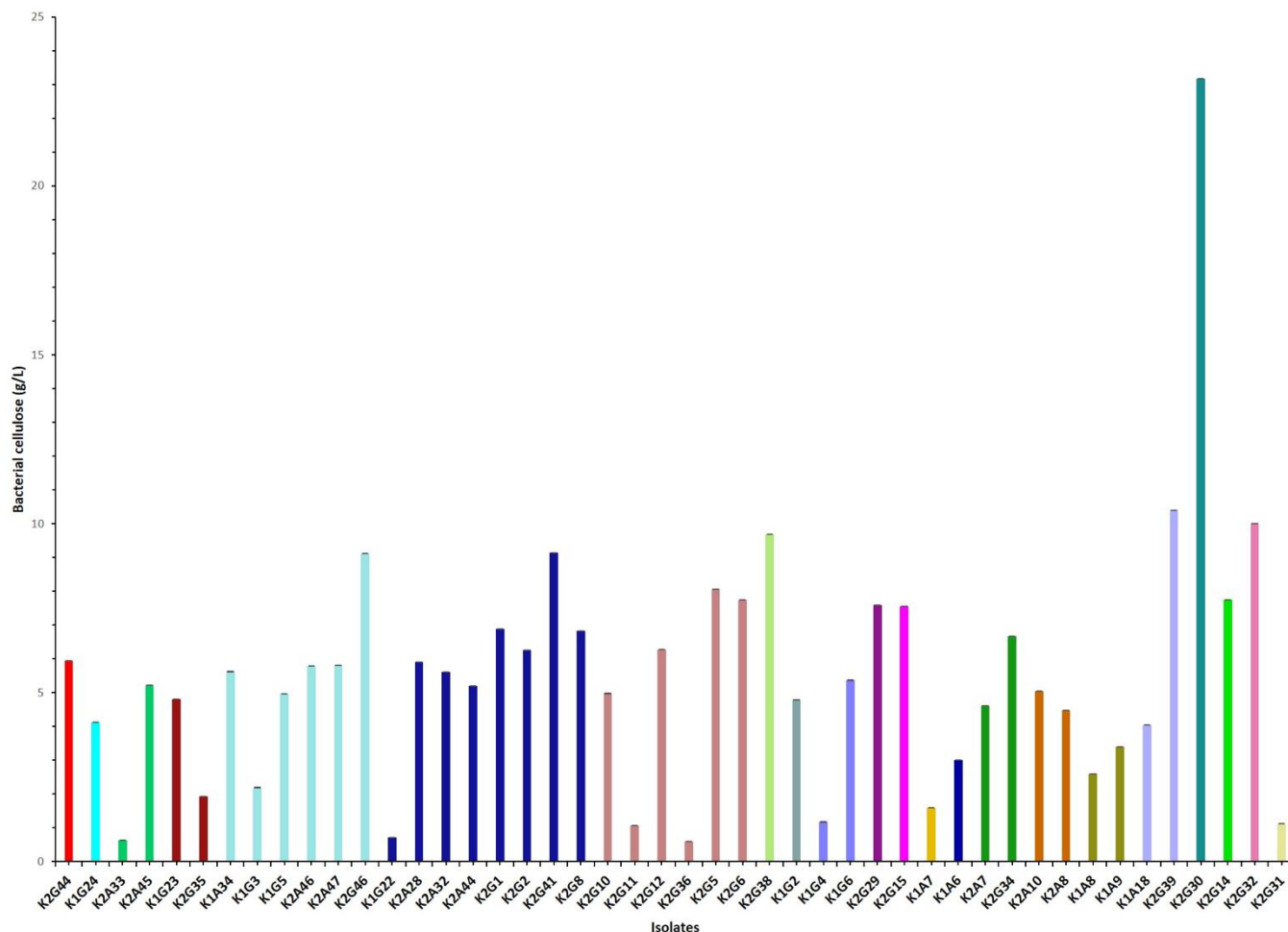


**Figure 3-1.** Bacterial cellulose yields of selected strains isolated from Kombucha tea. Each value is the mean of three parallel replicates  $\pm$  standard deviation.

### Diversity of Acetic Acid Bacteria from Kombucha Tea

The RFLP analysis on 16S rRNA, using *RsaI* and *AluI* restriction endonucleases, was conducted as a preliminary test to investigate the diversity of isolates recovered from kombucha tea samples. The mapping analysis based on the size of the fragments obtained by *RsaI* and *AluI* showed high homogeneous results, indicating the isolates as members of the same species. This evidence was in agreement with a previous study (Mamlouk and Gullo, 2013) which grouped *Komagataeibacter* strains according to *RsaI* and *AluI* restriction enzymes and observed similarities between the pattern of *K. xylinus* DSM 2004 with the *Komagataeibacter* strains investigated in this study. The low variability of the fingerprinting pattern is also consistent with previous studies on the high similarity of the 16S rRNA gene among the *Komagataeibacter* genus and especially within the *K. xylinus* species (Mamlouk and Gullo, 2013; Ludwig and Klenk, 2015).

From the genotyping of strains performed by using (GTG)<sub>5</sub> and ERIC fingerprinting techniques, two dendrograms were generated (Figure 3-2). Based on the cluster cut-off analysis, profiles

obtained using the amplification of interspersed tandem repeats GTG (Figure 3-2) were capable of discriminating between the strains considering a minimum percentage of similarity of 27.9%. A total of five major clades were created with a discrimination power of 0.42, calculated using the D index (Simpson index) (Hunter and Gaston, 1988). In order to improve the discrimination power of the analysis, we considered a minimum percentage of similarity of 70%. At this percentage of similarity, the resulted discrimination power was 0.94, defining 20 different biotypes. Among the detected clades, eight of them included just one isolate while seven were formed by two isolates. It was possible to distinguish two major clades, of which, one included nine isolates (clade 18) and another included five isolates (clade 19). The two reference strains, represented by K1G4 (=UMCC 2947) and K2G30 (=UMCC 2756) clustered into two different clades, represented by clades 19 and 7, respectively. The similarity percentage among the two references was 40.2%. The phylogenetic tree obtained from the digitized pattern profile using ERIC rep-PCR is represented in Figure 3-3. Based on the clustering cut-off analysis, ERIC was able to discriminate using a minimum similarity percentage of 40%, identifying five major clades, as in the case of (GTG)<sub>5</sub>. The clustering cut-off analysis discriminated a total of 19 biotypes, with a discrimination power of 0.95, slightly higher compared to (GTG)<sub>5</sub>. A total of six clades were represented by just one isolate, while the remaining isolates were well distributed among the detected clades. Three clades were represented by five isolates (clade 7, 16, and 17) and two clusters by four isolates (clade 8 and 9). The remaining clades were represented by three and two isolates. The number of detected clades was not so different compared to (GTG)<sub>5</sub> and, also in this case, the reference strains (K1G4 and K2G30) were found to be separated into two different groups (clade 15 for K1G4 and clade 12 for K2G30). The similarity of Dice indexes based on the patterns obtained from ERIC rep-PCR was 56.7%; quite similar to that obtained using (GTG)<sub>5</sub> rep-PCR (40.2%).

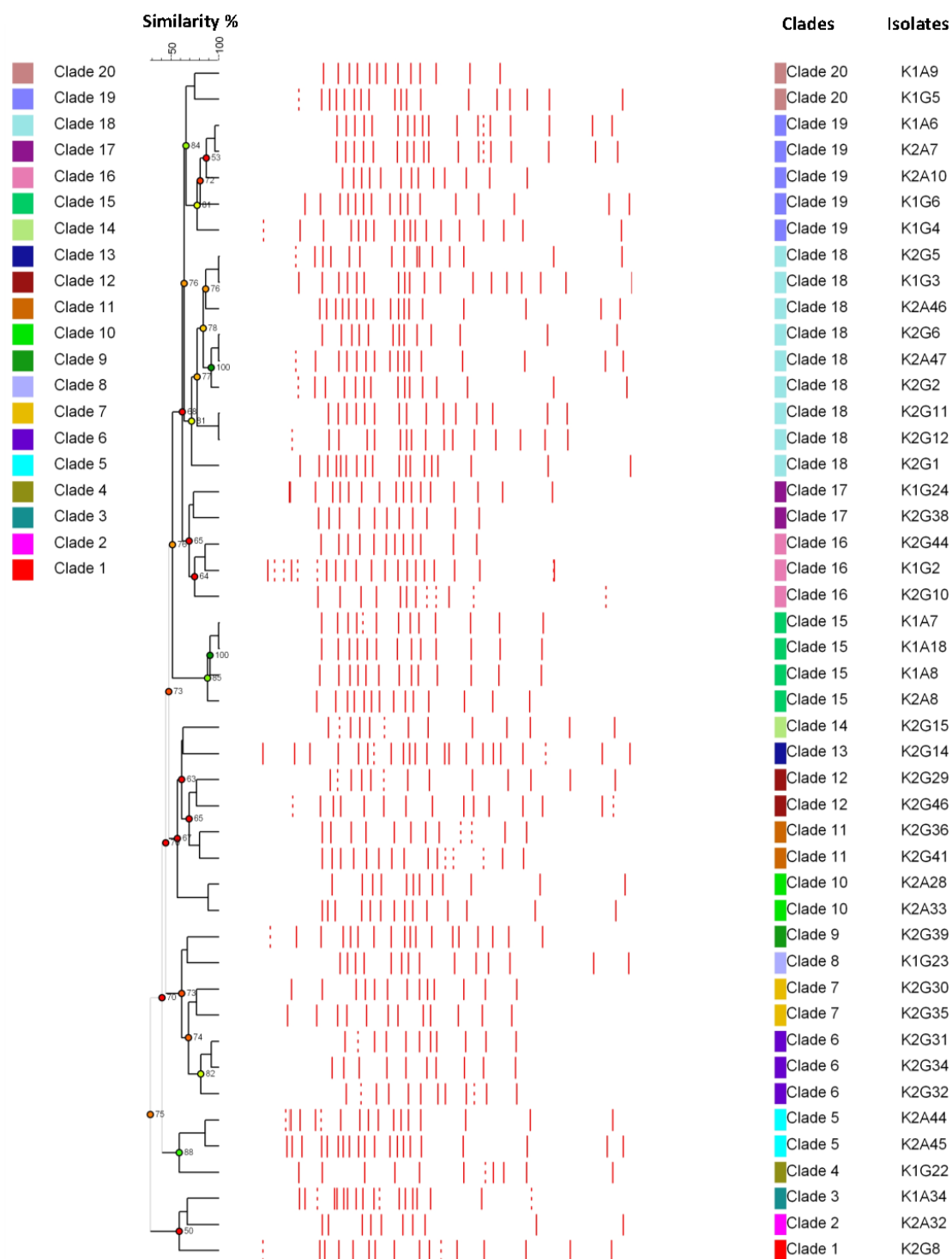


**Figure 3-2.** Dendrograms obtained from UPGMA analysis, using Dice's coefficient, of the digitized patterns obtained from (GTG)<sub>5</sub> rep-PCR. The similarity threshold for biotypes discrimination was 70%. The cophenetic coefficient is represented by numbers and dots colored as red–orange–yellow–green, based on the branch quality.

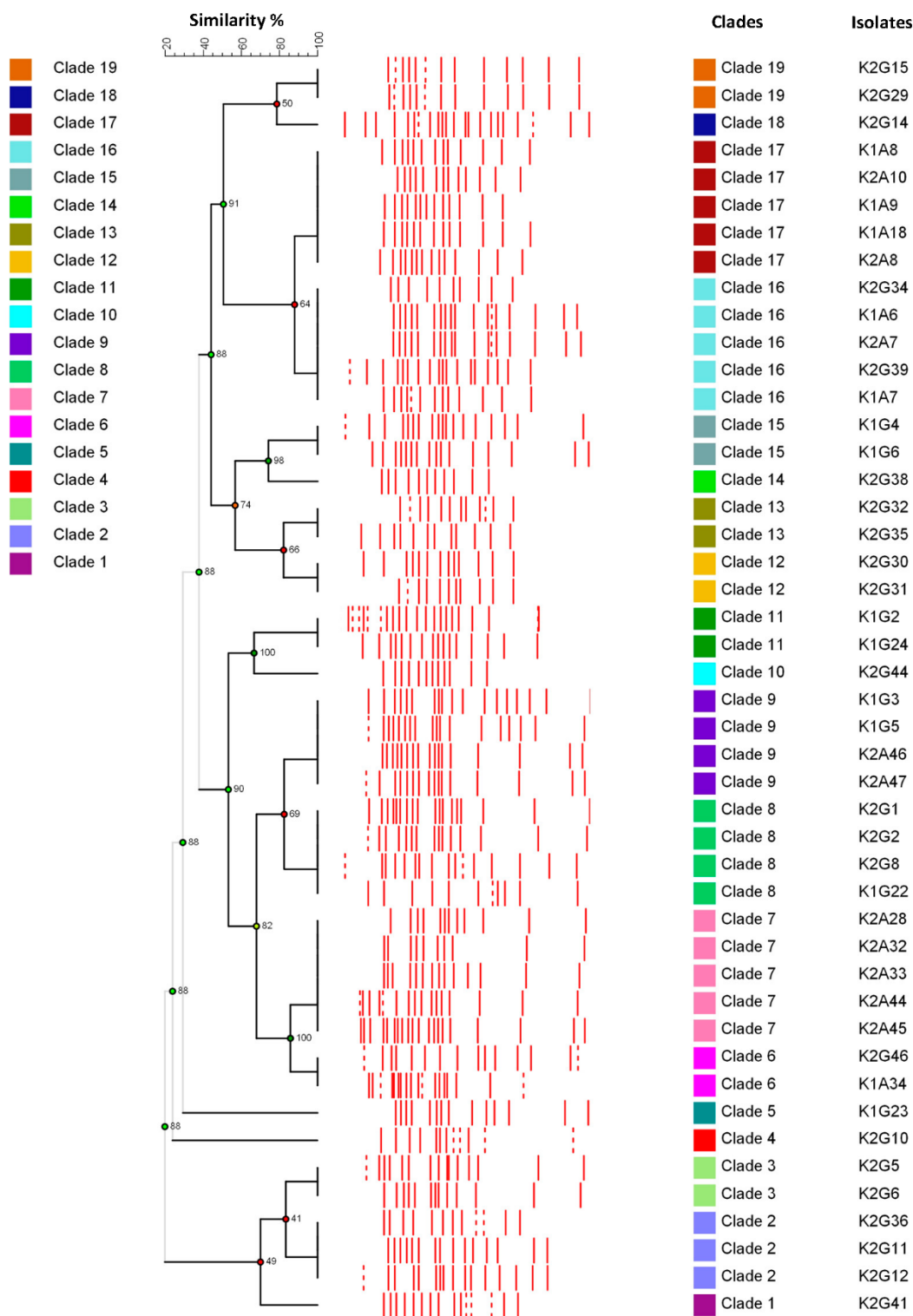


**Figure 3-3.** Dendrograms obtained from UPGMA analysis, using Dice's coefficient, of the digitized patterns obtained from ERIC rep-PCR. The similarity threshold for biotypes discrimination was 70%. The cophenetic coefficient is represented by numbers and dots colored as red–orange–yellow–green, based on the branch quality.

### Improving the Fingerprinting of *Komagataeibacter* Strains

In order to improve the sensitivity of the intraspecific discrimination, the data obtained from both rep-PCR assays were combined. The clustering analysis is reported in Figure 3-4. Based on the cluster cut-off analysis, the combination of  $(GTG)_5$  and ERIC rep-PCR allowed for discriminating the isolates, grouping them into 22 clades, considering a similarity percentage threshold of 94%.

The discrimination power, calculated as the Simpson index, was 0.94, mining a high intraspecies diversity. Most of the isolates were grouped into three clusters (clade 5, 6, and 7) representing 43.5% of the isolates ( $n = 20$ ). The remaining isolates ( $n = 26$ ) were dispersed in 19 clades, of which, most of them consisted of just one isolate ( $n = 12$ ). The reference strains were clustered into two different clades, as observed in both the case of (GTG)<sub>5</sub> and ERIC rep-PCR. Clade 10, in which K1G4 was clustered with K1G6, and clade 19, where K2G30 clustered alone, had a similarity percentage of Dice index of 84.9%, higher considering the separated results from (GTG)<sub>5</sub> and ERIC rep-PCR. This result is in agreement with the meaning of the combined analysis, since the two reference strains belong to the species of *K. xylinus*, as previously stated (Gullo et al., 2019; La China et al., 2020).

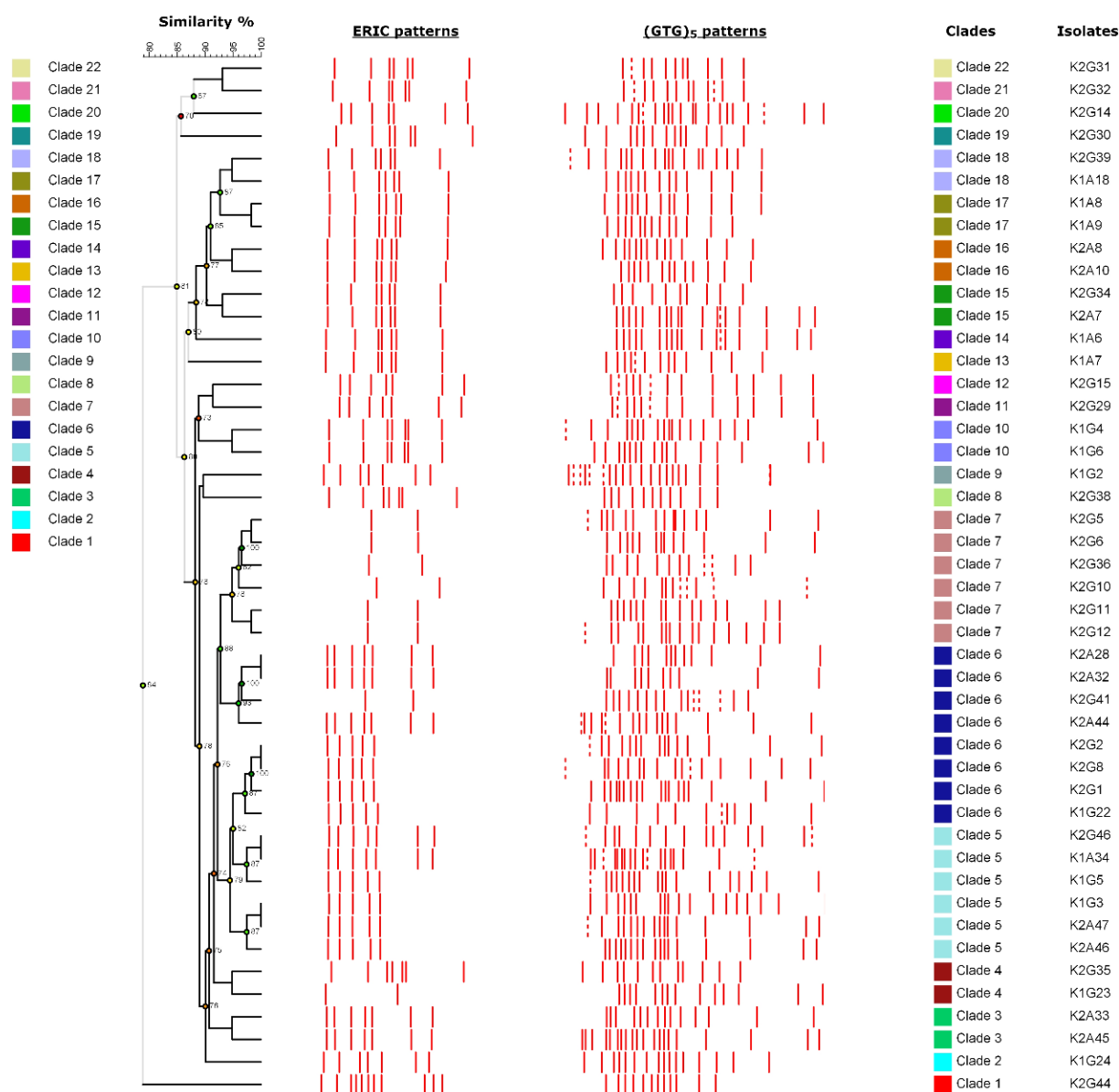


**Figure 3-4.** Dendrogram obtained combining the digitalized patterns from both (GTG)<sub>5</sub> rep-PCR and ERIC rep-PCR. The dendrogram was drawn from UPGMA analysis using Dice's coefficient. The discrimination of biotypes was performed considering a similarity threshold of 94%. The cophenetic coefficient is represented by numbers and dots colored as red–orange–yellow–green, based on the branch quality. Cluster colors were defined in agreement with the Figure 3-1.

## Correlation between Strains and Cellulose Yield

In order to understand putative correlation of the BC yield obtained from isolates with time and environmental factors, such as sampling fraction (pellicle or liquid) and clustering methods applied in this study, a Spearman correlation index was calculated. At the beginning all clades that resulted from the combined fingerprinting approach (Figure 3-4) were compared with all variables (3-5a). All factors seemed to strongly influence the BC yields. Only the time of sampling seemed to slightly influence BC production, but with a low value ( $R^2 = -0.38$ ,  $p = 0.009$ ). In order to understand how the sampling time could affect BC yield, the three most abundant clades, represented by clade 5, 6 and 7 were evaluated by calculating the Spearman coefficient, considering both time and sampling fraction. Regarding clade 5 ( $n = 6$ ) (Figure 3-5b), the time seems to correlate positively ( $R^2 = 0.84$ ,  $p = 0.03$ ). Indeed, the amount of BC (Figure 3-1) was higher for isolates sampled at day 12 (K2A46, K2A47, K2G46 and K1A34) and lower for isolates sampled at day 0 and from the preculture (K1G5 and K1G3 respectively). In clade 6 ( $n = 8$ ) (Figure 3-5c), BC yield seems to be not statistically correlated by the sampling time ( $R^2 = -0.70$ ,  $p > 0.05$ ). Regarding clade 7 ( $n = 6$ ) (Figure 3-5d), the sampling time negatively affects the BC amount ( $R^2 = -0.92$ ,  $p = 0.009$ ).

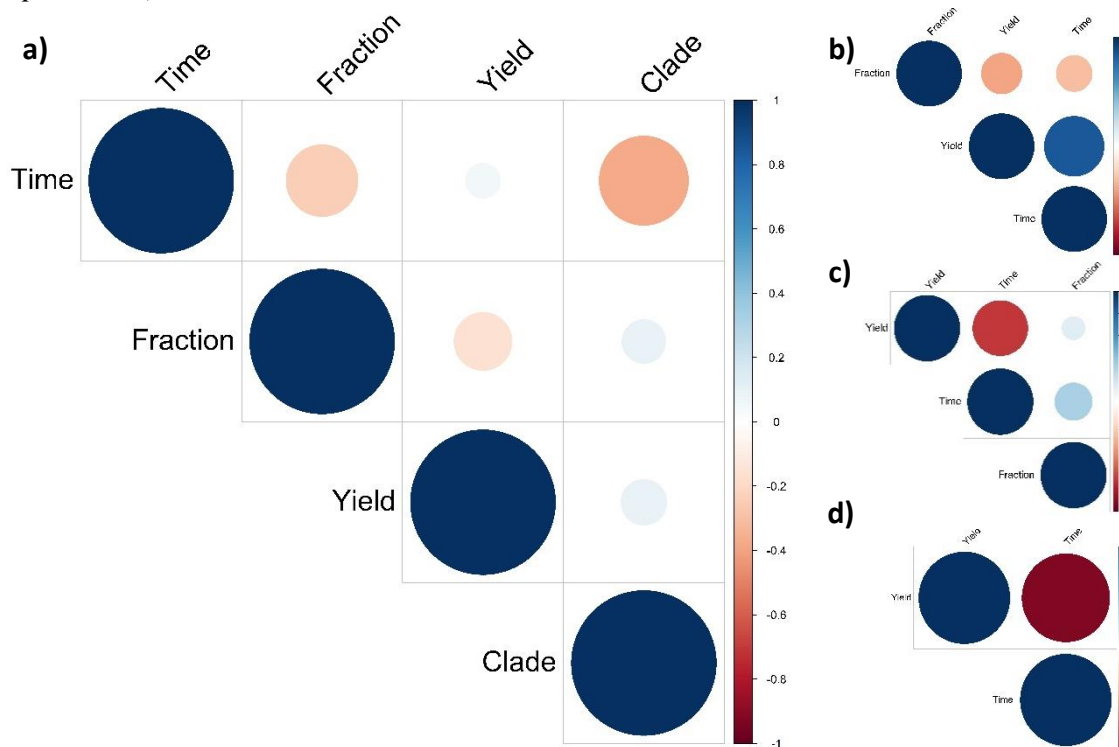


**Figure 3-5.** Correlation plot of the most abundant clades. Spearman correlation among time, environmental variables and obtained yields. (a) All retrieved clades were compared with time and environmental variables. Yield obtained within (b) clade 5, (c) clade 6 were compared with time and fraction variables. For clade 7 (d), includes only isolates sampled from liquid fraction.

## Discussion

Bacterial cellulose is receiving a great deal of attention due to several features that make it suitable for many biotechnological applications, such as biomedical devices, food packaging components and engineering materials (Robotti et al., 2018; Haghghi et al., 2020; Jakmuangpak et al., 2020).

It is well known from the literature that kombucha tea represents one of the most abundant reservoirs of BC producer bacteria, in particular, strains belonging to the *Komagataeibacter* genus (Sievers et al., 1995; Villarreal-Soto et al., 2018).

In this study, kombucha tea was chosen as a selective source for recovering cellulose producing bacteria. A total of 46 isolates were selected as the main components of the liquid and pellicle fractions of GTK and BTK kombucha tea samples and their phenotypic and genotypic variability was evaluated. RFLP of 16S rRNA gene and an analysis of the interspecific variability of isolates was conducted, and the results were discussed, considering the available genome sequences of strains K1G4 and K2G30.

The data obtained by RFLP analysis showed a very low variability in terms of the number of different species isolated from kombucha tea. This result is in agreement with previous studies reflecting both the low species diversity in kombucha tea (Sievers et al., 1995), as well as the difficulty of taxonomic assignment of *Acetobacteraceae* by using 16S rRNA gene, due to its similarity in high phylogenetic related organisms, as extensively reported in the literature (Cleenwerck et al., 2002).

Considering the analysis of the intraspecific variability within bacteria, usually, genotyping is performed using the amplification of highly conserved tandem repeat regions that are widely dispersed in the genome. The amplification of repeated elements of genomic DNA, such as (GTG)<sub>5</sub> and ERIC sequences, offers some advantages in terms of costs and rapidity, and is well developed for several Gram-negative and Gram-positive bacterial species, such as *Lactobacilli* (Gevers et al., 2001) and *Enterococci* (Švec et al., 2005) and acetic acid bacteria (De Vuyst et al., 2007).

In this study, the clustering analysis using the digitized patterns of (GTG)<sub>5</sub> elements revealed the clustering of the 46 isolates into five large clusters considering a cluster cut-off value of 50% in similarity. The discrimination power of this analysis was 0.94 considering a similarity threshold of 70%. At this similarity value, a total of 20 different biotypes were detected. Similar results were obtained using the amplification of ERIC repeated elements. Considering the cluster cut-off analysis, the comparison of the digitized patterns of ERIC rep-PCR showed a clustering of the 46 isolates with a similarity percentage of 50%, the same result obtained using (GTG)<sub>5</sub> rep-PCR. The discrimination power of ERIC fingerprint was 0.95, very similar to the (GTG)<sub>5</sub> rep-PCR, considering a similarity percentage of 70. Based on these results, a total of 19 different clades were identified, compared to the 20 obtained using (GTG)<sub>5</sub> rep-PCR. In both the fingerprint approaches, K1G4 and K2G30, previously identified as *K. xylinus* (Gullo et al., 2019; La China et al., 2020), were considered as reference strains and they were clustered into two different clades. Among the two reference strains, the percentage of similarity was 44.2% in the case of (GTG)<sub>5</sub> rep-PCR and 56.7% for ERIC rep-PCR. These results support the hypothesis that most of the strains analyzed belong to the *K. xylinus* species and that the discrimination was performed at the strain level.

In order to improve the genotyping analysis, a combined model of the two fingerprint assays was performed (Figure 3-3). The resulting analysis showed a clusterization of the isolates into seven clades based on the cluster cut-off value of 88% of pattern similarity. The discrimination power of this analysis was 0.94 at 94% of similarity. The number of biotypes defined by the combined model was 22; meaning that an improvement of the discrimination of the isolates was achieved compared to the single results obtained by the two approaches. Additionally, concerning the reference strains (K1G4 and K2G30) in this case, we observed a grouping into two different clades, with a similarity percentage of 84.9%, meaning that all the isolates with equal or major than that

value possibly belong to the species of *K. xylinus*. Based on this consideration, all of the isolates could be assigned to the *K. xylinus* except one isolate, the K2G44, clustering out of the group, with a similarity percentage of 78.8%. The data were in agreement with previous studies of the fingerprinting analysis of acetic acid bacteria (De Vuyst et al., 2007; Cleenwerck et al., 2009), in which the differences of strains among the same species (as *Komagataeibacter xylinus*) were about 80%. In this case, combining the two methods, the detection of different strains was improved.

The correlation analysis deriving from the combined strain clustering allowed us to link the BC yield with isolation time and environmental variables. A possible explanation of the obtained results may lie in the genetic plasticity features of acetic acid bacteria. It is well known in the literature that acetic acid bacteria are able to adapt themselves to environmental stressors, such as temperature and high concentration of organic acids, by acquiring genetic material from the environment or losing it. Indeed, acetic acid bacteria possess a large number of transposons genes and plasmids (Azuma et al., 2009). One example is provided by *Acetobacter* species which strains adapt themselves to environmental conditions along cultivation and fermentation cycles (Matsutani et al., 2013; Pothimon et al., 2020). In *Komagataeibacter* species the genetic plasticity has not yet been evaluated. However, we believe this aspect should be elucidated in the light to better understand the variability of BC yield within strains of *Komagataeibacter* genus.

The kombucha tea samples analyzed in this study allowed us to recover a pool of acetic acid bacteria strains, which have been characterized and deposited into the UMCC culture collection as promising candidates for BC production.



# Chapter 4

## Exploring K2G30 genome: A high bacterial cellulose producing strain in glucose and mannitol based media

Maria Gullo<sup>1</sup>, Salvatore La China<sup>1</sup>, Giulio Petroni<sup>2</sup>, Simona Di Gregorio<sup>2</sup> and Paolo Giudici<sup>1</sup>

<sup>1</sup>Department of Life Sciences, University of Modena and Reggio Emilia, Reggio Emilia, Italy

<sup>2</sup>Department of Biology, University of Pisa, Pisa, Italy

### **This chapter is published as:**

Gullo M, **La China S**, Petroni G, Di Gregorio S, Giudici P. Exploring K2G30 Genome: A high bacterial cellulose producing strain in glucose and mannitol based media. *Front Microbiol* (2019) 10:1-12. <https://doi.org/10.3389/fmicb.2019.00058>

## Abstract

Demands for renewable and sustainable biopolymers have rapidly increased in the last decades along with environmental issues. In this context, bacterial cellulose, as renewable and biodegradable biopolymer has received considerable attention. Particularly, acetic acid bacteria of the *Komagataeibacter xylinus* species can produce bacterial cellulose from several carbon sources. To fully exploit metabolic potential of cellulose producing acetic acid bacteria, an understanding of the ability of producing bacterial cellulose from different carbon sources and the characterization of the genes involved in the synthesis is required. Here, K2G30 (UMCC 2756) was studied with respect to bacterial cellulose production in mannitol, xylitol and glucose media. Moreover, the draft genome sequence with a focus on cellulose related genes was produced. A pH reduction and gluconic acid formation was observed in glucose medium which allowed to produce  $6.14 \pm 0.02$  g/L of bacterial cellulose; the highest bacterial cellulose production obtained was in 1.5% (w/v) mannitol medium ( $8.77 \pm 0.04$  g/L), while xylitol provided the lowest ( $1.35 \pm 0.05$  g/L) yield. Genomic analysis of K2G30 revealed a peculiar gene sets of cellulose synthase; three *bcs* operons and a fourth copy of *bcsAB* gene that encodes the catalytic core of cellulose synthase. These features can explain the high amount of bacterial cellulose produced by K2G30 strain. Results of this study provide valuable information to industrially exploit acetic acid bacteria in producing bacterial cellulose from different carbon sources including vegetable waste feedstocks containing mannitol.

## Introduction

Demands for renewable and sustainable biopolymers have rapidly increased in the last decades along with environmental issues. In this context, bacterial cellulose (BC), as biocompatible, renewable and biodegradable biopolymer has received considerable attention.

The primary structure of BC consists of a  $\beta$ -1,4-glucan chain which undergo aggregation events to form a ribbon-like structure (Saxena et al., 1994; Brown, 1996). These ribbons form the secondary structure that generate the well-structured 3D network, characteristic of BC (Koyama et al., 1997). The tertiary structure, as a result of intermolecular hydrogen bonds and van der Waals forces, stabilizes the entire structure through an intramolecular hydrogen bond network by hydroxyls and ring oxygen among glucose residues. Each repeating unit has a directional chemical asymmetry with respect to its molecular axis (a hemiacetal unit and hydroxyl group) (Koyama et al., 1997). The fibrous network forms a hydrogel film at air surface of culture media. Differently from its equivalent produced by plants, BC does not contain lignin and hemicellulose, it has higher degrees of purity, polymerization, crystallinity, tensile strength, water holding capacity, and biological adaptability (Costa et al., 2017; Gullo et al., 2018). Structurally, BC differs from plant cellulose on the basis of cellulose I $\alpha$  and I $\beta$  content (Atalla and VanderHart, 1984). These two allomorphs coexist always in nature and differ for the crystal system: the I $\alpha$  is characterized by triclinic system, whereas I $\beta$  by a monoclinic system. Cellulose I $\alpha$  is the predominant allomorph in BC, ranged from 60 to 80%. On the other hand, the allomorph I $\beta$  is the predominant form of plant cellulose (Nishiyama et al., 2002, 2003).

All BC properties are strictly linked to both intracellular biosynthesis and extracellular self-assembling mechanism. It is widely accepted that BC is synthesized within the bacterial cell as individual molecules. The biosynthesis occurs on the periplasmic space by cellulose synthase

(CS), a membrane protein complex formed by a series of subunits: BcsA, BcsB, BcsC, and BcsD, of which BcsA and BcsB represent the catalytic core of CS (Gullo et al., 2018). The CS genes are organized in an operon that, based on the genus, are divided into three classes, which differ in content and structure. The first class is represented by the operon originally described in the *Komagataeibacter xylinus* species. The second one, described for the first time in *E. coli*, contains also a divergent locus, which includes genes involved in natural BC modification (Thongsomboon et al., 2018). Finally, the third class of BC operon, described in *A. tumefaciens*, consists of two convergent operons. The first three genes are ortholog of *bcsA*, *bcsB*, and *bcsZ* from *K. xylinus*, while the others are typical of *A. tumefaciens* (Matthysse et al., 2005). Similar operons are also found in members of *Actinobacteria* and *Firmicutes* phyla (Römling and Galperin, 2015).

As material generally recognized as safe (GRAS) by the United States Food and drug administration (FDA) in 1992, BC can be utilized as a fiber for different applications in biomedical, cosmetics and food (Shi et al., 2014b). Main biomedical uses include supports as substitute artificial skin, hemostatic materials, wound healing scaffolds, and controlled drug delivery (Pavaloiu et al., 2014; Picheth et al., 2017). Recently very interestingly insights were obtained using BC as a biocarrier of dihydroxyacetone, in masking the symptoms of vitiligo by providing skin pigmentation (Stasiak-Róžańska et al., 2018).

In cosmetic field, BC is an ingredient for facial mask creams and as a powder in facial scrubs products in association with other natural materials (as olive oil, Vitamin C, Aloe vera extract, and powdered glutinous rice).

In food, BC can be used as dietary fiber and as adjuvant thanks to the ability to acquire flavors and colors. It occurs in the manufacturing of nata de coco, a Philippine dessert produced from fermented coconut water, and in Kombucha tea, a fermented beverage obtained from alcoholic and acetic fermentation of sugared tea (Gullo et al., 2018).

BC production was described for different bacterial species, comprising *Rhizobium leguminosarum*, *Burkholderia* spp., *Pseudomonas putida*, *Dickeya dadantii*, *Erwinia chrysanthemi*, *Agrobacterium tumefaciens*, *Escherichia coli*, and *Salmonella enterica* species (Chawla et al., 2009; Jahn et al., 2011). Within acetic acid bacteria (AAB), different genera were reported as BC producers including *Acetobacter*, *Gluconacetobacter* and *Komagataeibacter* (Mamlouk and Gullo, 2013). AAB are considered a very versatile group of bacteria involved in a wide range of industrial process for the production of different compounds, such as acetic acid in vinegar production, gluconic acid, 2-keto-L-gluconic acid, 5-keto-L-gluconic acid, 2-keto-gulonic acid, and dihydroxyacetone (Stasiak and Błaejak, 2009; La China et al., 2018). In vinegar production, other than acetic acid they can also form BC which is considered as a disadvantage because it negatively affects the process and the sensorial properties of the product (Gullo and Giudici, 2008; Gullo et al., 2016). On the other hands, vinegar has been used as an appropriate substrate for studying the mechanism of BC synthesis by AAB (Gullo et al., 2018). Species of the genus *Komagataeibacter* are widely detected in vinegar such as *K. europaeus* and its closely related species *K. xylinus*, which is considered as a model organism for BC synthesis (Römling, 2002).

Given the wide range of use of BC and the increasing of the market of bacteria cellulose-based materials, which is expected to exceed 500 million US dollars by 2023 (based on market research report1 ), there is a need to link the knowledge of science to its industrial scale-up. Although a

number of studies have highlighted great potential of application, others demonstrate limitations in term of process and economic sustainability (Gullo et al., 2017; Islam et al., 2017; Basu et al., 2018).

Main issues in BC production arise from the organism and the cultivation conditions, which affect the implementation of advantageous industrial processes. However, a number of works aiming at selecting robust wild strains and obtaining engineered strains are available. These studies mainly focuses *Komagataeibacter* species (*K. xylinus* and *K. hansenii*), tested in different culture conditions (Hwang et al., 1999; Kuo et al., 2010; Costa et al., 2017; Gullo et al., 2017). The most widely system of production is the static regime by which layers of different form and thickness are obtained, according to the ratio surface/volume (S/V) of vessels. Also the production by agitated cultivation system is reported, but it seems to provide a lower yield and generally BC is formed as spheres (Gullo et al., 2018).

Regarding the raw materials for producing BC, both the need to reduce costs and the need to provide more sustainable productions, encouraged the use of vegetable waste feedstocks containing suitable carbon sources (Kuo et al., 2010; Cheng et al., 2017b; Costa et al., 2017). Promising results were provided from lignocellulosic materials such as wheat straw, sugarcane bagasse, rice straw, hydrolysate fiber sludge, and corn steep liqu(Hwang et al., 1999; da Silva Filho et al., 2006; Cavka et al., 2013; Narh et al., 2018). Carbon sources mainly contained in these products are glucose, sucrose, and polyols as mannitol and xylitol, that are also naturally found in fruits, other vegetables, and also produced by bacteria and yeasts (Song and Vieille, 2009).

Focusing, on genes related to BC synthesis, in this work we present the genome sequencing of K2G30 (UMCC 2756), an AAB strain from Unimore Microbial Culture collection, previously selected as highly BC producing strain (Gullo et al., 2017). We also tested the BC production ability of K2G30 in two alternative carbon sources (mannitol and xylitol), which usually occur in waste vegetables.

## Materials and Methods

### Bacterial strain and culture conditions

K2G30 strain used in this study was previously isolated from pellicle fraction of Kombucha tea (Mamlouk, 2012) and safely deposited at the Unimore Microbial Culture Collection (UMCC) under the collection number UMCC 2756. The strain was cultivated in aerobic conditions at 28°C in GY broth (glucose 5.0% w/v and yeast extract 1.0% w/v; pH 4.46 (at time 0 of cultivation), when appropriate, agar (0.8% w/v) was supplemented. Bacterial cellulose was produced in GY, mannitol medium (1.5% mannitol (w/v), 2% yeast extract (w/v) and 0.5% polypeptone (w/v); pH 5.75 at time 0 of cultivation) (Oikawa et al., 1995b) and xylitol medium (5% xylitol (w/v), 1% yeast extract (w/v) and 1% tryptone (w/v); pH 5.65 at time 0 of cultivation) (Singhsa et al., 2018). Glucose, mannitol and xylitol were purchased from Merck KGaA, Darmstadt, Germany; yeast extract from Thermo Fisher Scientific Inc., All the media were sterilized by autoclaving at 121°C for 15 min prior the use.

## **Bacterial cellulose production in glucose, mannitol, and xylitol broths**

K2G30 was first cultivated in GY broth at 28°C for 5 days under static conditions. Aliquots were used to prepare preinocula in mannitol and xylitol broths, respectively. Triplicate assays were conducted in 500 mL beakers (diameter 8.7 cm) containing 150 mL of the respective broths inoculated with 5% (v/v) of the preinoculum culture. Cultures were incubated at 28 °C for 9 days under static conditions. Moreover, cultivation in agitated conditions (130 rpm/28 °C/5 days) was performed in 100 mL flasks using 40 mL of each broth inoculated with 5% (v/v) of the preinoculum.

## **Bacterial cellulose harvesting, purification and weighing**

BC pellicles collected at 3, 6, and 9 days of cultivation were washed with deionized water and treated with NaOH 1 M at 80 °C for 40 min to remove bacterial cells; they were washed several times with deionized water to reach neutral pH, and finally dried at 37 °C until constant weight. After performing experiments in triplicate, meaningful values were determined. The BC weight was expressed as previously reported (Gullo et al., 2017).

## **Analytic determinations**

D-glucose and D-Gluconic acid were measured by enzymatic kits (Megazyme Ltd., Bray, Ireland) according to the manufacturer's instructions. pH was measured using an automatic titrator (TitroLineQR EASY SCHOTT Instruments GmbH, Mainz, Germany), equipped with an SI Analytics electrode (SI Analytics, GmbH, Mainz, Germany). The samples were obtained collecting 5 mL of each culture medium in three-day intervals.

## **Genomic DNA extraction and sequencing**

Genomic DNA (gDNA) extraction from K2G30 was performed on a total 40 ml of GY culture, after 5 days of incubation at 28 °C. The liquid culture was centrifuged at 10,000 g/4°C/10 min. gDNA was extracted as previously described (Gullo et al., 2006) and it was quantified using Qubit 2.0 (Invitrogen, Carlsbad, CA, United States). A total 100 ng was used for sequencing. The whole genome of *K. xylinus* K2G30 was sequenced by Admera Health LCC (South Plainfield, NJ, United States) using Nextera XT DNA Sample Preparation Kits (Illumina) and sequenced using the Illumina HiSeq X.

## **De novo genome assembly and annotation**

The primary quality check was performed using FastQC and Trimmomatic v0.36 tool (Bolger et al., 2014) which was used to remove bases with a Phred score <20. Spades v1.10.1 (Bankevich et al., 2012) was used for de novo genome assembly using careful option and kmer size of 21, 33, and 55. The quality of consensus sequences was evaluated using Quast v4.5 (Gurevich et al., 2013) and reads with length lesser than 1 Kbp were discarded. Resulted contigs were used for genome annotation. Putative coding regions were identified by Prodigal v2.6.3 (Hyatt et al., 2010), while tRNA and rRNA were predicted using tRNAscan-SE v1.3.1 and RNAmmer (Lowe and Eddy, 1997; Lagesen et al., 2007). Functional annotation of translated coding regions was performed using Blastp v2.7.1 (McGinnis and Madden, 2004) against NCBI non-redundant database and Uniprot, setting E-value threshold as 1e-5. Hmmscan v3.1b2 (Mistry et al., 2013)

was used for protein domain annotation via Pfam database and protein family definitions via Tigrfam databases. Cluster of orthologous groups (COG) were retrieved using EggNog-mapper v1.0.3 (Huerta-Cepas et al., 2017). These data sources were combined and manually curated using Artemis genome browser (Carver et al., 2012) to assert a product description for each predicted protein. Genome ideogram reconstruction was performed using Circos v0.69 (Krzywinski et al., 2009). The genome version discussed in this study is the version K2G30\_v1.0. Fastq files and genome assembly fasta file are available at GeneBank, under the accession number QQBI000000000.

### Phylogenetic genome reconstruction

16S and 23S rRNA sequences and genome-to-genome sequence similarity analysis were performed. The related 16S and 23S rRNA sequences were downloaded from Silva SSU and LSU databases and from Joint Genome Institute (JGI) using IMG. Both 16S and 23S were separately aligned using Muscle aligner and then concatenated using MEGAX (Edgar, 2004; Kumar et al., 2018). From concatenated alignment, a maximum likelihood phylogenetic tree was generated using Tamura-Nei model (Tamura and Nei, 1993) with 1000 replicated, setting gamma distribution option. We used also alternative method to recognize K2G30 phylogeny, as digital DNA-DNA hybridization analysis. A total of 19 genomes of Komagataeibacter genus (taxid 1434011) retrieved from NCBI were used for analysis. The average nucleotide identity values using BLAST method (ANIb) and tetranucleotide usage patterns (TETRA) for all pairwise comparisons of 19 Komagataeibacter genomes were determined. ANIb and TETRA were calculated by the use the pyani module (Pritchard et al., 2016).

## Results and discussion

### K2G30 genome features and bacterial cellulose synthase genes

In order to describe the genetic organization of BC production related genes, the genome of K2G30 was sequenced, annotated and explored. The genome of K2G30 consists of 101 contigs with a total length of 3.63 Mbp and a coverage average of 700X (Figure 4-1). A total of 22 contigs were more or equal than 50 Kbp in size and N50 and L50 were 86.67 Kbp and 11, respectively. The G C content was 62.77%, which is near to the median G C content in sequenced genomes of *K. xylinus* strains. One operon of rRNA genes was retrieved including one copy of 5S, 16S, and 23S, respectively. The number of predicted coding DNA sequences (CDS) were 3380. The genome properties and statistics are summarized in Table 4-1. More than 75% of CDS were assigned to cluster of orthologous-group classification and functional categories (COG) (Table 4-2).

**Table 4-1.** K2G30 Genome features.

Properties	Value
Contigs	101
Lenght	3.63 Mbp
N50	86.67 Kbp
L50	11
Depth of coverage	700X
CDS	3380
rRNA	3
tRNA	51

tmRNA	1
Uniprot	64.70%
Pfam	87.66%
COG	78.04%
KEGG	50.5%

Based on Uniprot alignment, in K2G30 genome, three copies of *bcs* operons were annotated, of which only one (*bcs1*) contains the full enzymatic set of CS related genes (*BcsA*, *BcsB*, *BcsC*, and *BcsD*) and the accessory proteins *CMCax*, *ccpAx*, and *BglAx* (Figure 4-2). *Bcs1* operon was localized in contig 1, at the genomic position 256838-270633 bp. The full set of CS genes is represented by *bcsA*, *bcsB* (the catalytic core of CS), *bcsC*, *bcsD*, preceded by *cmcax*, and *ccpax* genes, in upstream position, while in downstream position *bglAx* was found. The sequences similarity span from 32.82% to 98.72% with and minimum e-value score of  $2e-19$ .

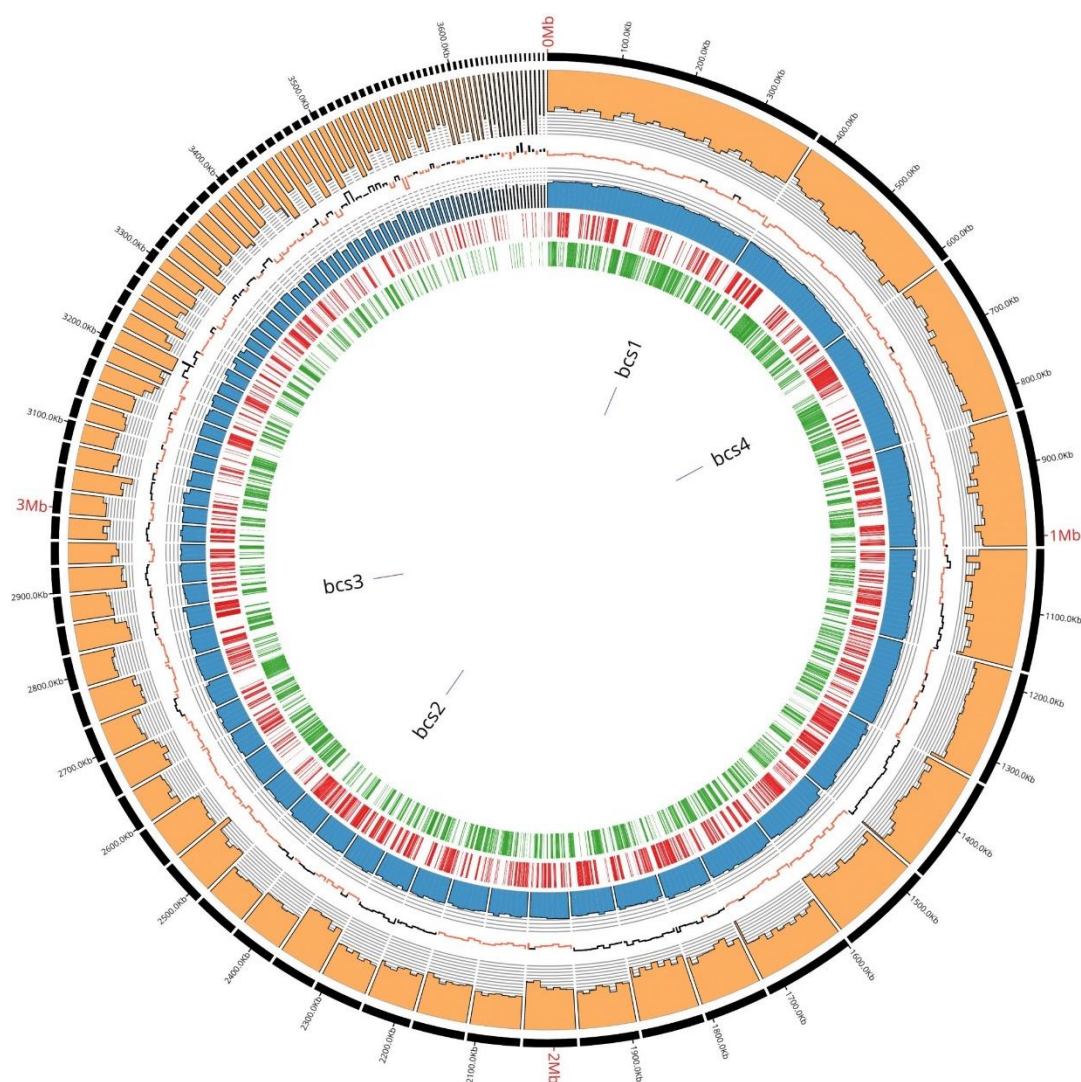


**Figure 4-1.** K2G30 genome circular representation. From outside to inside: contigs with relative lengths expressed in bp; coverage; GC skew expressed in positive changes in GC content (black) and negative (red); GC content expressed in percentage; forward CDS; reverse CDS; *bcs* operons genome localization.

*Cmcax* gene encodes for endo- $\beta$ -1,4-glucanase, while the *ccpax* role is not clear. However, it was hypothesized that it can be involved in the structural organization of the terminal complex,

cooperating with BcsD (Sunagawa et al., 2013). The downstream *bglax* gene encodes for  $\beta$ -glucosidase and seems to have also the glucosyltransferase activity (Tajima et al., 2001).

A second *bcs* operon (*bcs2*) was found in contig 19, located from 5579 to 16126 bp. This operon displays the classical architecture of *bcs2* described in other *Komagataeibacter* strains (Römling and Galperin, 2015). Differently from *bcs1* operon, in *bcs2*, the genes that encode for BcsA and BcsB subunits are fused, named *bcsAB*. No gene codifying for BcsD was detected, while the gene encoding for BcsC was detached from *bcsAB* by other two genes (*bcsX* and *bcsY*), generally described as peculiar in *bcs2* operon. The sequence similarity based on aminoacids sequences alignment was 78.79% for *bcsAB* (e-value of 0.0), instead for *bcsC* the sequence similarity was 70.24% (e-value of 0.0). The similarity of *bcsX* and *bcsY* were 92.83% and 80.05%, respectively.

**Table 4-2.** Genome cluster of orthologous groups classification and functional categories.

Categories	Functional group	Percentage (%)
C	Energy production and conversion	6.55
D	Cell cycle control, cell division, chromosome partitioning	0.96
E	Amino acid transport and metabolism	7.34
F	Nucleotide transport and metabolism	2.88
G	Carbohydrate transport and metabolism	5.31
H	Coenzyme transport and metabolism	3.81
I	Lipid transport and metabolism	2.28
J	Translation, ribosomal structure and biogenesis	5.31
K	Transcription	6.2
L	Replication, recombination and repair	7.55
M	Cell wall/membrane/envelope biogenesis	6.27
N	Cell motility	0.14
O	Posttranslational modification, protein turnover, chaperones	3.81
P	Inorganic ion transport and metabolism	6.98
Q	Secondary metabolites biosynthesis, transport and catabolism	1.17
S	Function unknown	26.81
T	Signal transduction mechanisms	2.67
U	Intracellular trafficking, secretion, and vesicular transport	2.49
V	Defense mechanisms	1.46

*bcs3* operon is located in contig 28 at position 28895-37149 bp and contains genes that encode for BcsA, BcsB and BcsC subunits. Also in this operon, the genes that codify for BcsA and BcsB were fused.



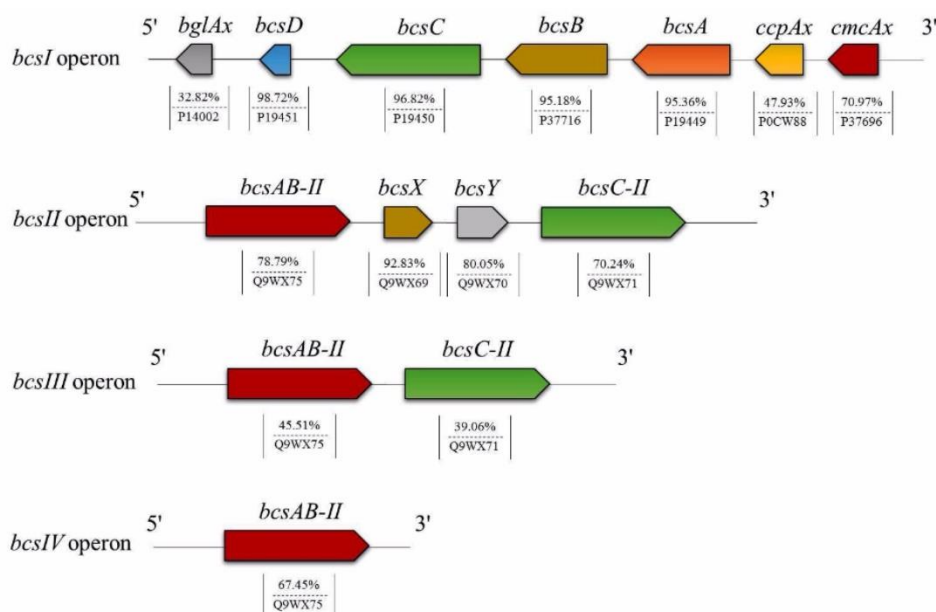


**Figure 4-2.** The arrangement of *bcs* operons and BC related genes organization in K2G30.

In addition, in K2G30, a fourth copy of *bcsAB* genes was retrieved in contig 3, having an amino acid sequence similarity of 67.45% (e-value score of 0.0). The high number of CS catalytic subunits can explain the high BC yield previously obtained from K2G30 (23 g/L) (Gullo et al., 2017). Only in another genome of *K. xylinus* species the fourth copy of *bcsAB* gene was described (Liu et al., 2018). Moreover, a variable copy number of *bcs* operon was previously reported for cellulose-producing AAB (Gullo et al., 2018). *K. hansenii* species were described to contain three copies of *bcs* operon (Iyer et al., 2010; Florea et al., 2016). In *K. xylinus*, the presence of one *bcs* operon was reported for a not BC producer strain (NBRC 3288) (Ogino et al., 2011), whereas two copies were retrieved in *K. xylinus* E25 (Kubiak et al., 2014).

## Phylogenetic Analysis

Individual alignment of 16S and 23S rRNA genes of 19 *Komagataeibacter* species were checked manually and clipped at the same length. A phylogenetic tree was generated from concatenated rRNA genes with a total length of 3687 nucleotides (nt): 16S (1118 nt) and 23S (2569 nt). The rRNA genes of two species of *Gluconobacter* genus (*G. albidus* LMG 1356<sup>T</sup> and *G. oxydans* DSM 3503<sup>T</sup>), were included in the dataset and used as outgroup. The ML tree (Figure 4-3) displays that *Komagataeibacter* species clustered in three major groups, the *K. hansenii*, the *K. europaeus* and the *K. intermedius* species. *K. medellinensis* and *K. rhaeticus* were closed in a single clade. K2G30 was clustered with the type strain (*K. xylinus* NBRC 15237<sup>T</sup>) and *K. nataicola* RZS01, with a bootstrap percentage of 78%.

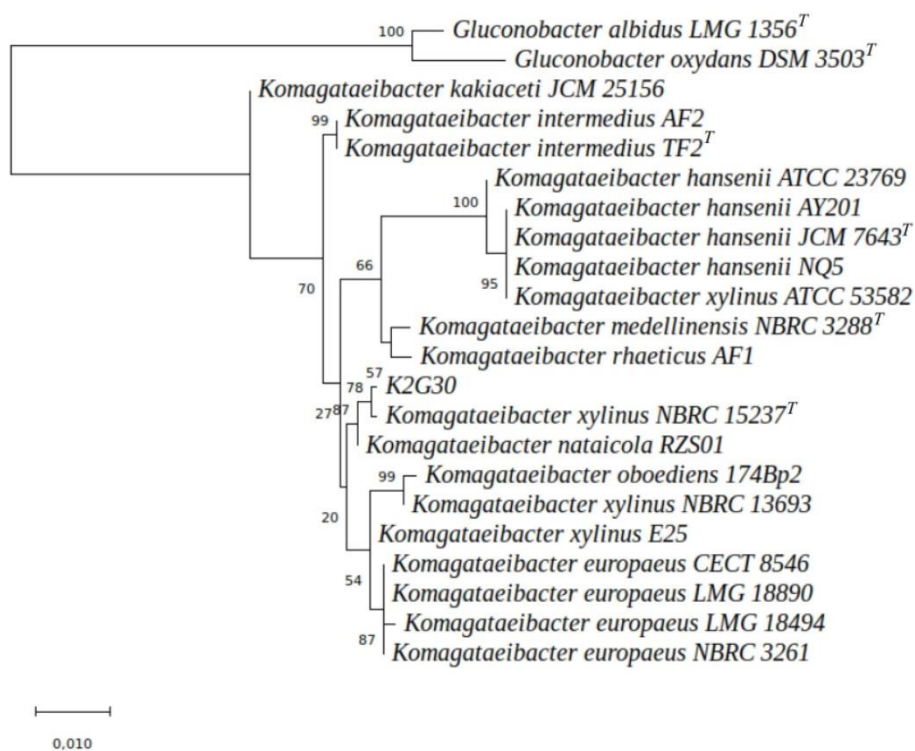


**Figure 4-3.** ML tree representing the phylogenetic distances among 19 *Komagataeibacter* genomes. The node numbers indicate the bootstrap values. The branch length was expressed in 0.010 unit.

The information gained from the phylogenetic analysis provides suitable depiction of the evolutionary position of K2G30 strain, but does not translate directly into the overall similarity of the genomes. Here, we used two approaches of digital DNA-DNA hybridization, ANIb and TETRA, which are considered two of the traditional “gold standard” for circumscribing bacterial species (Teeling et al., 2004; Konstantinidis and Tiedje, 2005). The required threshold to ascribe one species using ANIb (94% of genome sequence similarity) and TETRA (0.997) were previously defined (Richter et al., 2009).

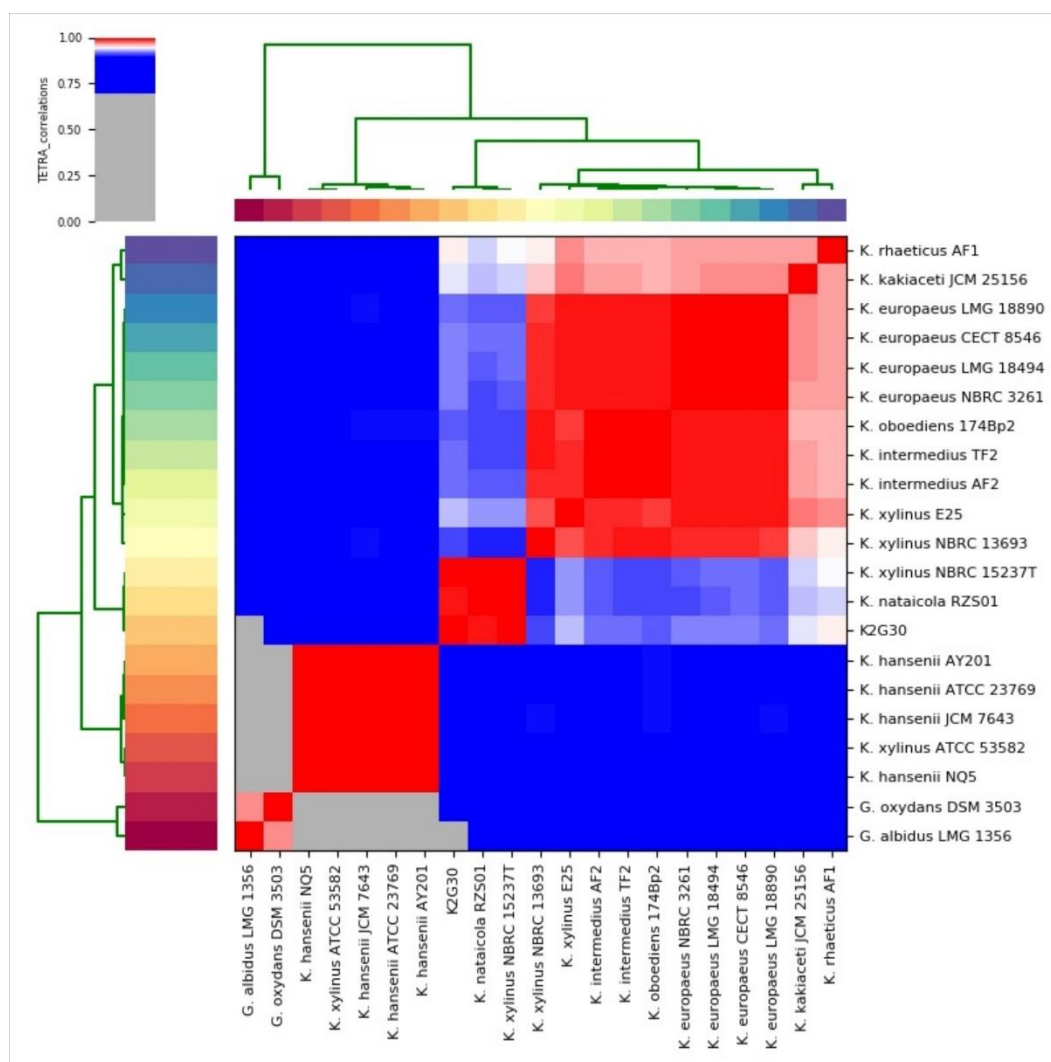


**Figure 44.** TETRA heatmap of 21 *Komagataeibacter* genomes sequences (derived from Supplementary Table S4-2). TETRA values are represented in the central bi-color gradient heatmap (red gradients  $\geq 96\%$ ; white = 95%; blue gradients  $\leq 94\%$ ).

We used the genome sequences of the species considered for ML tree reconstruction to produce the ANIb and TETRA distance matrices. As shown in Supplementary Table S4-1, the genome sequence similarity from the comparison of K2G30 and *K. xylinus* NBRC 15237<sup>T</sup> was 93.38%, just below the minimum threshold required to define a bacterial species. ANIb heatmap (Supplementary Figure S4-1) confirms the clustering order of the phylogenetic tree (Figure 4-3), showing the same three clades. The data from TETRA heatmap (Figure 4-4) were congruent with ANIb analysis and the ML tree, showing the same three large clades. The TETRA correlation value between K2G30 and *K. xylinus* NBRC 15237<sup>T</sup> was 0.9973, while the correlation value for the pairwise K2G30 and *K. nataicola* RSZ01 is 0.9952, lower than the threshold. It is clear from literature and from Figures 4-3, 4-4 and Supplementary Figure S4-1 of this study, that several strains attributed to the species *K. xylinus* do not associate with the type strain of the species (NBRC 15237<sup>T</sup>), but they cluster with other species of the genus (Lisdiyanti et al., 2006). Due to these misinterpretations, a critical revision of *K. xylinus* strains published and available in public culture collections is advisable.

Interestingly, in our analysis in which only sequenced genomes of *Komagataeibacter* are represented, just the strain we characterized (K2G30), clusters with *K. xylinus* type strain NBRC

15237<sup>T</sup> and could be confidently attributed to this species. For all those strains reported in literature as high BC producers that have been attributed *K. xylinus* species in the absence of genomic data, a critical re-examination and an identification using genomic data is needed. This would allow to verify if high BC production is indeed a specificity of *K. xylinus* or also of other species within the genus, which in former years and in absence of appropriate resolution tools, have been attributed to *K. xylinus*, but are indeed representatives of different species.

### Glucose, Mannitol, and Xylitol as Carbon Sources for Producing Bacterial Cellulose

With the aim to select the best cultivation system for obtaining BC pellicles from the strain K2G30, cultures were grown on GY broth, in both static and agitated conditions, and on GY agar medium. Well compacted BC membranes were obtained in static cultivation, whereas spheres of different size were produced in agitated cultivation system (Figures 4-5A,B).

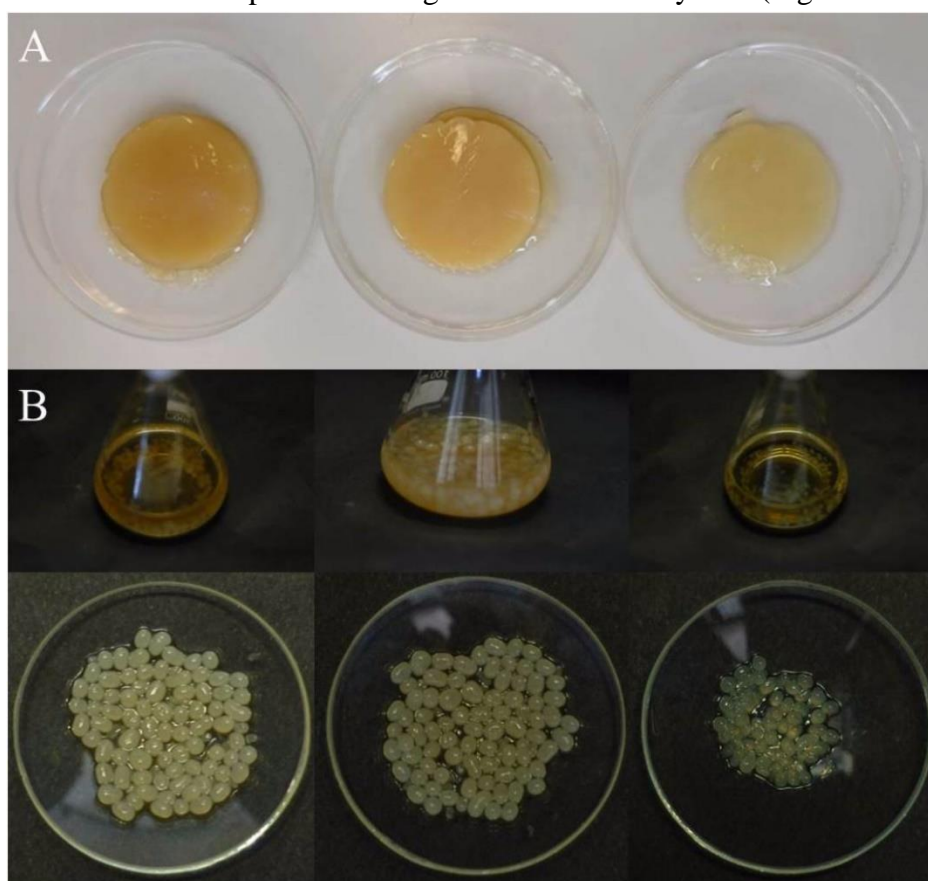


**Figure 4-5.** BC produced by K2G30 in static (A) and agitated (B) conditions. From left to right: BC produced in mannitol, glucose, and xylitol, respectively.

When we cultivated K2G30 on GY agar medium, we did not observe single colonies but a soft layer on the surface of the plates. An increase of BC yield has been obtained by different strategies including the use of double carbon sources e.g., glucose and ethanol, modified sugars and polyols (Oikawa et al., 1995a, 1995b; Canilha et al., 2008; Singhsa et al., 2018). In this study, BC production by K2G30 was tested using two polyols (mannitol and xylitol), as alternative carbon sources to glucose, by static cultivation system at 28 °C for a total of 9 days, according to Oikawa et al., 1995b and Singhsa et al., 2018, respectively. Assays were performed

in vessels (600 mL beakers) having a S/V ratio of 0.40 cm<sup>-1</sup>. BC pellicles were visible on the surface of all performed trials within 2 days of cultivation. However, different BC yields were reached in glucose broth (reference medium), mannitol and xylitol broths. The highest BC yield was observed in mannitol (1.5% (w/v) initial mannitol content) whereas xylitol broth (5% (w/v) initial xylitol content) was less performing in BC synthesis (Table 4-3).

**Table 4-3.** Bacterial cellulose production and pH values (S/V of vessel 0.40 cm<sup>-1</sup>)<sup>1</sup>.

Time (days)	Glucose (5% w/v)		Mannitol (1.5% w/v)		Xylitol (5% w/v)	
	BC (g/L)	pH	BC (g/L)	pH	BC (g/L)	pH
0	0	4.46±0.05	0	5.75±0.03	0	5.65±0.39
3	1.149±0.001	3.81±0.09	0.188±0.003	5.71±0.09	0.048±0.001	5.57±0.02
6	3.805±0.001	3.24±0.03	2.368±0.001	5.39±0.04	0.527±0.001	5.51±0.03
9	6.167±0.024	3.10±0.02	9.766±0.043	5.58±0.83	1.356±0.050	5.23±0.08

<sup>1</sup> The data are averages based on three trials, reporting the standard error values.

Within strains of the species *K. xylinus* the ability to produce BC from xylitol could be a variable trait, as previously observed by Singhsa et al., 2018, which tested five strains that produced low or moderate amount of BC, except for one strain that produced BC in higher amount (more than 1.0 g/L during 7 days cultivation).

In glucose broth (5% w/v of initial glucose content), the BC yield obtained was considerable, but less compared to the amount produced in mannitol broth (Table 4-3). From these results, it was shown that using mannitol the BC yield was increased of 43% than using glucose and that xylitol was not a preferred carbon source of K2G30 for producing BC.

In the BC production process, the accumulation of organic acids in the culture broth, such as gluconic acid and acetic acid, due to the oxidative metabolism of AAB, induces pH decreases far below the optimal value for BC production, that is estimated higher than 4 (Gullo and Giudici, 2008; Giudici et al., 2016). As previously reported the pH reduction at values below 4 is suboptimal for BC synthesis (Jonas and Farah, 1998; Gullo et al., 2017). In this study, a negligible production of gluconic acid, which induced a limited pH reduction, was observed in both mannitol and xylitol broths; whereas in glucose broth, BC formation was followed by glucose oxidation to gluconic acid and a pH decrease below 4 (Table 4-4). As in mannitol, also in xylitol broth the gluconic acid production was very low.

**Table 4-4** Gluconic acid (GlcA) production and pH values during BC production in glucose, mannitol and xylitol media (S/V of vessel 0.40 cm<sup>-1</sup>)<sup>1</sup>.

Time (days)	Glucose (5% w/v)		Mannitol (1.5% w/v)		Xylitol (5% w/v)	
	GlcA (g/L)	pH	GlcA (g/L)	pH	GlcA (g/L)	pH
0	1.353±0.741	4.46±0.05	0.927±0.017	5.75±0.03	0.530±0.044	5.65±0.39
3	12.887±0.027	3.81±0.09	1.121±0.021	5.71±0.09	1.182±0.029	5.57±0.02
6	19.580±0.091	3.24±0.03	1.109±0.033	5.39±0.04	1.144±0.028	5.51±0.03
9	29.779±0.046	3.10±0.02	1.243±0.014	5.58±0.83	1.193±0.060	5.23±0.08

<sup>1</sup> The data are averages based on three trials, reporting the standard error values.

This can be explained considering pentose and glucuronate metabolism (pathway ID KO00040), in which through different steps xylitol is converted into UDP-glucose, the precursor of BC.

Considering the metabolic pathways of mannitol and xylitol based on Kegg pathways maps, D-mannitol was converted to D-fructose and used to produce BC via galactose metabolism (pathway ID KO00051-KO00052). The candidate enzyme for this conversion seems to be D-mannitol dehydrogenase (EC 1.1.1.67). Differently from the membrane-bound enzyme polyol dehydrogenase (EC 1.1.5.2) that has low substrate specificity, D-mannitol dehydrogenase is a soluble enzyme characterized by high specificity for its substrate (Oikawa et al., 1997).

Contrary to D-mannitol, the production of BC from xylitol is a more complex pathway, involving several steps, which result less advantageous energetically for the cell.

## Conclusion

In the present study, K2G30 genome was sequenced and annotated in order to describe the key gene sets involved in BC synthesis. From genome analysis, four copies of the enzymatic core of CS and three copies of *bcs* operons were retrieved, explaining the high BC yield obtained from K2G30. From phylogenetic analysis, also the need of a re-examination within the *Komagataeibacter* genus was emphasized.

K2G30 is able to grow and to produce BC using different carbon sources, this is an additional attribute that highlights the versatility of the strain.

The choice of the carbon sources is one of the most important point in BC production, particularly for the obtainable yields. Effective BC production from glucose is questionable, due to the oxidative metabolism leading to gluconic acid production and concomitant pH decrease. Our evidences confirm the limit of using glucose as a carbon source and the suitability of other carbon sources, like mannitol, by which gluconic acid production is negligible. Considering that for industrial BC production, raw material remains a weighty production cost, the evaluation of waste feedstocks is a challenge. Since mannitol is found in a number of vegetal wastes, their use in producing BC could be promising. We therefore proposed a strategy that integrate information deriving from technological and genomic data as a platform for selecting strains and for optimizing bioprocessing for BC large-scale production.

# Chapter 5

## Genome sequencing and phylogenetic analysis of K1G4: a new *Komagataeibacter* strain producing bacterial cellulose from different carbon sources

Salvatore La China<sup>1</sup>, Andrea Bezzecchi<sup>1</sup>, Felipe Moya<sup>2</sup>, Giulio Petroni<sup>3</sup>, Simona Di Gregorio<sup>3</sup>, Maria Gullo<sup>1</sup>

<sup>1</sup>Department of Life Sciences, University of Modena and Reggio Emilia, Reggio Emilia, Italy.

<sup>2</sup>Department of Agrarian and Forestry Science, Catholic University of Maule, Talca, Chile.

<sup>3</sup>Department of Biology, University of Pisa, Pisa, Italy.

### This chapter is published as:

**La China S**, Bezzecchi A, Moya F, Petroni G, Di Gregorio S, Gullo M. Genome sequencing and phylogenetic analysis of K1G4: a new *Komagataeibacter* strain producing bacterial cellulose from different carbon sources. *Biotechnol Lett* (2020) 42:807-818. <https://doi.org/10.1007/s10529-020-02811-6>

## Abstract

The objective of this study was to evaluate the ability of a new *Komagataeibacter xylinus* strain in producing bacterial cellulose from glucose, mannitol and glycerol, and to assess the genome sequencing with special focus on bacterial cellulose related genes.

Bacterial cellulose production during 9 days of cultivation was tested in glucose, mannitol and glycerol, respectively. Differences in the bacterial cellulose kinetic formation was observed, with a final yield of 9.47 g/L in mannitol, 8.30 g/L in glycerol and 7.57 g/L in glucose, respectively. The draft genome sequencing of K1G4 was produced, revealing a genome of 3.09 Mbp. Two structurally completed cellulose synthase operons and a third copy of the catalytic subunit of cellulose synthase were found. By using phylogenetic analysis, on the entire rRNA operon sequence, K1G4 was found to be closely related to *Komagataeibacter xylinus* LMG 1515<sup>T</sup> and *K. xylinus* K2G30.

The different yields of bacterial cellulose produced on glucose, mannitol and glycerol can be correlated with the third copy of *bcsAB* operon harbored by K1G4, making it a versatile strain for industrial applications.

## Introduction

Cost-effective production of high value-added biomaterials by microbial transformations is a current challenge. Nowadays there is a great interest on the discovery and characterization of new biomaterials, especially focusing on the environmental impact and the biocompatibility features of materials (Mohite and Patil, 2014). In this scenario, bacterial cellulose (BC) plays a central role, as it is a naturally produced biopolymer from bacteria. BC is an ultra-fine polymer constituted by  $\beta$ -1,4-glucan chains. Synthesized extracellularly, BC is structurally formed by nanosized fibrils, held together by hydrogen bonds (Ross et al., 1991). The polymerization process leads to the formation of a coherent ultra-thin three-dimensional network of cellulose nanofibers aligned in parallel to the surface of a liquid medium. This network is called a pellicle and its geometry is determined by intra- and intermolecular hydrogen bonds, hydrophobic and van der Waals interactions (Gullo et al., 2018). Most of the properties that characterize BC derive from the synthesis and assembling processes. Properties like purity, high crystallinity and biocompatibility makes BC one of the most attractive polymers for biomedical, tissue engineering, food and environmental applications. Although native BC is considered adequate for different applications, the predominant research focuses on BC-based products with superior properties (Torres et al., 2019). For example, several desired features are shared between scaffolds used for different tissues, such as the possibility to modify the surface properties, the porosity, and the ability to design and shape three-dimensional structures (Bottan et al., 2015; Robotti et al., 2018; Stasiak-Róžańska et al., 2018).

Among different bacterial genera described as BC producers, *Komagataeibacter* genus and, particularly strains of the species *K. xylinus* are foremost BC producers (Römling and Galperin, 2015). Within the genus *Komagataeibacter*, a high phenotypic variability of its members is reported (Gullo et al., 2018). Considering BC synthesis, this variability can be observed within strains recovered not only from different fermenting sources, like vinegar (Gullo et al., 2016), but also from those of the same source but isolated at different time points of fermentation, which produces variable amount of BC (Valera et al., 2014; La China et al., 2018). Moreover, differences in the structure and yield can be attributed to the composition of cultivation media and the genetic organization of cellulose synthase (CS) related genes.



In this study, a new *Komagataeibacter* strain (K1G4) isolated from Kombucha tea is introduced. The BC production ability of K1G4 was evaluated using three different media, containing glucose, mannitol and glycerol, respectively. Since polyols such as glycerol and mannitol are widely distributed in higher plants, we considered them to the aim to provide information on the possibility to use vegetable waste feedstocks for producing BC. This is in line with the aim to reduce BC production costs and to the need to provide more sustainable productions. Moreover, media based on both mannitol and glycerol have already provided promising results for BC synthesis (Wang et al., 2018; Gullo et al., 2019) Glucose was chosen since it is the most common carbon source used for BC production, so it can be considered the reference carbon source to test BC production (Wang et al., 2018; Gullo et al., 2019).

Furthermore, genome sequencing was performed to understand the genetic organization of BC related genes in K1G4. To infer the phylogenetic position of K1G4 the entire operon sequence, including internal transcribed spacers (ITS) regions, was analysed.

## Materials and methods

### Bacterial strains and cultivation conditions

K1G4 strain was previously isolated from a liquid fraction of Kombucha tea, using GYC medium (10 g/L yeast extract, 50 g/L glucose, 15 g/L CaCO<sub>3</sub>, 9 g/L bacteriological agar; pH not adjusted). Kombucha tea was imported from the National Institute of Applied Sciences and Technology (INSAT), Tunisia and propagated by inoculation sterile tea (sucrose 10% w/v) of 3% w/v cellulose fraction and 10% (v/v) of fermented liquid broth from the previous culture. Fermentation was carried out at 28 °C for 15 days (Mamlouk, 2012). The strain K1G4 was deposited at UMCC (Unimore Microbial Culture Collection), under the collection code UMCC 2947.

The strains K1G4 and K2G30 were cultivated in aerobic conditions at 28 °C on glucose-yeast extract (GY) medium: 50 g/L glucose (Merck KGaA, Darmstadt, Germany) and 10 g/L yeast extract (Thermo Fisher Scientific Inc.). The medium was sterilized by autoclaving at 121 °C, 1 atm for 15 min prior the use.

### Genome DNA extraction and sequencing

Genomic DNA was extracted from a cell culture in 30 mL GY medium inoculated with 5% (v/v) of preinoculum and incubated at 28 °C for 5 days in static conditions. The liquid culture was centrifuged at 10,000g/4 °C/10 min. Genomic DNA extraction was conducted using chloroform/isoamylalcohol (Gullo et al., 2006) and it was quantified using Qubit 2.0 (Invitrogen, Carlsbad, CA, USA). A total 100 ng chromosomal DNA was used as input for the generation of Nextera XT PE library. The sequencing was performed on an Illumina HiSeq X platform in a 2 × 150 bp run by Admera Health LCC.

### Genome assembly and annotation

Genomic reads obtained from sequencing were quality filtered using Trimmomatic v0.36 tool (Bolger et al., 2014). Bases resulting with a Phred score lower than 20, were discarded. Resulting high quality reads were assembled into consensus sequences using SPAdes v1.10.1 (Bankevich et al., 2012), with k-mers size of 21, 33, 55, 77 and careful option. The quality of genome assembly was evaluated using Quast v4.5 (Gurevich et al., 2013). Contigs with length lower than 1 kbp were discarded. Genome

annotation was performed as previously described (Gullo et al., 2019). Genome raw data were deposited in NCBI SRA database, under accession number SRR9326342.

### **Phylogenetic genome reconstruction**

The phylogenetic reconstruction of K1G4 was carried out using the entire rRNA operon (*rrn*), including 16S, 23S, 5S rRNA genes and the ITS regions across those genes. A total of 37 genomes of *Komagataeibacter* genera were retrieved from NCBI genome database, using taxonomy ID 1434011. The operon sequence dataset was constructed as follows: the genomes were annotated using Barrnap v0.9 tool (<https://github.com/tseemann/barrnap>) to predict 16S, 23S and 5S rRNA genes. The coordinates obtained from rRNA gene prediction were used to retrieve the entire operon sequences in the genomes. Bedtools v2.27.1 (Quinlan and Hall, 2010) was used to obtain the sequences. In order to validate the datasets, a local blastn alignment was produced against the 16S ribosomal RNA sequences database from NCBI using Blast v2.7.1+ (McGinnis and Madden, 2004). The operon sequences of type strains *Acetobacter pasteurianus* LMG 1262 and *Acetobacter aceti* DSM 3508 were used as out-group. Retrieved sequences were aligned using Muscle v3.8.31 (Edgar, 2004). The alignment was imported into MEGAX (Kumar et al., 2018) and the non-matching sequence regions were clipped. From the alignment, a maximum likelihood (ML) phylogenetic tree was computed using Tamura-Nei DNA evolutionary model and a bootstrap value of 1000. A discrete Gamma distribution was used to model evolutionary rate differences among sites. MEGAX was also used to calculate a distance matrix among the 37 *Komagataeibacter* strains, applying Tamura-Nei substitution model, with a bootstrap value of 1000. In addition, a Gamma distribution was applied to model the evolutionary rate differences among sites. A genome-based taxonomic analysis was also performed using the average nucleotide identity based on blast (ANIb) using the python pyani module (Pritchard et al., 2016).

### **Bacterial cellulose production in glucose, mannitol and glycerol media**

K1G4 was first rehydrated from -80 °C storing conditions, by cultivation on GY broth, at 28 °C for 5 days, under static conditions. To release bacterial cells from the BC matrix, tube cultures were hand-shaken for 30 s. Then 5% v/v of culture was transferred in 30 mL of GY broth and cultivated at the same conditions. BC production was tested using the standard Hestrin-Schramm (HS) medium (yeast extract 20 g/L; 5 g/L polypeptone; 2.7 g/L disodium phosphate anhydrous and 1.15 g/L citric acid monohydrate) (Hestrin and Schramm, 1954). The carbon source, glucose, mannitol or glycerol was added at final concentration of 20 g/L, pH was adjusted to 6.20. All media were sterilized by autoclaving at 121 °C, 1 atm for 15 min. The cultivation was conducted in 600 mL beakers with a working volume of 150 mL, inoculated at 5% (v/v). Cultures were incubated at 28 °C for 9 days under static conditions. Each time-point (3, 6 and 9 days) was performed in triplicate.

### **Bacterial cellulose purification and analytical determination**

BC was collected at 3, 6 and 9 days of cultivation time and washed with deionized water. To remove bacterial cells, BC was treated with NaOH 1 M solution and incubated at 80 °C for 30 min. Subsequently, BC was washed with deionized water until neutral pH was reached. Dried BC layers were obtained by incubation at 30 °C up to a complete dehydration. BC weight was expressed as grams of dried BC per liter of broth.

For each time-point, gluconic acid (GlcA), D-glucose was measured using an enzymatic kit (Megazyme Ltd. Bray, Ireland), according to the manufacturer's instructions. The analytic

determination and pH were monitored by collecting 5 ml of culture medium at each time intervals. The pH was determined using an automatic titrator (TitroLine® EASY SCHOTT Instruments GmbH, Mainz, Germany), equipped with an SI Analytics electrode (SI Analytics, GmbH, Mainz, Germany). All determinations were conducted in triplicate.

## Results and discussion

### Genome statistics and cellulose synthase operon description of K1G4

K1G4 was previously isolated from the liquid fraction of Kombucha tea at time 0 of a fermentation trial conducted by back-sloping procedure (Mamlouk, 2012). The assembled genome of K1G4 covers 3.09 Mbp and consists of 169 contigs greater than 1 kbp, with an average in depth of 269 X (Figure 5-1).

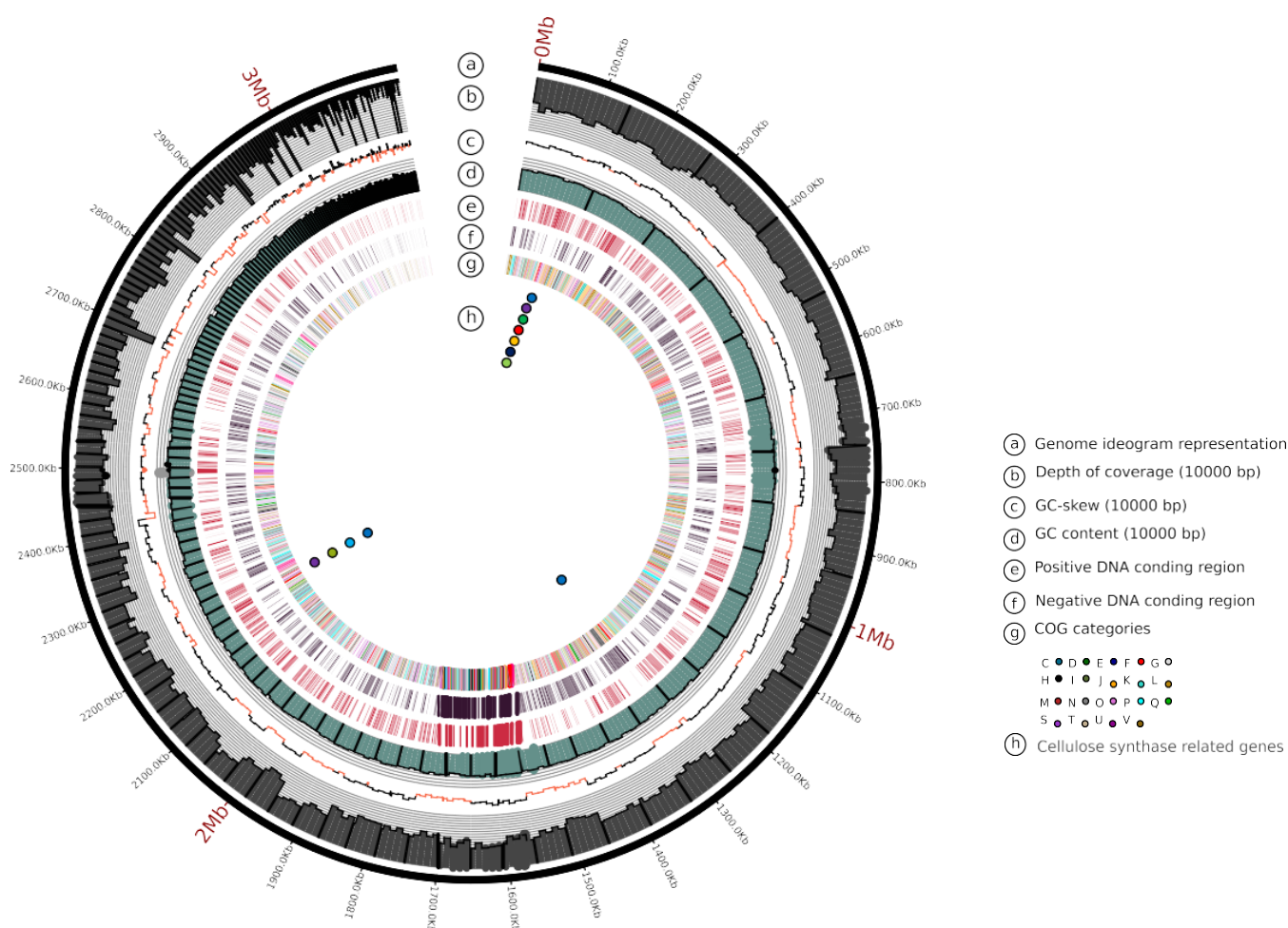


**Figure 5-1.** K1G4 genome representation. From outside to inside: (a) contigs size representations; (b) coverage (window size 10 kbp); (c) gc\_skew (window size 10 kbp; black positive changes and red negative changes); (d) GC content in percentage (window size 10 kbp); (e) positive coding DNA regions; (f) negative coding DNA regions; (g) colored-based COG annotation (the colors of each COG category is represented in the Figure legend); (h) cellulose synthase related genes colored as Figure 5-2.

A total of 2896 genes were predicted, of which 2842 are protein coding genes and 51 are tRNAs. One copy of rRNA operon was predicted, containing a single copy of 16S, 23S and 5S rRNA, respectively. According to the KO assignment and KEGG pathway mapping, 1531 (53.9%) could be classified into 226 pathways. The metabolic pathways consist of the most abundant gene set (454; 15.97% of total

CDS) in which the metabolic pathway related to BC production can be found (KEGG: 00500). According to COG classification, the total 2399 coding regions can be assigned to 19 categories, which are described in Table 5-1. Genome properties and statistics are summarized in Table 5-2.

**Table 5-1** COG categories retrieved in the K1G4genome

Categories	Functional group	Percentage (%)
C	Energy production and conversion	5.80
D	Cell cycle control, cell division, chromosome partitioning	0.82
E	Amino acid transport and metabolism	6.76
F	Nucleotide transport and metabolism	2.72
G	Carbohydrate transport and metabolism	5.04
H	Coenzyme transport and metabolism	3.83
I	Lipid transport and metabolism	2.38
J	Translation, ribosomal structure and biogenesis	4.97
K	Transcription	4.31
L	Replication, recombination and repair	5.49
M	Cell wall/membrane/envelope biogenesis	5.42
N	Cell motility	0.14
O	Posttranslational modification, protein turnover, chaperones	3.62
P	Inorganic ion transport and metabolism	5.11
Q	Secondary metabolites biosynthesis, transport and catabolism	1.03
S	Function unknown	20.68
T	Signal transduction mechanisms	2.45
U	Intracellular trafficking, secretion, and vesicular transport	2.17
V	Defense mechanisms	1.21

The bacteria capable of producing BC are characterized by differences in CS related genes organization and subunits composition. Two types of operons were described in the *Komagataeibacter* genus (Römling and Galperin, 2015).

**Table 5-2.** K1G4 genome assembly and annotation statistics

Properties	Value
Genome size	3.09 Mbp
Contigs	169
Coverage	269 x
Largest contigs	138 kbp
G+C content	63.67%
N50	49.9 kbp
L50	17
Total genes	2896
Of which CDS	2842
tRNA	51
tmRNA	1
Uniprot	64.70%
Proteins with COG function	82.94%
Proteins with Kegg function	53.9%
Proteins with Pfam	80.73%

The first type contains four genes that encode the key subunits of CS complex (*bcsA*, *bcsB*, *bcsC* and *bcsD*). In addition, three genes were described in the first operon type, two of which are located upstream (*cmcAx* and *ccpAx*) and one downstream (*bglAx*), the four *bcs* genes (Matsutani et al., 2015). The second operon type contains a total of four genes: *bcsAB*, *bcsX*, *bcsY* and *bcsC* (Römling and Galperin, 2015). It has been hypothesized that the strains that possess the second operon type are able

to produce an acetylated form of BC due to a high similarity of BcsY with transacylase (Umeda et al., 1999). Some differences in terms of operon copy number and presence/absence of the second operon type among *Komagataeibacter* species were previously described (Ryngajłło et al., 2018).

The number of *bcs* operons spans from 1 to 3 among *Komagataeibacter* genus. Only two *K. xylinus* strains were described to possess a fourth copy of *bcsAB* gene (Liu et al., 2018; Gullo et al., 2019). K1G4 genome analysis revealed the presence of the two *bcs* operon types structurally completed (Figure 5-2). Furthermore, a third copy of *bcsAB* has been found which can be correlated with the relatively high yield of BC produced.

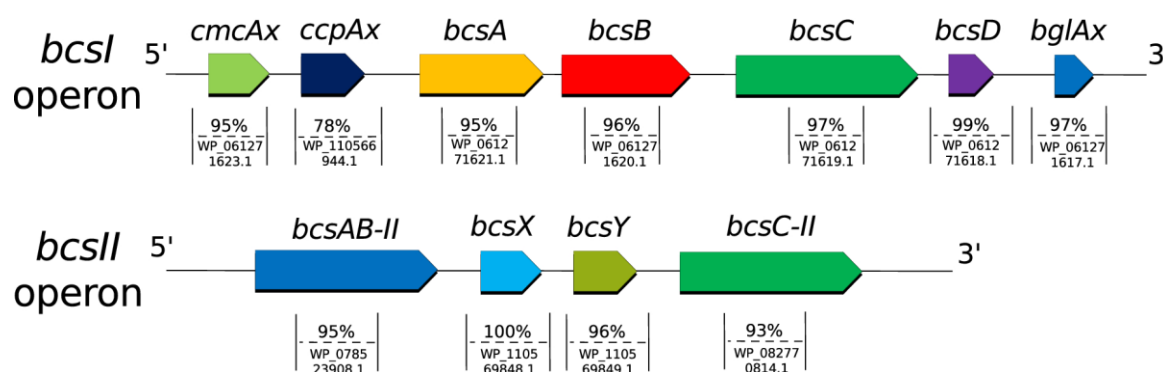


**Figure 5-2.** *Bcs* operons retrieved in K1G4 genome. The similarity percentage among the retrieved CDS and the reference sequence in Uniprot databases were indicated under each represented gene. BcsI is the type one of *bcs* operon, containing the full set of genes encoding CS. BcsII is the second type of operon, containing the genes codifying the CS catalytic core (*bcsAB*) and the genes encode for BcsC subunit. The role of *BcsX* remain unclear, whereas *bcsY* gene encode a protein probably responsible of the acetylated form of BC.

## Phylogenetic analysis of K1G4 strain

Considering that within *Komagataeibacter* genus, strains share a nucleotide 16S rRNA identity percentage higher than 98.1% (Cleenwerck et al., 2010), in this study, to assess the phylogenetic position of K1G4, the entire rRNA operon (*rrn*) including 16S, 23S, 5S rRNA genes and ITS regions was analysed.

Of the 37 *Komagataeibacter* genomes, one copy of *rrn* has been found, except for six of them, which display a variable *rrn* copy number (from 5 to 10) (Table 5-3).

**Table 5-3** *rrn* copy number among strains considered in this study and their isolation source

Organism	<i>rrn</i> copies	Base pairs (bp)	NCBI Assembly ID	Isolation source
<i>A. aceti</i> DSM 3508	1	5168	GCA_004341595.1	Vinegar
<i>A. pasteurianus</i> LMG 1262	1	5171	GCA_000285275.1	Beer
<i>K. cocois</i> WE7	1	5151	GCA_003311635.1	Coconut milk
<i>K. europaeus</i> CECT 8546	1	5208	GCA_001273645.1	Grape vinegar
<i>K. europaeus</i> LMG 18494	8	5207	GCA_000227545.1	Vinegar
<i>K. europaeus</i> NBRC 3261	1	5207	GCA_000964485.1	Vinegar
<i>K. europaeus</i> SRCM101446	5	5207	GCA_002173515.1	Vinegar
<i>K. hansenii</i> AY201	1	5165	GCA_001645805.1	–
<i>K. hansenii</i> HUM-1	1	5165	GCA_001938835.1	Hummingbird feeder
<i>K. hansenii</i> JCM 7643	1	5165	GCA_000964405.1	–
<i>K. hansenii</i> LMG 23726	1	5165	GCA_001938755.1	Kombucha tea
<i>K. hansenii</i> NQ5	1	5165	GCA_001645815.1	Sugar mill

Organism	<i>rrn</i> copies	Base pairs (bp)	NCBI Assembly ID	Isolation source
<i>K. hansenii</i> SC-3B	1	5165	GCA_001938745.1	Kombucha tea
<i>K. intermedius</i> TF2	1	5180	GCA_000964425.1	Kombucha tea
<i>K. kakiaceti</i> JCM 25156	1	5183	GCA_000613305.1	Kaki vinegar
<i>K. maltaceti</i> LMG 1529	1	5145	GCA_003206475.1	Malt vinegar
<i>K. medellinensis</i> NBRC 3288	5	5217	GCA_000182745.1	Vinegar
<i>K. nataicola</i> RZS01	5	5212	GCA_002009295.1	Rotten apples
<i>K. oboediens</i> 174Bp2	10	5177	GCA_000227565.1	Vinegar
<i>K. oboediens</i> LMG_18849	1	5177	GCA_003207815.1	Vinegar
<i>K. pomaceti</i> AV446	1	5147	GCA_003206055.1	Vinegar
<i>K. pomaceti</i> T5K1	1	5147	GCA_003207955.1	Vinegar
<i>K. rhaeticus</i> AF1	1	5206	GCA_000700985.1	Kombucha tea
<i>K. rhaeticus</i> iGEM	1	5206	GCA_900086575.1	Kombucha tea
<i>K. saccharivorans</i> CV1	5	5201	GCA_003546645.1	Vinegar
<i>K. saccharivorans</i> LMG 1582	1	5202	GCA_003207825.1	Beet juice
<i>K. saccharivorans</i> SRCM101450	1	5202	GCA_002878245.1	–
<i>K. sucrofermentans</i> LMG 18788	1	5250	GCA_003207865.1	Black cherry
<i>K. swingsii</i> LMG 22125	1	5241	GCA_003207895.1	Apple juice
<i>K. xylinus</i> BCRC 12334	1	5240	GCA_003416835.1	Vinegar
<i>K. xylinus</i> CGMCC 2955	1	5206	GCA_002762195.1	Vinegar
<i>K. xylinus</i> E25	1	5240	GCA_000550765.1	–
<i>K. xylinus</i> E26	1	5240	GCA_003416775.1	Vinegar
<i>K. xylinus</i> LMG 1515	1	5226	GCA_003207915.1	Mountains ash berries
K1G4 (This study)	1	5226		Kombucha tea
<i>K. xylinus</i> K2G30	1	5226	GCA_004302915.1	Kombucha tea
<i>K. xylinus</i> NBRC 13693	1	5177	GCA_000964505.1	–

– data not available

The phylogenetic tree based on 37 rRNA operon sequences (Figure 5-3) depicts diversification of *Komagataeibacter* strains in two large groups, which were supported by high bootstrap value (bootstrap value 100%). K1G4 has been found closely related to *K. xylinus* strain K2G30 and the type strain *K. xylinus* LMG 1515<sup>T</sup>. The phylogenetic position of K1G4 is well supported by the distance values of K1G4 and *K. xylinus* K2G30 and K1G4 and *K. xylinus* LMG 1515<sup>T</sup> that are 0 and 0.07%, respectively (Table S5-1). The total average of dissimilarities among all *Komagataeibacter* strains considered in this study is 0.01117, which means an average sequence similarity of 98.821%. Although the majority of *K. xylinus* strains are located in the second group, some of them clustered so far from the type strain *K. xylinus* LMG 1515<sup>T</sup>. Considering the cluster of *K. xylinus* E25, *K. xylinus* E26 and *K. xylinus* BCRC 12334, the distant matrix values range from 0.0045 to 0.0054. Concerning to *K. europaeus* strains, which are the closest relative to the cluster of *K. xylinus* E25, E26 and BCRC 12334, the average values of distance ranged from 0.0016 to 0.0022. A similar scenario can be observed for the strain *K. xylinus* CGMCC 2955, that is closely related to *K. rhaeticus* cluster, and *K. xylinus* NBRC 13693, clustering with *K. oboediens* group.

ANiB analysis was used as a digital DNA-DNA hybridization tool. The results from the pairwise matrix (Table S5-2) were consistent with the phylogenetic tree. As shown in ANiB heatmap, similar clusterization of rRNA operon-based tree can be observed (Figure 5-4).

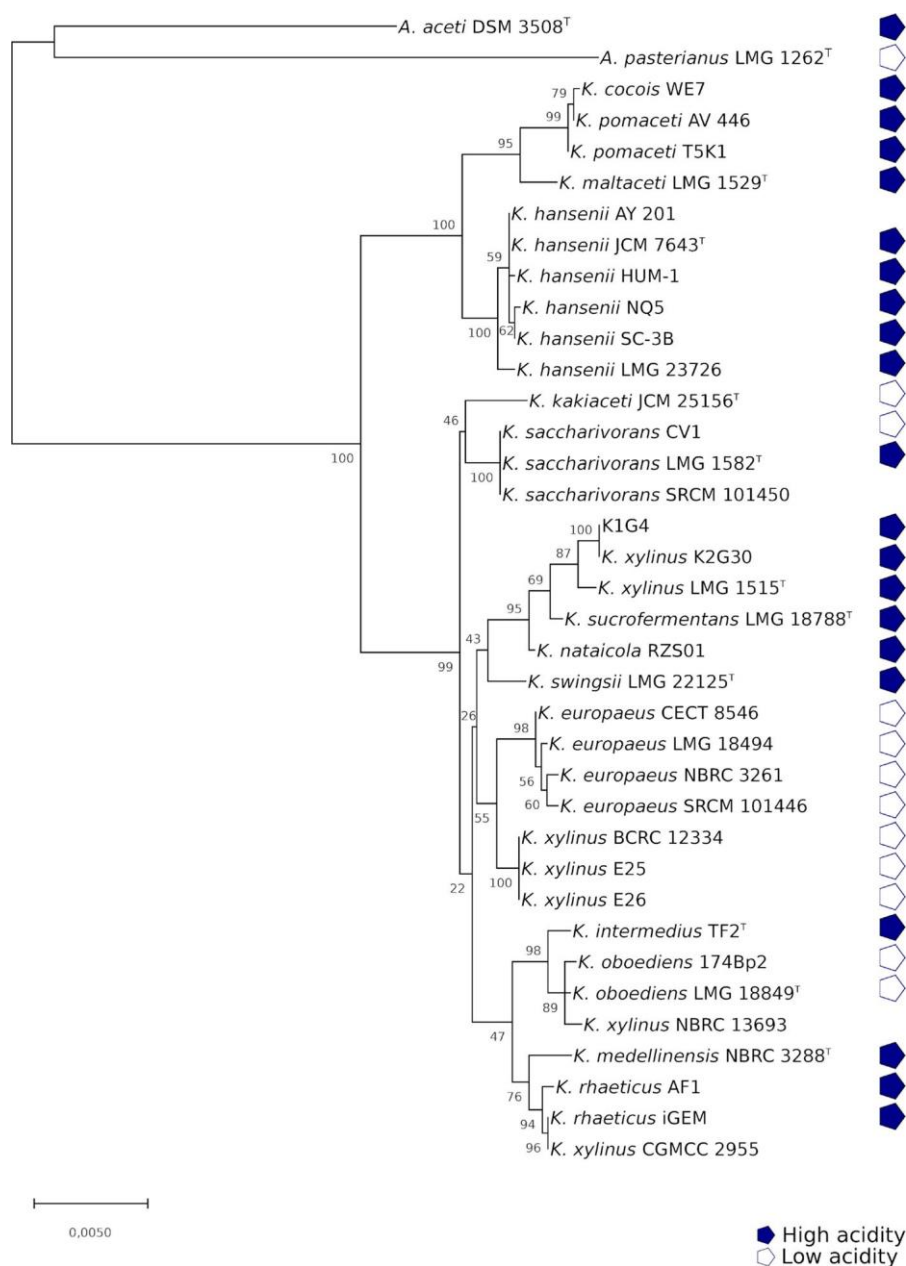


**Figure 5-3.** Phylogenetic tree based on *rrm* operon sequences. The strains clusters were highlighted based on the acidity of the different isolation matrices. (\*) Different acidity degree (blue/high or white/low). Data not retrieved were indicated as missing polygon.

K1G4 shows a genome sequence similarity of 99.93% with *K. xylinus* K2G30. This sequence similarity is more than the recommended threshold (94%) (Umeda et al., 1999), allowing us to classify K1G4 and *K. xylinus* K2G30 within the same species. About the ANI<sub>b</sub> value in the pairwise comparison of K1G4 and *K. xylinus* LMG 1515<sup>T</sup>, the similarity percentage is 93.34%, just under the recommended threshold. A possible explanation of this result could be due to the different isolation matrix of K1G4 and *K. xylinus* LMG 1515<sup>T</sup>. *K. xylinus* K1G4 and K2G30 were isolated from Kombucha tea, whereas *K. xylinus* LMG 1515<sup>T</sup> was isolated from mountain ash berries. Based on NCBI taxonomy and data retrieved from different microbial culture collection websites, the clusters showed in the phylogenetic tree (Figure 5-3) seem to follow the selective pressure of acetic acid content of the isolation matrices, except for the strains *K. kakiaceti* JCM 25156, *K. saccharivorans* CV1 and *K. intermedius* TF2. Based on the acetic acid content, the strains can be divided into three major groups: the *K. intermedius* group, well known to be isolated from vinegar with high acidity; the *K. hansenii* group, including

*Komagataeibacter* strains isolated from matrices at lower acetic acid content; *K. rhaeticus* cluster, including *K. medellinensis* strain and *K. xylinus* CGMCC 2955. Moreover, the group of the *K. xylinus* strains (E25, E26 and BCRC 12334) was probably misassigned, given the great correlation with *K. europaeus* strains and the isolation matrices.

Nevertheless, an intraspecies diversity may occur, probably due to the great variability from which the strains were isolated.

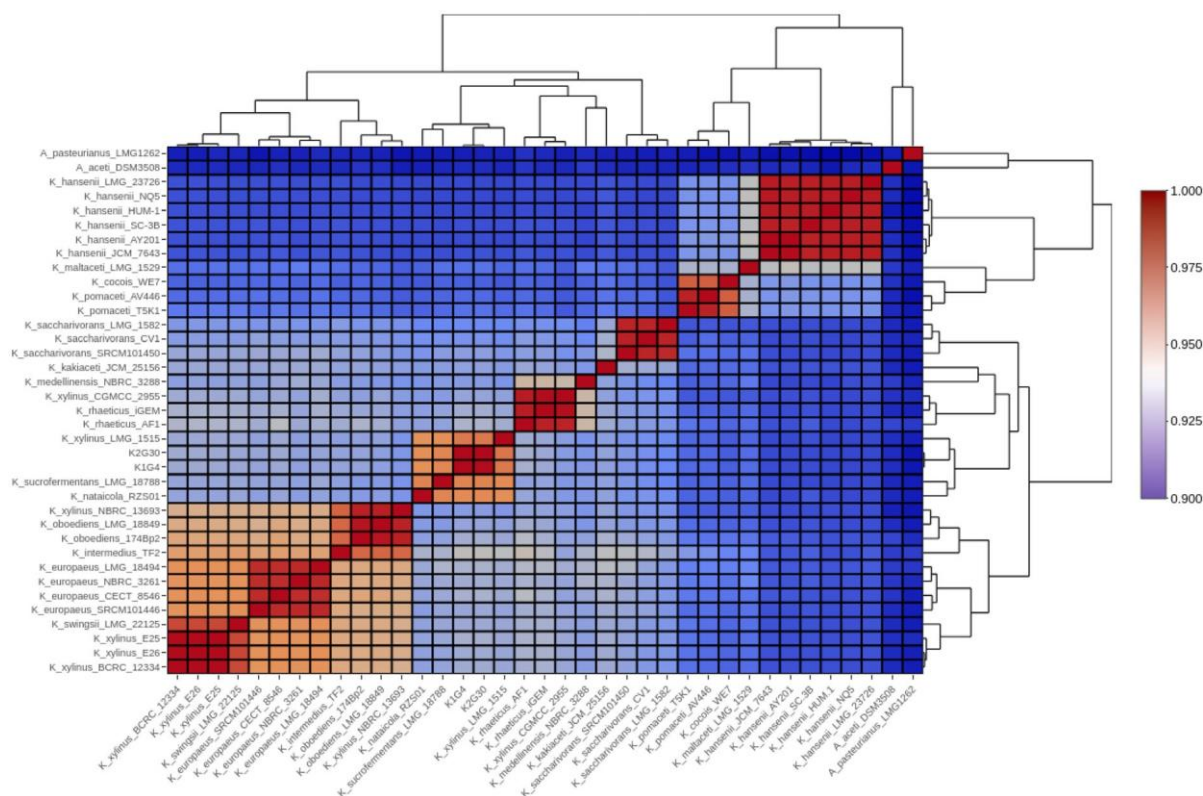


**Figure 5-4.** ANIb values of 37 *Komagataeibacter* strains pairwise comparisons. Values are represented in the central bi-color gradient heatmap (dark red gradients C 94%; white = 94%; dark blue gradients B 94%).

## Cellulose production using different carbon sources

The ability of K1G4 to synthesize BC was evaluated in HS medium supplemented with three different carbon sources: mannitol, glucose and glycerol, respectively. The standard HS medium was chosen in order to compare BC production by K1G4 with data retrieved from literature, which mainly provide information on HS.

K1G4 was able to grow on all three tested media. The best carbon source in our experiment was mannitol, in which a total of 9.47 g/L of BC was produced in 9 days. Considering the production trend in mannitol medium, after only 3 days of cultivation, the amount of BC was  $3.40 \pm 0.06$  g/L. An appreciable increase of the BC amount has been observed at 6 days ( $9.09 \pm 0.12$  g/L). From day 6 to day 9, BC production in mannitol was low compared to that produced from day 3 to day 6 (only 0.38 g/L) (Figure 5-5). The trends of BC production in glucose and glycerol are very similar. At the first time-point (day 3), BC production is roughly near to 0,  $0.192 \pm 0.014$  g/L in glucose medium and  $0.047 \pm 0.005$  in glycerol medium. From day 3 to day 6, BC amount reaches  $3.99 \pm 0.05$  g/L (glucose medium) and  $3.89 \pm 0.08$  g/L (glycerol medium). Unlike mannitol, at the final time-point (day 9), in glucose and glycerol, the amount of BC continues to increase considerably ( $7.57 \pm 0.08$  g/L and  $8.30 \pm 0.08$  g/L, respectively). The trend of BC production in mannitol can be explained considering its



metabolic pathway. As previously described by Oikawa and co-workers, a mannitol dehydrogenase (EC 1.1.1.67) having a high affinity for the substrate was found in *K. xylinus* KU-1.

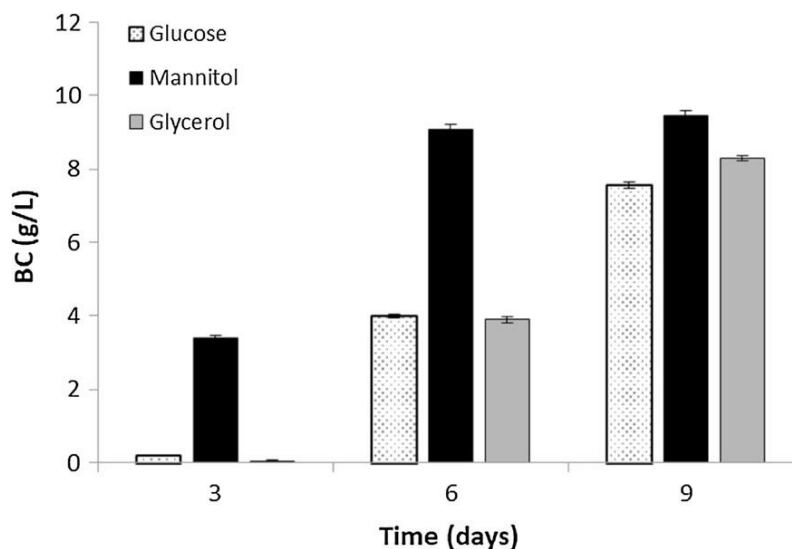


**Figure 5-5.** BC yields obtained during 9 days of cultivation using different carbon sources

The mannitol dehydrogenase converts mannitol in D-fructose, that can be easily used as substrate for BC production (Oikawa et al., 1997). In this study, we found one copy of mannitol dehydrogenase (97% of similarity) in K1G4 genome based on Refseq database (Refseq id WP\_082770678.1).

When glucose is used as a single carbon source, the multiple pathways in which it is involved must be considered. The pathway of BC production starts from the phosphorylation of glucose to glucose-6-phosphate (G6P) by the activity of hexokinase enzyme. The G6P can be addressed into different pathways, based on the needs of the cell. A reaction that carries the G6P in the BC pathways is the interconversion of G6P to glucose-1-phosphate by phosphoglucomutase. Acetic acid bacteria are also able to produce GlcA by the activity of glucose dehydrogenase, which converts the G6P into gluconolactone, an intermediate of GlcA pathway, by the glucose dehydrogenase (GDH) (Ameyama et al., 1981). From this point of view, it is possible to assume that the conversion of glucose into BC or in to GlcA depends on the enzymatic kinetic features of the phosphoglucomutase and the GDH, such as the substrate affinity. When glucose is oxidized to gluconic derivatives, a reduction of pH values is observed (Lu et al., 2015). In this study, in glucose medium (at day 9), a high amount of GlcA (11.98 g/L) was detected, which was responsible for pH reduction to 3.85 and a lower BC yield compared to that obtained in mannitol and glycerol media, respectively (Table 5-4).

**Table 5-4.** Correlation between GlcA and pH during the time frame of BC production.

Time (days)	Glucose		Mannitol		Glycerol	
	GlcA (g/L)	pH	GlcA (g/L)	pH	GlcA (g/L)	pH
0	—	6.24±0.01	—	6.19±0.02	—	6.22±0.02
3	3.64±0.6	4.79±0.07	1.74±0.37	5.42±0.02	1.18±0.19	5.33±0.06
6	10.02±0.58	3.87±0.05	1.72±0.04	5.51±0.01	2.02±0.18	5.52±0.04
9	11.98±1.48	3.85±0.01	1.89±0.21	5.5±0.01	2.08±0.08	5.53±0.03

The data were reported as the average among three replicates and the standard error was included

Knocking out of GDH seems to minimize this phenomenon, avoiding the acidification of the medium and increasing the BC yield (Kuo et al., 2015).

Considering glycerol medium, in a similar way of GDH, the activity of the membrane-bound polyol dehydrogenase (PQQ-GLDH) (EC 1.1.5.2) can affect BC yield. PQQ-GLDH can convert glycerol in dihydroxyacetone, reducing the carbon source availability for BC production (Matsushita et al., 2003; Stasiak and Błaejak, 2009).

High variability in terms of BC yield was observed using different *Komagataeibacter* species, like *K. hansenii* and *K. xylinus* (Gullo et al., 2018). Furthermore, intraspecies variability is also reported (Gullo et al., 2017). For example, Singhsa and co-workers tested four strains of *K. xylinus* species, obtaining different amount of BC (Singhsa et al., 2018). Besides, in our previous work, the differences that occur among strains isolated from the same matrix (Kombucha tea), after the same cultivation time, was observed. In particular, in static regime of cultivation, the cellulose layer formed by strains of the *K. xylinus* species can develop as a single or multilayer structure of different weight (Gullo et al., 2017). In this condition, the strain K2G30 produced a remarkable amount of BC using mannitol as carbon source (23 g/L in 10 days) (Gullo et al., 2019). To explain the differences in BC production among *Komagataeibacter* strains, we should consider also the CS operon's copy number. A higher copy number of the catalytic core of CS (BcsA; BcsB or BcsAB) can be correlated to a higher BC production (Florea et al., 2016). K1G4 possesses a total of three copies of the catalytic subunits, while *K. xylinus* K2G30 isolated from the same source was reported to possess four copies of the catalytic subunits (Cannon and Anderson, 1991). Moreover, the effect of an additional carbon source contributes to the maintenance of the basal metabolism of the bacterial cell. The HS medium used in this study contains citric acid a secondary carbon source that can be metabolized by bacterial cell to produce ATP via Krebs cycle (Cannon and Anderson, 1991), whereas the primary carbon sources (glucose, mannitol or glycerol) can be used for BC production.

## Conclusions

The strain K1G4 belonging to the species *K. xylinus* produces different BC yield growing on glucose, mannitol and glycerol, supplied as carbon sources. The highest BC production was observed on mannitol followed by glycerol and glucose, respectively.

Genome analysis revealed a third copy of *bcsAB* operon, which can be responsible for the high rate of BC. The versatility of K1G4 in producing BC suggests the possibility to exploit it by using different carbon sources, according to the specific industrial use.

# Chapter 6

## Characterization of bio-nanocomposite films based on gelatin/polyvinyl alcohol blend reinforced with bacterial cellulose nanowhiskers for food packaging applications

Hossein Haghghi<sup>1</sup>, Maria Gullo<sup>1</sup>, Salvatore La China<sup>1</sup>, Frank Pfeifer<sup>2</sup>, Heinz Wilhelm Siesler<sup>2</sup>, Fabio Licciardello<sup>1,3</sup>, Andrea Pulvirenti<sup>1,3</sup>

<sup>1</sup>Department of Life Sciences, University of Modena and Reggio Emilia, Reggio Emilia, Italy

<sup>2</sup>Department of Physical Chemistry, University of Duisburg-Essen, Essen, Germany

<sup>3</sup>Interdepartmental Research Centre BIOGEST-SITEIA, University of Modena and Reggio Emilia, Reggio Emilia, Italy

### This chapter is published as:

Haghghi H, Gullo M, **La China S**, Pfeifer F, Siesler HW, Licciardello F, Pulvirenti A. Characterization of bio-nanocomposite films based on gelatin/polyvinyl alcohol blend reinforced with bacterial cellulose nanowhiskers for food packaging applications. *Food Hydrocoll* (2020) 106454. <https://doi.org/10.1016/j.foodhyd.2020.106454>

## Abstract

Bacterial cellulose nanowhisker (BCNW) was synthesized from *Komagataeibacter xylinus* (strain K2G30; UMCC 2756) using sulfuric acid hydrolysis and it was incorporated into the gelatin-polyvinyl alcohol (GL/PVA) blend film matrix. The effect of BCNW content (1–10 wt% of biopolymer) on the microstructural, mechanical, optical, and water barrier properties of bio-nanocomposites was studied. The transmission electron microscopy image showed that BCNW had a needle shape structure with an average length of 600 nm and an average width of 30 nm. The crystallinity index of BCNW was 94.7% using X-ray diffraction. Scanning electron microscopy (SEM) illustrated good miscibility between GL/PVA blend film matrix and BCNW up to 7.5 wt%. Fourier-transform infrared spectroscopy in the attenuated total reflection mode showed molecular interactions between functional groups of the GL/PVA blend film matrix and BCNW. The incorporation of BCNW up to 7.5% into the GL/PVA blend enhanced the water vapor transmission rate and water vapor permeability by about 22% and 14%, respectively, while tensile strength, elongation at break, and elastic modulus increased by about 21.5%, 41% and 19%, respectively ( $p < 0.05$ ). Films transparency was not affected by the addition of BCNW ( $p > 0.05$ ) suggesting that the BCNW was dispersed uniformly at the nanoscale. All films were colorless ( $\Delta E^* < 2$ ) with low opacity value ( $< 2$ ) comparable to synthetic plastics. Overall, the characterization of functional properties revealed that GL/PVA blend film reinforced with BCNW could be used as an environmentally friendly packaging material to partially replace or reduce the use of the existing petroleum-based packaging materials available in the market.

## Introduction

Today, plastic is considered the most widely used polymers in our daily life which offers a broad range of functionalities optimized for each type of application from simple packing materials to complex engineering components (Philp et al., 2013). This is mainly due to its low price, lightness, strength, stability, flexibility, impermeability, and durability (Siracusa et al., 2008). However, the non-degradable nature of plastic leads to generate extensive volumes of post-consumer waste over the years and serious environmental issues (Hosseini et al., 2015). Annually, more than 350 million tons of plastics are produced in the world (Haghighi et al., 2020c). It is estimated that 85% of trash in the oceans is made of plastics and most of them are disposable items. According to a report from World Economic Forum in partnership with the Ellen MacArthur Foundation, there will be more plastic material than fish in terms of weight in the world's oceans by 2050 (Elias, 2017). Therefore, significant research has been proposed concerning the utilization of biopolymers as an alternative for partial replacement of conventional plastics (Brinchi et al., 2013; Abdul Khalil et al., 2016; De Leo et al., 2018; La China et al., 2018). In this sense, gelatin (GL) has been widely used for the development of biodegradable packaging thanks to its abundance, availability, and low cost (Etxabide et al., 2017). GL is a natural water-soluble protein, obtainable from the partial hydrolysis of collagen which is one of the most abundant proteins present in the skin, bone, and connective tissue of both land and marine animals (Chang et al., 2012). GL films have good barriers to oxygen, light, UV rays and can prevent photo-oxidation and lipid oxidation, thus allowing food quality preservation and shelf life (Rezaee et al., 2018). However, films made from GL have poor mechanical, thermal, and water barrier properties leading to a shorter food shelf life compared to conventional plastic material (George and Siddaramaiah, 2012; Haghighi et al.,

2019a). Blending GL with synthetic but biodegradable polymers such as polyvinyl alcohol (PVA) is purposed as a simple and effective way to overcome these limitations and to reduce the cost as well (Mendieta-Taboada et al., 2008).

PVA is a synthetic, non-toxic, water-soluble polymer, commercially obtainable from hydrolysis of polyvinyl acetate (Shahbazi et al., 2016). PVA has been evaluated for safety by the Joint FAO/WHO Expert Committee on Food Additives (JECFA) in 2003 (WHO, 2004) and it has also been approved for packaging meat and poultry products by the USDA (Kanatt et al., 2012; Bellelli et al., 2018). Despite its synthetic character, this polymer is biodegradable, and it shows high tensile strength, flexibility, and gas barrier properties (Aloui et al., 2016). The GL and PVA are highly miscible and compatible due to the presence of multifunctional groups in their polymer backbone. Films based on GL/PVA blend have been extensively studied as potential biodegradable packaging materials (Mendieta-Taboada et al., 2008; Pawde and Deshmukh, 2008; Carvalho et al., 2009; Bergo et al., 2012; Kanatt et al., 2017; Kariminejad et al., 2018). However, the hydrophilic nature of GL and PVA leads to the formation of films with poor water vapor permeability and high sensitivity to water (Cazón et al., 2019). This represents a major limitation for their industrial applications when applied to high moisture food products because these films may dissolve, swell or disintegrate upon contact with water (Gómez-Guillén et al., 2009; Suderman et al., 2018).

Recently, reinforcement of the polymer matrix with nanomaterials (i.e., bio-nanocomposites) has been proposed as a promising approach to optimizing the functional properties of packaging materials (Arfat et al., 2017). Uniform dispersion of nanomaterial leads to a very large interfacial and surface area (Dufresne, 2006; Hosseini et al., 2015). The ability to form a dense three-dimensional nanoscale network plays a critical role in changing molecular mobility, thereby leading to reinforcement and improvement in mechanical, optical, thermal, and water barrier properties (George and Siddaramaiah, 2012; Follain et al., 2013). Among nanomaterials, cellulose nanostructures (cellulose nanocrystals-CNC and cellulose nanofibers-CNF) have been widely studied as thin-layer coatings (Li et al., 2013, 2015a) and as reinforcement agents in different biopolymers such as alginate (Abdollahi et al., 2013), chitosan (Khan et al., 2012; Pereda et al., 2014), gelatin (Santos et al., 2014), pullulan (Trovatti et al., 2012), PVA (Cho and Park, 2011; Gonzalez et al., 2014; Asad et al., 2018; Spagnol et al., 2018), chitosan/PVA blend (Li et al., 2015b) and starch/PVA blend (Noshirvani et al., 2016). In this sense, cellulose nanostructures produced from bacteria (mainly *Komagataeibacter* species) have advantages over plant cellulose because they are free from hemicellulose and lignin, thus, reducing purification costs and environmental concerns derived from using harsh chemicals (Stasiak and Błaejak, 2009; Azeredo et al., 2017; Vasconcelos et al., 2017; Gullo et al., 2018). Besides high purity, bacterial cellulose has been reported to have a high degree of polymerization, high crystallinity (70–80%), biocompatibility, high water uptake capacity (up to 100 cc/g), excellent mechanical properties (very high elastic modulus and tensile strength) and outstanding oxygen barrier properties in medium to low relative humidity conditions (< 50% RH) which makes it a unique reinforcement nanomaterial in biopolymer matrix (Gabr et al., 2010; Marins et al., 2011; Wang et al., 2020). Blending GL with PVA to form a composite film could combine the advantages of the base polymers into a film with higher mechanical performances compared with those of each constituent. Besides, reinforcement of the GL/PVA film matrix with bacterial cellulose nanowhisker (BCNW) has been proposed as a promising approach to enhancing the water barrier properties and further improvement of mechanical properties of packaging materials (Wang et al.,

2020). To the best of our knowledge, literature about GL/PVA blend film reinforced with BCNW is not available. Therefore, the purpose of the present work was to characterize microstructural, physical, mechanical, optical and water barrier properties of GL/PVA blend films reinforced with different amounts of BCNWs produced by a selected acetic acid bacterium strain for food packaging applications.

## Material and methods

### Materials and reagents

PVA with a molecular weight of 27 kDa and 98% degree of hydrolysis was purchased from Fluka (Steinheim, Germany). GL (bloom 128 – 192°) was purchased from AppliChem GmbH (Darmstadt, Germany). Glycerol ( $\geq 99.5\%$ ) was purchased from Merck (Darmstadt, Germany). Sulfuric acid ( $\geq 99.99\%$ ) was obtained from Sigma Aldrich (St Louis, MO, USA).

### Bacterial strain and bacterial cellulose nanowhisker (BCNW) production

The strain K2G30 belonging to *Komagataeibacter xylinus* species was used to produce bacterial cellulose (Gullo et al., 2017). The strain is deposited at Unimore Microbial Culture Collection (UMCC) under the collection code UMCC 2756 and handled according to the standard procedures of the Microbial Resource Research Infrastructure-Italian Joint Research Unit (MIRRI-IT) (De Vero et al., 2019b).

The strain was cultivated in 1 L flasks (working volume 300 mL) using the standard Hestrin-Shramm (HS) medium (Hestrin and Schramm, 1954), inoculated with 5 wt% of preculture. The incubation was conducted at 28 °C in aerobic conditions for a total of 7 days. The obtained bacterial cellulose layers were collected washed and dried as previously described (Gullo et al., 2019). Dried bacterial cellulose was subjected to acid sulfuric hydrolysis (64 wt%) to break the hierarchical structure into rod-like crystalline structures called bacterial cellulose nanowhiskers (BCNWs) (Vasconcelos et al., 2017). Briefly, 0.6 g of dried bacterial and 60 mL of acid solution (1:100 ratio, w/v) were mixed at 45°C for 60 min with magnetic stirring (500 rpm). Hydrolysis was stopped by diluting with cold deionized water (15:1 ratio, v/v). The BCNWs were then washed with deionized water using 3 repeated centrifuge cycles (6000 rpm for 20 min at 20°C). The resulting suspension was ultrasonicated (180 w) by an ultrasound (Argo Lab DU45, Italy) for 3 min after each washing cycle. The BCNWs suspension was dialyzed in deionized water to reach neutral pH. Finally, the BCNW powder was obtained through freeze-drying with a yield of ~70 wt%.

### Preparation of film-forming solutions and nanocomposite films

Preparation of films was adapted from the procedure of (Alves et al., 2011) with slight modifications. Five GL/PVA blend films reinforced with different concentrations of BCNW (1, 2.5, 5, 7.5, and 10 wt% of biopolymer) were analyzed. Besides, GL/PVA blend without BCNW was used as control. The GL film-forming solution (FFS) (3 wt%) was prepared by hydrating GL in distilled water for 30 min and subsequently dissolved at 55 °C for an additional 30 min. The PVA FFS (3 wt%) was prepared by dissolving PVA in distilled water at 90°C for 30 min. Unplasticized GL and PVA films are very brittle and the resulting cast films are very difficult to

peel off. The addition of a plasticizer such as glycerol improves film flexibility, through the weakening of intermolecular interactions in the polymer network, also causing a reduction in tensile strength and thermal stability. Glycerol (25 g glycerol / 100 g dry polymer) was then added as into both FFSs, followed by additional stirring for 30 min. The GL/PVA blend FFS was prepared by mixing GL and PVA FFS at a 1:1 ratio. Different amounts of BCNWs (1–10 wt%) were added to the GL/PVA blend. All FFSs were degasified with a vacuum pump (70 kPa) for 15 min to remove bubbles. Films were obtained by casting 20 mL FFS into Petri dishes (14.4 cm in diameter) and drying at  $25 \pm 2$  °C in the chemical hood overnight at 45% relative humidity. The morphology and size of BCNW were characterized using scanning electron microscopy.

### **X-ray diffraction (XRD)**

XRD patterns of BCNW was recorded in an X-ray diffractometer (X'Pert Pro, PANalytical, Eindhoven, Netherlands) using Cu-K $\alpha$  radiation at 40 kV and 40 mA. A pure BCNW film was examined with a scanning angle of  $2\theta$  from 5-50 at a rate of 2.45°/min at room temperature. The crystallinity index was calculated by Eq. (1) as described by Segal et al. (1959):

$$\text{Crystallinity index (\%)}: (I_{\text{cry}} - I_{\text{am}} / I_{\text{cry}}) \times 100 \quad (1)$$

where  $I_{\text{cry}}$  is the maximum intensity of the diffraction peak in the crystalline region at an angle of  $2\theta \sim 22.5^\circ$ , and  $I_{\text{am}}$  is the minimum intensity in the amorphous region at an angle of  $2\theta \sim 18^\circ$ .

### **Transmission electron microscopy (TEM)**

The TEM image of the BCNW sample was obtained using a transmission electron microscope (Talos F200S G2, Thermo Scientific, Brno, Czech Republic) operating at a 200 kV acceleration voltage. A small quantity of the freeze-dried BCNW was dispersed in pure water with ultrasonication for 20 min. BCNW suspension was deposited on a formvar/carbon-coated copper (200-mesh) TEM grid. The average length and width of 100 randomly selected BCNWSs were measured by the ruler tool in TEM images using ImageJ software (v. 1.53a, National Institutes of Health, USA).

### **Scanning electron microscopy (SEM)**

The surface and cross-section images of films were obtained using SEM (Nova NanoSEM 450, FEI, USA). Film samples were fixed on stainless-steel support with a double-sided conductive adhesive. The analysis was conducted in a low vacuum (80 KPa) at an acceleration voltage of 10 kV.

### **Attenuated Total Reflection (ATR)/Fourier-Transform Infrared (FT-IR) Spectroscopy**

Infrared spectra of the different films were recorded in the ATR mode with a FT-IR spectrometer (type Alpha, Bruker Optik GmbH, Ettlingen, Germany). Spectra were collected from two different locations from the top and bottom side of the same samples in the 4000 – 400  $\text{cm}^{-1}$  wavenumber range by accumulating 64 scans with a spectral resolution of 4  $\text{cm}^{-1}$ .

## Thickness and mechanical properties

Film thickness was measured with a digital micrometer (Model IP65, SAMA Tools, Viareggio, Italy) at five different positions (one at the center and four at the edges). The means of these five separate measurements were recorded.

The tensile strength (TS), elongation at break (E%), and elastic modulus (EM) were determined using a dynamometer (Z1.0, Zwick/Roell, Ulm, Germany) according to ASTM standard method D882 (ASTM, 2001a). The films with known thickness were cut into rectangular strips ( $9.0 \times 1.5 \text{ cm}^2$ ). Initial grip separation and cross-head speed were set at 70 mm and 50 mm/min, respectively. Measurements were repeated 10 times from each type of film. The software TestXpert® II (V3.31) (Zwick/Roell, Ulm, Germany) was used to record the tensile strength curves. The tensile strength was calculated by dividing the maximum load to break the film by the cross-sectional area of the film and expressed in MPa. The elongation at break was calculated by dividing film elongation at rupture by the initial grip separation expressed in percentage (%). The elastic modulus was calculated from the initial slope of the stress-strain curve and expressed in MPa.

## UV-Vis light transmittance, opacity value, and color

The barrier properties of films against UV and visible light were determined at the UV (200, 280, and 350 nm) and the visible (400, 500, 600, 700, and 800 nm) wavelengths. This optical characteristic was estimated by a VWR® Double Beam UV×VIS 6300PC spectrophotometer (China) using square film samples ( $2 \times 2 \text{ cm}^2$ ). The opacity of the films was calculated by Eq. (2):

$$\text{Opacity value} = -\text{Log } T_{600} / x \quad (2)$$

where  $T_{600}$  is the fractional transmittance at 600 nm and  $x$  is the film thickness (mm). A larger opacity value represents lower film transparency. For each film, three readings were taken at different positions and average values were determined.

The color of films was measured with a colorimeter (CR – 400 Minolta, Minolta Camera, Co., Ltd., Osaka, Japan) at room temperature, with D65 illuminant and  $10^\circ$  observation angle. The instrument was calibrated with a white standard ( $L^* = 99.36$ ,  $a^* = -0.12$ ,  $b^* = -0.07$ ) before measurements. Results were expressed as  $L^*$  (lightness),  $a^*$  (redness/greenness) and  $b^*$  (yellowness/blueness) parameters. The total color difference ( $\Delta E^*$ ) was calculated using the following Eq. (3):

$$\Delta E^* = \sqrt{[(\Delta L^*)^2 + (\Delta a^*)^2 + (\Delta b^*)^2]} \quad (3)$$

where  $\Delta L^*$ ,  $\Delta a^*$ , and  $\Delta b^*$  are the differences between the corresponding color parameter of the samples and that of a standard white plate used as the film background. For each film, five readings were taken at different positions and the average values were determined from the top and bottom sides.

## Moisture content and water vapor transmission rate and water vapor permeability

Moisture content (MC) of the films ( $2 \times 2 \text{ cm}^2$ ) was determined as the percentage of weight loss upon drying to constant weight ( $M_d$ ) in an oven at  $105 \pm 2 \text{ }^\circ\text{C}$  and the initial weight ( $M_w$ ) according to the following Eq. (4):

$$\text{MC (\%)} = (M_w - M_d / M_w) \times 100 \quad (4)$$



Water vapor transmission rate (WVTR) of the films was determined gravimetrically according to the ASTM E96 method (ASTM, 2001b) with some modifications. Films were sealed on top of glass test cups with an internal diameter of 10 mm and a depth of 55 mm filled with 2 g anhydrous CaCl<sub>2</sub> (0% RH). The cups were placed in desiccators containing BaCl<sub>2</sub> (90% RH), which were maintained in incubators at 45 °C. WVTR was determined using the weight gain of the cups and was recorded and plotted as a function of time. Cups were weighed daily for 7 days to guarantee the steady-state permeation. The slope of the mass gain versus time was obtained by linear regression ( $r^2 \geq 0.99$ ). WVTR (g/day m<sup>2</sup>) and WVP (g mm/kPa day m<sup>2</sup>) were calculated according to the following Eqs. (5) and (6):

$$\text{WVTR} = \Delta W / \Delta t \times A \quad (5)$$

$$\text{WVP} = \text{WVTR} \times L / \Delta P \quad (6)$$

where  $\Delta W/\Delta t$  is the weight gain as a function of time (g/day), A is the area of the exposed film surface (m<sup>2</sup>), L is the mean film thickness (mm) and  $\Delta P$  is the difference of vapor pressure across the film (kPa). All measurements for MC, WVTR, and WVP were made in triplicate.

### Statistical analysis

The statistical analysis of the data was performed through analysis of variance (ANOVA) using SPSS statistical program (SPSS 20 for Windows, SPSS INC., IBM, New York). The experiment was performed in three replicates and the number of repeats varied from one analysis to another and was reported in each subsection. The differences between means were evaluated by Tukey's multiple range test ( $p < 0.05$ ). The data were expressed as the mean  $\pm$  SD (standard deviation).

## Results and discussion

### Bacterial cellulose production and characterization of bacterial cellulose nanowhisker

Bacterial cellulose was successfully produced in a static regime of cultivation by the strain K2G30, belonging to the species *K. xylinus*. This strain (originally isolated from Kombucha tea) was selected for its ability to produce bacterial cellulose from a variety of carbon sources. Previous studies showed high bacterial cellulose production yield from strain K2G30, especially growing on glucose and mannitol as carbon sources (Gullo et al., 2017, 2019). In this study, the ability of K2G30 to efficiently produce bacterial cellulose was confirmed.

The morphology and size of BCNW were characterized by transmission electron microscopy (TEM) (Figure 6-1a). The TEM image showed needle shape structure with an average length of 600 nm (ranging from 300 to 900 nm) and an average width of 30 nm (ranging from 15 to 45 nm) corresponding to an aspect ratio of 20 (Vasconcelos et al., 2017).

The XRD pattern of neat BCNW film is shown in Figure 6-1b. The BCNW showed three main characteristic peaks at  $2\theta = 14.19$ ,  $16.63$ , and  $22.5^\circ$  (Salari et al., 2018). Our previous studies showed that bacterial cellulose had a crystallinity index of 80% (Gullo et al., 2017). The crystallinity index of BCNW synthesized in this study was 94.7% which was greater than neat bacterial cellulose. This might be due to a reduction of the amorphous content in BCNW after sulfuric acid hydrolysis. A similar result was reported by Vasconcelos et al. (2017).

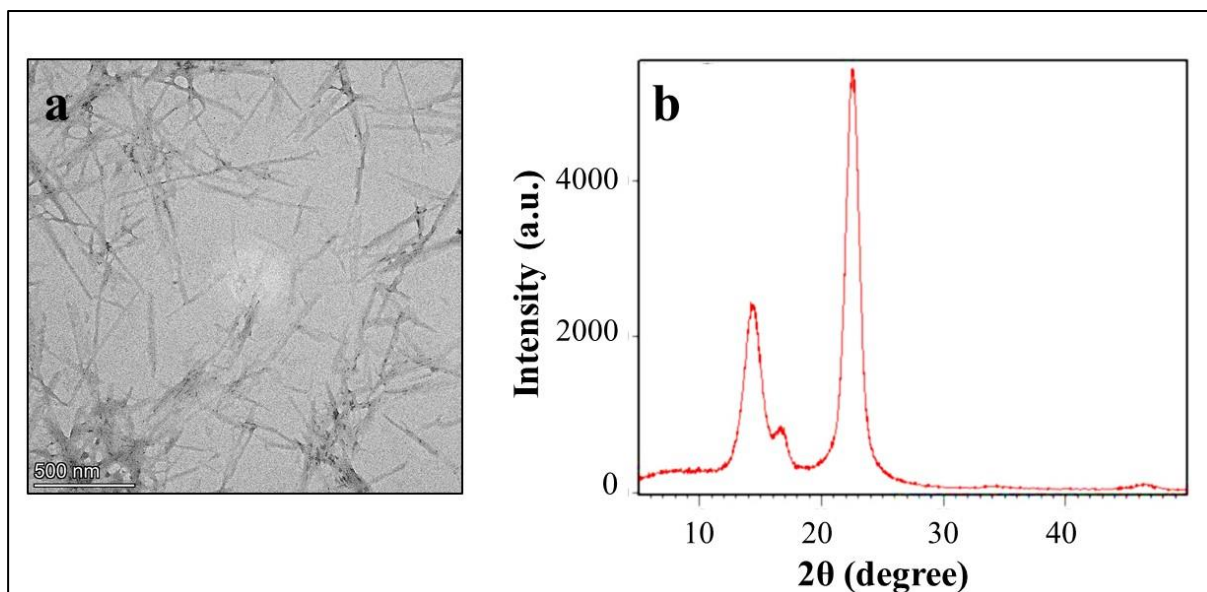


**Figure 6-1.** a) Transmission electron microscopy (TEM) image and b) X-ray diffraction (XRD) pattern of bacterial cellulose nanowhisiker (BCNW).

### Surface and cross-section morphology characterization by SEM

The surface and cross-section images of films based on a GL/PVA blend as control and those reinforced with BCNW (1–10 wt%) are presented in Figure 6-2 and Figure 6-3, respectively. The surface of the control film was smooth and homogenous without pores or cracks indicating good compatibility between GL and PVA (Figure 6-2a). This can be explained by a strong intermolecular association between the functional groups of GL and PVA (Ghaderi et al., 2019). Addition of BCNW up to 7.5 wt% did not affect the surface morphology indicating a uniform distribution of BCNW in the film matrix (Figure 6-2b, 6-2c, 6-2d, and 6-2e). However, a rough surface with small particles and aggregations were observed in GL/PVA/BCNW 10% (Figure 6-2f). This effect is mainly due to the strong interactions between the hydroxyl groups of the BCNWs at the highest loading level (10 wt%). At this condition, the nanowhisiker–nanowhisiker association becomes predominant over the nanowhisiker–biopolymer interaction (Chang et al., 2010; Reddy and Rhim, 2014; El Achaby et al., 2017).

A compact and continuous structure without irregularities such as air bubbles or pores and no evidence of phase separation can be observed in the cross-section of the control film (Figure 6-3a) indicating excellent structural integrity and compatibility between GL and PVA (Ghaderi et al., 2019). The cross-section of films reinforced with BCNWs up to 7.5 wt% showed a similar morphology (Figure 6-3b, 6-3c, 6-3d, and 6-3e) suggesting a good level of miscibility between the components and homogeneous dispersion of BCNW up to 7.5 wt% (Yadav and Chiu, 2019). The film containing 10 wt% BCNW showed irregular and sponge-shape structures (Figure 6-3f). This might be related to the agglomeration of BCNW in the film matrix at high concentrations mainly due to the poor interfacial bonding which resulted in disrupted structures (Ghaderi et al., 2019).

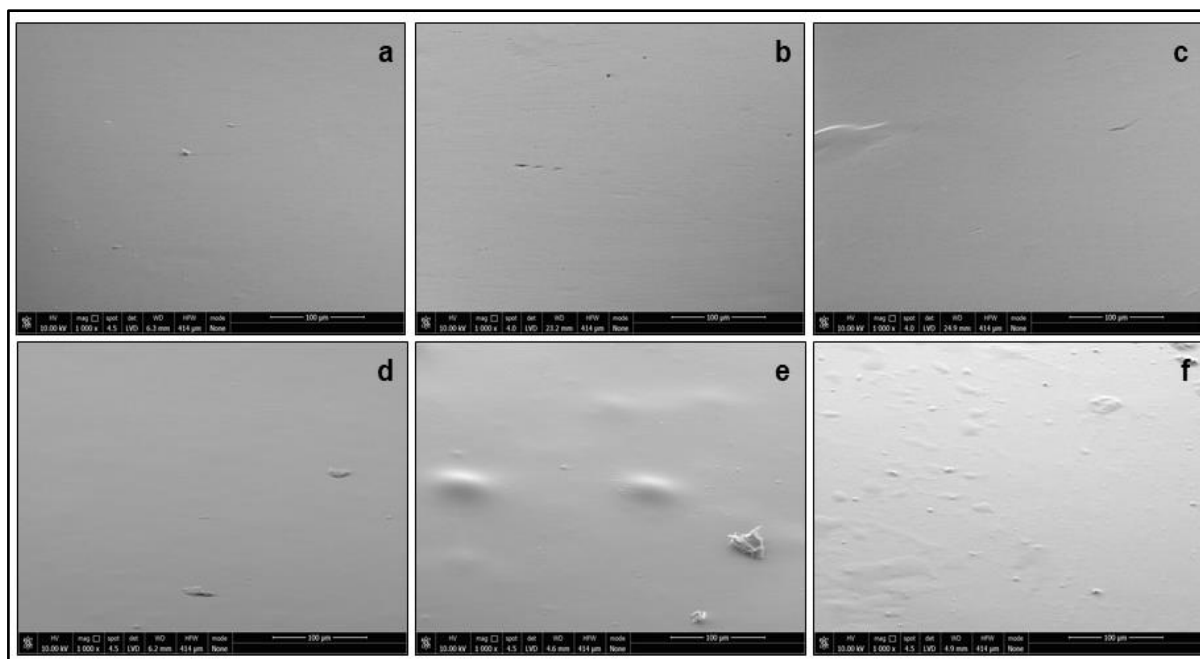


**Figure 6-2.** SEM images (surface) of films based on: a) GL/PVA blend, b) GL/PVA/BCNW1%, c) GL/PVA/BCNW2.5%, (d) GL/PVA/BCNW5%, (e) GL/PVA/BCNW7.5% and f) GL/PVA/BCNW10%.

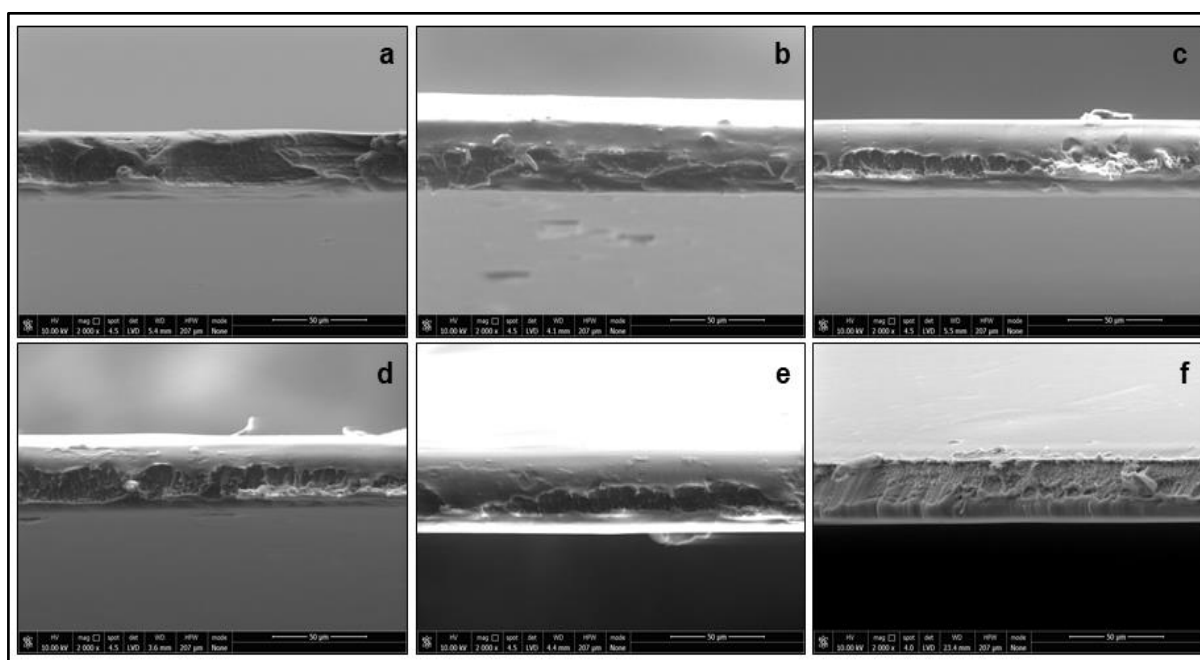


**Figure 6-3.** SEM images (cross-section) of films based on: a) Gelatin-Polyvinyl alcohol blend (GL/PVA), b) GL/PVA/Bacterial cellulose nanowhisker (BCNW) 1%, c) GL/PVA/BCNW2.5%, (d) GL/PVA/BCNW5%, (e) GL/PVA/BCNW7.5% and f) GL/PVA/BCNW10%.

### Attenuated Total Reflection (ATR) / Fourier-Transform Infrared (FT-IR) Spectroscopy

ATR/FT-IR spectroscopy was performed to characterize the structural and spectroscopic changes due to the incorporation of different amounts of BCNWs into the GL/PVA film matrix by measuring the spectra in the wavenumber range of  $4000 - 400 \text{ cm}^{-1}$  at a spectral resolution of  $4 \text{ cm}^{-1}$ . The spectrum of pure GL, PVA, and BCNW, respectively, are shown on top of Figure 6-4

in order to separately assign their specific absorption band. Comparison with the absorption bands observed in the GL/PVA blends with different amounts of BCNW then allow to draw conclusions regarding the interaction between GL and PVA and the incorporated BCNW. These interactions can result in peak shifts and intensity changes of existing peaks in the blend (Xu et al., 2019).

The spectrum of the pure GL film (Figure 6-4a) revealed the characteristic peaks at  $1630\text{ cm}^{-1}$  (amide-I) (typical signal for GL coil structure),  $1544\text{ cm}^{-1}$  (amide-II),  $1236\text{ cm}^{-1}$  (amide III),  $3292\text{ cm}^{-1}$  (amide-A),  $3080\text{ cm}^{-1}$  (amide-B) and the peak doublet at about  $2935/2877\text{ cm}^{-1}$  which can be assigned mainly to  $\nu_{\text{as}}(\text{CH}_2)/\nu_{\text{s}}(\text{CH}_2)$  and  $\nu(\text{CH})$  stretching vibrations. Similar results have been reported (Poverenov et al., 2014; Haghghi et al., 2019b).

The spectrum of the PVA film (Figure 6-4b) revealed a broad absorption band between  $3000 - 3500\text{ cm}^{-1}$  centered at  $3264\text{ cm}^{-1}$  which corresponds to  $\nu(\text{OH})$  stretching vibrations (Alves et al., 2011). This is mainly due to the presence of many hydroxyl groups on the PVA backbone which can form intramolecular and intermolecular hydrogen bonding (Mansur et al., 2004). The peak doublet at about  $2938/2910\text{ cm}^{-1}$  can be assigned to  $\nu_{\text{as}}(\text{CH}_2)/\nu_{\text{s}}(\text{CH}_2)$  stretching vibrations. The small bands around  $1720\text{ cm}^{-1}$  belong to  $\nu(\text{C}=\text{O})$  stretching vibrations of residual poly(vinylacetate) ( $\leq 2\%$ ) units due to the preparation of PVA from the hydrolysis of poly(vinylacetate) (Rouhi et al., 2017). The peak at  $1416\text{ cm}^{-1}$  belongs to the  $\delta(\text{CH}_2)$  bending vibration. The peak at  $1237\text{ cm}^{-1}$  is due to  $\text{CH}_2$  wagging vibrations. The peak at  $1142\text{ cm}^{-1}$  is assigned to a coupled  $\nu(\text{CC})$  and  $\nu(\text{CO})$  stretching vibration. This peak is related to PVA crystallinity (Castro et al., 2014). Characteristic peaks between  $1089$  and  $1040\text{ cm}^{-1}$  belong to  $\nu(\text{C}-\text{O})$  stretching vibrations, and that at  $918\text{ cm}^{-1}$  assigns to a  $\text{CH}_2$  rocking vibration (Haghghi et al., 2020b).

The spectrum of pure BCNW is reproduced in Figure 6-4c. The characteristic peaks at around  $3343\text{ cm}^{-1}$  ( $\nu(\text{O}-\text{H})$  stretching vibrations in different hydrogen bonding states),  $2894\text{ cm}^{-1}$  ( $\nu(\text{CH}_2)$  stretching vibrations),  $1640\text{ cm}^{-1}$  ( $\delta(\text{O}-\text{H})$  deformation vibration),  $1427\text{ cm}^{-1}$  ( $\delta(\text{CH}_2)$  bending vibration),  $1360\text{ cm}^{-1}$  (angular deformation of  $\text{C}-\text{H}$  bonds),  $1314\text{ cm}^{-1}$  ( $\omega_{\text{s}}(\text{CH}_2)$  bending vibration, assigned as a crystallinity-sensitive band of cellulose),  $1162\text{ cm}^{-1}$  ( $\nu_{\text{as}}(\text{C}-\text{O}-\text{C})$  stretching vibrations of  $\beta$ -(1-4) glycoside bonds),  $1107\text{ cm}^{-1}$  ( $\nu(\text{C}-\text{O})$  stretching vibrations). The strongest peaks across the BCNW spectrum at  $1054$  and  $1031\text{ cm}^{-1}$  are assigned to  $\nu(\text{C}-\text{O})$  stretching vibrations of aliphatic primary and secondary alcohol of cellulose (Voronova et al., 2015). The peak at  $812\text{ cm}^{-1}$  corresponds to a symmetric vibration of  $\text{C}-\text{O}-\text{S}$  bonds associated with  $\text{C}-\text{O}-\text{SO}_3^-$  groups due to sulfuric acid hydrolysis during BCNW production (Agustin et al., 2013; Santos et al., 2014). From the multiplicity of  $\nu(\text{O}-\text{H})$  absorption bands around  $3350\text{ cm}^{-1}$  in the BCNW spectrum, it can be inferred that the hydroxyl groups in BCNW contribute to the formation of various kinds of inter- and intramolecular hydrogen bonds (Chi and Catchmark, 2017; Vasconcelos et al., 2017).

Comparison of the spectra of the GL/PVA blend film (Figure 6-4d) and the pure GL film (Figure 6-4a) showed, that the amide-I peak of GL shifted from  $1630\text{ cm}^{-1}$  to  $1637\text{ cm}^{-1}$  in the blend indicating the interactions between the  $\text{C}=\text{O}$  groups of GL and the OH functionalities of PVA (Kariminejad et al., 2018). This change can be interpreted as a conformational change of the secondary structure of GL. The amide-II peak slightly shifts from  $1543$  to  $1549\text{ cm}^{-1}$  in the blend and also indicates changes in hydrogen bonding. Thus, our spectroscopic data showed that GL and PVA were miscible and blending GL and PVA resulted in conformational and hydrogen bonding changes. Similar results were reported by Silva et al. (2008).

The incorporation of BCNW into the GL/PVA blend caused some changes in the shape and intensity of the main peaks (Figure 6-4e and 6-4f). These changes were minor in films containing BCNW up to 7.5 wt% (see for example Figure 6-4e) (Khan et al., 2012). The GL/PVA blend film matrix containing 10 wt% BCNW (Figure 6-4f) showed shifts relative to the peaks between  $3500 - 3000 \text{ cm}^{-1}$ ,  $1637 \text{ cm}^{-1}$ , and  $1549 \text{ cm}^{-1}$  of GL/PVA only. Moreover, new peaks at  $1054 \text{ cm}^{-1}$  and  $1031 \text{ cm}^{-1}$ , corresponding to the C–O–C pyranose ring stretching vibrations of aliphatic primary and secondary alcohols of BCNW, were observed (Huq et al., 2012). These results suggest that hydrogen bonding takes place between hydroxyl groups of BCNW and carbonyl and hydroxyl groups of the GL/PVA matrix resulting in additional conformational changes. Similar results were reported by Cazón et al. (2018) and Santos et al. (2014).

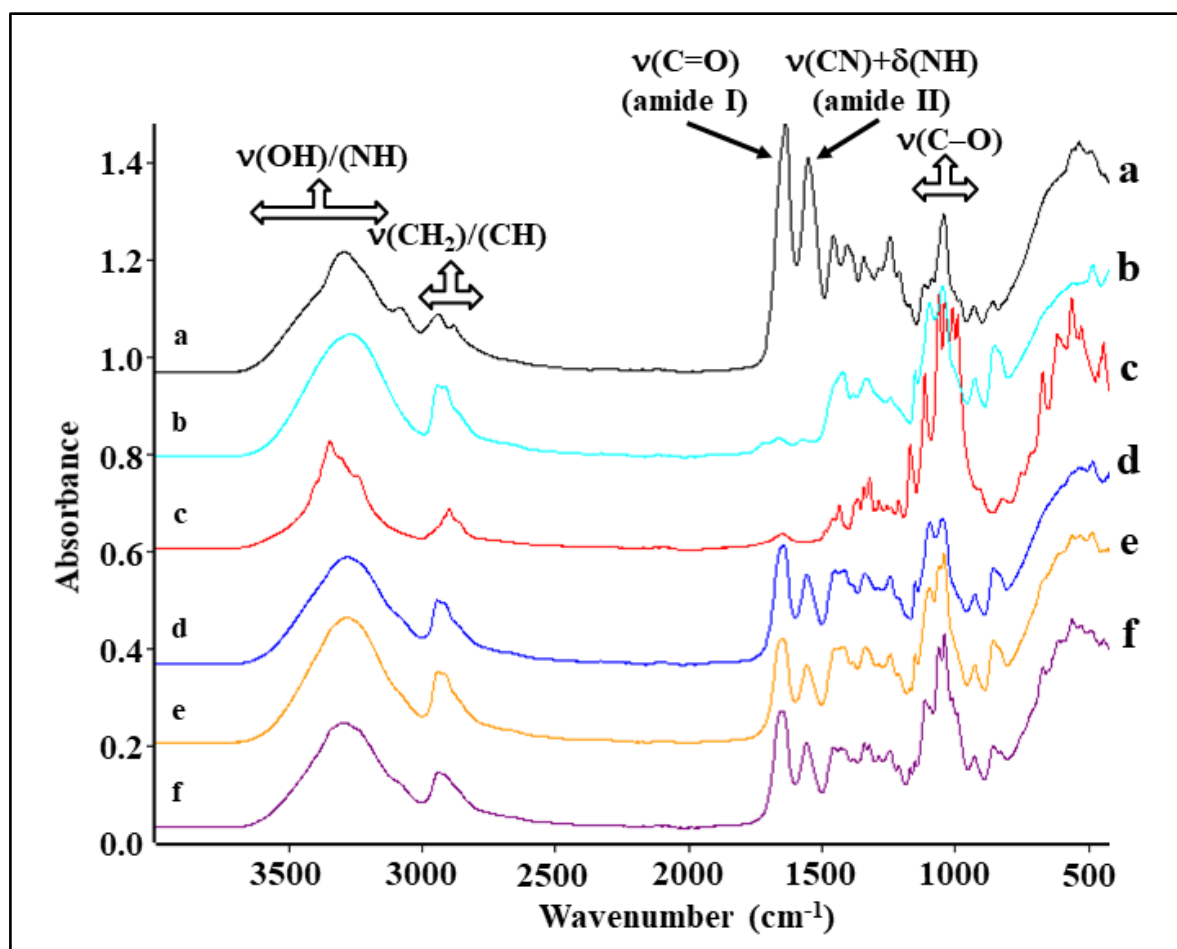


**Figure 6-4.** ATR/FT-IR spectra of films based on: a) Gelatin (GL), b) Polyvinyl alcohol (PVA), c) Bacterial cellulose nanowhisker (BCNW), d) GL/PVA blend, e) GL/PVA/BCNW5%, f) GL/PVA/BCNW10%.

### Thickness and mechanical properties

Adequate mechanical strength and extensibility are required to maintain the integrity and properties of foodstuff inside the packaging during processing, transportation, distribution, retailing, and storage. The thickness and mechanical properties including tensile strength (TS), elongation at break percentage (E%), and elastic modulus (EM) of films based on a GL/PVA blend as control and those reinforced with BCNW (1–10 wt%) are presented in Table 6-1. The thickness of the investigated films varied between 42 and 48  $\mu\text{m}$ . The GL/PVA blend showed the lowest

thickness value while the incorporation of BCNW above 2.5% significantly increased the thickness ( $p < 0.05$ ). The GL/PVA/BCNW10% film showed the highest thickness ( $p < 0.05$ ) due to the increase in the solid content (Pereda et al., 2014).

The TS increased from 21.8 MPa in the control film to 26.5 MPa by incorporation of BCNW up to 7.5 wt%. This behavior may be attributed to a strong interfacial interaction between BCNW and the GL/PVA blend film matrix (Agustin et al., 2013). A large number of hydroxyl functionalities are available on the surface of the BCNW to interact with the GL/PVA blend film matrix to form hydrogen bonds, resulting an increase in TS (Wang et al., 2017). However, this reinforcement effect of the BCNW was reduced in GL/PVA/BCNW10%, which scored TS as low as the control film, probably due to the agglomerations of BCNW, as observed in the SEM analysis (Figure 6-2f). At the highest amount of the BCNW (10 wt%), the nanowhisiker– biopolymer matrix interaction may be partially replaced by the nanowhisiker–nanowhisiker associations with a consequent drop in TS (Khan et al., 2012). The TS for the films containing BCNW up to 7.5 wt% were comparable with those of plastic films that are used widely in the market, such as high-density polyethylene (22–31 MPa) but slightly lower than that for polypropylene (31–38 MPa). The E% also significantly increased by the addition of BCNW up to 7.5 wt%, while further incorporation of BCNW into the film network resulted in a decrease of E% which can be explained by the restrictions to the consecutive motion at the filler–biopolymer interface (Yadav and Chiu, 2019). Aloui et al. (2016) and Rescignano et al. (2014) also reported that the addition of cellulose nanomaterial up to 5 wt% to PVA film caused an increase in E%. Similar behavior was observed for EM values. The significant decline in mechanical properties of the GL/PVA/BCNW10% film is also consistent with the SEM observation that the agglomeration of BCNW resulted in disrupted cross-section morphology. Similar mechanical performances have been reported for the addition of nanocellulose to other biopolymers such as agar, starch, and PVA (Agustin et al., 2013; Reddy and Rhim, 2014; Rescignano et al., 2014; Aloui et al., 2016). In contrast to these results, Khan et al. (2012) and Pereda et al. (2014) reported that the incorporation of nanocellulose to chitosan films significantly reduced the E%. Authors concluded that the strong interactions between nanocellulose and chitosan film matrix may limit the motion of the matrix and consequently cause a decrease in E%. Overall, the literature data regarding reinforcement effect of nanocellulose on elasticity values are partially controversial and are influenced by various factors such as types and concentration of the biopolymer and nanocellulose, the degree of dispersion, and interfacial interactions (Wang et al., 2017).

**Table 6-1** Thickness, tensile strength (TS), elongation at break percentage (E%), and elastic modulus (EM) of films based on: Gelatin-Polyvinyl alcohol blend (GL/PVA) as control and those reinforced with bacterial cellulose nanowhiskers (GL/PVA/BCNW 1-10%).

Film Sample	Thickness ( $\mu\text{m}$ )	TS (MPa)	E (%)	EM (MPa)
GL/PVA	42.0 $\pm$ 0.9 <sup>a</sup>	21.8 $\pm$ 2.3 <sup>a</sup>	28.9 $\pm$ 3.7 <sup>a</sup>	825.6 $\pm$ 32.9 <sup>a</sup>
GL/PVA/BCNW1%	42.9 $\pm$ 0.9 <sup>a</sup>	22.8 $\pm$ 0.9 <sup>ab</sup>	34.6 $\pm$ 4.7 <sup>b</sup>	936.1 $\pm$ 70.7 <sup>b</sup>
GL/PVA/BCNW2.5%	43.2 $\pm$ 1.0 <sup>b</sup>	24.1 $\pm$ 2.1 <sup>b</sup>	34.5 $\pm$ 4.2 <sup>b</sup>	911.8 $\pm$ 71.0 <sup>b</sup>
GL/PVA/BCNW5%	44.9 $\pm$ 0.9 <sup>b</sup>	24.2 $\pm$ 1.3 <sup>b</sup>	36.9 $\pm$ 1.2 <sup>b</sup>	891.3 $\pm$ 13.0 <sup>b</sup>
GL/PVA/BCNW7.5%	45.9 $\pm$ 1.0 <sup>b</sup>	26.5 $\pm$ 0.9 <sup>c</sup>	40.8 $\pm$ 3.1 <sup>c</sup>	983.3 $\pm$ 31.1 <sup>c</sup>
GL/PVA/BCNW10%	48.0 $\pm$ 2.2 <sup>c</sup>	21.1 $\pm$ 2.1 <sup>a</sup>	31.6 $\pm$ 2.3 <sup>ab</sup>	823.7 $\pm$ 89.2 <sup>a</sup>

Values are given as mean  $\pm$  SD (n = 3).

Different letters in the same column indicate significant differences ( $p < 0.05$ ).

## Color

The color parameters ( $L^*$ ,  $a^*$ , and  $b^*$ ) and total color difference ( $\Delta E^*$ ) of films based on a GL/PVA blend as control and those reinforced with BCNWs (1–10 wt%) are presented in Table 6-2. The values inside this table can be compared with commercial food packaging material and give a hint to the producer about the visual appearance, commercial success, and acceptability of products by consumers (Luzi et al., 2017). The  $L^*$  value, indicating lightness, was 99 – 99.2 without significant variations among treatments, showing that all films were highly clear irrespective of the incorporation of BCNW into the GL/PVA film matrix ( $p > 0.05$ ). Shankar and Rhim, (2016) also reported that the incorporation of cellulose nanofiber up to 10 wt% into the agar films did not significantly change the lightness. The  $a^*$  value, expressing the green-red color component, was negative for all films and did not show significant changes among different treatments ( $p > 0.05$ ). The  $b^*$  value, measuring the blue-yellow color component, slightly increased upon the addition of BCNW ( $p < 0.05$ ), reflecting a slight yellowish color in bio-nanocomposite films.  $\Delta E^*$  measures the overall color variation of a sample compared with a standard color. The  $\Delta E^*$  value varied from 0.92 in the control film to 1.6 in GL/PVA/BCNW10%. The addition of BCNW to the GL/PVA film matrix increased the  $\Delta E^*$  value ( $p < 0.05$ ) and the observed change can be attributed to the change in the colorimetric coordinate  $b^*$  and increase in film thickness upon addition of BCNW. Overall, the  $\Delta E^*$  value of the films under investigation was comparable with commercial plastic films (perceptibility threshold of  $\Delta E^* \sim 1$ ) available in the market (Thakhiew et al., 2013). Moreover,  $\Delta E^* = 2$  is the limit for the human eye perception, hence consumers shall not be able to perceive any color difference in the developed films by the naked eye (Luzi et al., 2017).

**Table 6-2.** Color parameters ( $L^*$ ,  $a^*$ , and  $b^*$ ) and total color difference ( $\Delta E^*$ ) of films based on: Gelatin-Polyvinyl alcohol blend (GL/PVA) as control and those reinforced with bacterial cellulose nanowhiskers (GL/PVA/BCNW 1-10%).

Film sample	Color parameters			
	$L^*$	$a^*$	$b^*$	$\Delta E^*$
GL/PVA	99.2 ± 0.2 <sup>a</sup>	-0.3 ± 0.02 <sup>a</sup>	0.8 ± 0.1 <sup>a</sup>	0.9 ± 0.2 <sup>a</sup>
GL/PVA/BCNW1%	99.1 ± 0.1 <sup>a</sup>	-0.3 ± 0.01 <sup>a</sup>	0.9 ± 0.1 <sup>ab</sup>	1.0 ± 0.1 <sup>ab</sup>
GL/PVA/BCNW2.5%	99.1 ± 0.2 <sup>a</sup>	-0.4 ± 0.03 <sup>a</sup>	0.9 ± 0.2 <sup>ab</sup>	1.1 ± 0.2 <sup>ab</sup>
GL/PVA/BCNW5%	99.1 ± 0.1 <sup>a</sup>	-0.4 ± 0.04 <sup>a</sup>	1.1 ± 0.1 <sup>b</sup>	1.2 ± 0.1 <sup>b</sup>
GL/PVA/BCNW7.5%	99.0 ± 0.1 <sup>a</sup>	-0.4 ± 0.02 <sup>a</sup>	1.4 ± 0.4 <sup>c</sup>	1.5 ± 0.3 <sup>c</sup>
GL/PVA/BCNW10%	99.1 ± 0.1 <sup>a</sup>	-0.4 ± 0.01 <sup>a</sup>	1.5 ± 0.4 <sup>c</sup>	1.6 ± 0.4 <sup>c</sup>

Values are given as mean ± SD (n = 3).

Different letters in the same column indicate significant differences ( $p < 0.05$ ).

## UV barrier, light transmittance, and opacity value

UV-Vis light barrier property is one of the key features in the development of films for the packaging of specific food categories since it allows to avoid or retard the oxidation of lipids, pigments, proteins, or vitamins. This feature is directly related to the food shelf life by preventing undesirable flavors, color, odors, loss of nutrients, thus preserving organoleptic and nutritional properties of the packed food (Cazón et al., 2019). The UV-Vis light transmittance and opacity value of films based on a GL/PVA blend as control and those reinforced with BCNWs (1–10 wt%) in the wavelength range between 200 to 800 are presented in Table 6-3. The control film was completely transparent with transmittance between 85.3 to 90.8% in the visible wavelength range (400 – 800 nm). Both GL and PVA films are well known for their transparency and their blends

also showed transparency mainly due to their high homogeneity and the compatibility of the components. Films containing BCNW up to 7.5 wt% also showed the same level of transparency, indicating a good dispersion of BCNW into GL/PVA blend film matrix, as observed by SEM images (Figure 6-2 and 6-3). Light transmission was slightly reduced and ranged between 81.3 to 84.5% in the film containing 10 wt% BCNW.

All films exhibited lower transmittance values at UV light (200 – 350 nm) than at visible light. Addition of BCNW into the GL/PVA film matrix did not affect the UV transmittance and all films showed similar values. Similar results were reported by Xu et al. (2019).

Opacity value of the films was calculated by measuring transmittance at 600 nm. Incorporation of BCNW into GL/PVA blend film up to 7.5 wt% did not affect the opacity value and these films showed a high level of transparency indicating the good interfacial adhesion between the BCNW and GL/PVA film matrix suggesting that the BCNW was dispersed homogeneously at the nanoscale (Aloui et al., 2016). However, a higher opacity value was observed at GL/PVA/BCNW10% ( $p < 0.05$ ) mainly due to the hindrance of light passage by agglomerated BCNW particles (Reddy and Rhim, 2014). Overall, all films can be considered as highly transparent due to the opacity value lower than 2. This is important for consumer preference to see the food items inside the packaging. This result was also in accordance with  $L^*$  value that showed all films were clear with  $L^*$  value above 99.

**Table 6-3.** UV and visible light transmittance (T%) and opacity value (600 nm) of the films based on: Gelatin-Polyvinyl alcohol blend (GL/PVA) as control and those reinforced with bacterial cellulose nanowhiskers (GL/PVA/BCNW 1-10%).

Film sample	Light transmission (%) at different wavelengths (nm)								Opacity (600 nm)
	200	280	350	400	500	600	700	800	
GL/PVA	0.04	49.3	77.1	85.3	88.9	90.1	90.6	90.8	1.1 ± 0.05 <sup>a</sup>
GL/PVA/BCNW1%	0.03	50.7	77.5	85.4	88.8	89.7	90.1	90.0	1.1 ± 0.03 <sup>a</sup>
GL/PVA/BCNW2.5%	0.03	49.7	77.4	85.7	89.2	90.2	90.6	90.6	1.0 ± 0.04 <sup>a</sup>
GL/PVA/BCNW5%	0.11	51.0	77.6	85.6	89.1	90.0	90.4	90.4	1.0 ± 0.06 <sup>a</sup>
GL/PVA/BCNW7.5%	0.03	48.4	75.4	83.5	87.5	88.9	89.4	89.6	1.1 ± 0.01 <sup>a</sup>
GL/PVA/BCNW10%	0.03	54.1	78.9	81.3	83.3	83.3	84.5	84.5	1.6 ± 0.20 <sup>b</sup>

Opacity values are given as mean ± SD (n = 3) while light transmission is given as mean (n = 3).

Different letters in the same column indicate significant differences ( $p < 0.05$ ).

## Moisture content, water vapor transmission rate, and water vapor permeability

The moisture content (MC), water vapor transmission rate (WVTR), and water vapor permeability (WVP) of films based on a GL/PVA blend as control and reinforced with BCNW (1–10 wt%) are presented in Table 6-4. The MC values ranged from 15.5 to 18%. The control film showed higher MC values than films containing BCNW ( $p < 0.05$ ) and by increasing the BCNW content, the MC value in the film was reduced ( $p < 0.05$ ). This might be attributed to the high surface area of BCNW and its strong interaction with GL/PVA chains leading to lower availability of free hydroxyl groups and, consequently, a reduction in hydrophilicity and MC value (Soykeabkaew et al., 2012; Yadav and Chiu, 2019).

One of the main drawbacks of GL and PVA films for packaging applications is their strong hydrophilic character causing poor moisture resistance. The hydroxyl groups in the polymer backbone make them polar substances able to attract water molecules from the surrounding environment. Reducing WVTR and WVP plays an important role in increasing the shelf life of



packed foodstuffs (Del Nobile et al., 2002). The WVTR of the control film was 1795.7 (g / day m<sup>2</sup>). With the increase in BCNW content up to 7.5 wt%, the WVTR values decreased and reached 1403 (g / day m<sup>2</sup>), corresponding to a decrease by about 22%. This is probably due to the impermeable crystalline structure of BCNW, which results in a slower water transmission rate (Xu et al., 2019). Further addition of BCNW caused an increase of WVTR in GL/PVA/BCNW10% (p<0.05) back to values similar to the control film. This effect can be attributed to the disrupted microstructure as it was observed in the SEM images (Figure 6-3f).

The WVP value of the control film was 8.7 (g mm / day kPa m<sup>2</sup>). The WVP values decreased with the increase in BCNW content up to 7.5 wt% reaching 7.5 (g mm / day kPa m<sup>2</sup>), corresponding to a decrease by about 14%. Further addition of BCNW caused a WVP increase in GL/PVA/BCNW10% (p<0.05). Addition of BCNW is an effective way of decreasing the film sensitivity to moisture. The improvement in WVP by addition of BCNW might be attributed both to the decreased hydrophilicity, resulting in turn from the lower availability of free hydroxyl groups, and to the tortuous network formed by the homogenous dispersion of BCNW in GL/PVA film, leading to slower diffusion of water molecules (Reddy and Rhim, 2014; Singh et al., 2018). Moreover, BCNW is less hygroscopic than GL/PVA blend due to a higher degree of molecular order (Ghanbari et al., 2018). Huq et al. (2012) reported that the addition of 5 wt% of cellulose nanocrystals into alginate-based films was effective to decrease WVP up to 31%. In contrast to these results, Wang et al. (2017) reported that addition of cellulose nanowhisker to alginate-based films caused an increase in WVP mainly due to the stronger hydrophilic nature of the cellulose nanowhisker compared to the polymer matrix. Overall, barrier property to water is an important feature to protect packaged products from the environment and maintain their quality for longer storage times in particular for moisture-sensitive foods. This feature is important for both fresh products such as fruits and vegetables, to avoid dehydration, and for dry foods such as bakery products (bread, biscuits, crackers, etc.) to avoid moisture uptake from the environment (Cazón et al., 2017).

**Table 6-4.** Moisture content (MC), water vapor transmission rate (WVTR), and water vapor permeability (WVP) of the films based on: Gelatin-Polyvinyl alcohol blend (GL/PVA) as control and those reinforced with bacterial cellulose nanowhiskers (GL/PVA/BCNW 1-10%).

Film sample	MC (%)	WVTR (g /day m <sup>2</sup> )	WVP 90:0% RH (g mm/kP day m <sup>2</sup> )
GL/PVA	18.03 ± 0.8 <sup>c</sup>	1795.7 ± 79.8 <sup>b</sup>	8.7 ± 0.4 <sup>b</sup>
GL/PVA/BCNW1%	17.23 ± 1.1 <sup>bc</sup>	1721.9 ± 141.4 <sup>ab</sup>	8.6 ± 0.7 <sup>b</sup>
GL/PVA/BCNW2.5%	16.34 ± 0.6 <sup>ab</sup>	1588.1 ± 135.0 <sup>ab</sup>	7.9 ± 0.3 <sup>a</sup>
GL/PVA/BCNW5%	15.73 ± 0.7 <sup>ab</sup>	1548.6 ± 55.5 <sup>ab</sup>	8.0 ± 0.3 <sup>a</sup>
GL/PVA/BCNW7.5%	15.53 ± 0.8 <sup>a</sup>	1403.0 ± 117.5 <sup>a</sup>	7.5 ± 0.6 <sup>a</sup>
GL/PVA/BCNW10%	15.50 ± 0.3 <sup>a</sup>	1790.6 ± 173.3 <sup>b</sup>	9.9 ± 0.9 <sup>c</sup>

Values are given as mean ± SD (n = 3).

Different letters in the same column indicate significant differences (p<0.05).

## Conclusion

In this study, BCNW was synthesized from *K. xylinus* (strain K2G30 = UMCC 2756) using sulfuric acid hydrolysis and it was incorporated into GL/PVA blend to form bio-nanocomposite films. SEM images showed homogenous dispersion of BCNW in GL/PVA film matrix up to 7.5 wt% while above this concentration agglomeration of BCNW occurred. All microstructural and

physical characterization analyses proved that incorporation of BCNW up to 7.5 wt% determined significant improvement in the film properties of interest for food packaging application. This concentration can be suggested as a threshold level for the incorporation of BCNW into the GL/PVA film matrix, since the significant deterioration of mechanical, optical, and water barrier properties occurred above this level, consistent with ATR/FT-IR observation highlighting band shifts and intensity changes. The total color difference of films was not detectable by the naked eye and the developed films showed high lightness and transparency values, comparable to synthetic plastic films available on the market. Overall, the present study demonstrates the reinforcement effect of BCNW on GL/PVA films and proposes such bio-nanocomposite as an effective and sustainable bioproduct to improve the mechanical and water barrier properties of GL/PVA films, which are especially critical for food preservation, thereby widening the potential range of application.

# Chapter 7

## Mechanical and structural properties of environmental green composites based on functionalized bacterial cellulose

Silvia Barbi<sup>1</sup>, Claudia Taurino<sup>1</sup>, Salvatore La China<sup>2</sup>, Kavitha Anguluri<sup>2</sup>, Maria Gullo<sup>2</sup>, Monia Montorsi<sup>1</sup>

<sup>1</sup>Department of Science and Methods for Engineering, University of Modena and Reggio Emilia, Reggio Emilia, Via Amendola 2, 42122, Italy

<sup>2</sup>Department of Life Sciences, University of Modena and Reggio Emilia, Reggio Emilia, Via Amendola 2, 42122, Italy

**This chapter is published as:**

Barbi S, Taurino C, **La China S**, Anguluri K, Gullo M, Montorsi M. Mechanical and structural properties of environmental green composites based on functionalized bacterial cellulose. *Cellulose* (2021) 1–12. <https://doi.org/10.1007/s10570-020-03602-y>

## Abstract

In this work TiO<sub>2</sub> and highly inorganic ceramic Clay were successfully immobilized into Bacterial Cellulose (BC), produced by *Komagataeibacter xylinus* K2G30 (UMCC 2756) strain, in different proportions. The morphology, structure, and mechanical properties of the composites, fabricated by wet mechanical mixing, were investigated through a multi-technique approach: density measurement, optical and electronic microscopy, FTIR spectroscopy, contact angle measurement and mechanical tensile testing, before and after aging, under UV light exposure. Results suggest completely different behavior by using TiO<sub>2</sub> or Clay. In fact, porous fragile structures were obtained by employing Clay, whereas more compact and plastic-like specimen by using TiO<sub>2</sub>, due to different chemical bonding developed through H-bonding, as confirmed by FTIR. Enhanced tensile resistance at break was found for a content of TiO<sub>2</sub> equal to 20 wt% and this result was not affected by aging, under UV light exposure. This study demonstrates how ceramic inorganic fillers for BC are able to act in completely different way, becoming of interests in different fields such as hydrophilic porous membranes for Clay and compact plastic-like film for textile industry with TiO<sub>2</sub> addition.

## Introduction

Bacterial cellulose (BC) is attracting the interest of the more recent research as remarkable versatile biomaterial employed in a wide range of applications including food packaging, biomedical, cosmetics, and engineering fields (Shah et al., 2013; Haghghi et al., 2020a). BC's production is the results of a hierarchical process, bacterial-direct formation and assembly steps that occur outside the cell (Gullo et al., 2018). It is formed starting from carbohydrates, like sugars or sugar-alcohol, in which the monomers are linked together by a  $\beta$ -1,4-bonding. The native glucan chain is secreted outside the cell, in which assembly phenomena occur to form microfibrils, and then self-assemble into final fibers. Finally, the crystalline fibers polymerize to each other in the pellicle, forming the cellulose layer (Brown, 2004). The polymer is characterized by a large surface area, resulting in a biomaterial with high biocompatibility, biodegradability and tensile strength (Esa et al., 2014). Furthermore, the presence of a large amount of hydroxyl groups makes BC the ideal candidate for in bulk and surface functionalization, easily promoting new materials design, motivated by consumers and market demand for high-performance and innovative commodities. For all these reasons, many studies focus first on the selection of suitable organisms for producing native BC. Among bacteria, the most representative species is *Komagataeibacter xylinus* (*K. xylinus*), which strains are recognized as effective BC producers (Valera et al., 2014; Gullo et al., 2017). Although limitations in the process for obtaining BC are reported, *K. xylinus* strains highlight high potential of synthesis in different culture conditions (La China et al., 2018). The intraspecific variability of strains belonging to the species *K. xylinus* offers a huge chance to study the mechanism of BC synthesis through different approaches. For instance, the investigations on the structure and differences of cellulose synthase genes organization and subunits composition, as well as the study of the most suitable carbon sources and culture conditions, provide the basis for a rational strain selection procedure, aimed to optimize the BC production for specific purposes (Liu et al., 2018; La China et al., 2020; Yang et al., 2020). On these bases the industrial exploitation of *K. xylinus* strains could be more feasible for scale up the production of BC as native and functionalized biomaterial.

Functional BC-based composites can be obtained by different approaches based on the cultivation methods and functionalization of BC films. Based on the cultivation methods, different shape can be obtained such as membrane (static cultivation), pellets (shake cultivation) and fibrous materials (Lee et al., 2011). Furthermore, by using the 3D printing, it is possible obtain a wide range of shapes and morphologies of the BC layer surface (Bottan et al., 2015; Schaffner et al., 2017). In addition, BC properties can be easily modified after the bioprocess, for example by coating with polymers or chemicals. Thereafter, different BC composites have been developed, exploiting BC porous nature able to act as a matrix for different reinforcement materials either through *in situ* or *ex situ* methods (UI-Islam et al., 2012; Shah et al., 2013; Keshk, 2014). Among them and focusing on BC functionalization with inorganic compounds much work has been reported on TiO<sub>2</sub> and SiO<sub>2</sub>-TiO<sub>2</sub> addition to BC for substrates with self-cleaning properties, thanks to an improved stability of the anatase phase due to SiO<sub>2</sub> inclusion (Chauhan and Mohanty, 2014; Khan et al., 2015; Monteiro et al., 2019). Moreover, mineral such as hydroxyapatite, calcium carbonate and clay have been investigated for biomedical applications, due to their biocompatible, non-toxic, hard tissue-mimicking nature, and reinforcing capability (UI-Islam et al., 2013; Torres et al., 2019). Furthermore, clay minerals, such as kaolinite, bentonite and montmorillonite, have received great attention as naturally available materials compatible with BC, due to their valuable reinforcing properties also considering that they can be synthesized without the use of toxic and expensive organic solvents (Giannelis et al., 1999; Gamelas and Ferraz, 2015; del Campo et al., 2018). In fact, clay has a large surface area that promotes strong physical contacts with the BC. Although, inorganic clay could be a promising alternative to more expensive and pure materials in a green economy perspective, much attention must be paid to the formation of aggregates due to the strong secondary bonding (e.g. Van der Waals or H-bond) among minerals (García et al., 2011). In addition, BC mixtures with inorganic compounds have demonstrated promising application in energy storage system into Li-S cells, as functional layer to restrain the shuttle effect of Li-S cells, avoiding the physical and chemical adsorption of polysulfides (Li et al., 2017a; Xie et al., 2018). Nevertheless, new fields of application are arising for BC-inorganic compounds composites, such as textile and bio-building. For the first, research is only at the very beginning, and the main driver is the need of more sustainable materials with functional properties (e.g. optoelectronic devices for smart textiles and anthropomorphic systems) (Radetić, 2013; Kamiński et al., 2020). On the other hand, bio-building research on BC-based materials is focused only on cementitious materials with enhanced compressive strength and reduced porosity, even if, possible application of BC as natural binder seems promising (Fu et al., 2017). In this context, attention must be paid both to the production method, which affects the fabrication cost, and to the use of toxic chemical reagents, that must be strongly reduced or avoided.

In this context, the aim of this study is to test if an easy method for composite production, based on wet BC as matrix and inorganic particle such as TiO<sub>2</sub> and Clay as reinforce, to reduce the economic and environmental impact of the production process, in an industrial scale up perspective. The first novelty of the study is to test an easy method such as mechanical wet mixing, already reported in literature as promising path for BC composite production, in new field of application such as high performance textiles for medical or sport purpose (Alves et al., 2019; Torres et al., 2019; Martins et al., 2020). Thereafter, structural, and mechanical properties of these composites have been tested in order to assess the ability of the material to fit and adhere to the body shape. In addition, in our knowledge, this is the first study in which composites are based on

BC that was produced by K2G30 (UMCC 2756) strain, which belong to *Komagataeibacter xylinus* species. This strain has been previously studied for its ability to produce high amount of BC from different carbon sources and it is still under a comprehensive study, including its genomic and technological properties (Gullo et al. 2017; Gullo et al. 2019).

## Materials and Methods

### Raw Materials

TiO<sub>2</sub> powder (D90<15 μm), with purity >99% (Sigma Aldrich), and Clay powder (D90<20 μm), with composition (wt %): 71SiO<sub>2</sub> - 19Al<sub>2</sub>O<sub>3</sub> - 5Na<sub>2</sub>O - 2.5K<sub>2</sub>O - 2.5FeO, were employed as filler for BC. BC was produced using *Komagataeibacter xylinus* K2G30 strain, which is deposited at Unimore Microbial Culture Collection under the collection code UMCC 2756 and maintained following the standard procedure of the Microbial Resource Research Infrastructure-Italian Joint Research Unit (MIRRI-IT) (Gullo et al., 2017; De Vero et al., 2019a). The strain was cultivated on the standard Hestrin-Shramm (HS) medium (w/v): D-glucose, 2%; yeast extract, 1%; polypepton, 0.5%; disodium phosphate anhydrous 0.27%; citric acid 0.115%) (Hestrin and Schramm 1954). The cultivation was carried out using 1 L flasks with a total working volume of 300 mL inoculated with 5 % v/v of the seed culture. The incubation was conducted at 28 °C for a total of 7 days, in aerobic conditions. The resulting native BC was collected, washed three times with distilled water and treated with 1% NaOH (Sigma Aldrich) at 90 °C for 1 h to eliminate the bacterial cells. Treated BC was washed with distilled water until reaching neutral pH and then used for bio-composite preparation.

### Bio-composite preparation

TiO<sub>2</sub> and Clay were separately mixed with BC following the composition reported in Table 7-1, obtaining batches of 15g for each sample. Wet mechanical mixing, through analytical mill (A10 basic, IKA), was done for each sample with a constant mixing time of 5 min. Slurries were poured separately into circular aluminum dishes (diameter= 7.5 cm) and allowed to cool and desiccate for 24 hours at room temperature. All specimens were conditioned in a controlled environment chamber at 25 °C and 50% relative humidity before characterization.

**Table 7-1.** Composition and bio-composite properties

	BC (wt%)	TiO <sub>2</sub> (wt%)	Clay (wt%)	Apparent Density (g/cm <sup>3</sup> )	True Density (g/cm <sup>3</sup> )	Porosity (%)	Contact Angle
<b>BC</b>	100			0.623 ± 0.023	--	--	64.5 ± 0.8
<b>T10</b>	90	10	-	1.076 ± 0.020	1.191	9.65	35.6 ± 0.8
<b>T20</b>	80	20	-	1.086 ± 0.034	1.338	18.85	19.8 ± 0.6
<b>T30</b>	70	30	-	0.993 ± 0.014	1.696	41.45	20.1 ± 0.8
<b>T40</b>	60	40	-	0.536 ± 0.010	2.054	73.90	18.3 ± 0.5
<b>C10</b>	90	-	10	0.413 ± 0.043	0.781	47.10	55.3 ± 0.7
<b>C20</b>	80	-	20	0.334 ± 0.020	0.938	64.41	49.6 ± 0.9
<b>C30</b>	70	-	30	0.309 ± 0.023	1.096	71.81	35.2 ± 0.8
<b>C40</b>	60	-	40	0.296 ± 0.032	1.254	76.39	20.8 ± 0.4

## Bio-composite characterization

The apparent density of the bio-composites was calculated by measuring the weight (W) and volume (V) of each sample after drying, using an analytical balance (sensitivity = 0.00001g) and an electronic digital micrometer (Mitutoyo, YY-T1BD-2GYE, Kawasaki, Japan) respectively. 15 different points of measure were taken, and the average value was considered as reference, together with its calculated standard deviation, to calculate sample's apparent density as W/V ratio. The true density of the composites was calculated by the mixture law considering the following material's density:  $\text{TiO}_2 = 4.2 \text{ g/cm}^3$  and  $\text{Clay} = 2.2 \text{ g/cm}^3$ . Composite's porosity (Table 7-1) was determined using the following equation (Mwaikambo and Ansell, 2001):

$$\text{Porosity} = \left( 1 - \frac{\text{Apparent Density}}{\text{True Density}} \right) * 100$$

The morphology of each sample was investigated by environmental scanning electron microscopy (ESEM, FEI XL-30) and optical microscopy (Leica microsystems, DM500). Surface behavior was measured through static contact angle measurement ( $\theta$ ). A water droplet technique was employed (OCA 20, Data Physics instrument) on each specimen in 10 different points of the surface and the average value was taken as reference for each sample, together with its calculated standard deviation.

The structural interaction between  $\text{TiO}_2$  and Clay with BC was analyzed by attenuated total reflectance Fourier transform infrared (FTIR-ATR) spectroscopy. The FTIR-ATR spectra were obtained with a Bruker Vertex 70 spectrophotometer in the range of  $400\text{--}4000 \text{ cm}^{-1}$ , with  $4 \text{ cm}^{-1}$  resolution and 30 scans.

The mechanical properties were determined through dynamic mechanical analysis (DMA, Q800 TA Instruments), employing a film tension clamp and fragments of the composites (30 mm x 10 mm). The specimens were conditioned at standard conditions (25 °C; 50% RH) for 24 hours before testing. The samples were then aligned, mounted in film clamps for the Q800 using the suitable fixture. The tensile properties of samples were monitored as the films were elongated with an applied force which was ramped to 18 N at a rate of  $0.05 \text{ N min}^{-1}$  from 0.05 N. Young's modulus (E) was calculated as the slope of the initial region of the stress-elongation curve from 0.05% to 0.25% of elongation according to EN ISO 527-1 method (BS EN ISO 527-5:2009, 2009). All samples were tested at room temperature and five replicates have been employed for each sample. Aging was evaluated after an overall UV irradiation time of 50 h on rectangular specimens (50 mm × 15 mm) in a closed chamber with fixed temperature equal to 25 °C and relative humidity equal to 65%. Tensile strength was measured before and after the UV exposure.

## Results and Discussion

### Bacterial cellulose and composites production

BC was produced by cultivation the selected acetic acid bacterium K2G30 (UMCC 2756) in static regime, according to a scaling up procedure, from tube test to flask, for obtaining BC dishes (Figure 7-1a). In this study K2G30 strain was chosen for its robustness and versatility in producing

BC from different carbon sources, such as glucose and mannitol-based media. BC's production has been previously assessed in repeated cultivation cycles, showing high performance in terms of yield ( $6.14 \pm 0.02$  g/L BC from 5% w/v of initial glucose content and  $8.77 \pm 0.04$  g/L BC from 1.5% (w/v) mannitol medium). Moreover, the native BC produced by K2G30 showed high degree of crystallinity (80%) and high water holding capacity (391%)(Gullo et al., 2017). Genome analysis of K2G30 strain revealed four copies of the enzymatic core of the cellulose synthase complex and three copies of *bcs* operons, which can explain the high BC yield production (Gullo et al., 2019). Based on all these traits, in this study, K2G30 was used as BC producer to build up the bio-based composites by immobilization of  $\text{TiO}_2$  and Clay, providing optimal outputs to produce BC to be functionalized.

Dried BC obtained after wet mixing and without addition of any filler, as control specimen is reported in Figure 7-1b. Whereas, two representatives composites obtained respectively with  $\text{TiO}_2$  and Clay addition (20 wt%), showing high macroscopic homogeneity, are reported in Figures 7-1c and 7-1d. Any relevant modification of the BC, as control specimen, was observed before and after the wet mechanical mixing without  $\text{TiO}_2$  or Clay addition.

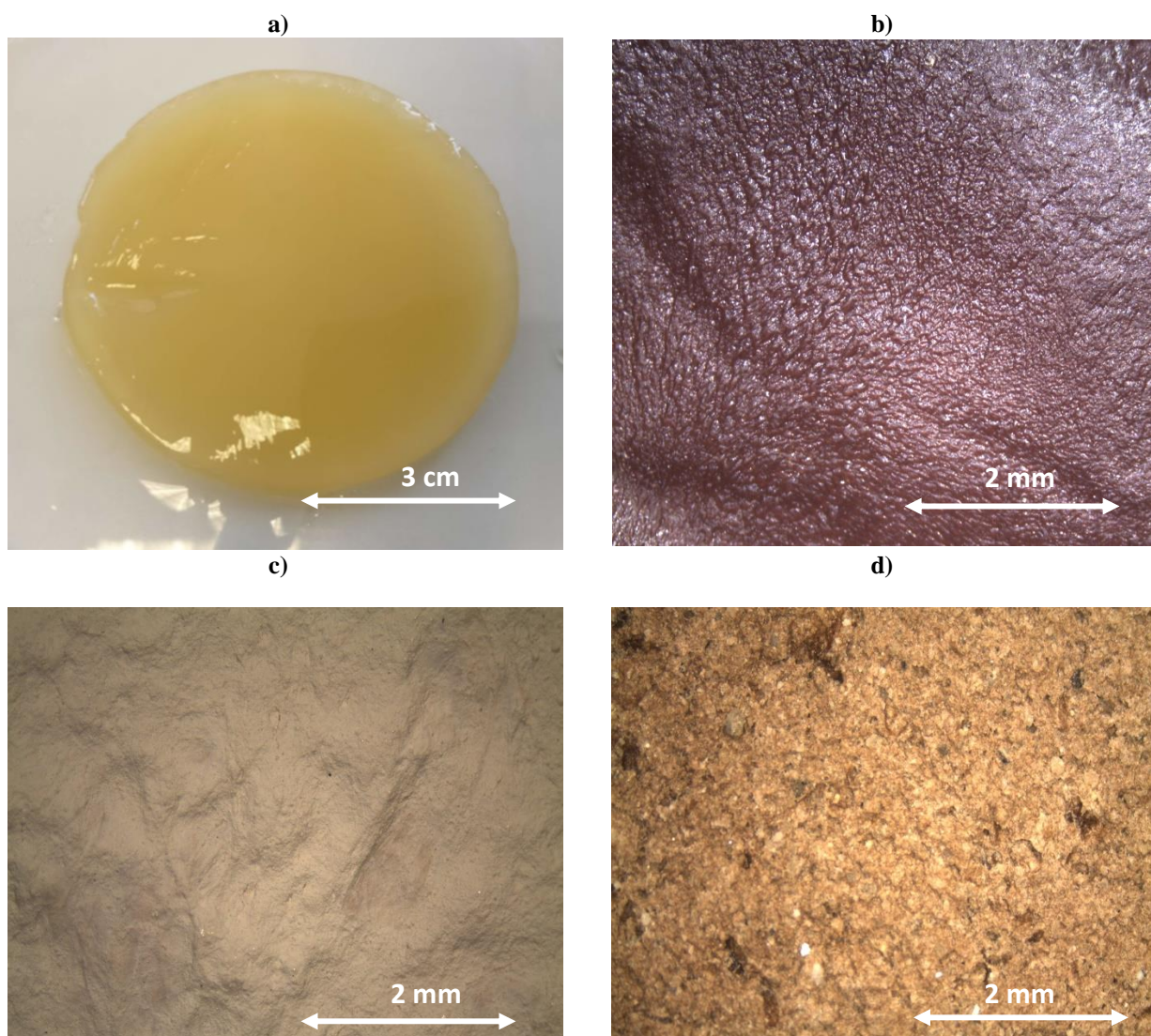
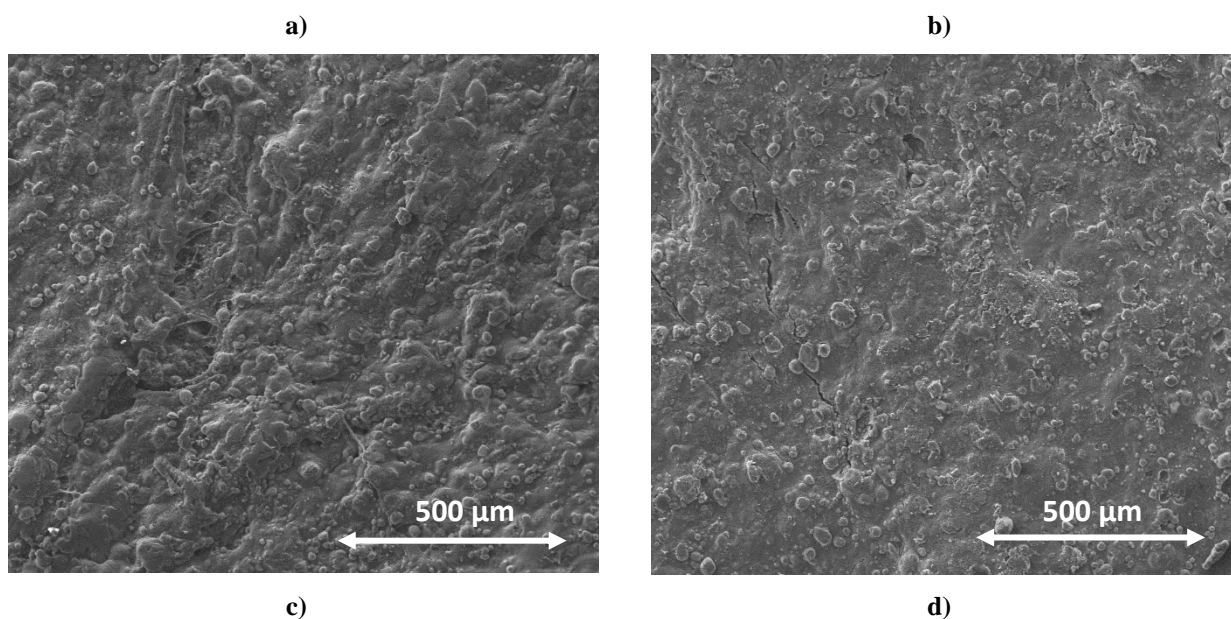




**Figure 7-1.** Native BC produced by K2G30 in static cultivation regime a) Wet BC b) Dry BC without any filler c) Dry BC with TiO<sub>2</sub> addition (20 wt%) d) Dry BC with Clay addition (20 wt%).

### Physical properties characterization

Density measurement of the bio-composites (Table 7-1) shows in general very restrained values around and below 1 g/cm<sup>3</sup>. In particular, it must be noted that for BC before mechanical mixing the value of the average density is equal  $0.620 \pm 0.020$  g/cm<sup>3</sup> and it can be considered as overlapped with the value obtained after mechanical mixing without any filler addition (Table 7-1), thereafter the wet mechanical mixing of BC do not show relevant modification of the BC density. This result is consistent with previous studies, suggesting the possible use of BC composites as lightweight materials (Cao et al., 2004; Sehaqui et al., 2010). In addition, as shown in Table 7-1, a further decreasing of density is observed moving from 10 wt% to 40 wt% of ceramic particle inclusion, even if some difference among TiO<sub>2</sub>-BC composites and Clay-BC composites must be considered. Since ceramic particles have in general density higher than 1 g/cm<sup>3</sup> (~ 4.2 g/cm<sup>3</sup> for TiO<sub>2</sub> and ~ 2.2 g/cm<sup>3</sup> for Clay) the decreasing in density must be associated to a rearrangement of the bio-composite structure, promoting a porous microstructure that can be tuned by controlling the amount of ceramic particle. In fact, by measuring the true density of the materials, porosity can be extrapolated employing the formula reported in the Material and Methods section, confirming an increasing porosity with the filler addition. This fact is even more stressed for the class of composites including TiO<sub>2</sub> for which, the much higher density of the filler, results in a strong increase in density of the sample T10 with respect to the BC sample (the one without filler addition), and in an higher porosity variation moving from T10 to T40. As a consequence, the further decreasing of density, with the increasing of filler is enhanced for the series with TiO<sub>2</sub> inclusion (- ~50 %) with respect to BC-Clay series of samples (- ~25 %), but it must be noted that lower density (0.296 g/cm<sup>3</sup>) is obtained for the sample containing 40 wt % of Clay as ceramic inclusion. In a similar way the highest porosity is obtained by the same sample (C40).



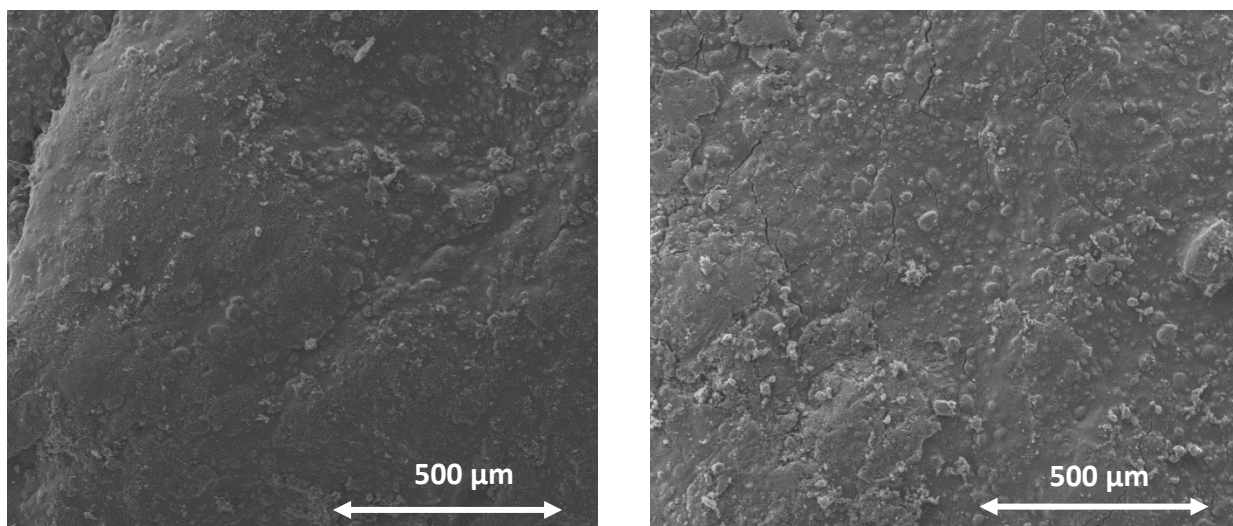


**Figure 7-2.** ESEM micrographs of TiO<sub>2</sub> containing composites: a) T10 b) T20 c) T30 d) T40

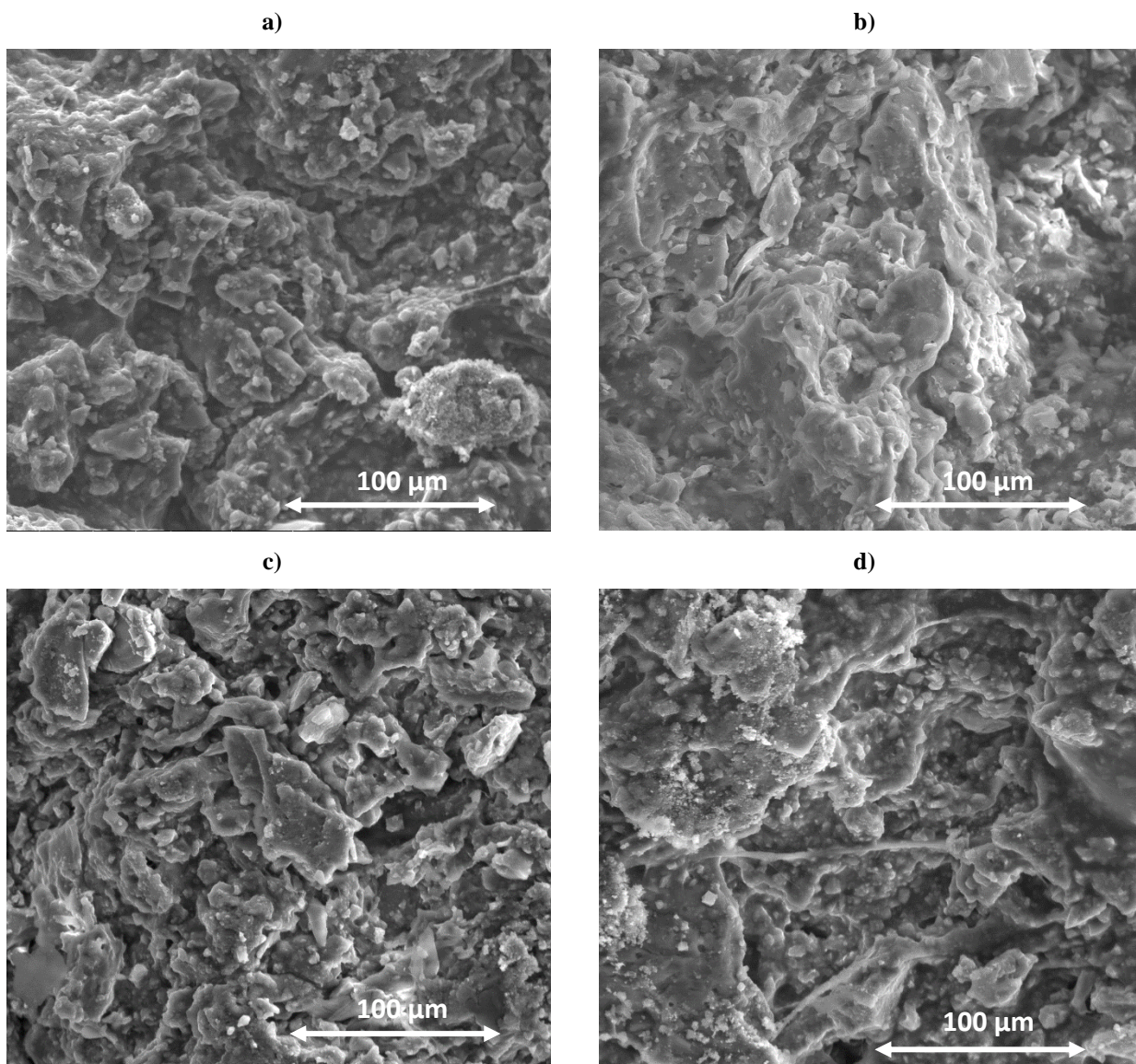


**Figure 7-3.** ESEM micrographs of Clay containing composites a) C10 b) C20 c) C30 d) C40

A morphological study of the BC-TiO<sub>2</sub> (Figure 7-2) and BC-Clay (Figure 7-3) composites was undertaken using ESEM in order to confirm the composite's synthesis by assessing the attachment of ceramic particles' onto the surface and their penetration into the matrix of BC. Moreover, the effects of ceramic particles concentration on these parameters and the overall morphological characteristics were also studied. Our results show that for both fillers, formation of aggregates or cluster of inorganic particles (which may be extremely difficult to break down), is not present, confirming the optimal dispersion and adhesion of the inorganic particles into BC obtained by mechanical wet mixing. As shown in Figure 7-2, bio-composites containing TiO<sub>2</sub> show in general smooth and clean surface with no specific pattern but including well-distributed TiO<sub>2</sub> particles (energy dispersive X-Ray spectroscopy spectra not reported), imparting surface roughness. The size of these particles is around 15-20  $\mu\text{m}$  (Figure 7-2) and this result agrees with the particle size of the raw powder employed, indicating that no cluster effect is present, independently of the TiO<sub>2</sub> content. Significant different results have been obtained for the series of bio-composites that include Clay; in fact, an interconnected sponge-like porous structure is present with randomly distributed pores (Figure 7-3).

To better highlight the different microstructure among TiO<sub>2</sub> and Clay based composites in Figure 7-4 ESEM pictures at higher magnitude have been shown. In Figure 7-4a, related to the sample T40, a more compact and homogenous structure has been detected with a great number of very small pores, having dimension around and below 1  $\mu\text{m}$ . On the other side, Figure 7-4b representing sample C40, shown a significantly more heterogeneous structure, with porosity more concentrated in specific areas and thereafter with less and bigger pores, when compared to T40. As confirmed by density measurement, BC-Clay composites are characterized by a strongly porous microstructure that ESEM indicate to be interconnected and randomly distributed

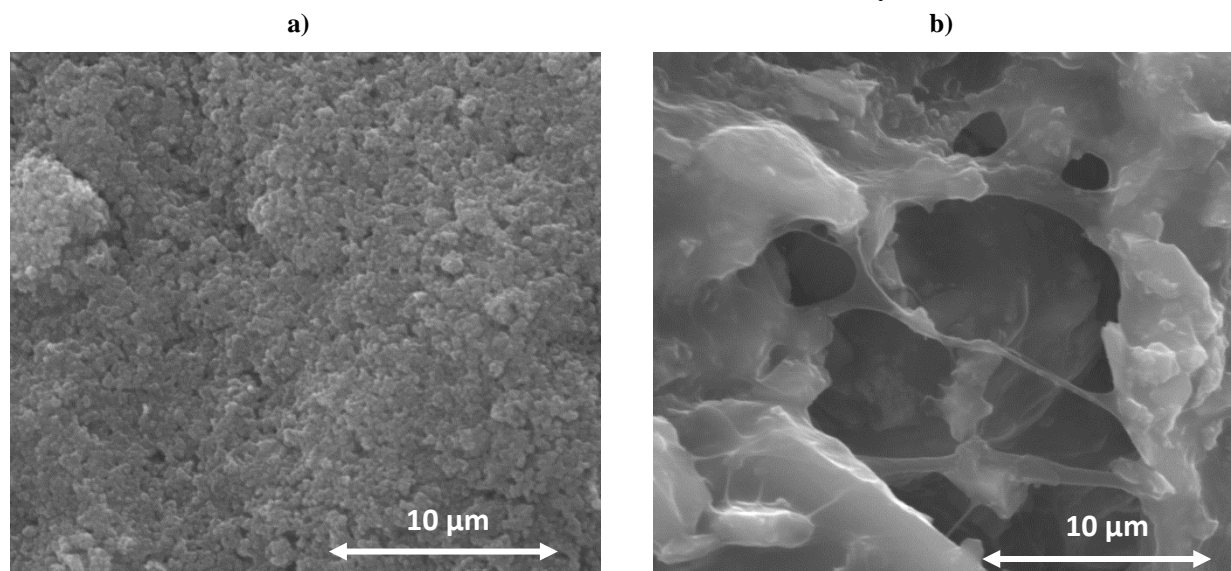


**Figure 7-4.** ESEM micrographs of significant sample at high-magnitude: a)T40 b)C40

### Structural properties characterization

To investigate more in-depth the structural modification of the composites, FT-IR (Figure 7-5 and Figure 7-6) has been performed on all the samples. Considering the FT-IR spectra of TiO<sub>2</sub> and Clay containing samples all of them show the typical principal bands and peaks for dried BC (Gullo et al., 2017): broad band of -OH alcoholic stretching vibrations between 3343  $\text{cm}^{-1}$  and

3232  $\text{cm}^{-1}$ , peak related to C–H stretching at around 2900  $\text{cm}^{-1}$ , peak associated to C=O vibration of the carboxylic group (–COOH) at around 1730  $\text{cm}^{-1}$  and the C–O–C and C–O carbonylic groups identified with peaks at around 1620  $\text{cm}^{-1}$ , 1420  $\text{cm}^{-1}$  and 1030  $\text{cm}^{-1}$ , respectively (Gullo et al. 2017). In  $\text{TiO}_2$  containing samples (Figure 7-5) the Ti–O–Ti stretching vibration at around 2361 and 2287  $\text{cm}^{-1}$  can be detected in sample T30 and T40 respectively, at the same time a further reduction of the bands related to -OH groups between 3343  $\text{cm}^{-1}$  and 3232  $\text{cm}^{-1}$  can be observed, as previously reported (Li et al., 2017b). Furthermore, it is reasonable to assume that the hydroxyl groups present into the BC may interact with the Ti–O through H-bonding, helping the bio-composite formation process and reducing the overall composites' stiffness as H-bonding are involved (Monteiro et al., 2019). For Clay containing samples (Figure 7-6) the main difference consists into the presence of peaks at 600  $\text{cm}^{-1}$ , corresponding to the Si–O–Si and C–Si bending (Voicu et al., 2017). Secondly, a variation of the shoulder around 1200  $\text{cm}^{-1}$  near the band placed at 1029  $\text{cm}^{-1}$  is observed depending on the increasing amount of Clay and it can be assigned to asymmetric Si–O–Si stretching vibrations (Barud et al., 2008). In addition, it must be cleared that for this series of samples the small peak at 2360  $\text{cm}^{-1}$  is related to Si–H group stretching vibration, indicating a restrained interaction among BC and Clay (mainly composed of  $\text{SiO}_2$ ) for samples C10 and C20 (Bugaev et al., 2012). Thereafter, the FT-IR spectra give clear evidence of the formation of a stronger structure for BC- $\text{TiO}_2$  composite with respect to BC-Clay, moving from 10 wt% to 40 wt% due to the H-bonding interaction between the OH groups and Ti–O, differently from Si–O bonding for BC-Clay composites.

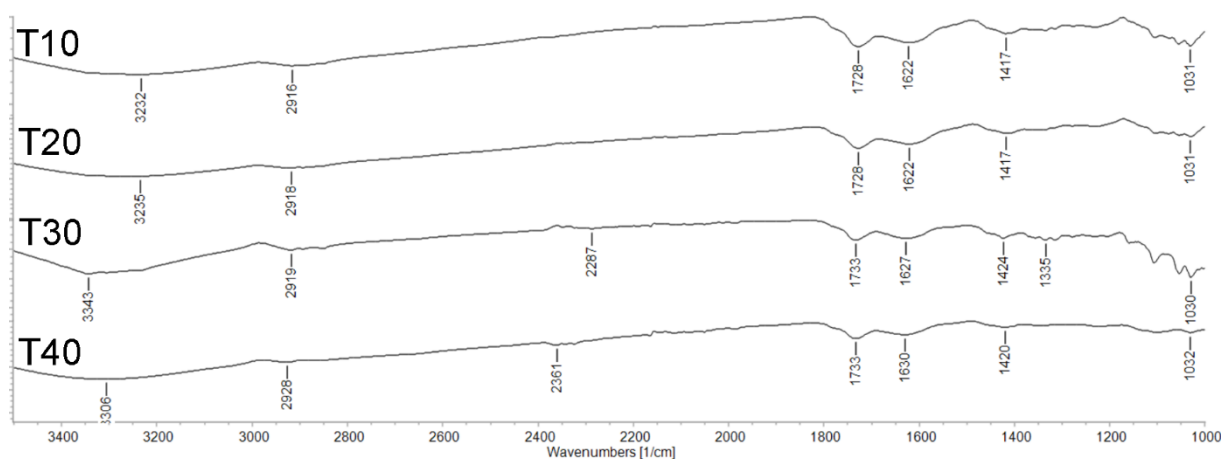


**Figure 7-5.** FTIR spectra of  $\text{TiO}_2$  containing composites

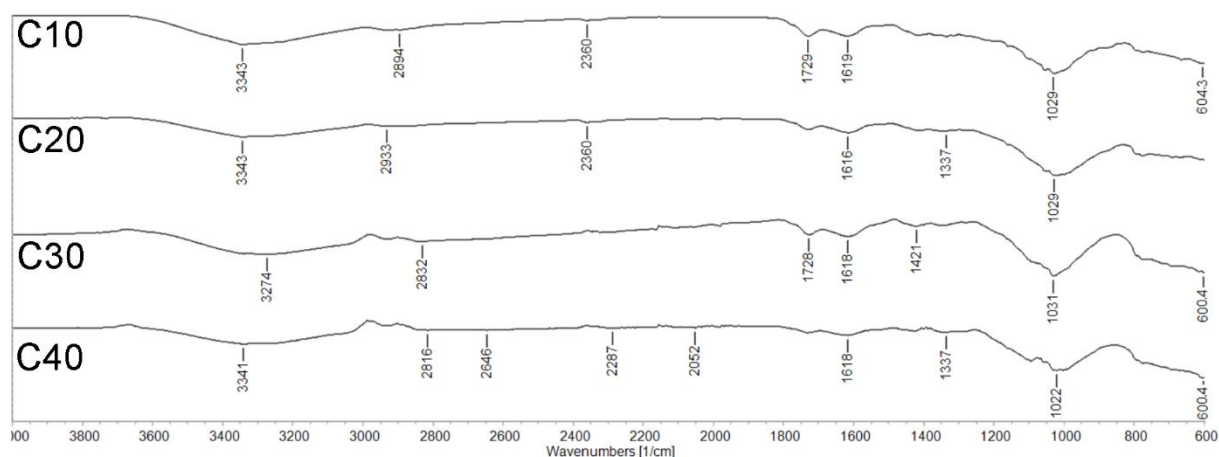
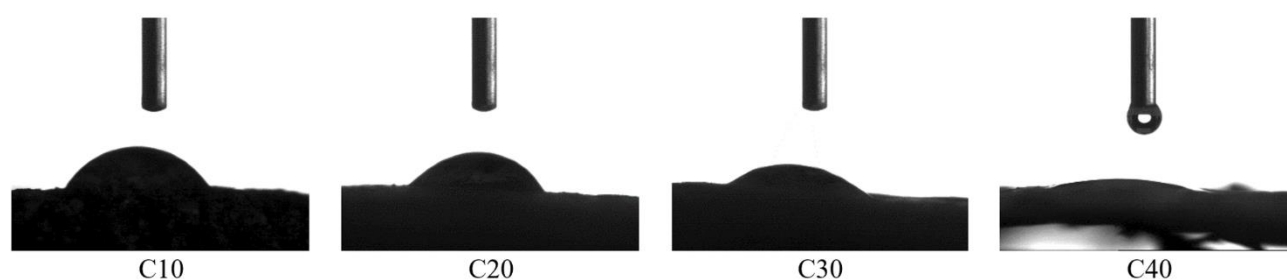


Figure 7-6. FTIR spectra of Clay containing composites

### Hydrophilic and mechanical properties characterization

According to the different morphology detected through optical and electronic microscopy, contact angle measurements have been considered (Table 7-1). It must be noted that no relevant modification of the contact angle has been measured before and after the wet mechanical mixing; in fact, the value reported in Table 7-1 can be considered as overlapped with the contact angle measured for the BC before wet mechanical mixing, equal to  $64.2 \pm 0.7$ . The surface wettability of the two series of bio-composites shows a strong hydrophilic behavior with low values of contact angle ( $< 60^\circ$ ) comparing to pure BC (Table 7-1). Even for this property, difference can be observed between the two series of bio-composites; in fact, no significant variation of contact angle can be detected for the series containing  $\text{TiO}_2$ , increasing the amount of ceramic particle inclusion. This behavior can be explained considering a not significant variation of the microstructure, as detected from ESEM measurement (Figure 7-2). For this group of composites, nevertheless the overall increasing porosity (Table 7-1), pores are characterized by restrained dimension and are homogeneously dispersed in all the material (Figure 7-4a). On the other hand, BC-Clay series of composites show a further decreasing of the contact angle from approximately  $55^\circ$  to  $20^\circ$  (Figure 7-7), with the increasing of Clay into composite matrix, demonstrating a further modification of the complex interconnected porous microstructure, which could be beneficial for higher hydrophilic applications e.g. membranes for medical application that must dissolve in aqueous solution. As shown in Figure 7-4b, the microstructure of a Clay based composite (C40) is strongly characterized by heterogeneous pore dimension and dispersion, leading to be more effected to physical property variation, such as contact angle, with respect to  $\text{TiO}_2$  based composites.



**Figure 7-7.** Contact angle measurements

In Figure 7-8 stress-elongation curves (average on five replicates) have been reported only for the series of samples containing TiO<sub>2</sub>, due to the fact that BC-Clay composites exhibit too fragile behavior for tensile deformation test. In fact, Clay particles occupy the pores within the matrix and serve as blockade layers, resulting in structures containing highly tortuous diffusion paths that can enhance the overall fragility of the structure as well as higher porosity of the structure (Gusev and Lusti, 2001). As shown in Figure 7-8, generally low values of elongation and stress are reported with respect to other composites system, including as reinforce plastic-like material more similar to BC, nevertheless they are consistent with other BC-inorganic materials (Ku et al., 2011). As expected, a general decrease of elongation was detected moving from 10 wt% of TiO<sub>2</sub> particle inclusion to 40 wt%, due to the ceramic nature of the particle reinforcement, too far from the plastic-like behavior of pure BC. On the other hand, a non-linear variation of stress at break was detected showing the highest value attributed to the sample containing 30 wt% of TiO<sub>2</sub>. This sample represents the optimal balance between the plastic-like behavior of the BC matrix and the fragile ceramic reinforcement. In fact, this sample containing as filler 30 wt% of TiO<sub>2</sub> promotes the best mechanical resistance: a further increasing of the reinforce will produce a downtrend of the tensile resistance, due to a too high physical density of TiO<sub>2</sub> particles in the same BC volume in the composite formulation. A similar non-linear trend can be detected for Young's modulus that can be derived from the stress-elongation curve. As shown in Figure 7-8 Young's modulus was found to increase significantly from 10 to 20 wt% of TiO<sub>2</sub> and decrease gradually from 20 wt% to 40 wt% of TiO<sub>2</sub>. The highest value of Young's modulus of this series, calculated following ISO 527 for sample T20 is equal to 129 MPa. Young's modulus and stress at break are lower than similar BC-inorganic composites, although elongation at break is higher (up to 35%), leading to a high potential for stretchable wound dressing (Luo et al., 2019). As expected, one of the most important factors having a major effect on the mechanical characteristics of particle-reinforced composite materials is the mass ratio between the matrix and fiber, and in this study, a non-linear effect has been found. The same behaviors and data have been checked after the aging test finding out that the UV exposure is not enough to affect sample's chemical bonding.

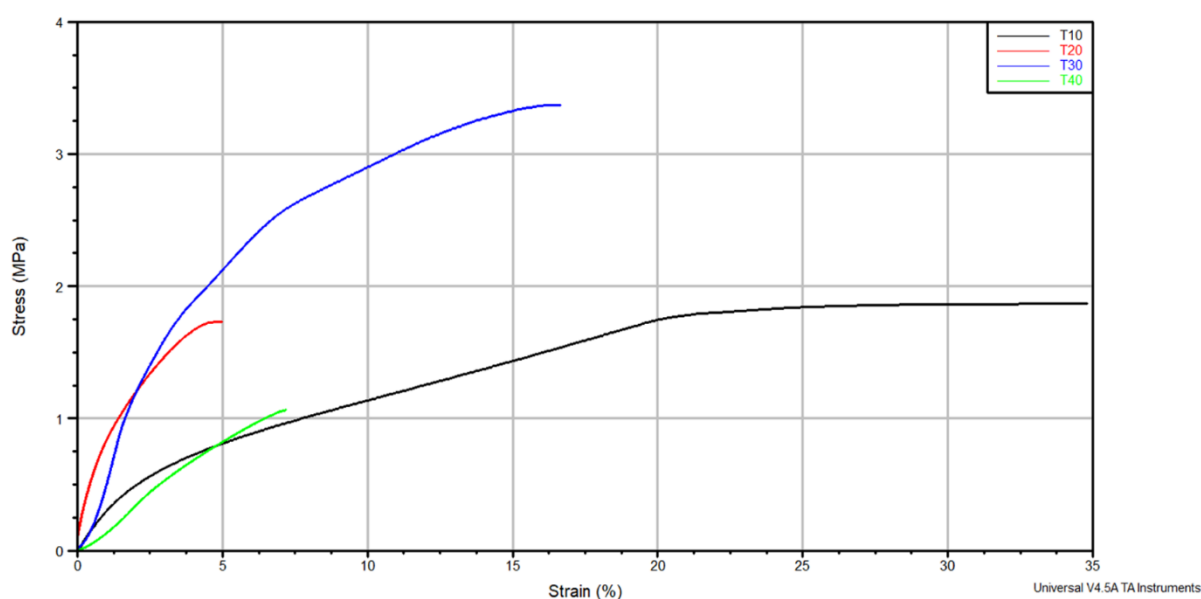


**Figure 7-8.** Tensile measurements

## Conclusion

In this study, a bottom up strategy for the immobilization of TiO<sub>2</sub> and Clay into BC was proposed to reduce the economic and environmental impact of the manufacturing process, in an industrial scale up perspective. The approach herein described for bio-composites formulation and preparation offer a versatile alternative and greener pathway for low cost and highly efficient devices such as membranes, textiles and lightweight materials, thanks to the low density, high elongation and biocompatible chemistry of the samples herein investigated. The degree of TiO<sub>2</sub> or Clay inclusion into the BC was varied from 10 wt% to 40 wt% and investigated to confirm that TiO<sub>2</sub> and Clay were well distributed into the BC through a wet mechanical mixing, although their interaction with BC were different, leading to tailored behavior in terms of physical and mechanical properties. In particular, has been founded that BC-TiO<sub>2</sub> composites exhibit interesting elongation at break to tensile deformation, higher than others reported in literature and particularly interesting for textile-like materials, thanks to OH-bond that cooperate to the formation of composites structure. On the other hand, BC-Clay composites, representing a further low-cost type of functionalization, have in general too fragile behavior to be tested for tensile deformation, but interesting properties arise from the contact angle measurement where a strong hydrophilic behavior has been detected, increasing its potential beneficial impact as lightweight membranes to be dissolved in aqueous solution.

# Chapter 8

General discussion and future perspectives



The aim of this thesis was to investigate the cellulose production mechanisms by acetic acid bacteria. Starting from the description of the microbiological diversity in Kombucha tea, representing one of the main matrix from which is possible to isolate *Komagataeibacter* strains, in this thesis we provide an overview moving from biological mechanisms, biochemical pathways, phylogenomic analysis and, at the end, promising industrial applications. In this chapter, we provide the general discussion of the results obtained in this thesis and place them in future perspective in order to improve the biological and molecular analysis of acetic acid bacteria and provide possible starting point for industrial applications.

## General discussion

### *Komagataeibacter* members as ubiquitous bacteria

*Komagataeibacter* strains could be considered as ubiquitous bacteria. As discussed in chapter 3, one of the most abundant matrix from which is possible to isolate high producer *Komagataeibacter* strains is Kombucha tea. Based on data retrieved in databases as NCBI or the Joint Genome Institute (JGI) and literature, *Komagataeibacter* strains were mostly isolated from beverages, as different kind of vinegars (Fernández et al., 2019), or food matrices, in particular fruits (Hollensteiner et al., 2020). The reason why *Komagataeibacter* strains populate a wide range of fruits probably could be understandable considering the interaction of some insect, as the fruit fly *Drosophila melanogaster*, with microbes that define their microbiome (Augimeri and Strap, 2015). It was well studied that acetic acid bacteria are one of the main components of the gut microbiome of insects (Dillon and Dillon, 2004; Smith and Newton, 2020), but have also been isolated from insect surfaces (Ren et al., 2007). Based on this consideration, insect as *Drosophila melanogaster* seems to play the key role as main vector of cellulose producer bacteria. The ecological role for *Komagataeibacter* genus was previously investigated, by studying the interaction between *Komagataeibacter* and fruits (Williams and Cannon, 1989). That role seems to be related to increase the environmental fitness thanks to the cellulose production, protecting themselves from desiccation and UV radiation. Basically, this highlights the importance in the study of interaction insect-fruit and fruit-bacteria in order to understand the environmental role of *Komagataeibacter*.

### Relevance of carbohydrate metabolism in *Komagataeibacter*

One of the main aspects to take into account when *Komagataeibacter* strains are studied is the metabolism of carbohydrates. This is because sugar or sugar alcohols represent the substrate for cellulose production. In order to understand which is the most suitable carbon source for cellulose production, one of the most important steps is to understand the biochemical pathways involved in the conversion of carbon sources into glucose, that is the substrate for cellulose production, and the kinetic of enzymes that catalyze target reactions. In chapter 4 and chapter 5, *K. xylinus* K2G30 (Gullo et al., 2019) and *K. xylinus* K1G4 (La China et al., 2020) were tested using different carbon sources, such as glucose and mannitol. Considering the pathways for cellulose production, the first chemical conversion is the phosphorylation of glucose into glucose-6-phosphate (G6P) (Jang et al., 2019). Basically, all the carbon sources that could be used for cellulose production, should be converted into G6P. Regarding mannitol, the conversion into glucose occurs through fructose, thanks to a mannitol dehydrogenase (Oikawa et al., 1997), which produces mannitol-1-phosphate. Apparently, the use of mannitol for cellulose production seems to be an expensive process in terms

of energy used. Considering the conversion rate of mannitol/glucose in to cellulose, which was estimated to be 38% of consumed carbon source converted in to cellulose for mannitol, compared to 8% in the case of glucose (Oikawa et al., 1995b), the reason of the higher yield obtained using mannitol is clear. The reason of this behavior could be attributed to the set of membrane-bound dehydrogenases that characterize acetic acid bacteria (Adachi and Yakushi, 2016). One of membrane-bound dehydrogenase, called glucose dehydrogenase is able to convert D-glucose in to gluconic acid (Deppenmeier et al., 2002; Iino et al., 2012; Sainz et al., 2016a). In this case, the carbon source resulted to be steal for cellulose production. Furthermore, from the results obtained in chapter 4 and chapter 5, the accumulation of gluconic acid in to the medium caused a decreasing of pH, making the environment conditions not favorable for cellulose production.

In order to better understand the metabolisms of *Komagataeibacter* strains, further analysis are required.

### **Combination of different composites and implementation of new techniques for the formulation of advanced material**

During last decades, BC received more attention due to its properties (Gullo et al., 2018). In particular, the main properties that were taken in to consideration were the biocompatibility and biodegradability. A large amount of devices and composites were developed during the last years considering this two main features of bacterial cellulose. In term of suitability of BC, the main fields in which a large number of researches were focused were the biomedical field and in the replacement of plastic-based materials in order to reduce the impact on the environment (Gallegos et al., 2016; Picheth et al., 2017). In detail, in chapters 6 and 7, we discussed about two approaches to develop composites in order to replace the plastic-based materials. One of this study was developed with the aim to create a cellulose-based film that could be promising for food packaging. In chapter 7, the two composites described could be suitable in two different applications. The blend of BC with TiO<sub>2</sub> showed high mechanical properties leading to high potential in wound dressing (Luo et al., 2019). The blended composites with BC and ceramic Clay showed a strong hydrophilic behavior, highlighting its potential as precursor to develop membrane able to dissolve in aqueous solution. Actually, a large number of researches are focusing in the functionalization of BC by blending it with organic or inorganic materials. Based on the material used, the obtained composites possess different properties and subsequently different applications (Douglass et al., 2018).

Regarding the uses of cellulose in biomedical field, differently from blended cellulose, in this case BC is used as naturally produced, without any modification in the film at structural level. One of the most interesting application of BC in biomedicine was developed in the field of biomedical devices (Robotti et al., 2018). In this case, BC was used as pure biopolymer in which the surface was modified by using assembly-based biolithography (GAB). Thanks to this technique, the resulted scaffolds was used for the implantation of biomedical devices, reducing the cell adhesion to the device, the inflammation process and subsequent reject reaction. Another interesting research in biomedical field was formulated by using BC produced by *K. xylinus* and the 3D-bioprinting (Shin et al., 2019). Bacterial cell in this case were used as ink and printed in a scaffold, obtaining tubular CNF/BC simulating the same behavior of blood vessels. Thanks to the development of high technological techniques in different fields will be reasonable to hypothesize that the biomedical field could be one of the most important area for BC-based materials.

## Future perspective

### Omics as a powerful tool in microbiological research

One of the biggest revolution in the modern microbiology research was the massive parallel sequencing tool development, such as Illumina sequencing and the third generation platforms as Nanopore and PacBio. Thanks to this technologies, the price of sequencing, intended as the cost per base, was reduced substantially, making these technologies more accessible to researches. Furthermore, the availability of public database, continuously improved and enriched by the new submission platforms, allow identification and the refinement of genome from all kingdoms. With the new sequencing platforms, the study of complex microbial communities, the interaction among them and their ecological roles are accessible (Gutleben et al., 2018).

One point that was not debated in this thesis was the full metabolic features of *Komagataeibacter* strains. In chapter 4 and chapter 5, metabolic pathways involved in cellulose production from glucose and mannitol were described. In literature, cellulose production was reported by using other alternative carbon sources, as raw material from food industrial wastes (Andriani et al., 2020). Based on these considerations, the metabolic network of *Komagataeibacter* strains need to be deeper studied. With the aim to elucidate the metabolic behavior, a combination of RNA sequencing and metabolomics studies could be the right approach. In this way it will be possible to understand not only the carbohydrate metabolism, directly linked to cellulose production, but also to elucidate the regulation of genic transcription and changes in other pathways possibly involved.

### Bacterial cellulose not only as innovative biomaterial. Trying to define the ecological role

As emerged from previous section of this chapter (*Komagataeibacter* members as ubiquitous bacteria), the ecological roles of *Komagataeibacter* members are not really defined. It seems to be limited to food matrices rich in sugars, especially fruits. Since the main vector for transmission of *Komagataeibacter* was recognized to be flies (Lee et al., 2019), it is reasonable to hypothesize that *Komagataeibacter* strains might be present also in different matrices. Based on this consideration, defining a possible ecological role of *Komagataeibacter* strains in complex matrices, as water or soil, could be the next approach in order to understand more about these bacteria. Naturally, bacterial cellulose is produced by bacteria as one of the main component of biofilm. Different members of the *Acetobacteraceae* family were detected in soil, as member of *Acetobacter* genus (Lisdiyanti et al., 2000). Biofilm is considered a micro-environment in which bacteria can survive and growth despite the adverse environmental conditions (Morris and Monier, 2003; Timmusk et al., 2011). Given this consideration, probably, the ecological role of *Komagataeibacter* strains could be to help the growth of themselves and other bacteria in the microbial community (Sriswasdi et al., 2017). Further studies should be addressed to assay the presence of *Komagataeibacter* in different matrices, as soil, water or plant root. These study could highlight new ecological roles for *Komagataeibacter* bacteria, allowing to understand more about their physiology and behavior.

## Concluding remarks

The results presented in this thesis elucidate the ecological and biological sides of *Komagataeibacter* genus, as the model organism in bacterial cellulose production. Starting from the description of the most important reservoir of *Komagataeibacter* strains, represented by Kombucha tea, we defined the genetic features, biochemical aspects and formulated two possible application of bacterial cellulose. We have highlight biochemical pathways involved in carbohydrate metabolism and the importance of a right phylogenetic assignment, not only based on 16S rRNA gene that seems to be highly conserved in *Komagataeibacter* genus. Nevertheless, as discussed before, further studies are needed to fill some gaps, especially regarding the metabolism of these bacteria and the ecological roles, in ordet to increase our knowledge and, subsequently, improve their application at real industrial scale.

# Supplementary materials

## Chapter 4

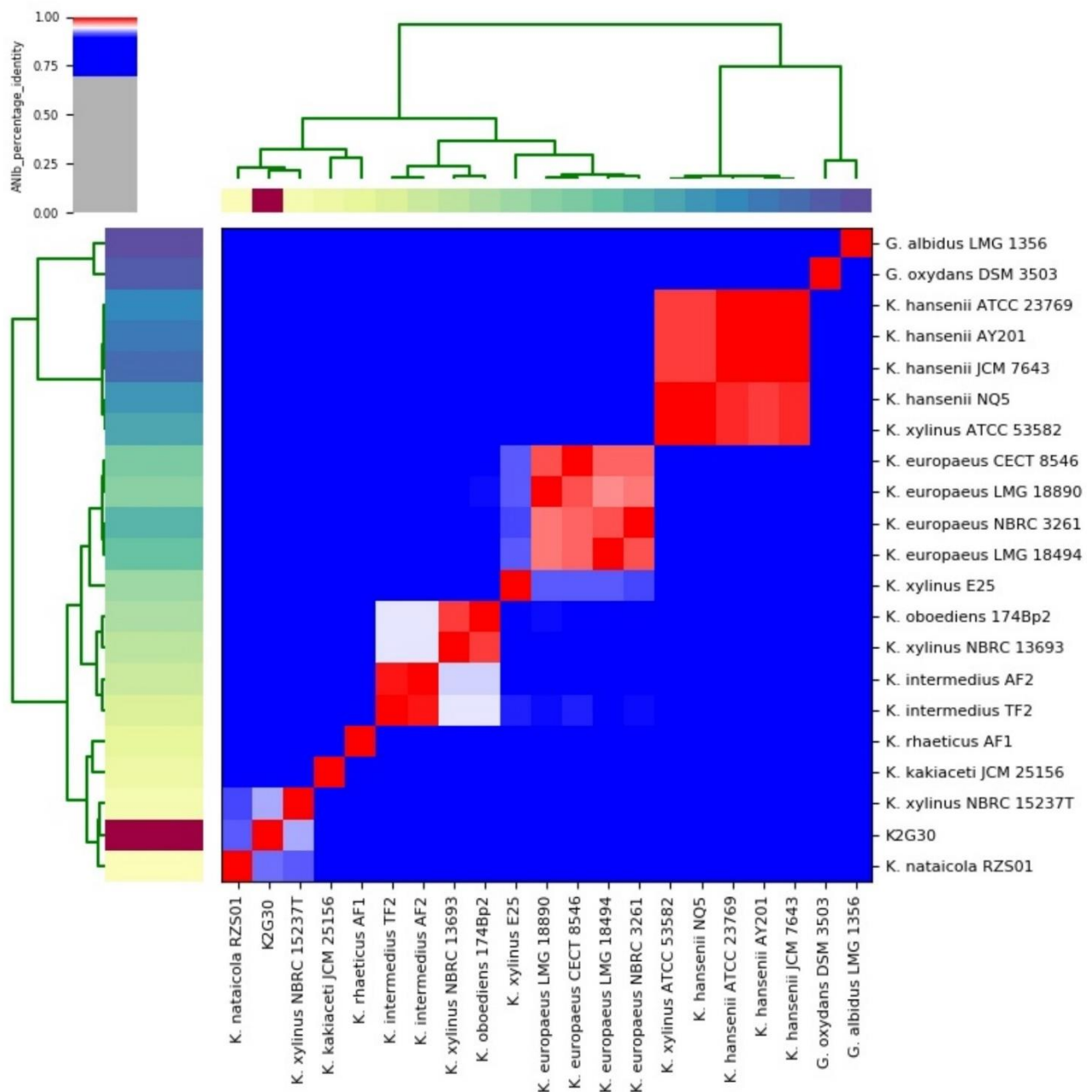


**Figure S4-1** ANiB heatmap of 21 *Komagataeibacter* genomes sequences (derived from Supplementary Table S1). ANiB values are represented in the central bi-color gradient heatmap (red gradients  $\geq 96\%$ ; white = 95%; blue gradients  $\leq 94\%$ ).

Table S4-1 ANIb pairwise similarity values for all *Komagataeibacter* genome sequences (n = 21).

	K. xylinus NBRC 15237T	K. intermedius	K. europaeus NBRC 3261	K. europaeus LMG 18494	K. xylinus ATCC 53582	K. nataicola RZ501	K.2G30	G. oxydans DSM 3503	K. europaeus LMG 18890	K. hansenii AY201	Genomes
	0.77	0.78	0.78	0.78	0.99	0.77	0.77	0.73	0.78	1.00	K. hansenii AY201
	0.84	0.90	0.98	0.98	0.78	0.84	0.84	0.73	1.00	0.78	K. europaeus LMG 18890
	0.73	0.73	0.73	0.74	0.72	0.73	0.73	1.00	0.74	0.73	G. oxydans DSM 3503
	0.93	0.86	0.85	0.85	0.77	0.92	1.00	0.73	0.85	0.77	K2G30
	0.91	0.85	0.84	0.84	0.77	1.00	0.92	0.73	0.84	0.77	K. nataicola RZ501
	0.77	0.78	0.78	0.78	1.00	0.77	0.77	0.73	0.78	0.99	K. xylinus ATCC 53582
	0.84	0.90	0.98	1.00	0.78	0.84	0.84	0.74	0.97	0.78	K. europaeus LMG 18494
	0.84	0.90	1.00	0.98	0.77	0.84	0.84	0.73	0.97	0.77	K. europaeus NBRC 3261
	0.84	1.00	0.89	0.89	0.78	0.84	0.84	0.73	0.89	0.78	K. intermedius TF2
	1.00	0.86	0.84	0.85	0.77	0.92	0.93	0.73	0.85	0.77	K. xylinus NBRC 15237T
	0.77	0.78	0.78	0.78	0.99	0.77	0.77	0.73	0.78	1.00	K. hansenii JCM 7643
	0.77	0.78	0.78	0.78	0.99	0.77	0.77	0.72	0.78	1.00	K. hansenii ATCC 23769
	0.84	0.86	0.85	0.86	0.78	0.84	0.84	0.74	0.85	0.78	K. katiaceti JCM 25156
	0.83	0.94	0.89	0.89	0.77	0.83	0.83	0.73	0.89	0.77	K. xylinus NBRC 13693
	0.77	0.78	0.78	0.78	1.00	0.77	0.77	0.73	0.78	0.99	K. hansenii NQ5
	0.84	0.94	0.89	0.89	0.77	0.83	0.84	0.73	0.90	0.78	K. oboediens 1748p2
	0.84	1.00	0.89	0.89	0.78	0.84	0.84	0.73	0.90	0.78	K. intermedius AF2
	0.84	0.90	0.91	0.92	0.78	0.84	0.85	0.73	0.92	0.78	K. xylinus E25
	0.73	0.73	0.74	0.74	0.72	0.73	0.73	0.86	0.73	0.73	G. albidus LMG 1356
	0.84	0.90	0.98	0.98	0.78	0.84	0.85	0.73	0.98	0.78	K. europaeus CECT 8546
	0.85	0.87	0.85	0.86	0.77	0.84	0.85	0.73	0.86	0.78	K. rhaeticus AF1

K. rhaeticus AF1	K. europaeus CECT 8546	G. albidus LMG 1356	K. xylinus E25	K. intermedius AF2	K. oboediens 1748p2	K. hansenii NQ5	K. xylinus NBRC 13693	K. kakiaceti JCM 25156	K. hansenii ATCC 23769	K. hansenii JCM 7643	Genomes
0.78	0.78	0.73	0.78	0.78	0.79	0.99	0.77	0.78	1.00	1.00	K. hansenii AY201
0.86	0.98	0.73	0.92	0.90	0.90	0.78	0.89	0.84	0.78	0.78	K. europaeus LMG 18890
0.73	0.73	0.86	0.73	0.74	0.74	0.73	0.73	0.73	0.72	0.73	G. oxydans DSM 3503
0.85	0.85	0.73	0.85	0.85	0.85	0.77	0.83	0.84	0.77	0.78	K2G30
0.84	0.84	0.73	0.84	0.84	0.84	0.77	0.83	0.83	0.77	0.78	K. nataicola RZ501
0.77	0.78	0.72	0.78	0.78	0.78	1.00	0.77	0.78	0.99	0.99	K. xylinus ATCC 53582
0.85	0.98	0.73	0.91	0.89	0.89	0.78	0.89	0.84	0.78	0.78	K. europaeus LMG 18494
0.84	0.98	0.73	0.91	0.89	0.89	0.78	0.89	0.84	0.77	0.78	K. europaeus NBRC 3261
0.85	0.89	0.73	0.89	0.99	0.94	0.78	0.94	0.84	0.78	0.78	K. intermedius TF2
0.85	0.85	0.73	0.85	0.85	0.84	0.77	0.83	0.83	0.77	0.78	K. xylinus NBRC 15237T
0.78	0.78	0.73	0.78	0.78	0.79	0.99	0.77	0.78	1.00	1.00	K. hansenii JCM 7643
0.77	0.78	0.72	0.77	0.78	0.78	0.99	0.77	0.78	1.00	1.00	K. hansenii ATCC 23769
0.85	0.85	0.74	0.85	0.85	0.85	0.78	0.84	1.00	0.78	0.78	K. kakiaceti JCM 25156
0.84	0.89	0.73	0.88	0.94	0.98	0.77	1.00	0.84	0.77	0.77	K. xylinus NBRC 13693
0.77	0.78	0.72	0.78	0.78	0.78	1.00	0.77	0.78	0.99	0.99	K. hansenii NQ5
0.85	0.90	0.73	0.89	0.94	1.00	0.77	0.99	0.84	0.78	0.78	K. oboediens 1748p2
0.86	0.89	0.73	0.89	1.00	0.94	0.78	0.94	0.84	0.78	0.78	K. intermedius AF2
0.85	0.92	0.73	1.00	0.89	0.89	0.78	0.88	0.84	0.78	0.78	K. xylinus E25
0.73	0.73	1.00	0.73	0.73	0.74	0.73	0.73	0.73	0.72	0.73	G. albidus LMG 1356
0.86	1.00	0.73	0.92	0.90	0.90	0.78	0.89	0.84	0.78	0.78	K. europaeus CECT 8546
1.00	0.86	0.73	0.85	0.86	0.86	0.77	0.84	0.84	0.77	0.78	K. rhaeticus AF1

Table S4-2 TETRA pairwise similarity values for all *Komagataeibacter* genome sequences (n = 21)

	K. hansenii NQ5	K. hansenii JCM 7643	K. hansenii AY201	K. hansenii ATCC 23769	K. europaeus NBRC 3261	K. europaeus LMG 18890	K. europaeus LMG 18494	K. europaeus CECT 8546	K2G30	G. oxydans DSM 3503	G. albidus LMG 1356	Genomes
	0.67	0.69	0.69	0.68	0.71	0.73	0.72	0.73	0.69	0.69	0.97	1
	0.66	0.69	0.68	0.68	0.74	0.76	0.75	0.75	0.74	1.00	0.97	G. albidus LMG 1356
	0.77	0.78	0.77	0.77	0.92	0.92	0.92	0.92	1.00	0.74	0.69	G. oxydans DSM 3503
	0.89	0.90	0.89	0.89	1.00	1.00	1.00	1.00	0.92	0.75	0.73	K2G30
	0.89	0.90	0.89	0.89	1.00	1.00	1.00	1.00	0.92	0.75	0.72	K. europaeus CECT 8546
	0.89	0.90	0.90	0.90	1.00	1.00	1.00	1.00	0.92	0.76	0.73	K. europaeus LMG 18494
	0.89	0.90	0.89	0.89	1.00	1.00	1.00	1.00	0.92	0.74	0.73	K. europaeus LMG 18890
	1.00	1.00	1.00	1.00	0.89	0.90	0.89	0.89	0.77	0.68	0.68	K. europaeus NBRC 3261
	1.00	1.00	1.00	1.00	0.89	0.90	0.89	0.89	0.77	0.68	0.69	K. hansenii ATCC 23769
	1.00	1.00	1.00	1.00	0.89	0.90	0.89	0.89	0.77	0.66	0.69	K. hansenii AY201
	1.00	1.00	1.00	1.00	0.89	0.89	0.89	0.89	0.77	0.66	0.69	K. hansenii JCM 7643
	0.89	0.90	0.90	0.89	0.99	1.00	1.00	1.00	0.92	0.76	0.74	K. hansenii NQ5
	0.89	0.90	0.90	0.89	1.00	1.00	1.00	1.00	0.92	0.75	0.73	K. intermedius AF2
	0.85	0.86	0.86	0.86	0.97	0.97	0.97	0.97	0.94	0.78	0.75	K. intermedius TF2
	0.76	0.78	0.77	0.77	0.91	0.91	0.92	0.92	1.00	0.75	0.72	K. kakiaceti JCM 25156
	0.89	0.90	0.90	0.90	0.99	0.99	0.99	0.99	0.92	0.76	0.74	K. nataicola RZ501
	0.83	0.85	0.84	0.84	0.97	0.97	0.97	0.97	0.95	0.77	0.73	K. oboediens 174Bp2
	1.00	1.00	1.00	1.00	0.89	0.89	0.89	0.89	0.77	0.66	0.67	K. rhaeticus AF1
	0.89	0.90	0.89	0.89	0.99	0.99	0.99	0.99	0.93	0.74	0.71	K. xylinus ATCC 53582
	0.89	0.90	0.90	0.90	0.99	0.99	0.99	0.99	0.91	0.73	0.70	K. xylinus E25
	0.76	0.78	0.77	0.77	0.92	0.92	0.92	0.92	1.00	0.75	0.71	K. xylinus NBRC 13693
												K. xylinus NBRC 15237T



K. xylinus NBRC 15237T	K. xylinus NBRC 13693	K. xylinus E25	K. xylinus ATCC 53582	K. rhaeticus AF1	K. oboediens 174Bp2	K. nataicola RZ501	K. kakiaceti JCM 25156	K. intermedius	K. intermedius AF2	Genomes
0.71	0.70	0.71	0.67	0.73	0.74	0.72	0.75	0.73	0.74	G. albidus LMG 1356
0.75	0.73	0.74	0.66	0.77	0.76	0.75	0.78	0.75	0.76	G. oxydans DSM 3503
1.00	0.91	0.93	0.77	0.95	0.92	1.00	0.94	0.92	0.92	K2G30
0.92	0.99	0.99	0.89	0.97	0.99	0.92	0.97	1.00	1.00	K. europaeus CECT 8546
0.92	0.99	0.99	0.89	0.97	0.99	0.92	0.97	1.00	1.00	K. europaeus LMG 18494
0.92	0.99	0.99	0.89	0.97	0.99	0.91	0.97	1.00	1.00	K. europaeus LMG 18890
0.92	0.99	0.99	0.89	0.97	0.99	0.91	0.97	1.00	0.99	K. europaeus NBRC 3261
0.77	0.90	0.89	1.00	0.84	0.90	0.77	0.86	0.89	0.89	K. hansenii ATCC 23769
0.77	0.90	0.89	1.00	0.84	0.90	0.77	0.86	0.90	0.90	K. hansenii AY201
0.78	0.90	0.90	1.00	0.85	0.90	0.78	0.86	0.90	0.90	K. hansenii JCM 7643
0.76	0.89	0.89	1.00	0.83	0.89	0.76	0.85	0.89	0.89	K. hansenii NQ5
0.92	0.99	0.99	0.89	0.96	1.00	0.91	0.97	1.00	1.00	K. intermedius AF2
0.91	1.00	0.99	0.89	0.96	1.00	0.91	0.97	1.00	1.00	K. intermedius TF2
0.94	0.96	0.98	0.85	0.96	0.96	0.94	1.00	0.97	0.97	K. kakiaceti JCM 25156
1.00	0.90	0.93	0.76	0.94	0.91	1.00	0.94	0.91	0.91	K. nataicola RZ501
0.91	0.99	0.99	0.89	0.96	1.00	0.91	0.96	1.00	1.00	K. oboediens 174Bp2
0.95	0.95	0.97	0.83	1.00	0.96	0.94	0.96	0.96	0.96	K. rhaeticus AF1
0.76	0.89	0.89	1.00	0.83	0.89	0.76	0.85	0.89	0.89	K. xylinus ATCC 53582
0.93	0.98	1.00	0.89	0.97	0.99	0.93	0.98	0.99	0.99	K. xylinus E25
0.90	1.00	0.98	0.89	0.95	0.99	0.90	0.96	1.00	0.99	K. xylinus NBRC 13693
1.00	0.90	0.93	0.76	0.95	0.91	1.00	0.94	0.91	0.92	K. xylinus NBRC 15237T

# Chapter 5

**Table S5-1** Distant matrix percentage values of pairwise comparisons for the 37 *Komagataeibacter* strains

<i>K. hansenii</i> HUM-1	<i>K. hansenii</i> AY201	<i>K. hansenii</i> ATCC53582	<i>K. europaeus</i> SRCM101446	<i>K. europaeus</i> NBRC3261	<i>K. europaeus</i> LMG18494	<i>K. europaeus</i> CECT8546	<i>K. coccoides</i> WIE7	<i>K. xylinus</i> K2G30	K1G4	Genomes
0.015	0.015	0.015	0.006	0.006	0.006	0.006	0.016	0.000		K1G4
0.015	0.015	0.015	0.006	0.006	0.006	0.006	0.016			<i>K. xylinus</i> K2G30
0.006	0.006	0.006	0.012	0.013	0.012	0.012				<i>K. coccoides</i> WIE7
0.010	0.010	0.010	0.000	0.001	0.000					<i>K. europaeus</i> CECT8546
0.011	0.010	0.010	0.001	0.001						<i>K. europaeus</i> LMG18494
0.011	0.011	0.011	0.001							<i>K. europaeus</i> NBRC 3261
0.011	0.011	0.011								<i>K. europaeus</i> SRCM101446
0.001	0.000									<i>K. hansenii</i> ATCC 53582
0.000										<i>K. hansenii</i> AY201
										<i>K. hansenii</i> HUM-1
										<i>K. hansenii</i> JCM17643
										<i>K. hansenii</i> LMG23726
										<i>K. hansenii</i> NQ5
										<i>K. hansenii</i> SC-3B
										<i>K. intermedius</i> TF2
										<i>K. kaikiae</i> JCM25156
										<i>K. maitakei</i> LMG1529
										<i>K. medellinensis</i> NBRC3288
										<i>K. naraicola</i> RZ501
										<i>K. oboediens</i> T74Bp2
										<i>K. oboediens</i> LMG18849
										<i>K. pomacei</i> AV446
										<i>K. pomacei</i> T5K1
										<i>K. rhaeticus</i> AF1
										<i>K. rhaeticus</i> IGEM
										<i>K. saccharivorans</i> CV1
										<i>K. saccharivorans</i> LMG1582
										<i>K. saccharivorans</i> SRCM101450
										<i>K. sucrofermentans</i> LMG18788
										<i>K. swingsii</i> LMG22125
										<i>K. xylinus</i> ATCC53582
										<i>K. xylinus</i> BCRC12334
										<i>K. xylinus</i> CGMCC2965
										<i>K. xylinus</i> E25
										<i>K. xylinus</i> E26
										<i>K. xylinus</i> LMG1515
										<i>K. xylinus</i> NBRC13693

<i>K. oboediens</i> LMG18849	<i>K. oboediens</i> 174Bp2	<i>K. natalicola</i> RZS01	<i>K. medellinensis</i> NBRC3288	<i>K. malitacei</i> LMG1529	<i>K. kakilacei</i> JCM25156	<i>K. intermedius</i> TF2	<i>K. hansenii</i> SC-3B	<i>K. hansenii</i> NQ5	<i>K. hansenii</i> LMG23726	<i>K. hansenii</i> JCM7643	Genomes
0.006	0.006	0.003	0.005	0.015	0.008	0.005	0.015	0.015	0.015	0.015	K1G4
0.006	0.006	0.003	0.005	0.015	0.008	0.005	0.015	0.015	0.015	0.015	<i>K. xylinus</i> K2G30
0.013	0.014	0.014	0.014	0.003	0.013	0.013	0.005	0.006	0.006	0.006	<i>K. coccois</i> WIE7
0.004	0.004	0.004	0.004	0.010	0.005	0.004	0.010	0.010	0.010	0.010	<i>K. europaeus</i> CECT8546
0.004	0.004	0.005	0.005	0.010	0.005	0.005	0.011	0.010	0.011	0.010	<i>K. europaeus</i> LMG18494
0.005	0.005	0.005	0.005	0.011	0.006	0.005	0.011	0.011	0.011	0.011	<i>K. europaeus</i> NBRC 3261
0.004	0.005	0.005	0.005	0.010	0.005	0.004	0.011	0.011	0.011	0.011	<i>K. europaeus</i> SRCM101446
0.012	0.012	0.013	0.013	0.005	0.012	0.012	0.000	0.000	0.002	0.000	<i>K. hansenii</i> ATCC 53582
0.012	0.012	0.013	0.013	0.005	0.012	0.012	0.000	0.000	0.001	0.000	<i>K. hansenii</i> AY201
0.012	0.013	0.013	0.013	0.005	0.012	0.012	0.000	0.001	0.001	0.000	<i>K. hansenii</i> HUM-1
0.012	0.012	0.013	0.013	0.005	0.012	0.012	0.000	0.000	0.001	0.000	<i>K. hansenii</i> JCM7643
0.012	0.013	0.013	0.013	0.005	0.012	0.012	0.000	0.000	0.001	0.000	<i>K. hansenii</i> LMG23726
0.012	0.012	0.013	0.013	0.005	0.012	0.012	0.000	0.002	0.001	0.000	<i>K. hansenii</i> NQ5
0.012	0.012	0.013	0.013	0.005	0.012	0.012	0.000	0.000	0.001	0.000	<i>K. hansenii</i> SC-3B
0.001	0.002	0.004	0.004	0.011	0.005	0.005	0.000	0.001	0.001	0.000	<i>K. intermedius</i> TF2
0.005	0.005	0.005	0.006	0.013	0.005	0.005	0.000	0.000	0.001	0.000	<i>K. kakilacei</i> JCM25156
0.012	0.012	0.013	0.013	0.005	0.012	0.012	0.000	0.000	0.001	0.000	<i>K. malitacei</i> LMG1529
0.004	0.004	0.004	0.013	0.004	0.012	0.012	0.000	0.002	0.001	0.000	<i>K. medellinensis</i> NBRC3288
0.005	0.005	0.005	0.006	0.013	0.012	0.012	0.000	0.000	0.001	0.000	<i>K. natalicola</i> RZS01
0.001	0.005	0.004	0.004	0.013	0.012	0.012	0.000	0.000	0.001	0.000	<i>K. oboediens</i> 174Bp2
											<i>K. oboediens</i> LMG18849
											<i>K. pomacei</i> AY446
											<i>K. pomacei</i> T5K1
											<i>K. rhaeticus</i> AF1
											<i>K. rhaeticus</i> IGEIM
											<i>K. saccharivorans</i> CV1
											<i>K. saccharivorans</i> LMG1582
											<i>K. saccharivorans</i> SRCM101450
											<i>K. sucrofermentans</i> LMG18788
											<i>K. swingsii</i> LMG22125
											<i>K. xylinus</i> ATCC53582
											<i>K. xylinus</i> BCR12334
											<i>K. xylinus</i> CGMCC2955
											<i>K. xylinus</i> E25
											<i>K. xylinus</i> E26
											<i>K. xylinus</i> LMG1515
											<i>K. xylinus</i> NBRC13693

<i>K. xylinus</i> BRC12334	<i>K. xylinus</i> ATCC3582	<i>K. swingsii</i> LMG22125	<i>K. saccharivorans</i> SRM101450	<i>K. saccharivorans</i> LMG1582	<i>K. saccharivorans</i> CV1	<i>K. rhaeticus</i> IGEM	<i>K. rhaeticus</i> AF1	<i>K. pomacei</i> T5K1	<i>K. pomacei</i> AV446	Genomes
0.006	0.015	0.005	0.006	0.006	0.006	0.005	0.005	0.016	0.016	K1G4
0.006	0.015	0.005	0.006	0.006	0.006	0.005	0.005	0.016	0.016	<i>K. xylinus</i> K2G30
0.011	0.006	0.013	0.012	0.012	0.012	0.012	0.012	0.000	0.000	<i>K. coccois</i> WIE7
0.002	0.010	0.003	0.004	0.004	0.004	0.004	0.003	0.012	0.011	<i>K. europaeus</i> CECT8546
0.002	0.010	0.003	0.004	0.004	0.004	0.004	0.003	0.012	0.012	<i>K. europaeus</i> LMG18494
0.002	0.011	0.004	0.005	0.005	0.005	0.005	0.004	0.013	0.012	<i>K. europaeus</i> NBRC 3261
0.002	0.011	0.004	0.004	0.004	0.004	0.004	0.004	0.012	0.012	<i>K. europaeus</i> SRCM101446
0.010	0.000	0.013	0.011	0.011	0.011	0.011	0.011	0.006	0.005	<i>K. hansenii</i> ATCC 53582
0.010	0.000	0.012	0.010	0.010	0.010	0.011	0.011	0.006	0.005	<i>K. hansenii</i> AY201
0.010	0.001	0.012	0.011	0.011	0.011	0.011	0.011	0.006	0.006	<i>K. hansenii</i> HUM-1
0.010	0.000	0.012	0.010	0.010	0.010	0.011	0.011	0.006	0.005	<i>K. hansenii</i> JCM7643
0.010	0.002	0.012	0.011	0.011	0.011	0.011	0.011	0.006	0.006	<i>K. hansenii</i> LMG23726
0.010	0.000	0.013	0.011	0.011	0.011	0.011	0.011	0.006	0.005	<i>K. hansenii</i> NQ5
0.010	0.000	0.012	0.011	0.011	0.011	0.011	0.011	0.005	0.005	<i>K. hansenii</i> SC-3B
0.005	0.012	0.005	0.004	0.004	0.004	0.003	0.003	0.012	0.012	<i>K. intermedius</i> TF2
0.004	0.012	0.005	0.003	0.003	0.003	0.006	0.006	0.013	0.013	<i>K. kakiaceti</i> JCM25156
0.010	0.005	0.013	0.012	0.012	0.012	0.012	0.011	0.002	0.003	<i>K. malliaceti</i> LMG1529
0.003	0.013	0.004	0.004	0.004	0.004	0.002	0.002	0.014	0.014	<i>K. medellinensis</i> NBRC3288
0.003	0.013	0.003	0.003	0.003	0.003	0.005	0.005	0.014	0.014	<i>K. nataricola</i> RZS01
0.005	0.012	0.006	0.005	0.005	0.005	0.003	0.003	0.014	0.013	<i>K. oboediensis</i> T74Bp2
0.005	0.012	0.006	0.005	0.005	0.005	0.003	0.003	0.013	0.013	<i>K. oboediensis</i> LMG18849
0.011	0.005	0.013	0.012	0.012	0.012	0.012	0.012	0.000	0.000	<i>K. pomacei</i> AV446
0.011	0.006	0.013	0.012	0.012	0.012	0.012	0.012	0.012	0.012	<i>K. pomacei</i> T5K1
0.003	0.011	0.005	0.003	0.003	0.003	0.000	0.000			<i>K. rhaeticus</i> AF1
0.004	0.011	0.005	0.003	0.003	0.003	0.003	0.003			<i>K. rhaeticus</i> IGEM
0.002	0.011	0.003	0.000	0.000	0.000					<i>K. saccharivorans</i> CV1
0.002	0.011	0.003	0.000	0.000	0.000					<i>K. saccharivorans</i> LMG1582
0.002	0.011	0.003	0.004	0.004	0.004					<i>K. saccharivorans</i> SRCM101450
0.004	0.013	0.004								<i>K. sacrofermentans</i> LMG18788
0.002	0.013	0.013								<i>K. swingsii</i> LMG22125
										<i>K. xylinus</i> ATCC53582
										<i>K. xylinus</i> BRC12334
										<i>K. xylinus</i> CGMCC2955
										<i>K. xylinus</i> E25
										<i>K. xylinus</i> E26
										<i>K. xylinus</i> LMG1515
										<i>K. xylinus</i> NBRC13693

<i>K. xylinus</i> NBRC13693	<i>K. xylinus</i> LMG1515	<i>K. xylinus</i> E26	<i>K. xylinus</i> E25	<i>K. xylinus</i> CGMCC2955	Genomes
0.006	0.001	0.006	0.006	0.005	K1G4
0.006	0.001	0.006	0.006	0.005	<i>K. xylinus</i> K2G30
0.013	0.015	0.011	0.011	0.012	<i>K. coccois</i> WIE7
0.004	0.004	0.002	0.002	0.004	<i>K. europaeus</i> CECT8546
0.004	0.005	0.002	0.002	0.004	<i>K. europaeus</i> LMG18494
0.005	0.005	0.002	0.002	0.005	<i>K. europaeus</i> NBRC 3261
0.004	0.005	0.002	0.002	0.004	<i>K. europaeus</i> SRCM101446
0.011	0.014	0.010	0.010	0.011	<i>K. hansenii</i> ATCC 53582
0.011	0.013	0.010	0.010	0.011	<i>K. hansenii</i> AY201
0.012	0.014	0.010	0.010	0.011	<i>K. hansenii</i> HUM-1
0.011	0.013	0.010	0.010	0.011	<i>K. hansenii</i> JCM7643
0.012	0.014	0.010	0.010	0.011	<i>K. hansenii</i> LMG23726
0.011	0.014	0.010	0.010	0.011	<i>K. hansenii</i> NQ5
0.011	0.014	0.010	0.010	0.011	<i>K. hansenii</i> SC-3B
0.001	0.007	0.005	0.005	0.003	<i>K. intermedius</i> TF2
0.006	0.007	0.004	0.004	0.006	<i>K. kakiaceti</i> JCM25156
0.011	0.014	0.010	0.010	0.012	<i>K. mallacetii</i> LMG1529
0.005	0.005	0.003	0.003	0.002	<i>K. medellinensis</i> NBRC3288
0.005	0.003	0.003	0.003	0.005	<i>K. nataricola</i> RZS01
0.001	0.007	0.005	0.005	0.003	<i>K. oboediensis</i> T74Bp2
0.001	0.007	0.005	0.005	0.003	<i>K. oboediensis</i> LMG18849
0.012	0.015	0.011	0.011	0.012	<i>K. pomacetii</i> AV446
0.013	0.015	0.011	0.011	0.012	<i>K. pomacetii</i> T5K1
0.003	0.006	0.003	0.003	0.000	<i>K. rhaeticus</i> AF1
0.003	0.006	0.004	0.004	0.000	<i>K. rhaeticus</i> IGEM
0.005	0.005	0.002	0.002	0.003	<i>K. saccharivorans</i> CV1
0.005	0.005	0.002	0.002	0.003	<i>K. saccharivorans</i> LMG1582
0.005	0.005	0.002	0.002	0.003	<i>K. saccharivorans</i> SRCM101450
0.006	0.002	0.004	0.004	0.005	<i>K. sacrofermentans</i> LMG18788
0.006	0.003	0.002	0.002	0.005	<i>K. swingsii</i> LMG22125
0.011	0.014	0.010	0.010	0.011	<i>K. xylinus</i> ATCC53582
0.005	0.005	0.000	0.000	0.004	<i>K. xylinus</i> BCR12334
0.003	0.006	0.004	0.004		<i>K. xylinus</i> CGMCC2955
0.005	0.005	0.000			<i>K. xylinus</i> E25
0.005	0.005				<i>K. xylinus</i> E26
0.007					<i>K. xylinus</i> LMG1515
					<i>K. xylinus</i> NBRC13693

Table S5-2 ANIb pairwise similarity matrix

<i>K. hansenii</i> HUM-1	<i>K. xylinus</i> K2630	<i>K. saccharivorans</i> CV1	<i>K. hansenii</i> LMG21726	<i>K. hansenii</i> SC-3B	<i>K. maltacetii</i> LMG1529	<i>K. hansenii</i> AY201	<i>K. xylinus</i> BCR12334	<i>K. pomacetii</i> T5K1	<i>K. xylinus</i> E26	Genomes
0.776	0.846	0.835	0.777	0.779	0.801	0.777	0.999	0.807	1.000	<i>K. xylinus</i> E26
0.829	0.795	0.787	0.828	0.828	0.852	0.832	0.802	1.000	0.804	<i>K. pomacetii</i> T5K1
0.776	0.847	0.834	0.777	0.778	0.801	0.778	1.000	0.807	0.999	<i>K. xylinus</i> BCR12334
0.988	0.771	0.774	0.986	0.985	0.863	1.000	0.776	0.831	0.777	<i>K. hansenii</i> AY201
0.860	0.798	0.791	0.861	0.859	1.000	0.863	0.798	0.853	0.800	<i>K. maltacetii</i> LMG1529
0.989	0.773	0.776	0.986	1.000	0.860	0.985	0.777	0.829	0.778	<i>K. hansenii</i> SC-3B
0.989	0.771	0.774	1.000	0.987	0.861	0.988	0.777	0.828	0.779	<i>K. hansenii</i> LMG21726
0.769	0.826	1.000	0.772	0.775	0.794	0.775	0.832	0.792	0.833	<i>K. saccharivorans</i> CV1
0.771	1.000	0.828	0.771	0.775	0.803	0.774	0.847	0.802	0.846	<i>K. xylinus</i> K2630
1.000	0.769	0.770	0.988	0.988	0.859	0.988	0.776	0.828	0.777	<i>K. hansenii</i> HUM-1
0.771	0.918	0.826	0.772	0.775	0.790	0.773	0.838	0.792	0.838	<i>K. naticicola</i> RZ501
0.989	0.770	0.770	0.988	0.987	0.861	0.987	0.775	0.828	0.776	<i>K. xylinus</i> ATCC53582
0.774	0.842	0.834	0.776	0.779	0.806	0.778	0.915	0.806	0.917	<i>K. europaeus</i> LMG18494
0.774	0.839	0.835	0.774	0.775	0.811	0.775	0.914	0.802	0.915	<i>K. europaeus</i> NBRC3261
0.771	0.835	0.829	0.772	0.776	0.786	0.775	0.848	0.783	0.843	<i>K. xylinus</i> CGMCC2955
0.775	0.840	0.834	0.777	0.780	0.800	0.779	0.891	0.801	0.892	<i>K. intermedius</i> TF2
0.775	0.844	0.835	0.776	0.778	0.803	0.777	0.961	0.810	0.962	<i>K. swingsii</i> LMG22125
0.769	0.933	0.825	0.771	0.775	0.796	0.772	0.843	0.798	0.843	<i>K. xylinus</i> LMG1515
0.828	0.787	0.788	0.827	0.828	0.850	0.832	0.792	0.948	0.793	<i>K. coccois</i> WE7
0.770	0.821	0.984	0.772	0.772	0.785	0.774	0.830	0.782	0.831	<i>K. saccharivorans</i> LMG1582
0.770	0.831	0.985	0.773	0.775	0.802	0.775	0.838	0.801	0.839	<i>K. saccharivorans</i> SRCM101450
0.989	0.772	0.773	0.989	0.987	0.860	1.000	0.777	0.829	0.778	<i>K. hansenii</i> LCM7643
0.766	0.831	0.822	0.772	0.772	0.812	0.769	0.835	0.794	0.836	<i>K. medellinensis</i> NBRC3288
0.989	0.771	0.771	0.988	0.987	0.862	0.988	0.776	0.829	0.777	<i>K. hansenii</i> ATCC53582
0.773	0.837	0.832	0.773	0.776	0.794	0.775	0.887	0.796	0.888	<i>K. aboedfiensis</i> LMG18849
0.770	0.924	0.827	0.772	0.772	0.801	0.772	0.841	0.796	0.841	<i>K. sacrofermentans</i> LMG18788
0.781	0.840	0.849	0.781	0.782	0.807	0.783	0.845	0.809	0.846	<i>K. khalifaei</i> JCM25156
0.773	0.831	0.828	0.772	0.773	0.787	0.773	0.883	0.789	0.884	<i>K. xylinus</i> NBRC3693
0.989	0.770	0.770	0.988	0.987	0.861	0.987	0.775	0.828	0.776	<i>K. hansenii</i> MQ5
0.770	0.998	0.824	0.770	0.774	0.794	0.772	0.841	0.792	0.841	K1G4
0.772	0.844	0.832	0.773	0.779	0.799	0.776	0.850	0.799	0.850	<i>K. rhaeticus</i> IGEN1
0.773	0.841	0.834	0.772	0.776	0.796	0.778	0.887	0.801	0.889	<i>K. aboedfiensis</i> 1748p2
0.829	0.795	0.798	0.829	0.830	0.852	0.833	0.797	0.985	0.798	<i>K. pomacetii</i> AV446
0.775	0.846	0.835	0.776	0.778	0.803	0.777	1.000	0.810	0.999	<i>K. xylinus</i> E25
0.775	0.845	0.836	0.776	0.778	0.805	0.782	0.915	0.808	0.917	<i>K. europaeus</i> CECT8546
0.775	0.842	0.840	0.776	0.780	0.805	0.778	0.914	0.804	0.916	<i>K. europaeus</i> SRCM101446
0.772	0.849	0.835	0.773	0.780	0.801	0.778	0.849	0.804	0.850	<i>K. rhaeticus</i> AFI

<i>K. saccharivorans</i> SRCM101450	<i>K. saccharivorans</i> LMG1582	<i>K. coccis</i> WE7	<i>K. xylinus</i> LMG1515	<i>K. swingsii</i> LMG22125	<i>K. intermedius</i> TF2	<i>K. xylinus</i> CGMCC2955	<i>K. europaeus</i> NBR3261	<i>K. europaeus</i> LMG18494	<i>K. xylinus</i> ATCC53582	<i>K. nativicola</i> RZ501	Genomes
0.843	0.832	0.792	0.844	0.961	0.903	0.846	0.915	0.917	0.716	0.841	<i>K. xylinus</i> E26
0.802	0.780	0.948	0.794	0.807	0.832	0.782	0.810	0.814	0.828	0.792	<i>K. pomacetii</i> TSK1
0.842	0.832	0.791	0.845	0.961	0.902	0.846	0.914	0.916	0.776	0.841	<i>K. xylinus</i> BCRC12334
0.773	0.775	0.832	0.771	0.777	0.782	0.775	0.780	0.783	0.988	0.771	<i>K. hanseii</i> AY201
0.804	0.783	0.849	0.793	0.802	0.820	0.785	0.821	0.819	0.862	0.793	<i>K. maltacetii</i> LMG1529
0.775	0.774	0.828	0.777	0.778	0.789	0.778	0.786	0.785	0.988	0.782	<i>K. hanseii</i> 5C-3B
0.774	0.773	0.828	0.770	0.778	0.785	0.775	0.781	0.785	0.989	0.772	<i>K. hanseii</i> LMG3726
0.983	0.984	0.788	0.825	0.833	0.855	0.829	0.838	0.842	0.770	0.828	<i>K. saccharivorans</i> CV1
0.837	0.822	0.790	0.932	0.845	0.862	0.841	0.848	0.851	0.771	0.921	<i>K. xylinus</i> K2G30
0.771	0.771	0.827	0.768	0.776	0.776	0.771	0.777	0.780	0.989	0.771	<i>K. hanseii</i> HUM-1
0.828	0.820	0.784	0.914	0.839	0.851	0.834	0.842	0.844	0.771	1.000	<i>K. nativicola</i> RZ501
0.772	0.772	0.828	0.769	0.776	0.777	0.772	0.779	0.781	1.000	0.771	<i>K. xylinus</i> ATCC53582
0.847	0.850	0.799	0.840	0.917	0.898	0.849	0.981	1.000	0.775	0.839	<i>K. europaeus</i> LMG18494
0.843	0.829	0.793	0.837	0.914	0.900	0.840	1.000	0.981	0.774	0.836	<i>K. europaeus</i> NBR3261
0.827	0.825	0.780	0.835	0.843	0.840	1.000	0.841	0.848	0.770	0.832	<i>K. xylinus</i> CGMCC2955
0.840	0.854	0.788	0.837	0.892	1.000	0.840	0.893	0.893	0.776	0.835	<i>K. intermedius</i> TF2
0.843	0.851	0.795	0.844	1.000	0.904	0.846	0.916	0.918	0.775	0.842	<i>K. swingsii</i> LMG22125
0.831	0.821	0.784	1.000	0.844	0.860	0.838	0.845	0.848	0.770	0.918	<i>K. xylinus</i> LMG1515
0.798	0.780	1.000	0.785	0.795	0.817	0.781	0.804	0.814	0.828	0.789	<i>K. coccis</i> WE7
0.980	1.000	0.779	0.822	0.831	0.845	0.826	0.832	0.832	0.771	0.824	<i>K. saccharivorans</i> LMG1582
1.000	0.984	0.794	0.827	0.840	0.859	0.830	0.845	0.855	0.772	0.828	<i>K. saccharivorans</i> SRCM101450
0.774	0.775	0.830	0.772	0.777	0.782	0.775	0.781	0.783	0.990	0.772	<i>K. hanseii</i> LCM7643
0.832	0.814	0.793	0.828	0.838	0.852	0.872	0.852	0.853	0.773	0.832	<i>K. medellinensis</i> NBR3288
0.772	0.772	0.829	0.770	0.777	0.777	0.772	0.780	0.782	1.000	0.772	<i>K. hanseii</i> ATCC53582
0.835	0.830	0.790	0.840	0.888	0.943	0.842	0.890	0.892	0.775	0.836	<i>K. oboediens</i> LMG18849
0.835	0.820	0.791	0.918	0.843	0.851	0.835	0.845	0.853	0.772	0.924	<i>K. sucrofermentans</i> LMG18788
0.854	0.843	0.805	0.836	0.845	0.861	0.839	0.852	0.859	0.781	0.838	<i>K. kakhiaeti</i> LCM21516
0.830	0.827	0.784	0.829	0.884	0.942	0.835	0.887	0.888	0.773	0.829	<i>K. xylinus</i> NBR3261
0.772	0.772	0.828	0.769	0.776	0.777	0.771	0.779	0.781	1.000	0.771	<i>K. hanseii</i> NQ5
0.829	0.820	0.785	0.931	0.842	0.855	0.836	0.844	0.846	0.769	0.922	K164
0.836	0.826	0.790	0.843	0.850	0.859	0.998	0.847	0.856	0.772	0.839	<i>K. rhoeticus</i> IGEN
0.839	0.829	0.794	0.838	0.888	0.943	0.838	0.889	0.892	0.774	0.834	<i>K. oboediens</i> 1749p2
0.804	0.783	0.947	0.793	0.801	0.826	0.784	0.811	0.816	0.828	0.791	<i>K. pomacetii</i> AY446
0.842	0.831	0.792	0.845	0.962	0.903	0.845	0.913	0.916	0.775	0.841	<i>K. xylinus</i> E25
0.844	0.850	0.798	0.844	0.916	0.903	0.845	0.978	0.978	0.776	0.842	<i>K. europaeus</i> CCT85-46
0.844	0.829	0.795	0.839	0.914	0.899	0.842	0.978	0.978	0.776	0.838	<i>K. europaeus</i> SRCM101446
0.836	0.827	0.794	0.846	0.850	0.867	0.989	0.851	0.855	0.773	0.842	<i>K. rhoeticus</i> AF1

<i>K. rhoeiticus</i> GEM	KL64	<i>K. hansenii</i> NQS	<i>K. xylinus</i> NBRC 13693	<i>K. kakaiceti</i> JCM21516	<i>K. sucrofermentans</i> LMG18788	<i>K. oboediens</i> LMG18849	<i>K. hansenii</i> ATCC33582	<i>K. medellinensis</i> NBRC3288	<i>K. hansenii</i> JCM7643	Genomes
0.851	0.843	0.777	0.885	0.844	0.842	0.888	0.777	0.838	0.780	<i>K. xylinus</i> E26
0.793	0.788	0.828	0.788	0.796	0.793	0.799	0.829	0.789	0.830	<i>K. pomaceti</i> T5K1
0.851	0.842	0.777	0.885	0.843	0.842	0.888	0.778	0.837	0.779	<i>K. xylinus</i> BCRG2334
0.774	0.770	0.988	0.774	0.779	0.772	0.776	0.988	0.770	0.998	<i>K. hansenii</i> AY201
0.796	0.793	0.862	0.789	0.800	0.798	0.794	0.863	0.809	0.860	<i>K. maffaceti</i> LMG1529
0.778	0.772	0.988	0.774	0.780	0.772	0.780	0.988	0.772	0.984	<i>K. hansenii</i> SC-3B
0.773	0.769	0.990	0.775	0.779	0.772	0.775	0.990	0.775	0.987	<i>K. hansenii</i> LMG23726
0.831	0.822	0.770	0.829	0.845	0.824	0.832	0.770	0.823	0.775	<i>K. saccharivorans</i> CV1
0.848	0.999	0.771	0.835	0.838	0.925	0.841	0.772	0.834	0.778	<i>K. xylinus</i> K2G30
0.770	0.768	0.989	0.775	0.779	0.769	0.775	0.989	0.766	0.987	<i>K. hansenii</i> HUM-1
0.837	0.920	0.771	0.831	0.834	0.925	0.834	0.771	0.830	0.776	<i>K. nataicola</i> R2S01
0.771	0.768	1.000	0.774	0.779	0.771	0.774	1.000	0.775	0.987	<i>K. xylinus</i> ATCC33582
0.850	0.839	0.775	0.887	0.845	0.844	0.888	0.776	0.844	0.780	<i>K. europaeus</i> LMG18494
0.842	0.836	0.775	0.888	0.845	0.838	0.887	0.776	0.847	0.778	<i>K. europaeus</i> NBRC3261
0.997	0.835	0.771	0.837	0.835	0.832	0.837	0.771	0.870	0.778	<i>K. xylinus</i> GCMC2955
0.844	0.835	0.776	0.945	0.840	0.837	0.942	0.776	0.836	0.782	<i>K. intermedius</i> T2
0.849	0.842	0.776	0.885	0.843	0.843	0.887	0.776	0.839	0.779	<i>K. swingsii</i> LMG22125
0.843	0.933	0.770	0.832	0.834	0.920	0.839	0.771	0.830	0.776	<i>K. xylinus</i> LMG1515
0.788	0.783	0.828	0.789	0.798	0.790	0.792	0.830	0.794	0.830	<i>K. cacaois</i> WE7
0.826	0.819	0.771	0.828	0.842	0.819	0.830	0.771	0.817	0.776	<i>K. saccharivorans</i> LMG1582
0.834	0.827	0.772	0.832	0.849	0.831	0.834	0.772	0.830	0.775	<i>K. saccharivorans</i> SRCM101450
0.774	0.770	0.990	0.774	0.779	0.772	0.777	0.990	0.770	1.000	<i>K. hansenii</i> JCM7643
0.873	0.829	0.773	0.829	0.831	0.833	0.830	0.773	1.000	0.772	<i>K. medellinensis</i> NBRC3288
0.772	0.768	1.000	0.774	0.779	0.772	0.775	1.000	0.775	0.988	<i>K. hansenii</i> ATCC33582
0.843	0.834	0.774	0.987	0.839	0.834	1.000	0.775	0.832	0.776	<i>K. oboediens</i> LMG18849
0.841	0.924	0.772	0.832	0.836	1.000	0.833	0.773	0.834	0.774	<i>K. sucrofermentans</i> LMG18788
0.843	0.840	0.782	0.842	1.000	0.838	0.841	0.783	0.839	0.784	<i>K. kakaiceti</i> JCM21516
0.837	0.830	0.773	1.000	0.836	0.828	0.984	0.773	0.828	0.774	<i>K. xylinus</i> NBRC13693
0.771	0.768	1.000	0.774	0.779	0.771	0.774	1.000	0.774	0.987	<i>K. hansenii</i> NQS
0.840	1.000	0.769	0.833	0.836	0.925	0.835	0.770	0.830	0.774	KL64
1.000	0.842	0.772	0.840	0.841	0.840	0.844	0.773	0.874	0.778	<i>K. rhoeiticus</i> GEM
0.843	0.835	0.773	0.986	0.841	0.833	0.993	0.775	0.834	0.778	<i>K. oboediens</i> L748p2
0.792	0.790	0.828	0.787	0.798	0.794	0.794	0.829	0.792	0.831	<i>K. pomaceti</i> AV446
0.851	0.842	0.776	0.884	0.843	0.842	0.888	0.776	0.838	0.779	<i>K. xylinus</i> E25
0.850	0.840	0.777	0.886	0.845	0.841	0.891	0.777	0.843	0.783	<i>K. europaeus</i> CCTC8546
0.847	0.839	0.776	0.885	0.842	0.840	0.883	0.776	0.838	0.782	<i>K. europaeus</i> SRCM101446
0.988	0.843	0.773	0.840	0.842	0.839	0.848	0.773	0.874	0.782	<i>K. rhoeiticus</i> AF1



<i>K. rhaeticus</i> AFI	<i>K. europaeus</i> SRCM101446	<i>K. europaeus</i> CECT8546	<i>K. xylinus</i> E25	<i>K. pomaceti</i> AV446	Genomes	<i>K. oboediens</i> 174Bp2
0.854	0.917	0.917	0.998	0.797	K1G4	0.894
0.805	0.799	0.808	0.805	0.985	<i>K. xylinus</i> K2G30	0.808
0.854	0.915	0.916	0.998	0.798	<i>K. coccois</i> WIE7	0.894
0.777	0.777	0.781	0.777	0.832	<i>K. europaeus</i> CECT8546	0.786
0.798	0.803	0.806	0.801	0.850	<i>K. europaeus</i> LMG18494	0.806
0.786	0.780	0.780	0.778	0.830	<i>K. europaeus</i> NBRC 3261	0.782
0.775	0.778	0.778	0.778	0.829	<i>K. europaeus</i> SRCM101446	0.779
0.834	0.840	0.837	0.834	0.798	<i>K. hansenii</i> ATCC 53582	0.839
0.853	0.844	0.851	0.850	0.796	<i>K. hansenii</i> AY201	0.849
0.772	0.775	0.776	0.776	0.828	<i>K. hansenii</i> HUM-1	0.778
0.838	0.835	0.839	0.840	0.788	<i>K. hansenii</i> JCM7643	0.837
0.772	0.776	0.778	0.775	0.828	<i>K. hansenii</i> LMG23726	0.780
0.849	0.980	0.977	0.915	0.803	<i>K. hansenii</i> NQ5	0.891
0.845	0.980	0.978	0.914	0.797	<i>K. hansenii</i> SC-3B	0.888
0.984	0.841	0.839	0.844	0.783	<i>K. intermedius</i> TF2	0.839
0.847	0.891	0.892	0.891	0.794	<i>K. kekulei</i> JCM25156	0.943
0.853	0.916	0.916	0.962	0.799	<i>K. maffaceti</i> LMG1529	0.891
0.848	0.841	0.847	0.845	0.791	<i>K. medellinensis</i> NBRC3288	0.844
0.794	0.796	0.805	0.793	0.947	<i>K. naticola</i> RZ501	0.805
0.829	0.830	0.831	0.833	0.780	<i>K. oboediens</i> 174Bp2	0.834
0.836	0.842	0.844	0.841	0.797	<i>K. oboediens</i> LMG18849	0.845
0.777	0.777	0.781	0.778	0.829	<i>K. pomaceti</i> AV446	0.785
0.873	0.837	0.844	0.837	0.791	<i>K. pomaceti</i> T5K1	0.838
0.773	0.777	0.779	0.776	0.829	<i>K. rhaeticus</i> AFI	0.781
0.849	0.886	0.893	0.888	0.791	<i>K. rhaeticus</i> IGEIM	0.992
0.839	0.842	0.844	0.843	0.793	<i>K. saccharivorans</i> CV1	0.839
0.846	0.847	0.852	0.848	0.804	<i>K. saccharivorans</i> LMG1582	0.851
0.838	0.885	0.886	0.884	0.785	<i>K. saccharivorans</i> SRCM101450	0.985
0.772	0.776	0.778	0.775	0.828	<i>K. sucrofermentans</i> LMG18768	0.780
0.844	0.839	0.843	0.842	0.790	<i>K. swingsii</i> LMG22125	0.840
0.986	0.848	0.851	0.852	0.792	<i>K. xylinus</i> ATCC53582	0.850
0.853	0.886	0.895	0.889	0.795	<i>K. xylinus</i> BCRC12334	1.000
0.799	0.802	0.806	0.799	1.000	<i>K. xylinus</i> CGMCC2955	0.804
0.853	0.914	0.916	1.000	0.798	<i>K. xylinus</i> E25	0.892
0.859	0.979	1.000	0.915	0.800	<i>K. xylinus</i> E26	0.898
0.847	1.000	0.979	0.913	0.802	<i>K. xylinus</i> LMG1515	0.888
1.000	0.848	0.859	0.851	0.796	<i>K. xylinus</i> NBRC19893	0.857

# References

- Abdel-Fattah, A. M., Gamal-Eldeen, A. M., Helmy, W. A., and Esawy, M. A. (2012). Antitumor and antioxidant activities of levan and its derivative from the isolate *Bacillus subtilis* NRC1aza. *Carbohydr. Polym.* doi:10.1016/j.carbpol.2012.02.041.
- Abdollahi, M., Alboofetileh, M., Behrooz, R., Rezaei, M., and Miraki, R. (2013). Reducing water sensitivity of alginate bio-nanocomposite film using cellulose nanoparticles. *Int. J. Biol. Macromol.* doi:10.1016/j.ijbiomac.2012.12.016.
- Abdul Khalil, H. P. S., Saurabh, C. K., Adnan, A. S., Nurul Fazita, M. R., Syakir, M. I., Davoudpour, Y., et al. (2016). A review on chitosan-cellulose blends and nanocellulose reinforced chitosan biocomposites: Properties and their applications. *Carbohydr. Polym.* doi:10.1016/j.carbpol.2016.05.028.
- Adachi, O., Tanasupawat, S., Yoshihara, N., Toyama, H., and Matsushita, K. (2003). 3-Dehydroquinone production by oxidative fermentation and further conversion of 3-dehydroquinone to the intermediates in the shikimate pathway. *Biosci. Biotechnol. Biochem.* 67, 2124–2131. doi:10.1271/bbb.67.2124.
- Adachi, O., and Yakushi, T. (2016). “Membrane-bound dehydrogenases of acetic acid bacteria,” in *Acetic Acid Bacteria: Ecology and Physiology* (Springer Japan), 273–297. doi:10.1007/978-4-431-55933-7\_13.
- Agustin, M. B., Ahmmad, B., De Leon, E. R. P., Buenaobra, J. L., Salazar, J. R., and Hirose, F. (2013). Starch-based biocomposite films reinforced with cellulose nanocrystals from garlic stalks. *Polym. Compos.* doi:10.1002/pc.22546.
- Aloui, H., Khwaldia, K., Hamdi, M., Fortunati, E., Kenny, J. M., Buonocore, G. G., et al. (2016). Synergistic effect of halloysite and cellulose nanocrystals on the functional properties of PVA based nanocomposites. *ACS Sustain. Chem. Eng.* doi:10.1021/acssuschemeng.5b00806.
- Alves, L., Ferraz, E., and Gamelas, J. A. F. (2019). Composites of nanofibrillated cellulose with clay minerals: A review. *Adv. Colloid Interface Sci.* 272, 101994. doi:10.1016/j.cis.2019.101994.
- Alves, P. M. A., Carvalho, R. A., Moraes, I. C. F., Luciano, C. G., Bittante, A. M. Q. B., and Sobral, P. J. A. (2011). Development of films based on blends of gelatin and poly(vinyl alcohol) cross linked with glutaraldehyde. *Food Hydrocoll.* doi:10.1016/j.foodhyd.2011.03.018.
- Ameyama, M., Osada, K., Shinagawa, E., Matsushita, K., and Adachi, O. (1981). Purification and characterization of aldehyde dehydrogenase of *Acetobacter aceti*. *Agric. Biol. Chem.* doi:10.1080/00021369.1981.10864803.
- Ameyama, M., Shinagawa, E., Matsushita, K., and Adachi, O. (1981). D-glucose dehydrogenase of *Gluconobacter suboxydans*: Solubilization, purification and characterization. *Agric. Biol. Chem.* 45, 851–861. doi:10.1271/bbb1961.45.851.
- Andres-Barrao, C., Falquet, L., Calderon-Copete, S. P., Descombes, P., Ortega Perez, R., and Barja,

- F. (2011). Genome sequences of the high-acetic acid-resistant bacteria *Gluconacetobacter europaeus* LMG 18890<sup>T</sup> and *G. europaeus* LMG 18494 (Reference Strains), *G. europaeus* 5P3, and *Gluconacetobacter oboediens* 174Bp2 (Isolated from Vinegar). *J. Bacteriol.* 193, 2670–2671. doi:10.1128/JB.00229-11.
- Andriani, D., Apriyana, A. Y., and Karina, M. (2020). The optimization of bacterial cellulose production and its applications: a review. *Cellulose*. doi:10.1007/s10570-020-03273-9.
- Ano, Y., Shinagawa, E., Adachi, O., Toyama, H., Yakushi, T., and Matsushita, K. (2011). Selective, high conversion of D-glucose to 5-keto-D-gluconate by *Gluconobacter suboxydans*. *Biosci. Biotechnol. Biochem.* doi:10.1271/bbb.100701.
- Arfat, Y. A., Ahmed, J., Hiremath, N., Auras, R., and Joseph, A. (2017). Thermo-mechanical, rheological, structural and antimicrobial properties of bionanocomposite films based on fish skin gelatin and silver-copper nanoparticles. *Food Hydrocoll.* doi:10.1016/j.foodhyd.2016.08.009.
- Arikan, M., Mitchell, A. L., Finn, R. D., and Gürel, F. (2020). Microbial composition of Kombucha determined using amplicon sequencing and shotgun metagenomics. *J. Food Sci.* 85, 455–464. doi:10.1111/1750-3841.14992.
- Asad, M., Saba, N., Asiri, A. M., Jawaid, M., Indarti, E., and Wanrosli, W. D. (2018). Preparation and characterization of nanocomposite films from oil palm pulp nanocellulose/poly (Vinyl alcohol) by casting method. *Carbohydr. Polym.* doi:10.1016/j.carbpol.2018.03.015.
- ASTM. (2001a). Standard test method for tensile properties of thin plastic sheeting. In Annual books of ASTM standards. Designation D882-01. Philadelphia: ASTM, American Society for Testing Materials.
- ASTM. (2001b). Standard test method for water vapor transmission of materials. In Annual books of ASTM Standards. Designation E 96-01, Philadelphia: ASTM, American Society for Testing Materials.
- Atalla, R. H., and VanderHart, D. L. (1984). Native cellulose: A composite of two distinct crystalline forms. *Science (80- )*. doi:10.1126/science.223.4633.283.
- Augimeri, R. V, and Strap, J. L. (2015). The phytohormone ethylene enhances cellulose production, regulates CRP/FNRKx transcription and causes differential gene expression within the bacterial cellulose synthesis operon of *Komagataeibacter (Gluconacetobacter) xylinus* ATCC 53582. *Front. Microbiol.* 6, 1459. doi:10.3389/fmicb.2015.01459.
- Azeredo, H. M. C., Rosa, M. F., and Mattoso, L. H. C. (2017). Nanocellulose in bio-based food packaging applications. *Ind. Crops Prod.* doi:10.1016/j.indcrop.2016.03.013.
- Azuma, Y., Hosoyama, A., Matsutani, M., Furuya, N., Horikawa, H., Harada, T., et al. (2009). Whole-genome analyses reveal genetic instability of *Acetobacter pasteurianus*. *Nucleic Acids Res.* 37, 5768–5783. doi:10.1093/nar/gkp612.
- Bae, S. O., and Shoda, M. (2005). Production of bacterial cellulose by *Acetobacter xylinum* BPR2001 using molasses medium in a jar fermentor. *Appl. Microbiol. Biotechnol.* 67, 45–51. doi:10.1007/s00253-004-1723-2.
- Bankevich, A., Nurk, S., Antipov, D., Gurevich, A. A., Dvorkin, M., Kulikov, A. S., et al. (2012).

- SPAdes: a new genome assembly algorithm and its applications to single-cell sequencing. *J. Comput. Biol.* 19, 455–77. doi:10.1089/cmb.2012.0021.
- Barbi, S., Taurino, C., La China, S., Anguluri, K., Gullo, M., and Montorsi, M. (2021). Mechanical and structural properties of environmental green composites based on functionalized bacterial cellulose. *Cellulose*, 1–12. doi:10.1007/s10570-020-03602-y.
- Bartowsky, E. J., and Henschke, P. A. (2008). Acetic acid bacteria spoilage of bottled red wine-A review. *Int. J. Food Microbiol.* doi:10.1016/j.ijfoodmicro.2007.10.016.
- Barud, H. S., Assunção, R. M. N., Martines, M. A. U., Dexpert-Ghys, J., Marques, R. F. C., Messaddeq, Y., et al. (2008). Bacterial cellulose-silica organic-inorganic hybrids. *J. Sol-Gel Sci. Technol.* 46, 363–367. doi:10.1007/s10971-007-1669-9.
- Basu, A., Vadanam, S. V., and Lim, S. (2018). A novel platform for evaluating the environmental impacts on bacterial cellulose production. *Sci. Rep.* 8, 5780. doi:10.1038/s41598-018-23701-y.
- Battikh, H., Chaieb, K., Bakhrouf, A., and Ammar, E. (2013). Antibacterial and antifungal activities of black and green kombucha teas. *J. Food Biochem.* 37, 231–236. doi:10.1111/j.1745-4514.2011.00629.x.
- Bellelli, M., Licciardello, F., Pulvirenti, A., and Fava, P. (2018). Properties of poly(vinyl alcohol) films as determined by thermal curing and addition of polyfunctional organic acids. *Food Packag. Shelf Life.* doi:10.1016/j.fpsl.2018.10.004.
- Benigar, E., Dogsa, I., Stopar, D., Jamnik, A., Cigić, I. K., and Tomšič, M. (2014). Structure and dynamics of a polysaccharide matrix: Aqueous solutions of bacterial levan. *Langmuir.* doi:10.1021/la500830j.
- Bergo, P., Moraes, I. C. F., and Sobral, P. J. A. (2012). Effects of different moisture contents on physical properties of PVA-gelatin films. *Food Biophys.* doi:10.1007/s11483-012-9273-0.
- Bolger, A. M., Lohse, M., and Usadel, B. (2014). Trimmomatic: a flexible trimmer for Illumina sequence data. *Bioinformatics* 30, 2114–20. doi:10.1093/bioinformatics/btu170.
- Bottan, S., Robotti, F., Jayathissa, P., Hegglin, A., Bahamonde, N., Heredia-Guerrero, J. A., et al. (2015). Surface-structured bacterial cellulose with guided assembly-based biolithography (GAB). *ACS Nano.* doi:10.1021/nn5036125.
- Brandt, J. U., Jakob, F., Behr, J., Geissler, A. J., and Vogel, R. F. (2016). Dissection of exopolysaccharide biosynthesis in *Kozakia baliensis*. *Microb. Cell Fact.* doi:10.1186/s12934-016-0572-x.
- Brinchi, L., Cotana, F., Fortunati, E., and Kenny, J. M. (2013). Production of nanocrystalline cellulose from lignocellulosic biomass: Technology and applications. *Carbohydr. Polym.* doi:10.1016/j.carbpol.2013.01.033.
- Brown, C., Leijon, F., and Bulone, V. (2012). Radiometric and spectrophotometric *in vitro* assays of glycosyltransferases involved in plant cell wall carbohydrate biosynthesis. *Nat. Protoc.* 7, 1634–1650. doi:10.1038/nprot.2012.089.

- Brown, R. M. (1996). The Biosynthesis of Cellulose. *J. Macromol. Sci. Part A* 33, 1345–1373. doi:10.1080/10601329608014912.
- Brown, R. M. (2004). Cellulose Structure and Biosynthesis: What is in store for the 21st Century? in *Journal of Polymer Science, Part A: Polymer Chemistry* doi:10.1002/pola.10877.
- BS EN ISO 527-5:2009 (2009). ISO 527-5:2009 Plastics — Determination of tensile properties. *Part 1*, 527–1.
- Bugaev, K. O., Zelenina, A. A., and Volodin, V. A. (2012). Vibrational spectroscopy of chemical species in silicon and silicon-rich nitride Thin Films. *Int. J. Spectrosc.* 2012, 1–5. doi:10.1155/2012/281851.
- Cañete-Rodríguez, A. M., Santos-Dueñas, I. M., Jiménez-Hornero, J. E., Ehrenreich, A., Liebl, W., and García-García, I. (2016). Gluconic acid: Properties, production methods and applications—An excellent opportunity for agro-industrial by-products and waste bio-valorization. Elsevier doi:10.1016/j.procbio.2016.08.028.
- Canilha, L., Carvalho, W., Felipe, M. das G. A., and de Almeida E Silva, J. B. (2008). Xylitol production from wheat straw hemicellulosic hydrolysate: hydrolysate detoxification and carbon source used for inoculum preparation. *Braz. J. Microbiol.* 39, 333–6. doi:10.1590/S1517-838220080002000025.
- Cannon, R. E., and Anderson, S. M. (1991). Biogenesis of bacterial cellulose. *Crit. Rev. Microbiol.* doi:10.3109/10408419109115207.
- Cao, J., Rusina, O., and Sieber, H. (2004). Processing of porous TiO<sub>2</sub>-ceramics from biological preforms. *Ceram. Int.* 30, 1971–1974. doi:10.1016/j.ceramint.2003.12.180.
- Carvalho, R. A., Maria, T. M. C., Moraes, I. C. F., Bergo, P. V. A., Kamimura, E. S., Habitante, A. M. Q. B., et al. (2009). Study of some physical properties of biodegradable films based on blends of gelatin and poly(vinyl alcohol) using a response-surface methodology. *Mater. Sci. Eng. C.* doi:10.1016/j.msec.2008.08.030.
- Carver, T., Harris, S. R., Berriman, M., Parkhill, J., and McQuillan, J. A. (2012). Artemis: an integrated platform for visualization and analysis of high-throughput sequence-based experimental data. *Bioinformatics* 28, 464–469. doi:10.1093/bioinformatics/btr703.
- Castro, C., Vesterinen, A., Zuluaga, R., Caro, G., Filpponen, I., Rojas, O. J., et al. (2014). *In situ* production of nanocomposites of poly(vinyl alcohol) and cellulose nanofibrils from *Gluconacetobacter* bacteria: Effect of chemical crosslinking. *Cellulose*. doi:10.1007/s10570-014-0170-1.
- Cavka, A., Guo, X., Tang, S.-J., Winstrand, S., Jönsson, L. J., and Hong, F. (2013). Production of bacterial cellulose and enzyme from waste fiber sludge. *Biotechnol. Biofuels* 6, 25. doi:10.1186/1754-6834-6-25.
- Cazón, P., Vázquez, M., and Velazquez, G. (2018). Novel composite films based on cellulose reinforced with chitosan and polyvinyl alcohol: Effect on mechanical properties and water vapour permeability. *Polym. Test.* doi:10.1016/j.polymertesting.2018.06.016.

- Cazón, P., Vázquez, M., and Velazquez, G. (2019). Composite films with UV-barrier properties based on bacterial cellulose combined with chitosan and Poly(vinyl alcohol): Study of puncture and water interaction properties. *Biomacromolecules* 20, 2084–2095. doi:10.1021/acs.biomac.9b00317.
- Cazón, P., Velazquez, G., Ramírez, J. A., and Vázquez, M. (2017). Polysaccharide-based films and coatings for food packaging: A review. *Food Hydrocoll.* 68, 136–148. doi:10.1016/j.foodhyd.2016.09.009.
- Chambert, R., Treboul, G., and Dedonder, R. (1974). Kinetic studies of levansucrase of *Bacillus subtilis*. *Eur. J. Biochem.* doi:10.1111/j.1432-1033.1974.tb03269.x.
- Chang, A. L., Tuckerman, J. R., Gonzalez, G., Mayer, R., Weinhouse, H., Volman, G., et al. (2001). Phosphodiesterase A1, a regulator of cellulose synthesis in *Acetobacter xylinum*, is a heme-based sensor. *Biochemistry*. doi:10.1021/bi0100236.
- Chang, P. R., Jian, R., Zheng, P., Yu, J., and Ma, X. (2010). Preparation and properties of glycerol plasticized-starch (GPS)/cellulose nanoparticle (CN) composites. *Carbohydr. Polym.* doi:10.1016/j.carbpol.2009.08.007.
- Chang, S. T., Chen, L. C., Lin, S. Bin, and Chen, H. H. (2012). Nano-biomaterials application: Morphology and physical properties of bacterial cellulose/gelatin composites via crosslinking. *Food Hydrocoll.* 27, 137–144. doi:10.1016/j.foodhyd.2011.08.004.
- Chau, C.-F., Yang, P., Yu, C.-M., and Yen, G.-C. (2008). Investigation on the lipid- and cholesterol-lowering abilities of biocellulose. *J. Agric. Food Chem.* 56, 2291–2295. doi:10.1021/jf7035802.
- Chauhan, I., and Mohanty, P. (2014). Immobilization of titania nanoparticles on the surface of cellulose fibres by a facile single step hydrothermal method and study of their photocatalytic and antibacterial activities. *RSC Adv.* 4, 57885–57890. doi:10.1039/c4ra07372j.
- Chawla, P. R., Bajaj, I. B., Survase, S. A., and Singhal, R. S. (2009). Microbial cellulose: Fermentative production and applications. *Food Technol. Biotechnol.*
- Chen, H. P., and Brown, R. M. (1996). Immunochemical studies of the cellulose synthase complex in *Acetobacter xylinum*. *Cellulose* 3, 63–75. doi:10.1007/BF02228791.
- Cheng, Z., Yang, R., Liu, X., Liu, X., and Chen, H. (2017a). Green synthesis of bacterial cellulose via acetic acid pre-hydrolysis liquor of agricultural corn stalk used as carbon source. *Bioresour. Technol.* 234, 8–14. doi:10.1016/j.biortech.2017.02.131.
- Cheng, Z., Yang, R., Liu, X., Liu, X., and Chen, H. (2017b). Green synthesis of bacterial cellulose via acetic acid pre-hydrolysis liquor of agricultural corn stalk used as carbon source. *Bioresour. Technol.* doi:10.1016/j.biortech.2017.02.131.
- Chi, K., and Catchmark, J. M. (2017). The influences of added polysaccharides on the properties of bacterial crystalline nanocellulose. *Nanoscale*. doi:10.1039/c7nr05615j.

- Cho, M. J., and Park, B. D. (2011). Tensile and thermal properties of nanocellulose-reinforced poly(vinyl alcohol) nanocomposites. *J. Ind. Eng. Chem.* doi:10.1016/j.jiec.2010.10.006.
- Chozhavendhan, S., Praveen Kumar, R., Elavazhagan, S., Barathiraja, B., Jayakumar, M., and Varjani, S. J. (2018). "Utilization of crude glycerol from biodiesel industry for the production of value-added bioproducts," in doi:10.1007/978-981-10-7431-8\_4.
- Christiansen, C., Abou Hachem, M., Janeček, Š., Viksø-Nielsen, A., Blennow, A., and Svensson, B. (2009). The carbohydrate-binding module family 20 - Diversity, structure, and function. *FEBS J.* 276, 5006–5029. doi:10.1111/j.1742-4658.2009.07221.x.
- Cleenwerck, I., De Vos, P., and De Vuyst, L. (2010). Phylogeny and differentiation of species of the genus *Gluconacetobacter* and related taxa based on multilocus sequence analyses of housekeeping genes and reclassification of *Acetobacter xylinus* subsp. *sucrofermentans* as *Gluconacetobacter sucrofermentans* (T). *Int. J. Syst. Evol. Microbiol.* doi:10.1099/ijs.0.018465-0.
- Cleenwerck, I., De Wachter, M., González, Á., De Vuyst, L., and De Vos, P. (2009). Differentiation of species of the family *Acetobacteraceae* by AFLP DNA fingerprinting: *Gluconacetobacter kombuchae* is a later heterotypic synonym of *Gluconacetobacter hansenii*. *Int. J. Syst. Evol. Microbiol.* 59, 1771–1786. doi:10.1099/ijs.0.005157-0.
- Cleenwerck, I., Vandemeulebroecke, K., Janssens, D., and Swings, J. (2002). Re-examination of the genus *Acetobacter*, with descriptions of *Acetobacter cerevisiae* sp. nov., and *Acetobacter malorum* sp. nov. *Int. J. Syst. Evol. Microbiol.* 52, 1551–1558. doi:10.1099/ijs.0.02064-0.
- Costa, A. F. S., Almeida, F. C. G., Vinhas, G. M., and Sarubbo, L. A. (2017). Production of bacterial cellulose by *Gluconacetobacter hansenii* using corn steep liquor as nutrient sources. *Front. Microbiol.* 8, 2027. doi:10.3389/fmicb.2017.02027.
- Coton, M., Pawtowski, A., Taminiau, B., Burgaud, G., Deniel, F., Coulloumme-Labarthe, L., et al. (2017). Unraveling microbial ecology of industrial-scale Kombucha fermentations by metabarcoding and culture-based methods. *FEMS Microbiol. Ecol.* 93. doi:10.1093/femsec/fix048.
- da Silva Filho, E. C., de Melo, J. C. P., and Airoidi, C. (2006). Preparation of ethylenediamine-anchored cellulose and determination of thermochemical data for the interaction between cations and basic centers at the solid/liquid interface. *Carbohydr. Res.* 341, 2842–2850. doi:10.1016/j.carres.2006.09.004.
- Dal Bello, F., Walter, J., Hertel, C., and Hammes, W. P. (2001). *In vitro* study of prebiotic properties of levan-type exopolysaccharides from *Lactobacilli* and non-digestible carbohydrates using denaturing gradient gel electrophoresis. *Syst. Appl. Microbiol.* doi:10.1078/0723-2020-00033.
- Davies, D. G., Parsek, M. R., Pearson, J. P., Iglewski, B. H., Costerton, J. W., and Greenberg, E. P. (1998). The involvement of cell-to-cell signals in the development of a bacterial biofilm. *Science* (80-. ). 280, 295–298. doi:10.1126/science.280.5361.295.
- De Leo, R., Quartieri, A., Haghghi, H., Gigliano, S., Bedin, E., and Pulvirenti, A. (2018). Application of pectin-alginate and pectin-alginate-laurolyl arginate ethyl coatings to eliminate *Salmonella*

- enteritidis* cross contamination in egg shells. *J. Food Saf.* doi:10.1111/jfs.12567.
- De Roos, J., and De Vuyst, L. (2018). Acetic acid bacteria in fermented foods and beverages. *Curr. Opin. Biotechnol.* 49, 115–119. doi:10.1016/j.copbio.2017.08.007.
- De Vero, L., Boniotti, M. B., Budroni, M., Buzzini, P., Cassanelli, S., Comunian, R., et al. (2019). Preservation, characterization and exploitation of microbial biodiversity: The perspective of the Italian network of culture collections. *Microorganisms.* doi:10.3390/microorganisms7120685.
- De Vero, L., Gullo, M., and Giudici, P. (2010). “Acetic Acid Bacteria, biotechnological applications,” in *Encyclopedia of Industrial Biotechnology* (Hoboken, NJ, USA: John Wiley & Sons, Inc.), 1–17. doi:10.1002/9780470054581.eib003.
- De Vuyst, L., Camu, N., De Winter, T., Vandemeulebroecke, K., Van De Perre, V., Vancanneyt, M., et al. (2007). Validation of the (GTG) 5-rep-PCR fingerprinting technique for rapid classification and identification of acetic acid bacteria, with a focus on isolates from Ghanaian fermented cocoa beans. doi:10.1016/j.ijfoodmicro.2007.02.030.
- De Vuyst, L., Vanderveken, F., Van De Ven, S., and Degeest, B. (1998). Production by and isolation of exopolysaccharides from *Streptococcus thermophilus* grown in a milk medium and evidence for their growth-associated biosynthesis. *J. Appl. Microbiol.* doi:10.1046/j.1365-2672.1998.00445.x.
- del Campo, M. M., Darder, M., Aranda, P., Akkari, M., Huttel, Y., Mayoral, A., et al. (2018). Functional hybrid nanopaper by assembling nanofibers of cellulose and sepiolite. *Adv. Funct. Mater.* 28, 1703048. doi:10.1002/adfm.201703048.
- Del Nobile, M. A., Fava, P., and Piergiovanni, L. (2002). Water transport properties of cellophane flexible films intended for food packaging applications. *J. Food Eng.* doi:10.1016/S0260-8774(01)00168-6.
- Deng, Y., Nagachar, N., Xiao, C., Tien, M., and Kao, T. (2013). Identification and characterization of non-cellulose-producing mutants of *Gluconacetobacter hansenii* generated by Tn5 transposon mutagenesis. *J. Bacteriol.* 195, 5072–83. doi:10.1128/JB.00767-13.
- Deppenmeier, U., Hoffmeister, M., and Prust, C. (2002). Biochemistry and biotechnological applications of *Gluconobacter* strains. *Appl. Microbiol. Biotechnol.* 60, 233–242. doi:10.1007/s00253-002-1114-5.
- Dikshit, P. K., and Moholkar, V. S. (2019). Batch and repeated-batch fermentation for 1,3-dihydroxyacetone production from waste glycerol using free, immobilized and resting *Gluconobacter oxydans* Cells. *Waste and Biomass Valorization.* doi:10.1007/s12649-018-0307-9.
- Dillon, R. J., and Dillon, V. M. (2004). The Gut Bacteria of Insects: Nonpathogenic Interactions. *Annu. Rev. Entomol.* doi:10.1146/annurev.ento.49.061802.123416.
- Donot, F., Fontana, A., Baccou, J. C., and Schorr-Galindo, S. (2012). Microbial exopolysaccharides: Main examples of synthesis, excretion, genetics and extraction. *Carbohydr. Polym.*



doi:10.1016/j.carbpol.2011.08.083.

- Douglass, E. F., Avci, H., Boy, R., Rojas, O. J., and Kotek, R. (2018). A review of cellulose and cellulose blends for preparation of bio-derived and conventional membranes, nanostructured thin films, and composites. *Polym. Rev.* 58, 102–163. doi:10.1080/15583724.2016.1269124.
- Du, J., Vepachedu, V., Cho, S. H., Kumar, M., and Nixon, B. T. (2016). Structure of the cellulose synthase complex of *Gluconacetobacter hansenii* at 23.4 Å Resolution. *PLoS One* 11, e0155886. doi:10.1371/journal.pone.0155886.
- Dufresne, A. (2006). Comparing the mechanical properties of high performances polymer nanocomposites from biological sources. *J. Nanosci. Nanotechnol.* doi:10.1166/jnn.2006.906.
- Edgar, R. C. (2004). MUSCLE: Multiple sequence alignment with high accuracy and high throughput. *Nucleic Acids Res.* 32, 1792–7. doi:10.1093/nar/gkh340.
- El Achaby, M., El Miri, N., Aboulkas, A., Zahouily, M., Bilal, E., Barakat, A., et al. (2017). Processing and properties of eco-friendly bio-nanocomposite films filled with cellulose nanocrystals from sugarcane bagasse. *Int. J. Biol. Macromol.* doi:10.1016/j.ijbiomac.2016.12.040.
- Elias, S. A. (2017). “Plastics in the ocean,” in *Encyclopedia of the Anthropocene* doi:10.1016/B978-0-12-809665-9.10514-2.
- ENTANI, E., OHMORI, S., MASAI, H., and SUZUKI, K.-I. (1985). *Acetobacter polyoxogenes* sp. nov., a new species of an acetic acid bacterium useful for producing vinegar with high acidity. *J. Gen. Appl. Microbiol.* 31, 475–490. doi:10.2323/jgam.31.475.
- Esa, F., Tasirin, S. M., and Rahman, N. A. (2014). Overview of bacterial cellulose production and application. *Agric. Agric. Sci. Procedia* 2, 113–119. doi:10.1016/J.AASPRO.2014.11.017.
- Esawy, M. A., Ahmed, E. F., Helmy, W. A., Mansour, N. M., El-Senousy, W. M., and El-Safty, M. M. (2011). Production of levansucrase from novel honey *Bacillus subtilis* isolates capable of producing antiviral levans. *Carbohydr. Polym.* doi:10.1016/j.carbpol.2011.05.035.
- Etxabide, A., Uranga, J., Guerrero, P., and de la Caba, K. (2017). Development of active gelatin films by means of valorisation of food processing waste: A review. *Food Hydrocoll.* doi:10.1016/j.foodhyd.2016.08.021.
- Euzéby, J. P. (1997). List of bacterial names with standing in nomenclature: A folder available on the internet. *Int. J. Syst. Bacteriol.* 47, 590–592. doi:10.1099/00207713-47-2-590.
- Fernández, J., Morena, A. G., Valenzuela, S. V., Pastor, F. I. J., Díaz, P., and Martínez, J. (2019). Microbial cellulose from a *Komagataeibacter intermedius* strain isolated from commercial wine vinegar. *J. Polym. Environ.* doi:10.1007/s10924-019-01403-4.
- Florea, M., Reeve, B., Abbott, J., Freemont, P. S., and Ellis, T. (2016). Genome sequence and plasmid transformation of the model high-yield bacterial cellulose producer *Gluconacetobacter hansenii* ATCC 53582. *Sci. Rep.* 6, 23635. doi:10.1038/srep23635.
- Follain, N., Belbekhouche, S., Bras, J., Siqueira, G., Marais, S., and Dufresne, A. (2013). Water

- transport properties of bio-nanocomposites reinforced by *Luffa cylindrica* cellulose nanocrystals. *J. Memb. Sci.* doi:10.1016/j.memsci.2012.09.048.
- Frensemeier, M., Koplín, C., Jaeger, R., Kramer, F., and Klemm, D. (2010). Mechanical properties of bacterially synthesized nanocellulose hydrogels. in *Macromolecular Symposia*, 38–44. doi:10.1002/masy.200900030.
- Fu, T., Moon, R. J., Zavattieri, P., Youngblood, J., and Weiss, W. J. (2017). *Cellulose nanomaterials as additives for cementitious materials*. Elsevier Ltd doi:10.1016/B978-0-08-100957-4.00020-6.
- Gabr, M. H., Elrahman, M. A., Okubo, K., and Fujii, T. (2010). A study on mechanical properties of bacterial cellulose/epoxy reinforced by plain woven carbon fiber modified with liquid rubber. *Compos. Part A Appl. Sci. Manuf.* 41, 1263–1271. doi:10.1016/j.compositesa.2010.05.010.
- Gaggìa, F., Baffoni, L., Galiano, M., Nielsen, D., Jakobsen, R., Castro-Mejía, J., et al. (2018). Kombucha beverage from green, black and rooibos teas: A comparative study looking at microbiology, chemistry and antioxidant activity. *Nutrients* 11, 1. doi:10.3390/nu11010001.
- Gallegos, A. M. A., Carrera, S. H., Parra, R., Keshavarz, T., and Iqbal, H. M. N. (2016). Bacterial cellulose: A sustainable source to develop value-added products - A review. *BioResources*. doi:10.15376/biores.11.2.Gallegos.
- Gamelas, J. A. F., and Ferraz, E. (2015). Composite films based on nanocellulose and nanoclay minerals as high strength materials with gas barrier capabilities: Key Points and Challenges. *BioResources* 10, 6310–6313. doi:10.15376/biores.10.4.6310-6313.
- Gao, L., Hu, Y., Liu, J., Du, G., Zhou, J., and Chen, J. (2014). Stepwise metabolic engineering of *Gluconobacter oxydans* WSH-003 for the direct production of 2-keto-l-gulonic acid from D-sorbitol. *Metab. Eng.* doi:10.1016/j.ymben.2014.04.003.
- Gao, X., Shi, Z., Liu, C., Yang, G., Sevostianov, I., and Silberschmidt, V. V. (2015). Inelastic behaviour of bacterial cellulose hydrogel: In aqua cyclic tests. *Polym. Test.* 44, 82–92. doi:10.1016/j.polymertesting.2015.03.021.
- García-García, I., Cañete-Rodríguez, A. M., Santos-Dueñas, I. M., Jiménez-Hornero, J. E., Ehrenreich, A., Liebl, W., et al. (2017). Biotechnologically relevant features of gluconic acid production by acetic acid bacteria. *Acetic Acid Bact.* doi:10.4081/aab.2017.6458.
- García, N., Guzmán, J., Benito, E., Esteban-Cubillo, A., Aguilar, E., Santarén, J., et al. (2011). Surface modification of sepiolite in aqueous gels by using methoxysilanes and its impact on the nanofiber dispersion ability. *Langmuir* 27, 3952–3959. doi:10.1021/la104410r.
- Gätgens, C., Degner, U., Bringer-Meyer, S., and Herrmann, U. (2007). Biotransformation of glycerol to dihydroxyacetone by recombinant *Gluconobacter oxydans* DSM 2343. *Appl. Microbiol. Biotechnol.* doi:10.1007/s00253-007-1003-z.
- George, J., and Siddaramaiah (2012). High performance edible nanocomposite films containing bacterial cellulose nanocrystals. *Carbohydr. Polym.* doi:10.1016/j.carbpol.2011.10.019.
- Gevers, D., Huys, G., and Swings, J. (2001). Applicability of rep-PCR fingerprinting for

- identification of *Lactobacillus* species . *FEMS Microbiol. Lett.* 205, 31–36. doi:10.1111/j.1574-6968.2001.tb10921.x.
- Ghaderi, J., Hosseini, S. F., Keyvani, N., and Gómez-Guillén, M. C. (2019). Polymer blending effects on the physicochemical and structural features of the chitosan/poly(vinyl alcohol)/fish gelatin ternary biodegradable films. *Food Hydrocoll.* doi:10.1016/j.foodhyd.2019.04.021.
- Ghanbari, A., Tabarsa, T., Ashori, A., Shakeri, A., and Mashkour, M. (2018). Preparation and characterization of thermoplastic starch and cellulose nanofibers as green nanocomposites: Extrusion processing. *Int. J. Biol. Macromol.* doi:10.1016/j.ijbiomac.2018.02.007.
- Giannelis, E. P., Krishnamoorti, R., and Manias, E. (1999). Polymer-silicate nanocomposites: Model systems for confined polymers and polymer brushes. *Adv. Polym. Sci.* 138, 108–147.
- Giudici, P., De Vero, L., Gullo, M., Solieri, L., and Lemmetti, F. (2016). Fermentation strategy to produce high gluconate vinegar. *Acetic Acid Bact.* 5. doi:10.4081/aab.2016.6067.
- Giudici, P., Gullo, M., and Solieri, L. (2009a). “Traditional balsamic vinegar,” in *Vinegars of the World* (Springer Milan), 157–177. doi:10.1007/978-88-470-0866-3\_10.
- Gómez-Guillén, M. C., Pérez-Mateos, M., Gómez-Estaca, J., López-Caballero, E., Giménez, B., and Montero, P. (2009). Fish gelatin: a renewable material for developing active biodegradable films. *Trends Food Sci. Technol.* doi:10.1016/j.tifs.2008.10.002.
- Gonzalez, J. S., Ludueña, L. N., Ponce, A., and Alvarez, V. A. (2014). Poly(vinyl alcohol)/cellulose nanowhiskers nanocomposite hydrogels for potential wound dressings. *Mater. Sci. Eng. C* 34, 54–61. doi:10.1016/j.msec.2013.10.006.
- Gullo, M., Caggia, C., De Vero, L., and Giudici, P. (2006). Characterization of acetic acid bacteria in “traditional balsamic vinegar.” *Int. J. Food Microbiol.* 106, 209–212. doi:10.1016/j.ijfoodmicro.2005.06.024.
- Gullo, M., De Vero, L., and Giudici, P. (2009). Succession of selected strains of *Acetobacter pasteurianus* and other acetic acid bacteria in traditional balsamic vinegar. *Appl. Environ. Microbiol.* doi:10.1128/AEM.02249-08.
- Gullo, M., and Giudici, P. (2008). Acetic acid bacteria in traditional balsamic vinegar: Phenotypic traits relevant for starter cultures selection. *Int. J. Food Microbiol.* 125, 46–53. doi:10.1016/j.ijfoodmicro.2007.11.076.
- Gullo, M., la China, S., Falcone, P. M. P. M., and Giudici, P. (2018). Biotechnological production of cellulose by acetic acid bacteria: current state and perspectives. *Appl. Microbiol. Biotechnol.* 102, 1–14. doi:10.1007/s00253-018-9164-5.
- Gullo, M., La China, S., Petroni, G., Di Gregorio, S., and Giudici, P. (2019). Exploring K2G30 genome: A high bacterial cellulose producing strain in glucose and mannitol based media. *Front. Microbiol.* 10, 1–12. doi:10.3389/fmicb.2019.00058.
- Gullo, M., Mamlouk, D., De Vero, L., and Giudici, P. (2012). *Acetobacter pasteurianus* strain AB0220: Cultivability and phenotypic stability over 9 years of preservation. *Curr. Microbiol.* 64, 576–580. doi:10.1007/s00284-012-0112-9.

- Gullo, M., Sola, A., Zanichelli, G., Montorsi, M., Messori, M., and Giudici, P. (2017). Increased production of bacterial cellulose as starting point for scaled-up applications. *Appl. Microbiol. Biotechnol.* 101, 8115–8127. doi:10.1007/s00253-017-8539-3.
- Gullo, M., Verzelloni, E., and Canonico, M. (2014). Aerobic submerged fermentation by acetic acid bacteria for vinegar production: Process and biotechnological aspects. Elsevier doi:10.1016/j.procbio.2014.07.003.
- Gullo, M., Zanichelli, G., Verzelloni, E., Lemmetti, F., and Giudici, P. (2016). Feasible acetic acid fermentations of alcoholic and sugary substrates in combined operation mode. *Process Biochem.* 51, 1129–1139. doi:10.1016/j.procbio.2016.05.018.
- Gupta, P., and Diwan, B. (2017). Bacterial exopolysaccharide mediated heavy metal removal: A Review on biosynthesis, mechanism and remediation strategies. *Biotechnol. Reports* 13, 58–71. doi:10.1016/J.BTRE.2016.12.006.
- Gurevich, A., Saveliev, V., Vyahhi, N., and Tesler, G. (2013). QUASt: quality assessment tool for genome assemblies. *Bioinformatics* 29, 1072–1075. doi:10.1093/bioinformatics/btt086.
- Gusev, A. A., and Lusti, H. (2001). Rational design of nanocomposites for barrier applications. *Adv. Mater. - ADVAN MATER* 13, 1641–1643. doi:10.1002/1521-4095(200111)13:213.0.CO;2-P.
- Gutleben, J., Chaib De Mares, M., van Elsas, J. D., Smidt, H., Overmann, J., and Sipkema, D. (2018). The multi-omics promise in context: from sequence to microbial isolate. *Crit. Rev. Microbiol.* 44, 212–229. doi:10.1080/1040841X.2017.1332003.
- Habibi, Y., Lucia, L. A., and Rojas, O. J. (2010). Cellulose nanocrystals: Chemistry, self-assembly, and applications. *Chem. Rev.* doi:10.1021/cr900339w.
- Haghighi, H., Biard, S., Bigi, F., De Leo, R., Bedin, E., Pfeifer, F., et al. (2019a). Comprehensive characterization of active chitosan-gelatin blend films enriched with different essential oils. *Food Hydrocoll.* doi:10.1016/j.foodhyd.2019.04.019.
- Haghighi, H., De Leo, R., Bedin, E., Pfeifer, F., Siesler, H. W., and Pulvirenti, A. (2019b). Comparative analysis of blend and bilayer films based on chitosan and gelatin enriched with LAE (lauroyl arginate ethyl) with antimicrobial activity for food packaging applications. *Food Packag. Shelf Life.* doi:10.1016/j.fpsl.2018.11.015.
- Haghighi, H., Gullo, M., La China, S., Pfeifer, F., Siesler, H. W., Licciardello, F., et al. (2020a). Characterization of bio-nanocomposite films based on gelatin/polyvinyl alcohol blend reinforced with bacterial cellulose nanowhiskers for food packaging applications. *Food Hydrocoll.*, 106454. doi:10.1016/j.foodhyd.2020.106454.
- Haghighi, H., Leugoue, S. K., Pfeifer, F., Siesler, H. W., Licciardello, F., Fava, P., et al. (2020b). Development of antimicrobial films based on chitosan-polyvinyl alcohol blend enriched with ethyl lauroyl arginate (LAE) for food packaging applications. *Food Hydrocoll.* doi:10.1016/j.foodhyd.2019.105419.
- Haghighi, H., Licciardello, F., Fava, P., Siesler, H. W., and Pulvirenti, A. (2020c). Recent advances on chitosan-based films for sustainable food packaging applications. *Food Packag. Shelf Life.*

doi:10.1016/j.fpsl.2020.100551.

- Han, Y. W., and Clarke, M. A. (1990). Production and characterization of microbial Levan. *J. Agric. Food Chem.* doi:10.1021/jf00092a011.
- Harrell, F.E., Jr.; Dupont, M.C. R Package Hmisc R Foundation for Statistical Computing, Vienna, Austria, 2014. CRAN <https://CRAN.R-project.org/package=Hmisc>. (Accessed on 03 Feb 2020)
- Hekmat, D., Bauer, R., and Fricke, J. (2003). Optimization of the microbial synthesis of dihydroxyacetone from glycerol with *Gluconobacter oxydans*. *Bioprocess Biosyst. Eng.* doi:10.1007/s00449-003-0338-9.
- Hermann, U., Merfort, M., Jeude, M., Bringer-Meyer, S., and Sahm, H. (2004). Biotransformation of glucose to 5-keto-D-gluconic acid by recombinant *Gluconobacter oxydans* DSM 2343. *Appl. Microbiol. Biotechnol.* 64, 86–90. doi:10.1007/s00253-003-1455-8.
- Hestrin, S., and Schramm, M. (1954). Synthesis of cellulose by *Acetobacter xylinum*. II. Preparation of freeze-dried cells capable of polymerizing glucose to cellulose. *Biochem. J.* 58, 345–352. doi:10.1042/bj0580345.
- Hidalgo, C., Vegas, C., Mateo, E., Tesfaye, W., Cerezo, A. B., Callejón, R. M., et al. (2010). Effect of barrel design and the inoculation of *Acetobacter pasteurianus* in wine vinegar production. *Int. J. Food Microbiol.* doi:10.1016/j.ijfoodmicro.2010.04.018.
- Hollensteiner, J., Poehlein, A., Kloskowski, P., Ali, T. T., and Daniel, R. (2020). Genome Sequence of *Komagataeibacter saccharivorans* strain JH1, isolated from fruit flies. *Microbiol. Resour. Announc.* 9. doi:10.1128/mra.00098-20.
- Hoshino, T., Sugisawa, T., Tazoe, M., Shinjoh, M., and Fujiwara, A. (1990). Metabolic pathway for 2-Keto-L-gulonic acid formation in *Gluconobacter melanogenus* IFO 3293. *Agric. Biol. Chem.* doi:10.1271/bbb1961.54.1211.
- Hosseini, S. F., Rezaei, M., Zandi, M., and Farahmandghavi, F. (2015). Fabrication of bio-nanocomposite films based on fish gelatin reinforced with chitosan nanoparticles. *Food Hydrocoll.* doi:10.1016/j.foodhyd.2014.09.004.
- Hu, S.-Q. S.-Q., Gao, Y.-G. Y.-G., Tajima, K., Sunagawa, N., Zhou, Y., Kawano, S., et al. (2010). Structure of bacterial cellulose synthase subunit D octamer with four inner passageways. *Proc. Natl. Acad. Sci.* 107, 17957–17961. doi:10.1073/pnas.1000601107.
- Huerta-Cepas, J., Forslund, K., Coelho, L. P., Szklarczyk, D., Jensen, L. J., von Mering, C., et al. (2017). Fast genome-wide functional annotation through orthology assignment by eggNOG-Mapper. *Mol. Biol. Evol.* 34, 2115–2122. doi:10.1093/molbev/msx148.
- Hunter, P. R., and Gaston, M. A. (1988). Numerical index of the discriminatory ability of typing systems: An application of Simpson's index of diversity. *J. Clin. Microbiol.* 26, 2465–2466. doi:10.1128/jcm.26.11.2465-2466.1988.
- Huq, T., Salmieri, S., Khan, A., Khan, R. A., Le Tien, C., Riedl, B., et al. (2012). Nanocrystalline cellulose (NCC) reinforced alginate based biodegradable nanocomposite film. *Carbohydr. Polym.* doi:10.1016/j.carbpol.2012.07.065.

- Hwang, J. W., Yang, Y. K., Hwang, J. K., Pyun, Y. R., and Kim, Y. S. (1999). Effects of pH and dissolved oxygen on cellulose production by *Acetobacter xylinum* BRC5 in agitated culture. *J. Biosci. Bioeng.* doi:10.1016/S1389-1723(99)80199-6.
- Hyatt, D., Chen, G.-L., Locascio, P. F., Land, M. L., Larimer, F. W., and Hauser, L. J. (2010). Prodigal: prokaryotic gene recognition and translation initiation site identification. *BMC Bioinformatics* 11, 119. doi:10.1186/1471-2105-11-119.
- Iguchi, M., Yamanaka, S., and Budhiono, A. (2000). Bacterial cellulose - a masterpiece of nature's arts. *J. Mater. Sci.* 35, 261–270. doi:10.1023/A:1004775229149.
- Iida, A., Ohnishi, Y., and Horinouchi, S. (2008). Control of acetic acid fermentation by quorum sensing via N-acylhomoserine lactones in *Gluconacetobacter intermedius*. *J. Bacteriol.* 190, 2546–55. doi:10.1128/JB.01698-07.
- Islam, M. U., Ullah, M. W., Khan, S., Shah, N., and Park, J. K. (2017). Strategies for cost-effective and enhanced production of bacterial cellulose. *Int. J. Biol. Macromol.* 102, 1166–1173. doi:10.1016/J.IJBIOMAC.2017.04.110.
- Iwata, T., Indrarti, L., and Azuma, J. I. (1998). Affinity of hemicellulose for cellulose produced by *Acetobacter xylinum*. *Cellulose* 5, 215–228. doi:10.1023/A:1009237401548.
- Iyer, P. R., Geib, S. M., Catchmark, J., Kao, T. -h., and Tien, M. (2010). Genome sequence of a cellulose-producing bacterium, *Gluconacetobacter hansenii* ATCC 23769. *J. Bacteriol.* 192, 4256–4257. doi:10.1128/JB.00588-10.
- Jahn, C. E., Selimi, D. A., Barak, J. D., and Charkowski, A. O. (2011). The *Dickeya dadantii* biofilm matrix consists of cellulose nanofibres, and is an emergent property dependent upon the type III secretion system and the cellulose synthesis operon. *Microbiology* 157, 2733–2744. doi:10.1099/mic.0.051003-0.
- Jakmuangpak, S., Prada, T., Mongkolthananuk, W., Harnchana, V., and Pinitsoontorn, S. (2020). Engineering bacterial cellulose films by nanocomposite approach and surface modification for biocompatible triboelectric nanogenerator. *ACS Appl. Electron. Mater.* 2, 2498–2506. doi:10.1021/acsaelm.0c00421.
- Jakob, F., Meißner, D., and Vogel, R. F. (2012a). Comparison of novel GH 68 levansucrases of levan-overproducing *Gluconobacter* species. *Acetic Acid Bact.* doi:10.4081/aab.2012.e2.
- Jakob, F., Pfaff, A., Novoa-Carballal, R., Rübsam, H., Becker, T., and Vogel, R. F. (2013). Structural analysis of fructans produced by acetic acid bacteria reveals a relation to hydrocolloid function. *Carbohydr. Polym.* doi:10.1016/j.carbpol.2012.10.054.
- Jakob, F., Steger, S., and Vogel, R. F. (2012b). Influence of novel fructans produced by selected acetic acid bacteria on the volume and texture of wheat breads. *Eur. Food Res. Technol.* 234, 493–499. doi:10.1007/s00217-011-1658-7.
- Jang, W. D., Kim, T. Y., Kim, H. U., Shim, W. Y., Ryu, J. Y., Park, J. H., et al. (2019). Genomic and metabolic analysis of *Komagataeibacter xylinus* DSM 2325 producing bacterial cellulose nanofiber. *Biotechnol. Bioeng.* 116, 3372–3381. doi:10.1002/bit.27150.

- Jayabalan, R., Marimuthu, S., and Swaminathan, K. (2007). Changes in content of organic acids and tea polyphenols during kombucha tea fermentation. *Food Chem.* 102, 392–398. doi:10.1016/j.foodchem.2006.05.032.
- Jiménez-Hornero, J. E., Santos-Dueñas, I. M., and García-García, I. (2009). Optimization of biotechnological processes. The acetic acid fermentation. Part I: The proposed model. *Biochem. Eng. J.* doi:10.1016/j.bej.2009.01.009.
- Jipa, I. M., Stoica-Guzun, A., and Stroescu, M. (2012). Controlled release of sorbic acid from bacterial cellulose based mono and multilayer antimicrobial films. *LWT - Food Sci. Technol.* 47, 400–406. doi:10.1016/J.LWT.2012.01.039.
- Jonas, R., and Farah, L. F. (1998). Production and application of microbial cellulose. *Polym. Degrad. Stab.* 59, 101–106. doi:10.1016/S0141-3910(97)00197-3.
- Jung, J. Y., Park, J. K., and Chang, H. N. (2005). Bacterial cellulose production by *Gluconacetobacter hansenii* in an agitated culture without living non-cellulose producing cells. *Enzyme Microb. Technol.* 37, 347–354. doi:10.1016/J.ENZMICTEC.2005.02.019.
- Kamiński, K., Jarosz, M., Grudzień, J., Pawlik, J., Zastawnik, F., Pandyra, P., et al. (2020). Hydrogel bacterial cellulose: a path to improved materials for new eco-friendly textiles. *Cellulose* 27, 5353–5365. doi:10.1007/s10570-020-03128-3.
- Kanatt, S. R., Jethwa, T., Sawant, K., and Chawla, S. P. (2017). PVA-gelatin films incorporated with tomato pulp: A potential primary food packaging film. *Int.J.Curr.Microbiol.App.Sci* 6, 1428–1441. doi:10.20546/ijcmas.2017.610.169.
- Kanatt, S. R., Rao, M. S., Chawla, S. P., and Sharma, A. (2012). Active chitosan-polyvinyl alcohol films with natural extracts. *Food Hydrocoll.* doi:10.1016/j.foodhyd.2012.03.005.
- Kariminejad, M., Sadeghi, E., Rouhi, M., Mohammadi, R., Askari, F., Taghizadeh, M., et al. (2018). The effect of nano-SiO<sub>2</sub> on the physicochemical and structural properties of gelatin-polyvinyl alcohol composite films. *J. Food Process Eng.* doi:10.1111/jfpe.12817.
- Kawano, S., Tajima, K., Uemori, Y., Yamashita, H., Erata, T., Munekata, M., et al. (2002). Cloning of cellulose synthesis related genes from *Acetobacter xylinum* ATCC23769 and ATCC53582: Comparison of cellulose synthetic ability between strains. *DNA Res.* 9, 149–156. doi:10.1093/dnares/9.5.149.
- Keiski, C. L., Harwich, M., Jain, S., Neculai, A. M., Yip, P., Robinson, H., et al. (2010). AlgK is a TPR-containing protein and the periplasmic component of a novel exopolysaccharide secretin. *Structure* 18, 265–273. doi:10.1016/j.str.2009.11.015.
- Keshk, S. M. (2014). Bacterial cellulose production and its industrial applications. *J. Bioprocess. Biotech.* 04. doi:10.4172/2155-9821.1000150.
- Khan, A., Khan, R. A., Salmieri, S., Le Tien, C., Riedl, B., Bouchard, J., et al. (2012). Mechanical and barrier properties of nanocrystalline cellulose reinforced chitosan based nanocomposite films. *Carbohydr. Polym.* doi:10.1016/j.carbpol.2012.07.037.
- Khan, S., Ul-Islam, M., Khattak, W. A., Ullah, M. W., and Park, J. K. (2015). Bacterial cellulose-

- titanium dioxide nanocomposites: nanostructural characteristics, antibacterial mechanism, and biocompatibility. *Cellulose* 22, 565–579. doi:10.1007/s10570-014-0528-4.
- Kittelmann, M., Stamm, W., Follmann, H., and Tröper, H. (1989). Isolation and classification of acetic acid bacteria from high percentage vinegar fermentations. *Appl. Microbiol. Biotechnol.* 30, 47–52. doi:10.1007/BF00255995.
- Kondo, T. (2007). “Nematic ordered cellulose: Its Structure and properties,” in *Cellulose: Molecular and Structural Biology* (Dordrecht: Springer Netherlands), 285–305. doi:10.1007/978-1-4020-5380-1\_16.
- Konstantinidis, K. T., and Tiedje, J. M. (2005). Genomic insights that advance the species definition for prokaryotes. *Proc. Natl. Acad. Sci. U. S. A.* 102, 2567–72. doi:10.1073/pnas.0409727102.
- Koyama, M., Helbert, W., Imai, T., Sugiyama, J., and Henrissat, B. (1997). Parallel-up structure evidences the molecular directionality during biosynthesis of bacterial cellulose. *Proc. Natl. Acad. Sci. U. S. A.* 94, 9091–9095. doi:10.1073/pnas.94.17.9091.
- Krystynowicz, A., Czaja, W., Wiktorowska-Jezierska, A., Gonçalves-Miśkiewicz, M., Turkiewicz, M., and Bielecki, S. (2002). Factors affecting the yield and properties of bacterial cellulose. *J. Ind. Microbiol. Biotechnol.* doi:10.1038/sj.jim.7000303.
- Krzywinski, M., Schein, J., Birol, I., Connors, J., Gascoyne, R., Horsman, D., et al. (2009). Circos: An information aesthetic for comparative genomics. *Genome Res.* 19, 1639–1645. doi:10.1101/gr.092759.109.
- Ku, H., Wang, H., Pattarachaiyakoop, N., and Trada, M. (2011). A review on the tensile properties of natural fiber reinforced polymer composites. *Compos. Part B Eng.* 42, 856–873. doi:10.1016/j.compositesb.2011.01.010.
- Kubiak, K., Kurzawa, M., Jędrzejczak-Krzepkowska, M., Ludwicka, K., Krawczyk, M., Migdalski, A., et al. (2014). Complete genome sequence of *Gluconacetobacter xylinus* E25 strain-Valuable and effective producer of bacterial nanocellulose. *J. Biotechnol.* 176, 18–19. doi:10.1016/j.jbiotec.2014.02.006.
- Kumar, S., Stecher, G., Li, M., Knyaz, C., and Tamura, K. (2018). MEGA X: Molecular Evolutionary Genetics Analysis across computing platforms. *Mol. Biol. Evol.* 35, 1547–1549. doi:10.1093/molbev/msy096.
- Kuo, C.-H. H., Teng, H.-Y. Y., and Lee, C.-K. K. (2015). Knock-out of glucose dehydrogenase gene in *Gluconacetobacter xylinus* for bacterial cellulose production enhancement. *Biotechnol. Bioprocess Eng.* 20, 18–25. doi:10.1007/s12257-014-0316-x.
- Kuo, C. H., Chen, J. H., Liou, B. K., and Lee, C. K. (2016). Utilization of acetate buffer to improve bacterial cellulose production by *Gluconacetobacter xylinus*. *Food Hydrocoll.* doi:10.1016/j.foodhyd.2014.12.034.
- Kuo, C. H., Lin, P. J., and Lee, C. K. (2010). Enzymatic saccharification of dissolution pretreated waste cellulosic fabrics for bacterial cellulose production by *Gluconacetobacter xylinus*. *J. Chem. Technol. Biotechnol.* doi:10.1002/jctb.2439.



- La China, S., Bezzecchi, A., Moya, F., Petroni, G., Di Gregorio, S., and Gullo, M. (2020). Genome sequencing and phylogenetic analysis of K1G4: a new *Komagataeibacter* strain producing bacterial cellulose from different carbon sources. *Biotechnol. Lett.* 42, 807–818. doi:10.1007/s10529-020-02811-6.
- La China, S., Zanichelli, G., De Vero, L., and Gullo, M. (2018). Oxidative fermentations and exopolysaccharides production by acetic acid bacteria: a mini review. doi:10.1007/s10529-018-2591-7.
- Lagesen, K., Hallin, P., Rødland, E. A., Staerfeldt, H.-H., Rognes, T., and Ussery, D. W. (2007). RNAMmer: consistent and rapid annotation of ribosomal RNA genes. *Nucleic Acids Res.* 35, 3100–8. doi:10.1093/nar/gkm160.
- Lairson, L. L., Henrissat, B., Davies, G. J., and Withers, S. G. (2008). Glycosyltransferases: Structures, functions, and mechanisms. *Annu. Rev. Biochem.* 77, 521–555. doi:10.1146/annurev.biochem.76.061005.092322.
- Laureys, D., Britton, S. J., and De Clippeleer, J. (2020). Kombucha Tea fermentation: A review. *J. Am. Soc. Brew. Chem.* 78, 165–174. doi:10.1080/03610470.2020.1734150.
- Lee, H. Y., Lee, S. H., Lee, J. H., Lee, W. J., and Min, K. J. (2019). The role of commensal microbes in the lifespan of *Drosophila melanogaster*. *Aging (Albany, NY)*. doi:10.18632/aging.102073.
- Lee, K. Y., Quero, F., Blaker, J. J., Hill, C. A. S., Eichhorn, S. J., and Bismarck, A. (2011). Surface only modification of bacterial cellulose nanofibres with organic acids. *Cellulose*. doi:10.1007/s10570-011-9525-z.
- Li, F., Biagioni, P., Bollani, M., Maccagnan, A., and Piergiovanni, L. (2013). Multi-functional coating of cellulose nanocrystals for flexible packaging applications. *Cellulose*. doi:10.1007/s10570-013-0015-3.
- Li, F., Mascheroni, E., and Piergiovanni, L. (2015a). The potential of nanocellulose in the packaging field: A review. *Packag. Technol. Sci.* 28, 475–508. doi:10.1002/pts.2121.
- Li, F., Wang, G., Wang, P., Yang, J., Zhang, K., Liu, Y., et al. (2017a). High-performance lithium-sulfur batteries with a carbonized bacterial cellulose/TiO<sub>2</sub> modified separator. *J. Electroanal. Chem.* 788, 150–155. doi:10.1016/j.jelechem.2016.11.058.
- Li, G., Nandgaonkar, A. G., Wang, Q., Zhang, J., Krause, W. E., Wei, Q., et al. (2017b). Laccase-immobilized bacterial cellulose/TiO<sub>2</sub>functionalized composite membranes: Evaluation for photo- and bio-catalytic dye degradation. *J. Memb. Sci.* 525, 89–98. doi:10.1016/j.memsci.2016.10.033.
- Li, H.-Z., Chen, S.-C., and Wang, Y.-Z. (2015b). Preparation and characterization of nanocomposites of polyvinyl alcohol/cellulose nanowhiskers/chitosan. *Compos. Sci. Technol.* 115, 60–65. doi:10.1016/j.compscitech.2015.05.004.
- Li, M. hua, Wu, J., Liu, X., Lin, J. ping, Wei, D. zhi, and Chen, H. (2010). Enhanced production of dihydroxyacetone from glycerol by overexpression of glycerol dehydrogenase in an alcohol dehydrogenase-deficient mutant of *Gluconobacter oxydans*. *Bioresour. Technol.*

doi:10.1016/j.biortech.2010.05.065.

- Li, Y., Tian, C., Tian, H., Zhang, J., He, X., Ping, W., et al. (2012). Improvement of bacterial cellulose production by manipulating the metabolic pathways in which ethanol and sodium citrate involved. *Appl. Microbiol. Biotechnol.* 96, 1479–1487. doi:10.1007/s00253-012-4242-6.
- Iino, T., Suzuki, R., Kosako, Y., Ohkuma, M., Komagata, K., and Uchimura, T. (2012). *Acetobacter okinawensis* sp. nov., *Acetobacter papayae* sp. nov., and *Acetobacter persicus* sp. nov.; novel acetic acid bacteria isolated from stems of sugarcane, fruits, and a flower in Japan. *J. Gen. Appl. Microbiol.* 58, 235–243. doi:10.2323/jgam.58.235.
- Lisdiyanti, P., Kawasaki, H., Seki, T., Yamada, Y., Uchimura, T., and Komagata, K. (2000). Systematic study of the genus *Acetobacter* with descriptions of *Acetobacter indonesiensis* sp. nov., *Acetobacter tropicalis* sp. nov., *Acetobacter orleanensis* (Henneberg 1906) comb. nov., *Acetobacter lovaniensis* (Frateur 1950) comb. nov., and *Acetobacter estunensis* (Carr 1958) comb. nov. *J. Gen. Appl. Microbiol.* 46, 147–165. doi:10.2323/jgam.46.147.
- Lisdiyanti, P., Navarro, R. R., Uchimura, T., and Komagata, K. (2006). Reclassification of *Gluconacetobacter hansenii* strains and proposals of *Gluconacetobacter saccharivorans* sp. nov. and *Gluconacetobacter nataicola* sp. nov. *Int. J. Syst. Evol. Microbiol.* doi:10.1099/ijs.0.63252-0.
- Liu, M., Liu, L., Jia, S., Li, S., Zou, Y., and Zhong, C. (2018). Complete genome analysis of *Gluconacetobacter xylinus* CGMCC 2955 for elucidating bacterial cellulose biosynthesis and metabolic regulation. *Sci. Rep.* 8, 6266. doi:10.1038/s41598-018-24559-w.
- Lowe, T. M., and Eddy, S. R. (1997). tRNAscan-SE: A Program for Improved Detection of Transfer RNA Genes in Genomic Sequence. *Nucleic Acids Res.* doi:10.1093/nar/25.5.955.
- Lu, H., Jia, Q., Chen, L., and Zhang, L. (2015). Effect of organic acids on bacterial cellulose produced by *Acetobacter xylinum*. *J. Microbiol. Biotechnol.*
- Lu, L., Wei, L., Zhu, K., Wei, D., and Hua, Q. (2012). Combining metabolic engineering and adaptive evolution to enhance the production of dihydroxyacetone from glycerol by *Gluconobacter oxydans* in a low-cost way. *Bioresour. Technol.* doi:10.1016/j.biortech.2012.03.013.
- Ludwig, W., and Klenk, H. (2015). “Overview: A phylogenetic backbone and taxonomic framework for procaryotic systematics,” in *Bergey’s Manual of Systematics of Archaea and Bacteria* doi:10.1002/9781118960608.bm00020.
- Luo, M. T., Huang, C., Li, H. L., Guo, H. J., Chen, X. F., Xiong, L., et al. (2019). Bacterial cellulose based superabsorbent production: A promising example for high value-added utilization of clay and biology resources. *Carbohydr. Polym.* 208, 421–430. doi:10.1016/j.carbpol.2018.12.084.
- Lux, S., and Siebenhofer, M. (2013). Synthesis of lactic acid from dihydroxyacetone: Use of alkaline-earth metal hydroxides. *Catal. Sci. Technol.* doi:10.1039/c3cy20859a.
- Luzi, F., Fortunati, E., Giovanale, G., Mazzaglia, A., Torre, L., and Balestra, G. M. (2017). Cellulose nanocrystals from *Actinidia deliciosa* pruning residues combined with carvacrol in PVA\_CH

- films with antioxidant/antimicrobial properties for packaging applications. *Int. J. Biol. Macromol.* doi:10.1016/j.ijbiomac.2017.05.176.
- Macauley, S., McNeil, B., and Harvey, L. M. (2001). The genus *Gluconobacter* and its applications in biotechnology. *Crit. Rev. Biotechnol.* doi:10.1080/20013891081665.
- Mamlouk, D. (2012). Insight into Physiology and Functionality of Acetic Acid Bacteria Through a Multiphasic Approach. Dissertation, University of Modena and Reggio Emilia, Modena.
- Mamlouk, D., and Gullo, M. (2013). Acetic acid bacteria: Physiology and carbon sources oxidation. Springer doi:10.1007/s12088-013-0414-z.
- Mansur, H. S., Oréface, R. L., and Mansur, A. A. P. (2004). Characterization of poly(vinyl alcohol)/poly(ethylene glycol) hydrogels and PVA-derived hybrids by small-angle X-ray scattering and FTIR spectroscopy. *Polymer (Guildf)*. 45, 7193–7202. doi:10.1016/j.polymer.2004.08.036.
- Marins, J. A., Soares, B. G., Dahmouche, K., Ribeiro, S. J. L., Barud, H., and Bonemer, D. (2011). Structure and properties of conducting bacterial cellulose-polyaniline nanocomposites. *Cellulose*. doi:10.1007/s10570-011-9565-4.
- Martins, D., de Carvalho Ferreira, D., Gama, M., and Dourado, F. (2020). Dry bacterial cellulose and carboxymethyl cellulose formulations with interfacial-active performance: processing conditions and redispersion. *Cellulose* 27, 6505–6520. doi:10.1007/s10570-020-03211-9.
- Mas, A., Torija, M. J., García-Parrilla, M. D. C., and Troncoso, A. M. (2014). Acetic acid bacteria and the production and quality of wine vinegar. *Sci. World J.* doi:10.1155/2014/394671.
- Matsushita, K., Fujii, Y., Ano, Y., Toyama, H., Shinjoh, M., Tomiyama, N., et al. (2003). 5-keto-D-gluconate production is catalyzed by a quinoprotein glycerol dehydrogenase, major polyol dehydrogenase, in *Gluconobacter* species. *Appl. Environ. Microbiol.* 69, 1959–66. doi:10.1128/AEM.69.4.1959-1966.2003.
- Matsushita, K., Toyama, H., and Adachi, O. (1994). Respiratory chains and bioenergetics of acetic acid bacteria. *Adv. Microb. Physiol.* doi:10.1016/s0065-2911(08)60181-2.
- Matsutani, M., Ito, K., Azuma, Y., Ogino, H., Shirai, M., Yakushi, T., et al. (2015). Adaptive mutation related to cellulose producibility in *Komagataeibacter medellinensis* (*Gluconacetobacter xylinus*) NBRC 3288. *Appl. Microbiol. Biotechnol.* 99, 7229–7240. doi:10.1007/s00253-015-6598-x.
- Matsutani, M., Nishikura, M., Saichana, N., Hatano, T., Masud-Tippayasak, U., Theergool, G., et al. (2013). Adaptive mutation of *Acetobacter pasteurianus* SKU1108 enhances acetic acid fermentation ability at high temperature. *J. Biotechnol.* doi:10.1016/j.jbiotec.2013.03.006.
- Matthysse, A. G., Marry, M., Krall, L., Kaye, M., Ramey, B. E., Fuqua, C., et al. (2005). The effect of cellulose overproduction on binding and biofilm formation on roots by *Agrobacterium tumefaciens*. *Mol. Plant-Microbe Interact.* 18, 1002–1010. doi:10.1094/MPMI-18-1002.
- McDougald, D., Rice, S. A., Barraud, N., Steinberg, P. D., and Kjelleberg, S. (2012). Should we stay or should we go: mechanisms and ecological consequences for biofilm dispersal. *Nat. Rev.*

- Microbiol.* 10, 39–50. doi:10.1038/nrmicro2695.
- McGinnis, S., and Madden, T. L. (2004). BLAST: at the core of a powerful and diverse set of sequence analysis tools. *Nucleic Acids Res.* 32, W20–W25. doi:10.1093/nar/gkh435.
- McNamara, J. T., Morgan, J. L. W., and Zimmer, J. (2015). A molecular description of cellulose biosynthesis. *Annu. Rev. Biochem.* 84, 895–921. doi:10.1146/annurev-biochem-060614-033930.
- Mehta, K., Pfeffer, S., and Brown, R. M. (2015). Characterization of an *acsD* disruption mutant provides additional evidence for the hierarchical cell-directed self-assembly of cellulose in *Gluconacetobacter xylinus*. *Cellulose* 22, 119–137. doi:10.1007/s10570-014-0521-y.
- Méndez-Lorenzo, L., Porras-Domínguez, J. R., Raga-Carbajal, E., Olvera, C., Rodríguez-Alegría, M. E., Carrillo-Nava, E., et al. (2015). Intrinsic levanase activity of *Bacillus subtilis* 168 levansucrase (SacB). *PLoS One*. doi:10.1371/journal.pone.0143394.
- Méndez, C., and Salas, J. A. (2001). The role of ABC transporters in antibiotic-producing organisms: Drug secretion and resistance mechanisms. *Res. Microbiol.* doi:10.1016/S0923-2508(01)01205-0.
- Mendieta-Taboada, O., Sobral, P. J. do A., Carvalho, R. A., and Habitante, A. M. B. Q. (2008). Thermomechanical properties of biodegradable films based on blends of gelatin and poly(vinyl alcohol). *Food Hydrocoll.* doi:10.1016/j.foodhyd.2007.10.001.
- Merfort, M., Herrmann, U., Bringer-Meyer, S., and Sahm, H. (2006). High-yield 5-keto-D-gluconic acid formation is mediated by soluble and membrane-bound gluconate-5-dehydrogenases of *Gluconobacter oxydans*. *Appl. Microbiol. Biotechnol.* doi:10.1007/s00253-006-0467-6.
- Mistry, J., Finn, R. D., Eddy, S. R., Bateman, A., and Punta, M. (2013). Challenges in homology search: HMMER3 and convergent evolution of coiled-coil regions. *Nucleic Acids Res.* 41, e121–e121. doi:10.1093/nar/gkt263.
- Mohite, B. V., and Patil, S. V. (2014). A novel biomaterial: Bacterial cellulose and its new era applications. *Biotechnol. Appl. Biochem.* 61, 101–110. doi:10.1002/bab.1148.
- Monteiro, A. S., Domenegueti, R. R., Wong Chi Man, M., Barud, H. S., Teixeira-Neto, E., and Ribeiro, S. J. L. (2019). Bacterial cellulose–SiO<sub>2</sub>@TiO<sub>2</sub> organic–inorganic hybrid membranes with self-cleaning properties. *J. Sol-Gel Sci. Technol.* 89, 2–11. doi:10.1007/s10971-018-4744-5.
- Morgan, J. L. W. W., Strumillo, J., and Zimmer, J. (2013). Crystallographic snapshot of cellulose synthesis and membrane translocation. *Nature* 493, 181–186. doi:10.1038/nature11744.
- Morris, C. E., and Monier, J. M. (2003). The ecological significance of biofilm formation by plant-Associated bacteria. *Annu. Rev. Phytopathol.* doi:10.1146/annurev.phyto.41.022103.134521.
- Murali, N., Fernandez, S., and Ahring, B. K. (2017). Fermentation of wet-exploded corn stover for the production of volatile fatty acids. *Bioresour. Technol.* doi:10.1016/j.biortech.2016.12.012.
- Mwaikambo, L. Y., and Ansell, M. P. (2001). The determination of porosity and cellulose content of

- plant fibers by density methods. *J. Mater. Sci. Lett.* 20, 2095–2096. doi:10.1023/A:1013703809964.
- Nakai, T., Nishiyama, Y., Kuga, S., Sugano, Y., and Shoda, M. (2002). ORF2 gene involves in the construction of high-order structure of bacterial cellulose. *Biochem. Biophys. Res. Commun.* 295, 458–462. doi:10.1016/S0006-291X(02)00696-4.
- Nakai, T., Sugano, Y., Shoda, M., Sakakibara, H., Oiwa, K., Tuzi, S., et al. (2013). Formation of highly twisted ribbons in a carboxymethylcellulase gene-disrupted strain of a cellulose-producing bacterium. *J. Bacteriol.* 195, 958–964. doi:10.1128/JB.01473-12.
- Narh, C., Frimpong, C., Mensah, A., and Wei, Q. (2018). Rice bran, an alternative nitrogen source for *Acetobacter xylinum* bacterial cellulose synthesis. *BioResources* 13, 4346–4363. doi:10.15376/biores.13.2.4346-4363.
- Ndoye, B., Lebecque, S., Dubois-Dauphin, R., Tounkara, L., Guiro, A. T., Kere, C., et al. (2006). Thermoresistant properties of acetic acids bacteria isolated from tropical products of Sub-Saharan Africa and destined to industrial vinegar. *Enzyme Microb. Technol.* doi:10.1016/j.enzmitec.2006.01.020.
- Ng, C. C., and Shyu, Y. T. (2004). Development and production of cholesterol-lowering *Monascus-nata* complex. *World J. Microbiol. Biotechnol.* 20, 875–879. doi:10.1007/s11274-004-0873-9.
- Nishiyama, Y., Langan, P., and Chanzy, H. (2002). Crystal structure and hydrogen-bonding system in cellulose I $\beta$  from synchrotron X-ray and neutron fiber diffraction. *J. Am. Chem. Soc.* 124, 9074–9082. doi:10.1021/ja0257319.
- Nishiyama, Y., Sugiyama, J., Chanzy, H., and Langan, P. (2003). Crystal structure and hydrogen bonding system in cellulose I $\alpha$  from synchrotron X-ray and neutron fiber diffraction. *J. Am. Chem. Soc.* doi:10.1021/ja037055w.
- Noro, N., Sugano, Y., and Shoda, M. (2004). Utilization of the buffering capacity of corn steep liquor in bacterial cellulose production by *Acetobacter xylinum*. *Appl. Microbiol. Biotechnol.* 64, 199–205. doi:10.1007/s00253-003-1457-6.
- Noshirvani, N., Ghanbarzadeh, B., Fasihi, H., and Almasi, H. (2016). Starch–PVA nanocomposite film incorporated with cellulose nanocrystals and MMT: A comparative Study. *Int. J. Food Eng.* 12, 37–48. doi:10.1515/ijfe-2015-0145.
- Nowell, A. R. M., and Church, M. (1979). Turbulent flow in a depth-limited boundary layer. *J. Geophys. Res.* 84, 4816–4824. doi:10.1029/JC084iC08p04816.
- Ogino, H., Azuma, Y., Hosoyama, A., Nakazawa, H., Matsutani, M., Hasegawa, A., et al. (2011). Complete genome sequence of NBRC 3288, a unique cellulose-nonproducing strain of *Gluconacetobacter xylinus* isolated from vinegar. *J. Bacteriol.* 193, 6997–8. doi:10.1128/JB.06158-11.
- Oikawa, T., Morino, T., and Ameyama, M. (1995a). Production of cellulose from D -Arabitol by *Acetobacter xylinum* KU-1. *Biosci. Biotechnol. Biochem.* 59, 1564–1565. doi:10.1271/bbb.59.1564.

- Oikawa, T., Nakai, J., Tsukagawa, Y., and Soda, K. (1997). A novel type of D-Mannitol dehydrogenase from *Acetobacter xylinum*: Occurrence, purification, and basic properties. *Biosci. Biotechnol. Biochem.* 61, 1778–1782. doi:10.1271/bbb.61.1778.
- Oikawa, T., Ohtori, T., and Ameyama, M. (1995b). Production of cellulose from D-Mannitol by *Acetobacter xylinum* KU-1. *Biosci. Biotechnol. Biochem.* doi:10.1271/bbb.59.331.
- Oikawa, T., Ohtori, T., and Ameyama, M. (1995c). Production of cellulose from D -Mannitol by *Acetobacter xylinum* KU-1. *Biosci. Biotechnol. Biochem.* 59, 331–332. doi:10.1271/bbb.59.331.
- Okamoto-Kainuma Akiko, A., Ishikawa, M., Nakamura, H., Fukazawa, S., Tanaka, N., Yamagami, K., et al. (2011). Characterization of rpoH in *Acetobacter pasteurianus* NBRC3283. *J. Biosci. Bioeng.* doi:10.1016/j.jbiosc.2010.12.016.
- Omadjela, O., Narahari, A., Strumillo, J., Melida, H., Mazur, O., Bulone, V., et al. (2013). BcsA and BcsB form the catalytically active core of bacterial cellulose synthase sufficient for *in vitro* cellulose synthesis. *Proc. Natl. Acad. Sci.* 110, 17856–17861. doi:10.1073/pnas.1314063110.
- Osma, J. F., Toca-Herrera, J. L., and Rodríguez-Couto, S. (2010). Uses of laccases in the food industry. *Enzyme Res.* doi:10.4061/2010/918761.
- Pagliaro, M., Ciriminna, R., Kimura, H., Rossi, M., and Della Pina, C. (2007). From glycerol to value-added products. *Angew. Chemie - Int. Ed.* doi:10.1002/anie.200604694.
- Pappenberger, G., and Hohmann, H. P. (2013). Industrial production of L-Ascorbic acid (Vitamin C) and D-isoascorbic acid. *Adv. Biochem. Eng. Biotechnol.* doi:10.1007/10\_2013\_243.
- Passos da Silva, D., Schofield, M. C., Parsek, M. R., and Tseng, B. S. (2017). An update on the sociomicrobiology of quorum sensing in gram-negative biofilm development. *Pathogens* 6, 51. doi:10.3390/pathogens6040051.
- Pasteur, L. (1864). Mémoire sur la fermentation acétique. *Ann. Sci. l'École Norm. supérieure.* doi:10.24033/asens.4.
- Pavaloiu, R. D., Stroescu, M., and Parvulescu, O. (2014). Composite hydrogels of bacterial cellulose -carboxymethyl cellulose for drug release. *Rev. Chim.* 65, 852–855. doi:10.1016/j.btre.2017.07.002
- Pawde, S. M., and Deshmukh, K. (2008). Characterization of polyvinyl alcohol/gelatin blend hydrogel films for biomedical applications. *J. Appl. Polym. Sci.* 109, 3431–3437. doi:10.1002/app.28454.
- Pereda, M., Dufresne, A., Aranguren, M. I., and Marcovich, N. E. (2014). Polyelectrolyte films based on chitosan/olive oil and reinforced with cellulose nanocrystals. *Carbohydr. Polym.* 101, 1018–1026. doi:10.1016/j.carbpol.2013.10.046.
- Petersen, N., and Gatenholm, P. (2011). Bacterial cellulose-based materials and medical devices: current state and perspectives. *Appl. Microbiol. Biotechnol.* 91, 1277–1286. doi:10.1007/s00253-011-3432-y.
- Pfeffer, S., Mehta, K., Brown, R. M., and Jr. (2016). Complete genome sequence of a

- Gluconacetobacter hansenii* ATCC 23769 isolate, AY201, producer of bacterial cellulose and important model organism for the study of cellulose biosynthesis. *Genome Announc.* 4. doi:10.1128/genomeA.00808-16.
- Philp, J. C., Bartsev, A., Ritchie, R. J., Baucher, M. A., and Guy, K. (2013). Bioplastics science from a policy vantage point. *N. Biotechnol.* doi:10.1016/j.nbt.2012.11.021.
- Picheth, G. F., Pirich, C. L., Sierakowski, M. R., Woehl, M. A., Sakakibara, C. N., de Souza, C. F., et al. (2017). Bacterial cellulose in biomedical applications: A review. *Int. J. Biol. Macromol.* 104, 97–106. doi:10.1016/j.ijbiomac.2017.05.171.
- Pokalwar, S. U., Mishra, M. K., and Manwar, A. V (2010). Pproduction of cellulose by *Gluconoasctobacter* sp. *Recent Res. Sci. Technol.* 2, 14–19. Available at: [www.recent-science.com](http://www.recent-science.com).
- Pothimon, R., Gullo, M., La China, S., Thompson, A. K., and Krusong, W. (2020). Conducting high acetic acid and temperature acetification processes by *Acetobacter pasteurianus* UMCC 2951. *Process Biochem.* 98, 41–50. doi:10.1016/j.procbio.2020.07.022.
- Poverenov, E., Rutenberg, R., Danino, S., Horev, B., and Rodov, V. (2014). Gelatin-Chitosan composite films and edible coatings to enhance the quality of food products: Layer-by-Layer vs. blended formulations. *Food Bioprocess Technol.* 7, 3319–3327. doi:10.1007/s11947-014-1333-7.
- Pritchard, L., Glover, R. H., Humphris, S., Elphinstone, J. G., and Toth, I. K. (2016). Genomics and taxonomy in diagnostics for food security: soft-rotting enterobacterial plant pathogens. *Anal. Methods* 8, 12–24. doi:10.1039/C5AY02550H.
- Qi, Y., Rao, F., Luo, Z., and Liang, Z.-X. (2009). A flavin cofactor-binding PAS domain regulates c-di-GMP synthesis in *Ax* DGC2 from *Acetobacter xylinum*. *Biochemistry* 48, 10275–10285. doi:10.1021/bi901121w.
- Qi, Z., Wang, W., Yang, H., Xia, X., and Yu, X. (2014). Mutation of *Acetobacter pasteurianus* by UV irradiation under acidic stress for high-acidity vinegar fermentation. *Int. J. Food Sci. Technol.* doi:10.1111/ijfs.12324.
- Quinlan, A. R., and Hall, I. M. (2010). BEDTools: A flexible suite of utilities for comparing genomic features. *Bioinformatics.* doi:10.1093/bioinformatics/btq033.
- R Core Team. R: A Language and Environment for Statistical Computing. R Foundation for Statistical Computing: Vienna, Austria, 2017. Available online: <https://www.R-project.org/>. (Accessed on 03 Feb 2020).
- R. Navarro, R., Uchimura, T., and Komagata, K. (1999). Taxonomic heterogeneity of strains comprising *Gluconacetobacter hansenii*. *J. Gen. Appl. Microbiol.* 45, 295–300. doi:10.2323/jgam.45.295.
- Rabin, N., Zheng, Y., Opoku-Temeng, C., Du, Y., Bonsu, E., and Sintim, H. O. (2015). Biofilm formation mechanisms and targets for developing antibiofilm agents. *Future Med. Chem.* 7, 493–512. doi:10.4155/fmc.15.6.

- Radetić, M. (2013). Functionalization of textile materials with TiO<sub>2</sub> nanoparticles. *J. Photochem. Photobiol. C Photochem. Rev.* 16, 62–76. doi:10.1016/j.jphotochemrev.2013.04.002.
- Rairakhwada, D., Pal, A. K., Bhathena, Z. P., Sahu, N. P., Jha, A., and Mukherjee, S. C. (2007). Dietary microbial levan enhances cellular non-specific immunity and survival of common carp (*Cyprinus carpio*) juveniles. *Fish Shellfish Immunol.* doi:10.1016/j.fsi.2006.06.005.
- Rajwade, J. M., Paknikar, K. M., and Kumbhar, J. V. (2015). Applications of bacterial cellulose and its composites in biomedicine. *Appl. Microbiol. Biotechnol.* 99, 2491–2511. doi:10.1007/s00253-015-6426-3.
- Reddy, J. P., and Rhim, J. W. (2014). Characterization of bionanocomposite films prepared with agar and paper-mulberry pulp nanocellulose. *Carbohydr. Polym.* doi:10.1016/j.carbpol.2014.04.056.
- Ren, C., Webster, P., Finkel, S. E., and Tower, J. (2007). Increased internal and external bacterial load during *Drosophila* aging without life-span trade-off. *Cell Metab.* 6, 144–152. doi:10.1016/j.cmet.2007.06.006.
- Rescignano, N., Fortunati, E., Montesano, S., Emiliani, C., Kenny, J. M., Martino, S., et al. (2014). PVA bio-nanocomposites: A new take-off using cellulose nanocrystals and PLGA nanoparticles. *Carbohydr. Polym.* doi:10.1016/j.carbpol.2013.08.061.
- Rezaee, M., Askari, G., EmamDjomeh, Z., and Salami, M. (2018). Effect of organic additives on physiochemical properties and anti-oxidant release from chitosan-gelatin composite films to fatty food simulant. *Int. J. Biol. Macromol.* doi:10.1016/j.ijbiomac.2018.03.122.
- Richter, M., Rosselló-Móra, R., and Rossello-Mora, R. (2009). Shifting the genomic gold standard for the prokaryotic species definition. *Proc. Natl. Acad. Sci.* 106, 19126–19131. doi:10.1073/pnas.0906412106.
- Roberfroid, M. B., Van Loo, J. A. E., and Gibson, G. R. (1998). The bifidogenic nature of chicory inulin and its hydrolysis products. *J. Nutr.* doi:10.1093/jn/128.1.11.
- Robotti, F., Bottan, S., Frascetti, F., Mallone, A., Pellegrini, G., Lindenblatt, N., et al. (2018). A micron-scale surface topography design reducing cell adhesion to implanted materials. *Sci. Rep.* doi:10.1038/s41598-018-29167-2.
- Roehr, M., Kubicek, C. P., and Komínek, J. (2001). “Gluconic Acid,” in *Biotechnology Set* (Wiley), 347–362. doi:10.1002/9783527620999.ch10f.
- Rogers, P., Chen, J. S., and Zidwick, M. J. (2014). “Organic acid and solvent production: Acetic, lactic, gluconic, succinic, and polyhydroxyalkanoic acids,” in *The Prokaryotes: Applied Bacteriology and Biotechnology* (Springer-Verlag Berlin Heidelberg), 3–75. doi:10.1007/978-3-642-31331-8\_23.
- Römling, U. (2002). Molecular biology of cellulose production in bacteria. *Res. Microbiol.* 153, 205–212. doi:10.1016/S0923-2508(02)01316-5.
- Römling, U., and Galperin, M. Y. (2015). Bacterial cellulose biosynthesis: Diversity of operons, subunits, products, and functions. NIH Public Access doi:10.1016/j.tim.2015.05.005.



- Ross, P., Mayer, R., and Benziman, M. (1991). Cellulose biosynthesis and function in bacteria. *Microbiol. Rev.* 55, 35–58. doi:10.1016/j.bbalip.2012.08.009.
- Ross, P., Weinhouse, H., Aloni, Y., Michaeli, D., Weinberger-Ohana, P., Mayer, R., et al. (1987). Regulation of cellulose synthesis in *Acetobacter xylinum* by cyclic diguanylic acid. *Nature* 325, 279–281. doi:10.1038/325279a0.
- Rouhi, M., Razavi, S. H., and Mousavi, S. M. (2017). Optimization of crosslinked poly(vinyl alcohol) nanocomposite films for mechanical properties. *Mater. Sci. Eng. C.* doi:10.1016/j.msec.2016.11.135.
- Rühmkorf, C., Jungkuntz, S., Wagner, M., and Vogel, R. F. (2012). Optimization of homoexopolysaccharide formation by *Lactobacilli* in gluten-free sourdoughs. *Food Microbiol.* doi:10.1016/j.fm.2012.07.002.
- Ruka, D. R., Simon, G. P., and Dean, K. M. (2012). Altering the growth conditions of *Gluconacetobacter xylinus* to maximize the yield of bacterial cellulose. *Carbohydr. Polym.* 89, 613–622. doi:10.1016/j.carbpol.2012.03.059.
- Ryngajłło, M., Kubiak, K., Jędrzejczak-Krzepkowska, M., Jacek, P., and Bielecki, S. (2018). Comparative genomics of the *Komagataeibacter* strains—Efficient bionanocellulose producers. *Microbiologyopen.* doi:10.1002/mbo3.731.
- Saichana, N., Matsushita, K., Adachi, O., Frébort, I., and Frebortova, J. (2015). Acetic acid bacteria: A group of bacteria with versatile biotechnological applications. *Biotechnol. Adv.* doi:10.1016/j.biotechadv.2014.12.001.
- Sainz, F., Jesús Torija, M., Matsutani, M., Kataoka, N., Yakushi, T., Matsushita, K., et al. (2016a). Determination of dehydrogenase activities involved in D-glucose oxidation in *Gluconobacter* and *Acetobacter* strains. *Front. Microbiol.* 7, 1358. doi:10.3389/fmicb.2016.01358.
- Sainz, F., Navarro, D., Mateo, E., Torija, M. J., and Mas, A. (2016b). Comparison of D-gluconic acid production in selected strains of acetic acid bacteria. *Int. J. Food Microbiol.* 222, 40–47. doi:10.1016/j.ijfoodmicro.2016.01.015.
- Saito, Y., Ishii, Y., Hayashi, H., Imao, Y., Akashi, T., Yoshikawa, K., et al. (1997). Cloning of genes coding for L-sorbose and L-sorbosone dehydrogenases from *Gluconobacter oxydans* and microbial production of 2-keto-L-gulonate, a precursor of L-ascorbic acid, in a recombinant *G. oxydans* strain. *Appl. Environ. Microbiol.* doi:10.1128/aem.63.2.454-460.1997.
- Salari, M., Sowti Khiabani, M., Rezaei Mokarram, R., Ghanbarzadeh, B., and Samadi Kafil, H. (2018). Development and evaluation of chitosan based active nanocomposite films containing bacterial cellulose nanocrystals and silver nanoparticles. *Food Hydrocoll.* 84, 414–423. doi:10.1016/j.foodhyd.2018.05.037.
- Santos, T. M., Souza Filho, M. de S. M., Caceres, C. A., Rosa, M. F., Morais, J. P. S., Pinto, A. M. B., et al. (2014). Fish gelatin films as affected by cellulose whiskers and sonication. *Food Hydrocoll.* doi:10.1016/j.foodhyd.2014.04.001.
- Saxena, I. M., and Brown, R. M. (1995). Identification of a second cellulose synthase gene (*acsAII*)

- in *Acetobacter xylinum*. *J. Bacteriol.* 177, 5276–5283. doi:10.1128/jb.177.18.5276-5283.1995.
- Saxena, I. M., Kudlicka, K., Okuda, K., and Brown, R. M. (1994). Characterization of genes in the cellulose-synthesizing operon (acs operon) of *Acetobacter xylinum*: Implications for cellulose crystallization. *J. Bacteriol.* 176, 5735–5752. doi:10.1128/jb.176.18.5735-5752.1994.
- Schaffner, M., Rühs, P. A., Coulter, F., Kilcher, S., and Studart, A. R. (2017). 3D printing of bacteria into functional complex materials. *Sci. Adv.* 3, eaao6804. doi:10.1126/sciadv.aao6804.
- Segal, L., Creely, J. J., Martin, A. E., and Conrad, C. M. (1959). An empirical method for estimating the degree of crystallinity of native cellulose using the X-Ray diffractometer. *Text. Res. J.* doi:10.1177/004051755902901003.
- Sehaqui, H., Salajková, M., Zhou, Q., and Berglund, L. A. (2010). Mechanical performance tailoring of tough ultra-high porosity foams prepared from cellulose i nanofiber suspensions. *Soft Matter* 6, 1824–1832. doi:10.1039/b927505c.
- Semjonovs, P., Ruklisha, M., Paegle, L., Saka, M., Treimane, R., Skute, M., et al. (2017). Cellulose synthesis by *Komagataeibacter rhaeticus* strain P 1463 isolated from Kombucha. *Appl. Microbiol. Biotechnol.* 101, 1003–1012. doi:10.1007/s00253-016-7761-8.
- Sengun, I. Y., and Karabiyikli, S. (2011). Importance of acetic acid bacteria in food industry. *Food Control* 22, 647–656. doi:10.1016/j.foodcont.2010.11.008.
- Seto, A., Saito, Y., Matsushige, M., Kobayashi, H., Sasaki, Y., Tonouchi, N., et al. (2006). Effective cellulose production by a coculture of *Gluconacetobacter xylinus* and *Lactobacillus mali*. *Appl. Microbiol. Biotechnol.* 73, 915–921. doi:10.1007/s00253-006-0515-2.
- Shah, N., Ul-Islam, M., Khattak, W. A., and Park, J. K. (2013). Overview of bacterial cellulose composites: A multipurpose advanced material. *Carbohydr. Polym.* 98, 1585–1598. doi:10.1016/j.carbpol.2013.08.018.
- Shahbazi, M., Rajabzadeh, G., Rafe, A., Ettelaie, R., and Ahmadi, S. J. (2016). The physico-mechanical and structural characteristics of blend film of poly (vinyl alcohol) with biodegradable polymers as affected by disorder-to-order conformational transition. *Food Hydrocoll.* doi:10.1016/j.foodhyd.2016.03.038.
- Shankar, S., and Rhim, J. W. (2016). Preparation of nanocellulose from micro-crystalline cellulose: The effect on the performance and properties of agar-based composite films. *Carbohydr. Polym.* doi:10.1016/j.carbpol.2015.08.082.
- Shaw, T., Winston, M., Rupp, C. J., Klapper, I., and Stoodley, P. (2004). Commonality of elastic relaxation times in biofilms. *Phys. Rev. Lett.* doi:10.1103/PhysRevLett.93.098102.
- Shi, L., Li, K., Zhang, H., Liu, X., Lin, J., and Wei, D. (2014a). Identification of a novel promoter gHp0169 for gene expression in *Gluconobacter oxydans*. *J. Biotechnol.* doi:10.1016/j.jbiotec.2014.01.035.
- Shi, Z., Zhang, Y., Phillips, G. O., and Yang, G. (2014b). Utilization of bacterial cellulose in food. *Food Hydrocoll.* 35, 539–545. doi:10.1016/J.FOODHYD.2013.07.012.

- Shigematsu, T., Takamine, K., Kitazato, M., Morita, T., Naritomi, T., Morimura, S., et al. (2005). Cellulose production from glucose using a glucose dehydrogenase gene (gdh)-deficient mutant of *Gluconacetobacter xylinus* and its use for bioconversion of sweet potato pulp. *J. Biosci. Bioeng.* 99, 415–422. doi:10.1263/JBB.99.415.
- Shin, S., Kwak, H., Shin, D., and Hyun, J. (2019). Solid matrix-assisted printing for three-dimensional structuring of a viscoelastic medium surface. *Nat. Commun.* doi:10.1038/s41467-019-12585-9.
- Shinagawa, E., Matsushita, K., Adachi, O., and Ameyama, M. (1983). Selective production of 5-Keto-D-gluconate by *Gluconobacter* strains. *J. Ferment. Technol. (Osaka. 1977)*.
- Shinjoh, M., and Toyama, H. (2016). “Industrial application of acetic acid bacteria (vitamin C and others),” in *Acetic Acid Bacteria: Ecology and Physiology* (Springer Japan), 321–338. doi:10.1007/978-4-431-55933-7\_15.
- Shoseyov, O., Shani, Z., and Levy, I. (2006). Carbohydrate binding modules: biochemical properties and novel applications. *Microbiol. Mol. Biol. Rev.* 70, 283–95. doi:10.1128/MMBR.00028-05.
- Sievers, M., Lanini, C., Weber, A., Schuler-Schmid, U., and Teuber, M. (1995). Microbiology and fermentation balance in a kombucha beverage obtained from a tea fungus fermentation. *Syst. Appl. Microbiol.* 18, 590–594. doi:10.1016/S0723-2020(11)80420-0.
- Sievers, M., Sellmer, S., and Teuber, M. (1992). *Acetobacter europaeus* sp. nov., a Main Component of industrial vinegar fermenters in central Europe. *Syst. Appl. Microbiol.* 15, 386–392. doi:10.1016/S0723-2020(11)80212-2.
- Silva, G. G. D., Sobral, P. J. A., Carvalho, R. A., Bergo, P. V. A., Mendieta-Taboada, O., and Habitante, A. M. Q. B. (2008). Biodegradable films based on blends of gelatin and poly (vinyl alcohol): Effect of PVA type or concentration on some physical properties of films. *J. Polym. Environ.* 16, 276–285. doi:10.1007/s10924-008-0112-9.
- Sima, F., Mutlu, E. C., Eroglu, M. S., Sima, L. E., Serban, N., Ristoscu, C., et al. (2011). Levan nanostructured thin films by MAPLE assembling. *Biomacromolecules* 12, 2251–2256. doi:10.1021/bm200340b.
- Singh, S., Gaikwad, K. K., and Lee, Y. S. (2018). Antimicrobial and antioxidant properties of polyvinyl alcohol bio composite films containing seaweed extracted cellulose nano-crystal and basil leaves extract. *Int. J. Biol. Macromol.* doi:10.1016/j.ijbiomac.2017.10.057.
- Singh, O. V., and Kumar, R. (2007). Biotechnological production of gluconic acid: Future implications. *Appl. Microbiol. Biotechnol.* 75, 713–722. doi:10.1007/s00253-007-0851-x.
- Singhsa, P., Narain, R., and Manuspiya, H. (2018). Physical structure variations of bacterial cellulose produced by different *Komagataeibacter xylinus* strains and carbon sources in static and agitated conditions. *Cellulose* 25, 1571–1581. doi:10.1007/s10570-018-1699-1.
- Siracusa, V., Rocculi, P., Romani, S., and Rosa, M. D. (2008). Biodegradable polymers for food packaging: a review. *Trends Food Sci. Technol.* doi:10.1016/j.tifs.2008.07.003.
- Smith, E. A., and Newton, I. L. G. (2020). Genomic signatures of honey bee association in an acetic acid symbiont. *Genome Biol. Evol.* 12, 1882–1894. doi:10.1093/gbe/evaa183.

- Sokollek, S. J., and Hammes, W. P. (1997). Description of a starter culture preparation for vinegar fermentation. *Syst. Appl. Microbiol.* 20, 481–491. doi:10.1016/S0723-2020(97)80017-3.
- Son, H.-J., Heo, M.-S., Kim, Y.-G., and Lee, S.-J. (2001). Optimization of fermentation conditions for the production of bacterial cellulose by a newly isolated *Acetobacter* sp.A9 in shaking cultures. *Biotechnol. Appl. Biochem.* 33, 1. doi:10.1042/ba20000065.
- Song, S. H., and Vieille, C. (2009). Recent advances in the biological production of mannitol. *Appl. Microbiol. Biotechnol.* 84, 55–62. doi:10.1007/s00253-009-2086-5.
- Sonoyama, T., Tani, H., and Matsuda, K. (1982). Production of 2-keto-L-gulonic acid from D-glucose by two-stage fermentation. *Appl. Environ. Microbiol.* doi:10.1128/aem.43.5.1064-1069.1982.
- Soykeabkaew, N., Laosat, N., Ngaokla, A., Yodsuwan, N., and Tunkasiri, T. (2012). Reinforcing potential of micro- and nano-sized fibers in the starch-based biocomposites. *Compos. Sci. Technol.* doi:10.1016/j.compscitech.2012.02.015.
- Spagnol, C., Fragal, E. H., Witt, M. A., Follmann, H. D. M., Silva, R., and Rubira, A. F. (2018). Mechanically improved polyvinyl alcohol-composite films using modified cellulose nanowhiskers as nano-reinforcement. *Carbohydr. Polym.* doi:10.1016/j.carbpol.2018.03.001.
- Srikanth, R., Siddartha, G., Sundhar Reddy, C. H. S. S., Harish, B. S., Janaki Ramaiah, M., and Uppuluri, K. B. (2015). Antioxidant and anti-inflammatory levan produced from *Acetobacter xylinum* NCIM2526 and its statistical optimization. *Carbohydr. Polym.* 123, 8–16. doi:10.1016/j.carbpol.2014.12.079.
- Sriswasdi, S., Yang, C. C., and Iwasaki, W. (2017). Generalist species drive microbial dispersion and evolution. *Nat. Commun.* doi:10.1038/s41467-017-01265-1.
- Standal, R., Iversen, T. G., Coucheron, D. H., Fjaervik, E., Blatny, J. M., and Valla, S. (1994). A new gene required for cellulose production and a gene encoding cellulolytic activity in *Acetobacter xylinum* are colocalized with the bcs operon. *J. Bacteriol.* 176, 665–672. doi:10.1128/jb.176.3.665-672.1994.
- Stasiak-Róžańska, L., Płoska, J., Stasiak-Róžańska, L., and Płoska, J. (2018). Study on the use of microbial cellulose as a biocarrier for 1,3-Dihydroxy-2-propanone and its potential Application in industry. *Polymers (Basel)*. 10, 438. doi:10.3390/polym10040438.
- Stasiak, L., and Błaejak, S. (2009). Acetic acid bacteria-perspectives of application in biotechnology-a review. *Polish J. Food Nutr. Sci.*
- Stoodley, P., Dodds, I., Boyle, J. D., and Lappin-Scott, H. M. (1998). Influence of hydrodynamics and nutrients on biofilm structure. *J. Appl. Microbiol.* 85, 19S-28S. doi:10.1111/j.1365-2672.1998.tb05279.x.
- Stottmeister, U., Aurich, A., Wilde, H., Andersch, J., Schmidt, S., and Sicker, D. (2005). White biotechnology for green chemistry: Fermentative 2-oxocarboxylic acids as novel building blocks for subsequent chemical syntheses. in *Journal of Industrial Microbiology and Biotechnology* (Springer), 651–664. doi:10.1007/s10295-005-0254-x.
- Suderman, N., Isa, M. I. N., and Sarbon, N. M. (2018). The effect of plasticizers on the functional

- properties of biodegradable gelatin-based film: A review. *Food Biosci.* doi:10.1016/j.fbio.2018.06.006.
- Sugisawa, T., Hoshino, T., Nomura, S., Fujiwara, A., and Akiko, A. F. (1991). Isolation and characterization of membrane-bound L-Sorbose dehydrogenase from *Gluconobacter melanogenus* UV10. *Agric. Biol. Chem.* 55, 363–370. doi:10.1271/bbb1961.55.363.
- Sunagawa, N., Fujiwara, T., Yoda, T., Kawano, S., Satoh, Y., Yao, M., et al. (2013). Cellulose complementing factor (Ccp) is a new member of the cellulose synthase complex (terminal complex) in *Acetobacter xylinum*. *J. Biosci. Bioeng.* 115, 607–612. doi:10.1016/j.jbiosc.2012.12.021.
- Švec, P., Vancanneyt, M., Seman, M., Snauwaert, C., Lefebvre, K., Sedláček, I., et al. (2005). Evaluation of (GTG)<sub>5</sub>-PCR for identification of *Enterococcus* spp. *FEMS Microbiol. Lett.* 247, 59–63. doi:10.1016/j.femsle.2005.04.030.
- Taiyun, W.; Viliam, S. R package "corrplot": Visualization of a Correlation Matrix. Version 0.84. 2017. Available from <https://github.com/taiyun/corrplot>. (Accessed on 03 Feb 2020).
- Tajima, K., Nakajima, K., Yamashita, H., Shiba, T., Munekata, M., and Takai, M. (2001). Cloning and sequencing of the beta-glucosidase gene from *Acetobacter xylinum* ATCC 23769. *DNA Res.* 8, 263–269. doi:10.1093/dnares/8.6.263.
- Tamura, K., and Nei, M. (1993). Estimation of the number of nucleotide substitutions in the control region of mitochondrial DNA in humans and chimpanzees. *Mol. Biol. Evol.* 10, 512–26. doi:10.1093/oxfordjournals.molbev.a040023.
- Teeling, H., Waldmann, J., Lombardot, T., Bauer, M., and Glöckner, F. O. (2004). TETRA: A web-service and a stand-alone program for the analysis and comparison of tetranucleotide usage patterns in DNA sequences. *BMC Bioinformatics.* doi:10.1186/1471-2105-5-163.
- Thakhiew, W., Devahastin, S., and Soponronnarit, S. (2013). Physical and mechanical properties of chitosan films as affected by drying methods and addition of antimicrobial agent. *J. Food Eng.* doi:10.1016/j.jfoodeng.2013.05.020.
- Thompson, D. N., and Hamilton, M. A. (2001). Production of bacterial cellulose from alternate feedstocks. in *Applied Biochemistry and Biotechnology - Part A Enzyme Engineering and Biotechnology* (Appl Biochem Biotechnol), 503–513. doi:10.1385/ABAB:91-93:1-9:503.
- Thongsomboon, W., Serra, D. O., Possling, A., Hadjineophytou, C., Hengge, R., and Cegelski, L. (2018). Phosphoethanolamine cellulose: A naturally produced chemically modified cellulose. *Science (80-. )*. 359, 334–338. doi:10.1126/science.aao4096.
- Timmusk, S., Paalme, V., Pavlicek, T., Bergquist, J., Vangala, A., Danilas, T., et al. (2011). Bacterial distribution in the rhizosphere of wild barley under contrasting microclimates. *PLoS One.* doi:10.1371/journal.pone.0017968.
- Tonouchi, N., Tahara, N., Tsuchida, T., Yoshinaga, F., Beppu, T., and Horinouchi, S. (1995). Addition of a small amount of an endoglucanase enhances cellulose production by *Acetobacter xylinum*. *Biosci. Biotechnol. Biochem.* 59, 805–808. doi:10.1271/bbb.59.805.

- Torres, F. G., Arroyo, J. J., and Troncoso, O. P. (2019). Bacterial cellulose nanocomposites: An all-nano type of material. *Mater. Sci. Eng. C* 98, 1277–1293. doi:10.1016/J.MSEC.2019.01.064.
- Toyama, H., Soemphol, W., Moonmangmee, D., Adachi, O., and Matsushita, K. (2005). Molecular properties of membrane-bound FAD-containing D-sorbitol dehydrogenase from thermotolerant *Gluconobacter frateurii* isolated from Thailand. *Biosci. Biotechnol. Biochem.* 69, 1120–1129. doi:10.1271/bbb.69.1120.
- Trovatti, E., Fernandes, S. C. M., Rubatat, L., Perez, D. da S., Freire, C. S. R., Silvestre, A. J. D., et al. (2012). Pullulan-nanofibrillated cellulose composite films with improved thermal and mechanical properties. *Compos. Sci. Technol.* doi:10.1016/j.compscitech.2012.06.003.
- Ua-Arak, T., Jakob, F., and Vogel, R. F. (2016). Characterization of growth and exopolysaccharide production of selected acetic acid bacteria in buckwheat sourdoughs. *Int. J. Food Microbiol.* 239, 103–112. doi:10.1016/j.ijfoodmicro.2016.04.009.
- Ua-Arak, T., Jakob, F., and Vogel, R. F. (2017). Fermentation pH modulates the size distributions and functional properties of *Gluconobacter albidus* TMW 2.1191 Levan. *Front. Microbiol.* 8, 807. doi:10.3389/fmicb.2017.00807.
- Ul-Islam, M., Khan, T., Khattak, W. A., and Park, J. K. (2013). Bacterial cellulose-MMTs nanoreinforced composite films: Novel wound dressing material with antibacterial properties. *Cellulose* 20, 589–596. doi:10.1007/s10570-012-9849-3.
- Ul-Islam, M., Khan, T., and Park, J. K. (2012). Nanoreinforced bacterial cellulose-montmorillonite composites for biomedical applications. *Carbohydr. Polym.* 89, 1189–1197. doi:10.1016/j.carbpol.2012.03.093.
- Ullah, H., Santos, H. A., and Khan, T. (2016). Applications of bacterial cellulose in food, cosmetics and drug delivery. *Cellulose* 23, 2291–2314. doi:10.1007/s10570-016-0986-y.
- Umeda, Y., Hirano, A., Ishibashi, M., Akiyama, H., Onizuka, T., Ikeuchi, M., et al. (1999). Cloning of cellulose synthase genes from *Acetobacter xylinum* JCM 7664: Implication of a novel set of cellulose synthase genes. *DNA Res.* 6, 109–115. doi:10.1093/dnares/6.2.109.
- Valera, M. J., Torija, M. J., and Mas, A. (2018). “Detrimental effects of acetic acid bacteria in foods,” in *Acetic Acid Bacteria* (CRC Press), 299–320. doi:10.1201/9781315153490-14.
- Valera, M. J., Mas, A., Streit, W. R., and Mateo, E. (2016). GqqA, a novel protein in *Komagataeibacter europaeus* involved in bacterial quorum quenching and cellulose formation. *Microb. Cell Fact.* 15, 88. doi:10.1186/s12934-016-0482-y.
- Valera, M. J., Torija, M. J., Mas, A., and Mateo, E. (2014). Cellulose production and cellulose synthase gene detection in acetic acid bacteria. *Appl. Microbiol. Biotechnol.* 99, 1349–1361. doi:10.1007/s00253-014-6198-1.
- Vasconcelos, N. F., Feitosa, J. P. A., da Gama, F. M. P., Morais, J. P. S., Andrade, F. K., de Souza Filho, M. de S. M., et al. (2017). Bacterial cellulose nanocrystals produced under different hydrolysis conditions: Properties and morphological features. *Carbohydr. Polym.* doi:10.1016/j.carbpol.2016.08.090.

- Versalovic, J., Koeuth, T., and Lupski, R. (1991). Distribution of repetitive DNA sequences in eubacteria and application to finerprinting of bacterial enomes. *Nucleic Acids Res.* 19, 6823–6831. doi:10.1093/nar/19.24.6823.
- Versalovic, J., Schneider, M., Bruijn, F. J. De, and Lupski, J. R. (1994). Genomic fingerprinting of bacteria using repetitive sequence-based polymerase chain reaction. *Methods Mol. Cell. Biol.* 5, 25–40.
- Vidra, A., and Németh, Á. (2018). Bio-produced acetic acid: A review. *Period. Polytech. Chem. Eng.* 62, 245–256. doi:10.3311/PPch.11004.
- Villarreal-Soto, S. A., Beaufort, S., Bouajila, J., Souchard, J.-P., and Taillandier, P. (2018). Understanding kombucha tea fermentation: A review. *J. Food Sci.* 83, 580–588. doi:10.1111/1750-3841.14068.
- Voicu, G., Jinga, S. I., Drosu, B. G., and Busuioc, C. (2017). Improvement of silicate cement properties with bacterial cellulose powder addition for applications in dentistry. *Carbohydr. Polym.* 174, 160–170. doi:10.1016/j.carbpol.2017.06.062.
- Voronova, M. I., Surov, O. V., Guseinov, S. S., Barannikov, V. P., and Zakharov, A. G. (2015). Thermal stability of polyvinyl alcohol/nanocrystalline cellulose composites. *Carbohydr. Polym.* 130, 440–447. doi:10.1016/j.carbpol.2015.05.032.
- Wang, B., Shao, Y., Chen, T., Chen, W., and Chen, F. (2015). Global insights into acetic acid resistance mechanisms and genetic stability of *Acetobacter pasteurianus* strains by comparative genomics. *Sci. Rep.* 5, 18330. doi:10.1038/srep18330.
- Wang, L., Chen, C., Wang, J., Gardner, D. J., and Tajvidi, M. (2020). Cellulose nanofibrils versus cellulose nanocrystals: Comparison of performance in flexible multilayer films for packaging applications. *Food Packag. Shelf Life.* doi:10.1016/j.fpsl.2020.100464.
- Wang, L. F., Shankar, S., and Rhim, J. W. (2017). Properties of alginate-based films reinforced with cellulose fibers and cellulose nanowhiskers isolated from mulberry pulp. *Food Hydrocoll.* doi:10.1016/j.foodhyd.2016.08.041.
- Wang, S. S., Han, Y. H., Chen, J. L., Zhang, D. C., Shi, X. X., Ye, Y. X., et al. (2018). Insights into bacterial cellulose biosynthesis from different carbon sources and the associated biochemical transformation pathways in *Komagataeibacter* sp. W1. *Polymers (Basel)*. doi:10.3390/polym10090963.
- Watanabe, K., and Yamanaka, S. (1995). Effects of oxygen tension in the gaseous phase on production and physical properties of bacterial cellulose formed under static culture conditions. *Biosci. Biotechnol. Biochem.* doi:10.1080/bbb.59.65.
- Wei, S., Song, Q., and Wei, D. (2007). Repeated use of immobilized *Gluconobacter oxydans* cells for conversion of glycerol to dihydroxyacetone. *Prep. Biochem. Biotechnol.* 37, 67–76. doi:10.1080/10826060601040954.
- WHO Technical Report Series 922 Evaluation of certain food additives and contaminants. Sixty-first

- report of the Joint FAO/WHO Expert Committee on Food Additives.
- Williams, W. S., and Cannon, R. E. (1989). Alternative environmental roles for cellulose produced by *Acetobacter xylinum*. *Appl. Environ. Microbiol.* 55.
- Wong, H. C., Fear, A. L., Calhoon, R. D., Eichinger, G. H., Mayer, R., Amikam, D., et al. (1990). Genetic organization of the cellulose synthase operon in *Acetobacter xylinum*. *Proc. Natl. Acad. Sci. U. S. A.* doi:10.1073/pnas.87.20.8130.
- Wu, J., Gullo, M., Chen, F., and Giudici, P. (2010). Diversity of *Acetobacter pasteurianus* strains isolated from solid-state fermentation of cereal vinegars. *Curr. Microbiol.* 60, 280–286. doi:10.1007/s00284-009-9538-0.
- Xie, H., Yang, C., Fu, K. (Kelvin), Yao, Y., Jiang, F., Hitz, E., et al. (2018). Flexible, scalable, and highly conductive garnet-polymer solid electrolyte templated by bacterial cellulose. *Adv. Energy Mater.* 8, 1–7. doi:10.1002/aenm.201703474.
- Xu, J., Xia, R., Zheng, L., Yuan, T., and Sun, R. (2019). Plasticized hemicelluloses/chitosan-based edible films reinforced by cellulose nanofiber with enhanced mechanical properties. *Carbohydr. Polym.* 224, 115164. doi:10.1016/j.carbpol.2019.115164.
- Xu, S., Wang, X., Du, G., Zhou, J., and Chen, J. (2014). Enhanced production of L-sorbose from D-sorbitol by improving the mRNA abundance of sorbitol dehydrogenase in *Gluconobacter oxydans* WSH-003. *Microb. Cell Fact.* 13, 146. doi:10.1186/s12934-014-0146-8.
- Yadav, M., and Chiu, F. C. (2019). Cellulose nanocrystals reinforced  $\kappa$ -carrageenan based UV resistant transparent bionanocomposite films for sustainable packaging applications. *Carbohydr. Polym.* doi:10.1016/j.carbpol.2019.01.114.
- Yang, Y., Lu, Y. T., Zeng, K., Heinze, T., Groth, T., and Zhang, K. (2020). Recent progress on cellulose-based ionic compounds for biomaterials. *Adv. Mater.* doi:10.1002/adma.202000717.
- Yasutake, Y., Kawano, S., Tajima, K., Yao, M., Satoh, Y., Munekata, M., et al. (2006). Structural characterization of the *Acetobacter xylinum* endo- $\beta$ -1,4-glucanase CMCax required for cellulose biosynthesis. *Proteins Struct. Funct. Bioinforma.* 64, 1069–1077. doi:10.1002/prot.21052.
- Yoo, S. H., Yoon, E. J., Cha, J., and Lee, H. G. (2004). Antitumor activity of levan polysaccharides from selected microorganisms. *Int. J. Biol. Macromol.* 34, 37–41. doi:10.1016/j.ijbiomac.2004.01.002.
- Zhang, H., Xu, X., Chen, X., Yuan, F., Sun, B., Xu, Y., et al. (2017). Complete genome sequence of the cellulose-producing strain *Komagataeibacter nataicola* RZS01. *Sci. Rep.* 7. doi:10.1038/s41598-017-04589-6.
- Zheng, Y., Wang, J., Bai, X., Chang, Y., Mou, J., Song, J., et al. (2018). Improving the acetic acid tolerance and fermentation of *Acetobacter pasteurianus* by nucleotide excision repair protein UvrA. *Appl. Microbiol. Biotechnol.* 102, 6493–6502. doi:10.1007/s00253-018-9066-6.
- Zhong, C., Zhang, G. C., Liu, M., Zheng, X. T., Han, P. P., and Jia, S. R. (2013). Metabolic flux analysis of *Gluconacetobacter xylinus* for bacterial cellulose production. *Appl. Microbiol.*



*Biotechnol.* 97, 6189–6199. doi:10.1007/s00253-013-4908-8.

Zogaj, X., Nimt, M., Rohde, M., Bokranz, W., and Römling, U. (2001). The multicellular morphotypes of *Salmonella typhimurium* and *Escherichia coli* produce cellulose as the second component of the extracellular matrix. *Mol. Microbiol.* 39, 1452–1463. doi:10.1046/j.1365-2958.2001.02337.x.



# Acknowledgments

This thesis was in part developed in collaboration with University of Pisa, Department of Biology, King Abdullah University of Science and Technology (Kaust) and the Department of engineering of University of Modena and Reggio Emilia. Acetaia San Giacomo srl and Boschetto maremma Toscana are acknowledged for partial economic support.

When I started my experience getting a doctorate in 2017, I really did not realize how much experience was gaining in my career. Although there is only one name in the cover of this thesis, there are many people without whom, thanks to their scientific insights, mental support and practical help this PhD work would not be possible.

Maria, you hired me when I was just a research fellow in another University, without any experience in microbiology wet lab. Over the years, you gave me all the necessary inputs for experimental design. I was not always sure on my research activities, but you were reassuring and at the end, we develop all the chapter of this thesis. I want to thank you for giving me some opportunities during these years as to attend the workshop from the Joint Genome Institute and the period in Saudi Arabia, at Kaust University. Thank you to support my success and my failures and to gave me the opportunity to present our work in to three international conferences.

Luciana, your contribution was important to reach this achievement. Your technical advices and your suggestions when I was not so confident in lab improved many experimental plans.

Much gratitude is extended to Stefano. We develop some parts of future project on this topic. We shared many coffee breaks especially when the labs was empty, talking about new ideas and frustrations for some bioinformatics analysis. Thanks a lot for sharing this moment.

One experience stand out from my PhD. I am taking about the period in Kaust University. I want to thank Prof. Daffonchio for giving me this opportunity and to share his amazing scientific support. A big thanks is addressed to Ramona, whit her scientific rigor improved some experimental plans and, subsequently, my professional skills. I want to thank also the others team members, especially Alan, Elisa and Matteo for sharing their expertise and funny moments during my staying in Kaust.

A special thanks is addressed to Prof. Giulio Petroni and Dr Simona Di Gregorio from University of Pisa, for their scientific contribution and crital revisions of some parts of this PhD project.

I want to thank my colleagues from food packaging lab to develop some parts of this project. Thank you for sharing your expertize and technical advices. Especially I want to tanks Nima for his support as colleague and for sharing fanny moments outside the lab.

My gratitude is addressed to Prof. Monia Montorsi and her staff, in particular Dr. Silvia Barbi and for the development of parts of this project. It was a pleasure share with you our expertize.

I want to thank the STEBA school and in particular the Dean Prof. Alessandro Ulrici for the management of the PhD school.

Special thanks is addressed to Serena. We may not have worked together directly, but shared a lot

of funny moments and coffee breaks during these years, inside and outside the lab, discussing about projects, frustrations, present life and the future. Your support was a morale-boost for whole period, so thanks a lot.

During PhD years, a particular experience changed everything and was to meet you, Ying. Thank you to believe in me and gave me the push to complete this step of my career. Wherever our adventures take us next, I will be happy to share them with you.

I want to thank my flat mate, Sebastiano, Valeria, Laura, Filippo e Luigi for sharing with me funny moments, for celebrating my success and for dealing my complaints.

My gratitude goes also to my family, who supported me during this long journey and during my frustrations.

# Curriculum vitae and list of publications

Salvatore La China was born on the 18<sup>th</sup> of March 1986, in Agrigento, Italy. After completing his secondary education at Leonardo Da Vinci college, he started the bachelor program in molecular biological sciences at Pisa University. After his graduation, the same year he started the master program in biology applied to biomedicine, at University of Pisa and graduated in 2014. After two year, in 2016, he was research fellow at Center for Algorithmic biotechnology (CAB) lab in St. Petersburg in the group of Prof. Alla Lapidus, where he acquired bioinformatics skills in genomic and metagenomics analysis. The same year, he started a research fellowship at University of Pisa, where he was focused on environmental microbiology, especially in the study of microbial community in contaminated soil. In 2017 he started the PhD programme on bacterial cellulose produced from *Komagataeibacter* strains isolated from food matrices at University of Modena and Reggio Emilia in the food microbiology group of Dr. Maria Gullo. During these years he was winner of the 3<sup>rd</sup> of “Premio Stanca” for his scientific contribution to the doctorate school. The results of the research conducted for his PhD are described in this thesis book.

## List of publications

**La China, S.**, De Vero, L., Anguluri, K., Brugnoli, M., Mamlouk, D., Gullo, M. (2021) Kombucha tea as a reservoir of cellulose producing bacteria: Assessing diversity among *Komagataeibacter* isolates. *Appl. Sci.* 11, 1595. doi:10.3390/app11041595.

Krusong, W., Pothimon, R., **La China, S.**, and Thompson, A. K. (2021). Consecutive bacterial cellulose production by luffa sponge enmeshed with cellulose microfibrils of *Acetobacter xylinum* under continuous aeration. *3 Biotech.* 11, 6. doi:10.1007/s13205-020-02569-8.

Barbi, S., Taurino, C., **La China, S.**, Anguluri, K., Gullo, M., and Montorsi, M. (2021). Mechanical and structural properties of environmental green composites based on functionalized bacterial cellulose. *Cellulose*, 1–12. doi:10.1007/s10570-020-03602-y.

Haghighi, H., Gullo, M., **La China, S.**, Pfeifer, F., Siesler, H. W., Licciardello, F., et al. (2021). Characterization of bio-nanocomposite films based on gelatin/polyvinyl alcohol blend reinforced with bacterial cellulose nanowhiskers for food packaging applications. *Food Hydrocoll.* 113, 4. doi:10.1016/j.foodhyd.2020.106454.

Chicca, I., Becarelli, S., Dartiahl, C., **La China, S.**, De Kievit, T., Petroni, G., et al. (2020). Degradation of BTEX mixture by a new *Pseudomonas putida* strain: role of the quorum sensing in the modulation of the upper BTEX oxidative pathway. *Environ. Sci. Pollut. Res.* 27, 36203–36214. doi:10.1007/s11356-020-09650-y.

Pothimon, R., Gullo, M., **La China, S.**, Thompson, A. K., and Krusong, W. (2020). Conducting High acetic acid and temperature acetification processes by *Acetobacter pasteurianus* UMCC 2951. *Process Biochem.* 98, 41–50. doi:10.1016/j.procbio.2020.07.022.

Becarelli, S., **La China, S.**, Lapidus, A., Prijibelski, A., Polev, D., Petroni, G., et al. (2020). A new *Thioalkalivibrio* sp. strain isolated from petroleum-contaminated Brackish estuary sediments: A new candidate for bio-based application for sulfide oxidation in halo-alkaline conditions. *Water* 12, 1385. doi:10.3390/w12051385.

**La China, S.**, Bezzecchi, A., Moya, F., Petroni, G., Di Gregorio, S., and Gullo, M. (2020). Genome sequencing and phylogenetic analysis of K1G4: a new *Komagataeibacter* strain producing bacterial cellulose from different carbon sources. *Biotechnol. Lett.* 42, 807–818. doi:10.1007/s10529-020-02811-6.

Becarelli, S., Chicca, I., Siracusa, G., **La China, S.**, Gentini, A., Lorenzi, R., et al. (2019). Hydrocarbonoclastic Ascomycetes to enhance co-composting of total petroleum hydrocarbon (TPH) contaminated dredged sediments and lignocellulosic matrices. *N. Biotechnol.* 50, 27–36. doi:10.1016/j.nbt.2019.01.006.

Gullo, M., **La China, S.**, Petroni, G., Di Gregorio, S., and Giudici, P. (2019). Exploring K2G30 genome: A high bacterial cellulose producing strain in glucose and mannitol based media. *Front. Microbiol.* 10, 1–12. doi:10.3389/fmicb.2019.00058.

Spennati, F., Mora, M., Tigini, V., **La China, S.**, Di Gregorio, S., Gabriel, D., et al. (2019). Removal of quebracho and tara tannins in fungal bioreactors: Performance and biofilm stability analysis. *J. Environ. Manage.* 231, 137–145. doi:10.1016/j.jenvman.2018.10.001.

**La China, S.**, Zanichelli, G., De Vero, L., and Gullo, M. (2018). Oxidative fermentations and exopolysaccharides production by acetic acid bacteria: a mini review. *Biotechnol. Lett.* 40, 1289–1302. doi:10.1007/s10529-018-2591-7.

Gullo, M., **La China, S.**, Falcone, P. M. P. M., and Giudici, P. (2018). Biotechnological production of cellulose by acetic acid bacteria: current state and perspectives. *Appl. Microbiol. Biotechnol.* 102, 1–14. doi:10.1007/s00253-018-9164-5.

